FLORIDA INTERNATIONAL UNIVERSITY

Miami, Florida

# THE ROLE OF INOSITOL POLYPHOSPHATE-4-PHOSPHATASE TYPE II B (INPP4B) IN NORMAL AND NEOPLASTIC PHYSIOLOGY OF DIET-INDUCED OBESE MOUSE MODELS

A dissertation submitted in partial fulfillment of

the requirements for the degree of

DOCTOR OF PHILOSOPHY

in

BIOMEDICAL SCIENCES

by

Yasemin Ceyhan

2022

To: Dean Juan C. Cendan
College of Medicine

This dissertation, written by Yasemin Ceyhan, and entitled The Role of Inositol Polyphosphate-4-Phosphatase Type II B (INPP4B) in Normal and Neoplastic Physiology of Diet-Induced Obese Mouse Models, having been approved in respect to style and intellectual content, is referred to you for judgment.

We have read this dissertation and recommend that it be approved.

_____
Alexander Agoulnik

_____
Charles Dimitroff

_____
Yuan Liu

_____
Xiangxi Xu

_____
Irina Agoulnik, Major Professor

Date of Defense: November 7, 2022

The dissertation of Yasemin Ceyhan is approved.

_____
Dean Juan C. Cendan
College of Medicine

_____
Andrés G. Gil
Vice President for Research and Economic Development
and Dean of the University Graduate School

Florida International University, 2022

DEDICATION

I dedicate this dissertation to my mother, S. Lale Millik Ceyhan, and to loving memory of my grandmother, Muadelet Ceyhan. Their love and strength inspired me to become who I am today.

ACKNOWLEDGMENTS

I would like to acknowledge numerous people without whom this dissertation would not be possible. First of all, I would like to express my gratitude to my major professor Dr. Irina Agoulnik for her constant support and excellent mentorship during my graduate studies. While I had the opportunity of working in various amazing projects in Dr. Agoulnik's laboratory, her mentorship allowed me to improve my scientific writing, research, and presentation skills. I will always be in debt to Dr. Agoulnik for her kindness and compassion, which helped me become a better scientist and a better person in these last five years.

I would like to extend my gratitude to my committee members, Dr. Alexander Agoulnik, Dr. Yuan Liu, Dr. Charles Dimitroff, and Dr. Xiangxi Xu for their guidance and feedback. I would like to give a special thanks to Dr. Agoulnik as our Biomedical Sciences PhD program director, for always making sure that I am on track and making progress. In addition, I would like to thank our program coordinator Ms. Odalys De La Rosa for helping us with all kinds of administrative issues and making our lives much easier.

Moreover, I would like to acknowledge former and current members of Dr. Irina Agoulnik's laboratory. Judy Vasquez and Dr. Manqi Zhang taught me all of the methodologies that I used to exert this research, and our discussions, which helped me improve my scientific knowledge. I will be always grateful for their patience, kindness, and friendship. I would like to thank Carlos Sandoval and Adrian Rodriguez for their assistance and their research fellowship. In addition, I would like to extend my thanks to the members of Dr. Alexander Agoulnik's laboratory for their invaluable contributions in our projects. Dr. Agoulnik has supervised our testis project, Courtney Myhr assisted us in

flow cytometry experiments, and Dr. Elena Kaftanovskaya provided us immense help and support in our histology experiments.

Moreover, I would like to express my gratitude to our collaborators. Dr. Jean Vacher provided our mouse model, Dr. Haiwei Gu provided us expertise in the metabolomics and lipidomics, Dr. Lubov Nathanson helped us immensely in the analysis of gene expression profile, and Dr. Zaohua Huang taught us sperm count analysis.

I would like to recognize National Cancer Institute and Baptist Health South Florida for funding my stipend and research, as well as Herbert Wertheim College of Medicine and 2022 Summer University Graduate School Dissertation Year Fellowship for the financial support.

I would like to acknowledge and thank PLoS One publishing group as the original publisher of "Deletion of inositol polyphosphate 4-phosphatase type-II B affects spermatogenesis in mice", 2020, doi: 10.1371/journal.pone.0233163 and Oxford University Press as the original publisher of "Expression patterns and the roles of phosphatidylinositol phosphatases in testis", 2022, doi: 10.1093/biolre/ioac132 for allowing me to use the manuscripts in my dissertation.

Finally, I would like to thank my family and friends. My friends and colleagues Marissa Pokharel and Marko Manevski made graduate school a more fun place, I will always cherish our impromptu meetings and laughs. I will be always grateful for my dear parents, Drs. S. Lale Millik Ceyhan and Onen Ceyhan, for their unconditional love, always believing in me, and encouraging me to pursue my dreams, as well as my beloved brother, Sinan Ceyhan, for his constant support and inspirational talks before my presentations.

Special thanks to my fiancé, Veli Bugra Ozdemir, for being my rock all these years. Nothing would be the same without you.

ABSTRACT OF THE DISSERTATION

THE ROLE OF INOSITOL POLYPHOSPHATE-4-PHOSPHATASE TYPE II B (INPP4B) IN NORMAL AND NEOPLASTIC PHYSIOLOGY OF DIET-INDUCED OBESE MOUSE MODELS

by

Yasemin Ceyhan

Florida International University, 2022

Miami, Florida

Professor Irina Agoulnik, Major Professor

Obesity is a risk factor for various endocrine diseases including metabolic syndrome, cancer, and infertility, and its increasing incidence in society poses a major health concern. INPP4B is a tumor suppressor in breast cancer and a metabolic regulator that was shown to protect male mice from obesity and type 2 diabetes. Despite the wide expression pattern of INPP4B, its role in normal physiology is not fully described. It is also not known whether loss of INPP4B plays a role in obesity-associated increase in breast cancer initiation and progression or whether it alters tumor metabolism. In this dissertation, I showed that INPP4B loss affects the metabolic health of female mice, mammary gland development, and ERBB2- driven tumorigenesis in females. I found that *Inpp4b*$^{-/-}$ females develop high-fat diet (HFD) induced obesity, hyperglycemia, nonalcoholic fatty liver disease (NAFLD), and adipose tissue inflammation. I determined that NAFLD is due to increased hepatic lipid synthesis, while hyperglycemia is caused by insulin resistance, increased gluconeogenesis, and reduction in hypothalamic FGF21/FGFR1 signaling. Increased *de novo* lipogenesis in

liver, decreased fat combustion in adipose tissue, and hypothalamic leptin resistance contributed to diet- induced obesity and inflammation of visceral adipose tissue.

In mammary glands, I showed that INPP4B stimulates ductal branching by stabilizing progesterone receptor levels and inducing its transcriptional activity. The mammary glands of *Inpp4b*- knockout females on an HFD have elevation of AKT and p53 levels, as well as dysregulated leptin signaling and inflammation. In ERBB2 driven mammary gland tumorigenesis, both INPP4B loss of function and HFD accelerate tumor incidence and progression by reducing p53 expression and activity and increasing lipid synthesis. I also found that INPP4B plays an important role in male reproductive function. *Inpp4b*$^{-/-}$ males exhibit smaller testis and fewer sperm due to reduced rates of meiosis and increased apoptosis. In men, the expression of *INPP4B* is highest in post-meiotic germ cells and it declines significantly in testes of infertile men that lack mature sperm. Thus, INPP4B emerges as a new regulator of metabolic and reproductive health as well as in obesity-induced tumorigenesis.

TABLE OF CONTENTS

CHAPTER PAGE

LIST OF TABLES

TABLE PAGE

TABLE OF FIGURES

FIGURES PAGE

# LIST OF ABBREVIATIONS

| | |
|---|---|
| ADGRE1 | F4/80 antigen |
| AKT | Protein kinase B |
| ApoB | Apolipoprotein B |
| AR | Androgen receptor |
| AS160 | AKT substrate of 160 kDa |
| AUC | Area under curve |
| BAR | Bin/Amphiphysin/Rvs |
| BMI | Body mass index |
| CD36 | Cluster of Differentiation 36 |
| CD68 | Cluster of Differentiation 68 |
| CIDEC | Cell Death Inducing DFFA Like Effector C |
| CMV | Cytomegalovirus |
| CYP11A1 | Cytochrome P450 Family 11 Subfamily A Member 1 |
| CYP17A1 | Cytochrome P450 Family 17 Subfamily A Member 1 |
| CYP19 | Aromatase |
| DAG | Diacylglycerol |
| DPP | Days postpartum |
| EEA1 | Early endosome antigen |
| EGFR | Epidermal growth factor receptor family |
| EGR1 | Early Growth Response 1 |
| EGR3 | Early Growth Response 3 |

| | |
|---|---|
| ERBB2 | Oncogenic receptor tyrosine protein kinase erbB-2 |
| ERK | Extracellular signal-regulated kinases |
| FABP4 | Fatty acid-binding protein 4 |
| FGF1 | Fibroblast growth factor 1 |
| FGF21 | Fibroblast growth factor 21 |
| FGFR1 | Fibroblast growth factor receptor 1 |
| FOXO1 | Forkhead Box O1 |
| FSH | Follicle stimulating hormone |
| GDNF | Glial cell line-derived neurotrophic factor |
| GLP-1 | Glucagon-like peptide-1 |
| GLUT4 | Glucose transporter 4 |
| GOLPH3 | Golgi PI4P-binding protein |
| GPCR | G-protein coupled receptor |
| GSK3B | glycogen synthase kinase-3-beta |
| HC | Hypostained |
| HER2 | Human epidermal growth factor receptor 2 |
| HFD | High fat diet |
| HPG | Hypothalamic-pituitary-gonadal |
| Hsd17b3 | 17 beta-hydroxysteroid dehydrogenase |
| Hsd3b6 | Hydroxy-delta-5-steroid dehydrogenase, 3 beta |
| HYP | Hypothalamus |
| ICV | Intracerebroventricular |

| | |
|---|---|
| IGF1 | Insulin growth factor |
| Il1b | Interleukin 1 beta |
| Il6 | Interleukin 6 |
| INNPL1 | Inositol Polyphosphate Phosphatase Like 1 |
| INPP4A | Inositol Polyphosphate-4-Phosphatase Type I A |
| INPP4B | Inositol polyphosphate 4- phosphatase Type-II B |
| INPP5B/E | Inositol Polyphosphate-5-Phosphatase B/E |
| IP | Intraperitoneal |
| IPTT | Intraperitoneal pyruvate tolerance test |
| IR | Insulin receptor |
| IRS1/2 | Insulin receptor substrate 1/2 |
| ITT | Insulin tolerance test |
| KLB | Beta-klotho |
| LEPR | Leptin receptor |
| LFD | Low fat diet |
| LH | Luteinizing hormone |
| LHCGR | LH receptor |
| MAPK | Mitogen-activated protein kinases |
| MEA | Mammary epithelial area |
| MetS | Metabolic syndrome |
| MOGAT1 | Monoacylglycerol O-Acyltransferase 1 |
| MS | Multiple sclerosis |

| | |
|---|---|
| MTM | Myotubularin |
| MTMR | Myotubularin Related Protein |
| mTOR | Mammalian target of rapamycin |
| mTORC1 | Mammalian target of rapamycin catalytic subunit 1 |
| mTORC2 | Mammalian target of rapamycin catalytic subunit 2 |
| NAFLD | Non-alcoholic fatty liver disease |
| NHR2 | Nervy Homology 2 |
| NMR | Nuclear magnetic resonance |
| NPY/AgRP | Neuropeptide Y/ Agouti-related protein |
| NR5A1, | Steroidogenic factor 1 |
| OGTT | Oral glucose tolerance test |
| PDGF | Platelet-derived growth factor |
| PDK1 | Phosphoinositide dependent protein kinase 1 |
| PH | Pleckstrin homology |
| PHD | Plant homeodomain |
| PI | Phosphoinositides |
| PI3K | Phosphatidylinositol 3 kinase |
| PI4KIIIβ | PI 4-kinase IIIβ |
| PIP | Phosphoinositide polyphosphates |
| PITP | Class I PI transfer protein |
| PKC | Protein kinase C |
| PLC | Phospholipase C |

| | |
|---|---|
| PLIN4 | Perilipin 4 |
| POMC | Neuropeptide pro-opiomelanocortin |
| PPAR | Peroxisome proliferator activated receptor |
| PPARA | Peroxisome proliferator activated receptor alpha |
| PPARG/Pparg | Peroxisome proliferator activated receptor gamma |
| PPARGC1A | PPARG coactivator 1 alpha |
| PPARGC1B | PPARG coactivator 1 beta |
| PR/PGR | Progesterone receptor |
| PTEN | Phosphatase and tensin homolog |
| PTP | Protein tyrosine phosphatase |
| PX | Phox domain |
| ROS | Reactive oxygen species |
| SCF | Stem cell factor |
| Ser | Serine |
| SGK3 | Serum/Glucocorticoid Regulated Kinase Family Member 3 |
| SNP | Single nucleotide polymorphism |
| SNX9 | Sorting nexin 9 |
| Srd5a1 | Steroid 5-alpha-reductase |
| SREBP1 | Sterol regulatory binding protein 1 |
| SSC | Spermatogonial stem cells |
| STAR | Steroidogenic acute regulatory protein |
| SYNJ1/2 | Synaptojanin 1/2 |

| | |
|---|---|
| T2D | Type II diabetes |
| Thr | Threonine |
| TMEM 55A/B | Transmembrane Protein 55A/B |
| TNBC | Triple-negative breast cancers |
| TNFA | Tumor necrosis factor-alpha |
| TPTE | Transmembrane Phosphatase with Tensin Homology |
| US | United States |
| WAT | White adipose tissue |
| WT | Wild-type |
| XLMTM | X-linked myotubular myopathy |
| ZP | Zona pellucida |
| γH2A.X | Gamma histone 2A.X |

# 1. CHAPTER 1: INTRODUCTION

## 1.1. Preface: Phosphoinositide-4 phosphatase INPP4B is involved in obesity-associated disorders

Obesity is a global health issue, and the rate of obesity has tripled since 1975 due to sedentary lifestyle and increased consumption of foods high in fat and sugars [1]. Currently, 42% of the adult population in the United States (U.S.) is obese [2], and obesity-associated disorders are responsible for the death of 41 million people annually [3].

Obesity is a risk factor for various endocrine disorders including metabolic syndrome, cancer, and infertility [4]. Lipid second messengers phosphoinositides (PIs) are central to the etiology of obesity and associated disorders, which mediate signaling cascades from insulin receptor (IR) to phosphatidylinositol 3 kinase (PI3K) and protein kinase B (PKB/AKT). IR/PI3K signaling is the main pathway in insulin resistance, which is common in obese patients and is the underlying cause of diabetes [5]. Aberrant activation of PI3K/AKT pathway is frequent in primary tumors and nearly universal in advanced metastatic cancers [6-8]. Spatiotemporal regulation of cellular PI levels plays an important role in male germ cell production and homeostasis [9, 10].

The cellular concentrations of PIs are tightly regulated by specific PI kinases and phosphatases [11]. The subject of this dissertation research is one of the PI-4 phosphatases, Inositol polyphosphate 4- phosphatase type-II B (INPP4B), as well as its roles in obesity and obesity-associated disorders.

## 1.2. Inositol polyphosphate 4- phosphatase type II B (INPP4B)

### 1.2.1. Gene information, protein structure, enzymatic activity, and expression pattern of INPP4B

INPP4B was first identified by Norris et al. [12, 13]. In humans, *INPP4B* is located on chromosome locus 4q31.21 (position 142,023,160-142,847,432) (Ensembl). Mouse ortholog (*Inpp4b*) is located on chromosome 8 (Ensembl). In 2006, Ferron et al. characterized two isoforms of *Innp4b* in mice: INPP4Bα and INPP4Bβ. The two isoforms have different number of amino acids and subcellular localization [14].

The protein sequence of INPP4B shows a substantial conservation between humans and mice with 96% sequence identity [14]. For both species, the protein structure consists of an N-terminal C2 lipid-binding domain with 91% similarity [12, 14], an internal Nervy Homology 2 (NHR2) domain that induces protein-protein interactions, and a conserved dual phosphatase motif, $C_{842}X5R_{848}$ or CKSAKDRT, within the C-terminal phosphatase domain [13-15].

INPP4B is a dual-specificity phosphatase, which can dephosphorylate both phospholipids and phosphoproteins [16]. Substrates of lipid phosphatase activity are phosphoinositides $PI(3,4)P_2$, $PI(4,5)P_2$, and $PI(3,4,5)P_3$, as well as the inositol $Ins(1,3,4)P_3$ [16-18]. Protein phosphatase activity substrates are phospho-serine and phospho-threonine residues on the phosphatase and tensin homolog (PTEN), and phospho-tyrosine, phospho-serine, and phospho-threonine residues on AKT [16, 19]. The subcellular localizations and functions of lipid substrates and products of INPP4B are covered in detail in the section 1.2.2.

In order to characterize the contributions of different amino acids to the protein tyrosine phosphatase (PTP) and lipid phosphatase activities, our laboratory produced four different

mutations: C842A, K846M, D847E, and K843M. In C842A and D847E mutations, both lipid phosphatase and PTP activities are significantly reduced, and K846M mutation affects only lipid phosphatase activity. Intriguingly, while reducing lipid phosphatase activity, K843M mutation increases PTP activity [16].

INPP4B is expressed ubiquitously in a variety of mouse tissues [20]. Moreover, *INPP4B* expression is highly variable among human tissues and between different individuals (Figure 1.1).

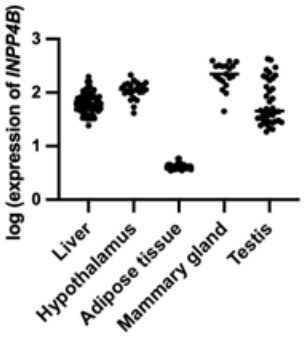


**Figure 1.1.** Relative expression of *INPP4B* in human tissues.
Data from datasets GSE126848 (liver), GSE1147 (hypothalamus), GSE27951 (adipose tissue), GSE21422 (mammary gland), and E-TABM-1214 (testis) was used for comparative analysis of *INPP4B* expression.

In mice, the highest expression of *Inpp4b* was detected in the testis, followed by the mammary gland and adipose tissue, whose physiology is affected by obesity and associated diseases [13, 20].

### 1.2.2. Subcellular localizations and functions of INPP4B-associated PIs

PIs are membrane phospholipids that are the derivates of phosphatidylinositol and synthesized in endoplasmic reticulum. PIs are formed by the linkage of the two fatty acids to a water-soluble inositol group by a glycerol backbone. Phosphorylation and dephosphorylation of the hydroxyl groups on the inositol ring of phosphatidylinositol at D-3, D-4, or D-5 positions give rise to seven functionally distinct PIs: PI(3,4,5)$P_3$, PI(3,5)$P_2$, PI(3,4)$P_2$, PI(4,5)$P_2$, PI(3)P, PI(4)P, and PI(5)P [21-24]. The maintenance of PI homeostasis is required for various cellular events in which they can directly bind to effector proteins and act as a substrate or a second messenger [25, 26]. INPP4B is one of the PI-4- phosphatases that dephosphorylates the D-4 position of the inositol ring. The lipid substrates and products of INPP4B are shown in Figure 1.2.

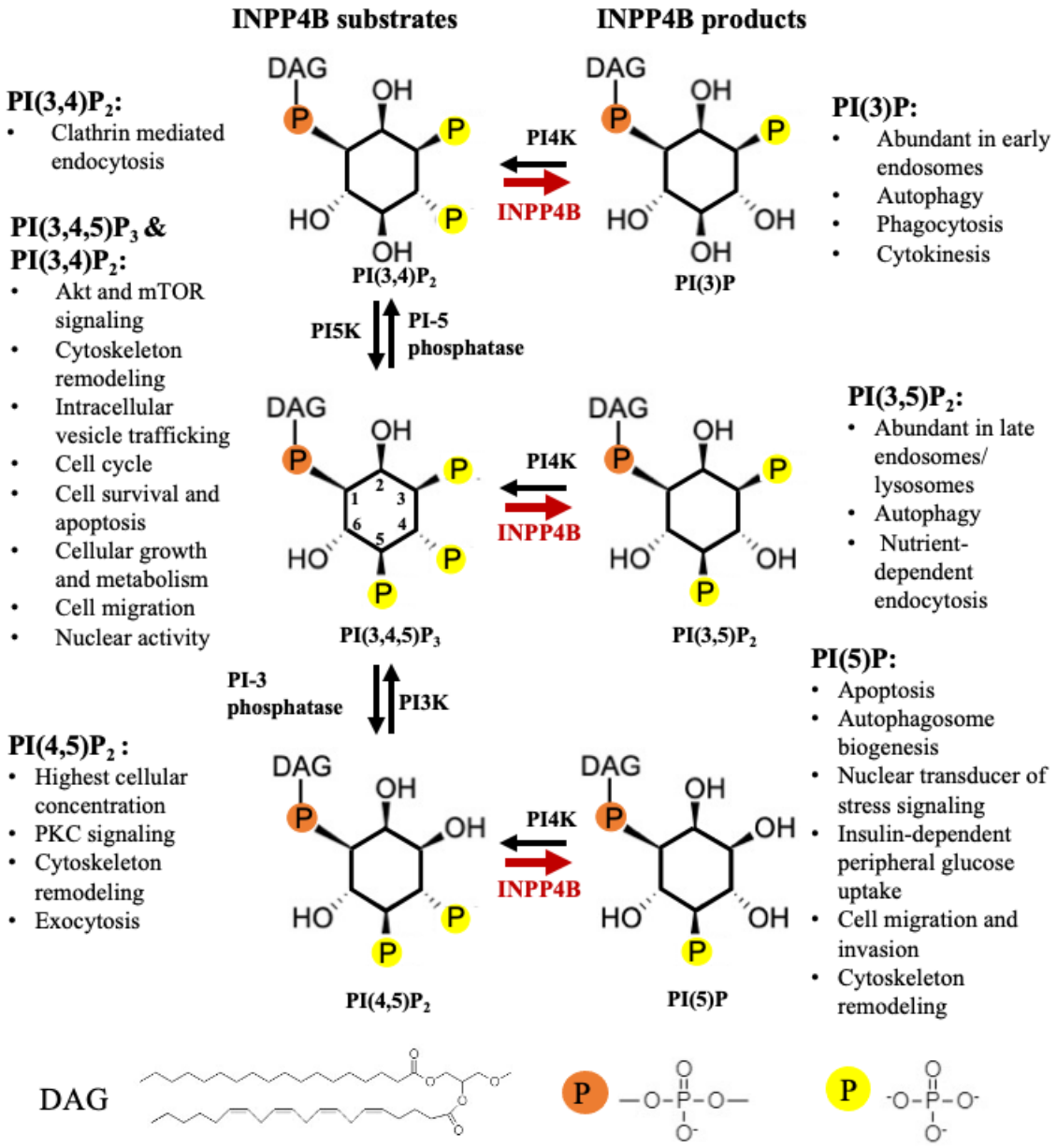


**Figure 1.2.** Lipid substrates and products of INPP4B

Lipid substrates of INPP4B enzymatic activity: $PI(3,4,5)P_3$, $PI(3,4)P_2$, and $PI(4,5)P_2$. Products of INPP4B enzymatic activity: $PI(3,5)P_2$, PI(3)P, and PI(5)P, respectively. Subcellular localizations and functions are summarized for each lipid molecule.

INPP4B substrates, PI(3,4,5)$P_3$ and PI(3,4)$P_2$, are essential for various cellular activities such as intracellular vesicle trafficking, cytoskeleton remodeling, chemotaxis, cell metabolism, survival, and apoptosis through AKT and mammalian or mechanistic target of rapamycin (mTOR) signaling pathways [25, 26]. PI3K produces PI(3,4)$P_2$ and PI(3,4,5)$P_3$, which bind to the pleckstrin homology (PH) domain of AKT and/or phosphoinositide dependent protein kinase 1 (PDK1), and active PKB/AKT signaling [27]. mTOR consists of two catalytic subunits, mTORC1 and mTORC2 [28]. PI(3,4,5)$P_3$ binds to PH domain on the mTORC2 inhibiting protein SIN1, and activates mTORC2 [29]. In the absence of growth factors and during nutrient deprivation, PI(3,4)$P_2$ binds Raptor subunit of mTORC1 and inhibits mTORC1 activity [30].

Activated AKT phosphorylates fork head box transcription factors O 1 (FOXO1) and causes its export from the nucleus [31]. This triggers expression of Cyclin D1, which leads to G1-S transition. FOXO1 nuclear exclusion also prevents the transcription of pro-apoptotic proteins [32]. Activation of AKT and mTORC1 promotes insulin-dependent glucose uptake, *de novo* lipogenesis, and amino acid biosynthesis [33]. In addition, PI(3,4,5)$P_3$ is involved in vesicle trafficking, cytoskeleton remodeling, and cell migration through activation of AKT or other effector molecules such as Rab proteins, nucleotide exchange protein GRP, and Rac exchange factors [34, 35]. Recent reports show that PI(3,4,5)$P_3$ also has a nuclear function. Gavgani et al. reported nucleolar localization of PI(3,4,5)$P_3$ and its interacting partners, which are involved in RNA processing/splicing, cytokinesis, and DNA repair [36]. Chen et al. demonstrated that formation of p53-PI(3,4,5)$P_3$ signalosome in the nucleoplasm under genotoxic stress causes nuclear activation of AKT and inhibits DNA damage and FOXO-regulated cell death [37].

In addition to activating AKT and mTOR pathways, $PI(3,4)P_2$ mediates phospholipase C/ protein kinase C (PLC/PKC) signaling, vesicular trafficking, cytoskeletal rearrangements, and cellular invasion and motility[38]. $PI(3,4)P_2$ mediates cellular motility and invasion by stimulating maturation of lamellipodia, podosomes, and invadopodia [39, 40]. It activates clathrin-mediated endocytosis by binding Phox domain (PX) or Bin/Amphiphysin/Rvs (BAR) domains of protein sorting nexin 9 (SNX9) [41]. Binding of $PI(3,4)P_2$ to the PH-domain of adaptor protein TAPP1 in response to platelet-derived growth factor (PDGF) triggers the reorganization of actin cytoskeleton, leading to the formation of dorsal ruffles on plasma membrane and subsequent micropinocytosis [42].

$PI(4,5)P_2$ has the highest concentration in cell membranes among phosphoinositides and is the most well-studied INPP4B substrate. It regulates cytoskeleton remodeling by interacting with actin-binding proteins such as profilin, gelsolin, capZ, vinculin, and WASP [43]. Moreover, $PI(4,5)P_2$ is the first PI that was studied in endocytosis/exocytosis, which are important for cell migration, autophagy, and recycling of membrane receptors such as epidermal growth factor receptor [44]. $PI(4,5)P_2$ is a substrate for PLC, which cleaves it into inositol $Ins(1,4,5)P_3$ and diacylglycerol (DAG). $Ins(1,4,5)P_3$ triggers the opening of $Ca^{2+}$ channels on the sarcoplasmic reticulum and increases $Ca^{2+}$ concentration in the cytosol. DAG binds to functional C1 domain of PKC, causing a conformational change that activates PKC [45]. Furthermore, $PI(4,5)P_2$ stabilizes and activates G-protein coupled receptors and inward-rectifier potassium channel by acting as a docking phospholipid [46, 47].

The product of INPP4B reaction, PI(3)P, is abundant in early endosomal membranes and is synthesized by Class 3 PI3K VPS34 [48] or produced by dephosphorylation of $PI(3,4)P_2$

by INPP4B. It is required for autophagy, phagocytosis, and cytokinesis [49, 50]. Loss of *Inpp4b* in mouse embryonic fibroblasts leads to over-activation of VPS34 and subsequent increase in PI(3)P levels, which causes severe lysosomal enlargement [51]. PI(3)P binds to the FYVE domain [52], which is present in various endosomal and autophagosomal effector proteins such as early endosome antigen 1 (EEA1) and cytokinesis factor FYVE-CENT [53]. Recently, Ajazi et al. has shown that elevated levels of PI(3)P binds and activates VPS34-VPS15-ATG6/Beclin1-VPS38 complex, which impairs amino acid metabolism and sensitizes cells to replication stress by modulating mTORC1 pathway [54]. The product of PI(3,4,5)$P_3$ dephosphorylation by INPP4B, PI(3,5)$P_2$, can also be produced from PI(3)P by kinase PIKFYVE in the late endosomes. PI(3,5)$P_2$ inhibits autophagy and promotes nutrient dependent endocytosis of plasma membrane proteins through activation of mTORC1 pathway [55, 56]. Under nutrient rich conditions, INPP4B produces PI(3)P from PI(3,4)$P_2$ in late endosomes, which is used as a substrate for the synthesis of PI(3,5)$P_2$ for the lysosomal maturation during basal autophagy [57, 58].

Dephosphorylation of PI(4,5)$P_2$ by INPP4B produces PI(5)P, which has a lower cellular concentration compared to other PIs. Kinases PIKFYVE and PIP4K are the two main enzymes that are responsible for the production and recycling of PI(5)P, respectively [59]. PI(5)P promotes autophagosome biogenesis during glucose starvation via AMPK activation [60, 61]. High PI(5)P levels stimulate insulin dependent glucose uptake via glucose transporter (GLUT4) and cytoskeleton remodeling in adipocytes and myocytes [62, 63]. Cell migration and invasion are increased by the activation of adaptor proteins Rac1 and Tiam1 through high PI(5) levels in cancer cells [64, 65]. Increased levels of PI(5)P, which are caused by the inhibition of PIP4Kβ, result in oxidative stress. In the

nucleus, PI(5)P binds to plant homeodomain (PHD) of nuclear effector protein ING2 and induces p53 acetylation and p53-dependent apoptosis [66, 67].

Thus, substrates and products of INPP4B lipid phosphatase activity regulate the signaling pathways PI3K/AKT, PKC, and mTOR, which are involved in cancer progression, metabolic health, and male fertility. While PI3K/AKT pathway is activated in 100% of advanced cancers, multiple isoforms of PKC modulate breast cancer progression [68, 69]. In metabolism, PI3K/AKT is the main mediator of insulin signaling, PKC pathway is a marker of insulin sensitivity, and mTOR pathway is a nutrient sensor and regulator of lipid metabolism [70, 71]. In addition, PI3K/AKT and PKC pathways are essential for male germ cell production and maturation [10]. The role of INPP4B and downstream signaling in breast cancer is further discussed in section 1.3, in metabolic health in section 1.4, and in male fertility in section 1.5.

### 1.2.3. Phenotypes of *Inpp4b*- knockout mouse models

The first *Inpp4b*-knockout mouse model was developed by Dr. Jean Vacher's group. The knockout of *Inpp4b* was generated by the flanking of exon 11 by loxP sites and crossing these animals with CMV-Cre transgenic mice, which resulted in the deletion of exon 11 and the frame shift, changing codon 217 to a stop codon. Truncated protein completely lacks phosphatase domain and is undetectable in mouse tissues on a protein level. Ferron et al. showed that *Inpp4b*$^{-/-}$ null mice develop osteoporosis due to increased osteoclast differentiation, leading to decreased bone mass [18]. Of note, this particular mouse model was used in the execution of this dissertation research.

Another *Inpp4b*-knockout mouse was generated by Kofuji et al. in 2015, which is produced by the deletion of exon 21, which encodes the catalytic motif in the phosphatase domain.

The deletion was achieved via introducing loxP sites in introns 20 and 21 and crossing *Inpp4b*$^{+/flox}$ animals with MeuCre40 mice. Neither mRNA nor protein levels were detected in tissues on the knockout animals [17]. Similar to Dr. Vacher's model, these *Inpp4b*$^{-/-}$ mice do not develop tumors; however, *Inpp4b*$^{-/-}$*; Pten*$^{+/-}$ mice developed thyroid hyperplasia caused by the hyperactivation of AKT2 signaling [17].

In addition to the role in cancer biology and osteoporosis, Lemcke et al reported the involvement of INPP4B in nerve conduction velocity in multiple sclerosis (MS) [72]. A patient cohort showed a positive correlation between INPP4B polymorphism and susceptibility to MS. A rodent variant of *Inpp4b* has been identified, S474R/H548P, which causes cortical motor evoked potential latency [72]. Ji et al. reported that the loss of *Inpp4b* halted the callosal axon development during embryogenesis [73].

### 1.3. INPP4B in breast cancer

While there is a strong epidemiological data demonstrating tumor suppressor role of INPP4B in cancer, not all signaling pathways regulated by INPP4B are known [74].

#### 1.3.1. Molecular subtypes of breast cancer

Breast cancer is one of the endocrine cancers in women that is affected by obesity. It is divided into four molecular subtypes based on the expression levels of steroid hormone receptors, estrogen receptor alpha (ERα) and progesterone receptor (PR), and oncogenic receptor tyrosine protein kinase erbB-2/ human epidermal growth factor receptor 2 (ERBB2/ HER2) [75, 76] (Table 1).

More than 70% of breast cancers are hormone-dependent, and loss of the steroid hormone receptor expression is correlated with poor prognosis in breast cancer patients [77].

Mounting evidence suggests that INPP4B expression is another potential marker of breast cancer progression.

INPP4B is co-expressed in the normal luminal epithelium with ERα and PR [78]. INPP4B is expressed in ER-positive breast cancers and its levels positively correlate with ERα expression. INPP4B levels are greatly reduced in triple-negative breast cancers (TNBC) [78, 79] (Table 1). Loss of INPP4B is shown to be the strongest prognostic markers in TNBC with an odds ratio of 108 [80].

**Table 1.** ERα, PR, HER2, and INPP4B expression in the molecular subtypes of breast cancer

| | ERα | PR | HER2 | INPP4B |
|---|---|---|---|---|
| Luminal A | positive | positive | negative | present |
| Luminal B | positive | positive | positive | present |
| HER2- positive | negative | negative | positive | intermediate |
| TNBC | negative | negative | negative | absent |

### 1.3.2. HER2-positive breast cancers

Approximately 25% to 30% of the breast cancers overexpress HER2. These cases have second worst survival rate after TNBC [81]. ERBB2/HER2 is a receptor tyrosine kinase and belongs to the epidermal growth factor receptor family (EGFR). ERBB2 forms obligatory heterodimers with ERRB3 and upregulates mitogen-activated protein kinases/ extracellular signal-regulated kinases (MAPK/ERK) and PI3K/AKT/mTOR pathways, which promote proliferation and survival, and reduce apoptosis [82, 83]. Since INPP4B is well known to oppose PI3K/AKT pathway, it is plausible that INPP4B plays a tumor suppressive role in HER2-positive breast cancers. Data analysis from three breast cancer cohorts in Table 2 shows that concomitant alterations in both ERBB2 and INPP4B lead to the worst survival rate compared to patients with mutations in only one of the genes or

patients without mutations in both genes (cBioPortal, [84]), suggesting functional interaction between INPP4B and HER2.

**Table 2.** Comparison of the total number of mutations in *ERBB2* and *INPP4B* genes and median survival in breast cancer patients

| | Number of cases | Number of genetic alterations | Median Survival (95% CI) |
|---|---|---|---|
| Unaltered | 3811 | 1353 | 168.30 (159.20 - 176.10) |
| Only ERBB2 | 693 | 274 | 140.60 (119.97 - 158.53) |
| Only INPP4B | 28 | 8 | 98.70 (58.67 - NA) |
| INPP4B, ERBB2 | 9 | 6 | 89.53 (38.03 - NA) |

### 1.3.3. Molecular mechanisms of INPP4B in breast cancer

Multiple reports show that INPP4B can act both as a tumor suppressor and an oncogene depending on the downstream effectors expressed in individual cancer [74, 85-91] (Figure 1.3).

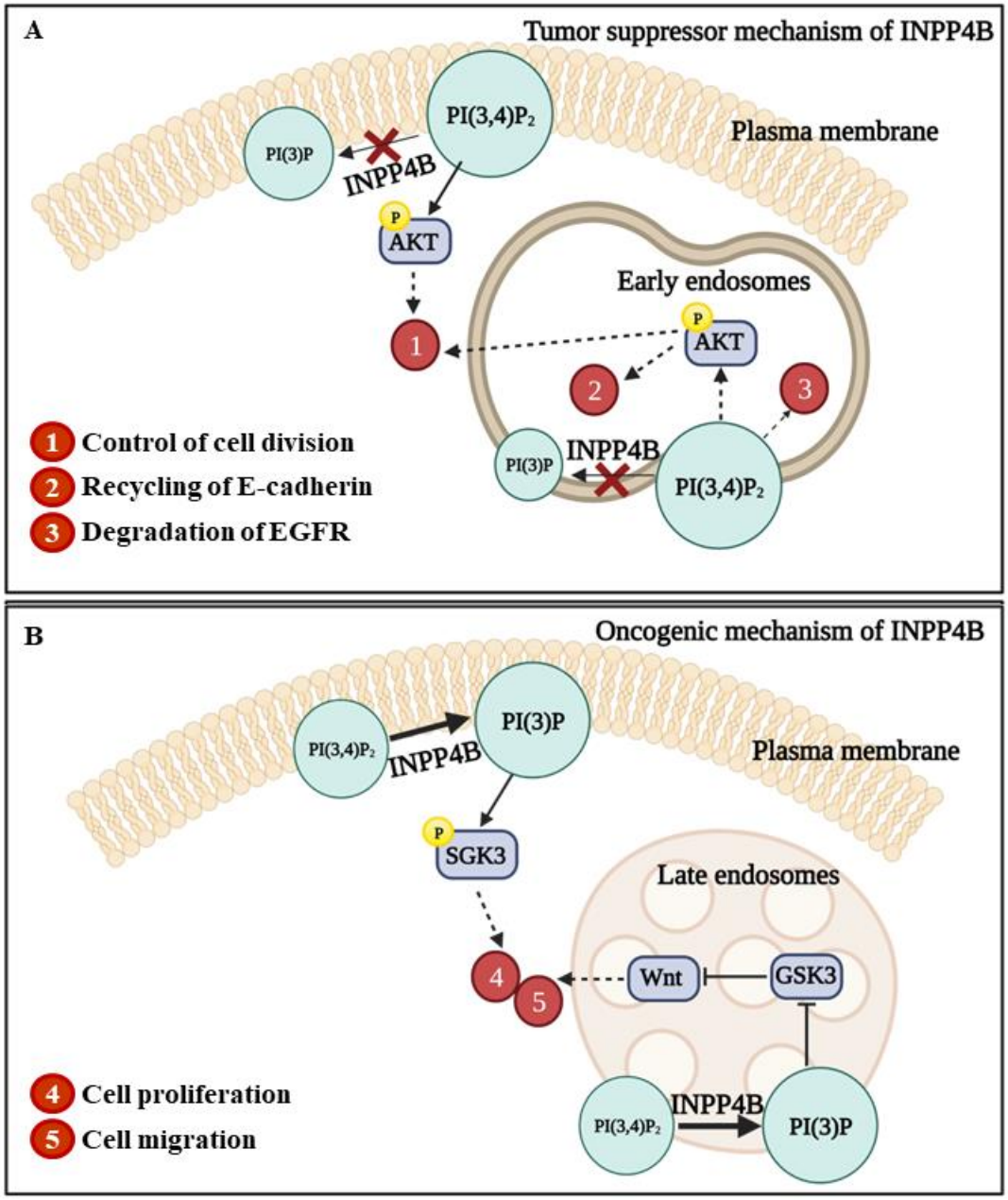


**Figure 1.3.** Molecular mechanisms of INPP4B mediated (A) tumor suppression and (B) oncogenesis in cancer.
A) Tumor suppressor activities of INPP4B. In the plasma membrane, enzymatic activity of INPP4B inhibits AKT A) INPP4B dephosphorylates PI(3,4,5)P3 and PI(3,4)P2 lipids that activate AKT stimulating cellular survival and proliferation (1). $PI(3,4)P_2$ localized to early endosomes is dephosphorylated by INPP4B (1). PI(3)P production stimulates endosome maturation, allowing E-cadherin cycling and EGFR degradation (2-3). B) Overexpression of INPP4B leads to the accumulation of PI(3)P. At the plasma membrane, PI(3)P binds and activates SGK3, stimulating cell proliferation and migration (4-5). At the late endosomes, PI(3)P accumulation results in the activation of Wnt mediated cellular proliferation (4). The thickness of arrows and the size of PIs reflect INPP4B activity in both panels.

As a tumor suppressor, loss of INPP4B suppresses cell proliferation and tumorigenesis by dephosphorylating PI(3,4,5)$P_3$ and PI(3,4)$P_2$, which bind and activate AKT pathway [78, 87, 91]. In ER-positive breast cancers, downregulation of INPP4B leads to the phosphorylation and activation of AKT, triggering G1/S transition and increased cellular proliferation [92]. INPP4B overexpression inhibits proliferation by reducing pAKT levels in TNBC cell line MDA-MD-231 [93]. In pancreatic and thyroid cancers, INPP4B produces PI(3) from PI(3,4)$P_2$ in early endosomal membranes, stimulating the disposal of cadherin as well as reducing endosomal AKT2 activity [85, 88]. Using the same mechanism in breast cancer, INPP4B promotes the sorting of EGFR from early to late endosomes, leading to EGFR degradation and preventing tumor initiation [87].

Oncogenic activities of INPP4B include stimulation of the DNA repair [94, 95], inactivating dephosphorylation of PTEN [19], and activation of SGK3 pathway [96-98]. Overexpression of INPP4B leads to increased dephosphorylation of PI(3,4)$P_2$ and produces PI(3)P, which binds to and activates SGK3. In turn, activated SGK3 triggers the proteolytic degradation of tumor suppressor NRDG1, promoting cell proliferation and migration [96]. In ERα positive breast cancer cell lines MCF-7 and T47D, PI(3)P production by INPP4B induces late endosome formation and enhances Wnt/β-catenin dependent cell proliferation and tumor growth [99].

### 1.4. INPP4B regulated pathways in metabolic health

While activation of AKT due to INPP4B loss has been described in different cancers by independent investigators [17, 86, 87, 89, 91], pathways inhibited by INPP4B, such as PI3K/AKT, PKC, and mTOR, are key regulators of metabolic homeostasis in both mice and men.

### 1.4.1. Body weight is a balance between appetite, energy expenditure, and gender

Body weight is one of the main indicators of metabolic health and is maintained, in part, by the hypothalamus through two main mechanisms [100]. The first one is the regulation of food intake via feeling of satiety and suppression of appetite. The second one is the regulation of energy expenditure [100]. There are differences in fat storage and energy expenditure in men and women due to the hormonal levels, such as adipokine leptin levels and the effect of estrogen on hepatic lipid metabolism [101]. Consistent with the physiological differences, the prevalence and severity of obesity is two times higher in women compared to men [102]. In addition to the genetic and physiological factors, consumption of foods with high calorie content and a sedentary lifestyle cause a drastic increase in the rates of obesity in the last few decades. In the US, more than one- third of the adult population is obese [103].

### 1.4.2. Obesity and gender affect the predisposition to metabolic diseases

Obesity is one of the most modifiable risk factors for various metabolic diseases including type II diabetes (T2D) and non-alcoholic fatty liver disease (NAFLD) [104, 105]. The prevalence of T2D and NAFLD are rising in parallel with obesity. Over 80% of diabetic patients are obese and hepatic steatosis score increases from 3% to 40% in severely obese patients compared to non-obese individuals [106, 107]. The main consequences of obesity are insulin resistance, increased inflammation, and disrupted lipid metabolism [108]. Lipid substrates and products of INPP4B enzymatic activity modulate signaling pathways that regulate obesity and metabolic homeostasis. These pathways are described in greater detail in the sections 1.3.3-1.3.5. Similar to obesity, metabolic dysfunction is sexually dimorphic. Unlike in obesity, men are under higher risk of developing T2D and NAFLD than women

[109, 110]. Currently, the molecular pathways that protect women and lean people from NAFLD and T2D are poorly characterized.

### 1.4.3. Dysregulation of central leptin and insulin signaling pathways leads to obesity

Hypothalamic leptin signaling is the master regulator of weight control. Leptin is an adipokine that is produced and secreted by adipocytes, and its circulating levels are proportionate to the volume of adipose tissue [111]. Central and peripheral actions of leptin are mediated by leptin receptor (LEPR) [112]. Activation of LEPR in hypothalamus increases energy expenditure and reduces food intake opposing weight gain [112]. In obese patients, expansion of the adipose tissue leads to an increase in leptin levels and results in leptin resistance [113]. People with mutations in leptin or LEPR and mice with whole body knockout of leptin or *Lepr*, *ob/ob* and *db/db*, respectively, exhibit severe obesity [114-116]. Hypothalamus- specific knockout of *Lepr* leads to severe obesity similar to *ob/ob* and *db/db* mice, underlining the importance of hypothalamic leptin signaling in weight control [117]. In addition to leptin, hypothalamic insulin signaling contributes to weight control by reducing food intake [118]. The knockout of insulin receptor in the central nervous system causes weight gain and higher serum leptin levels in both genders but significantly increases food intake only in female mice [119]. The crosstalk between leptin and insulin signaling is important for the metabolic homeostasis, as resistance in one pathway promotes the resistance of the other [120].

### 1.4.4. Insulin and metabolic fibroblast growth factors modulate blood glucose levels and lipid metabolism

Insulin is a postprandial hormone, which is secreted from pancreatic β-cells in response to high blood glucose levels and regulates glucose and lipid metabolism [121]. The liver is the main target of insulin, where it inhibits gluconeogenesis and glycogenolysis and promotes glycolysis, glycogenesis, and *de novo* lipogenesis [121]. In one of essential target peripheral tissues, white adipose tissue (WAT), insulin promotes glucose uptake and inhibits lipolysis [121]. As mentioned before, the hypothalamus is another target of insulin. Hypothalamic insulin signaling reduces hepatic glucose production (HGP) by suppressing the expression of gluconeogenesis enzymes to control blood glucose levels [122].

Metabolic fibroblast growth factors (FGFs), FGF1 and FGF21, are additional components of the metabolic homeostasis, which signal through hypothalamic fibroblast growth factor receptor1 (FGFR1) to maintain normal blood glucose levels. The knockout mouse models of both FGF1 and FGF21 develop metabolic abnormalities including hyperglycemia and fatty liver when fed high fat or ketogenic diets [123, 124]. Both intraperitoneal (IP) and intracerebroventricular (ICV) injections of FGF1 and FGF21 restore insulin sensitivity and result in sustained reduction of blood glucose levels in obese or diabetic mice [125-128]. In addition, IP injection of FGF1 in *ob/ob* mice reduces lipolysis and HGP through insulin-independent pathways in WAT [129].

### 1.4.5. The INPP4B-associated molecular signaling pathways that are impaired in obesity and MetS

Impaired insulin signaling is at the center of metabolic diseases [130]. The main insulin signaling cascade in metabolism is mediated by IR/PI3K/AKT pathway [131]. The binding

of insulin to the insulin receptor triggers the phosphorylation and activation of docking protein insulin receptor substrate 1/2 (IRS1/2) [132]. Phosphorylated IRS2 leads to the activation of catalytic p110 subunit of PI3K and the generation of $PI(3,4,5)P_3$ from $PI(4,5)P_2$ [132]. As described previously, $PI(3,4,5)P_3$ activates the downstream AKT pathway. Some of the substrates downstream of AKT are FOXO1, glycogen synthase kinase-3-beta (GSK3β), mTOR, and AKT substrate of 160 kDa (AS160) [130]. PKC pathway is another component of insulin signaling that is regulated by INPP4B-substrate $PI(4,5)P_2$. Hydrolysis of $PI(4,5)P_2$ generates DAG and activates multiple PKC isoforms. IR/PI3K/AKT and IR/PKC pathways in liver, WAT, and hypothalamus maintain metabolic homeostasis and are dysregulated in metabolic diseases (Figure 1.4-1.5).

In the liver, activation of the PI3K/AKT pathway inhibits expression of gluconeogenesis associated enzymes and promotes glycogenesis by the phosphorylation and nuclear export of the transcription factors FOXO1 and GSK3β [133, 134]. Activation of AKT and PKC signaling promotes hepatic *de novo* lipogenesis by increasing proteolytic cleavage and nuclear translocation of the transcription factor Sterol regulatory binding protein 1 (SREBP1), which activates transcription of lipogenic enzymes and lipid transporters [135-137]. In the insulin-resistant patients, hyperactivation of PI3K/AKT pathway fails to inactivate FOXO1 and GSK3β, causing hyperglycemia. In addition to hyperglycemia, these patients have high levels of circulating free fatty acids due to the increased lipolysis, further activating multiple PKC isoforms [138]. The accumulating data shows that PKCσ, PKCθ, and PKCε are among the isoforms which contribute to hepatic insulin resistance. In particular, PKCε inhibits insulin receptor tyrosine kinase activity [139], and PKCθ

phosphorylates the Ser1101 residues on IRS1 to prevent its activation via the insulin receptor [140].

In the WAT, AS160 phosphorylation via PI3K/ AKT and PKC pathways contributes to the translocation of GLUT4 to the plasma membrane to induce glucose uptake [141-143]. Similar to liver, PKCε regulates insulin signaling in the WAT. Deletion of PKCε in WAT ameliorates glucose tolerance by modulating hepatic gene expression and lipid metabolism [144].

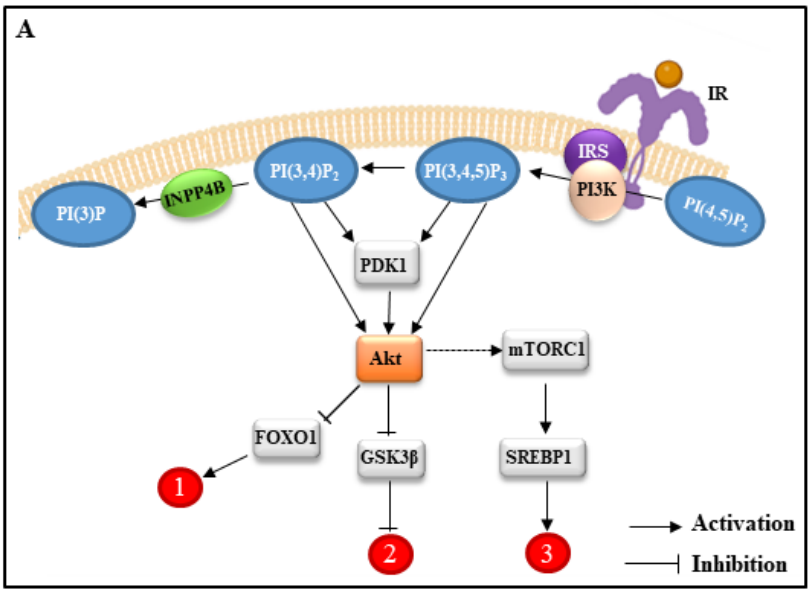


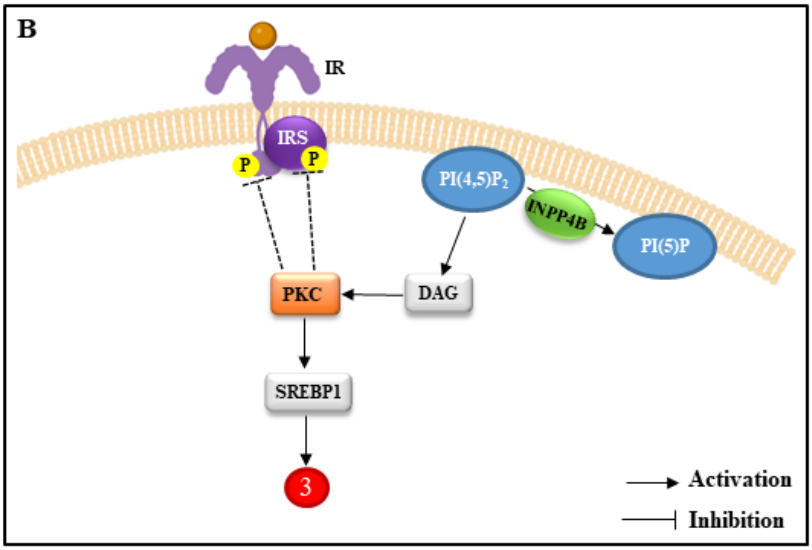


| C | Normal conditions | Insulin resistance |
|---|---|---|
| 1 Gluconeogenesis | ↓ | ↑ |
| 2 Glycogen synthesis | ↑ | ↓ |
| 3 *De novo* lipogenesis | ↑ | ↑↑ |

**Figure 1.4**. An overview of PI3K/AKT and PKC pathways in the liver.
(A) IR/PI3K/AKT pathway in the liver. Binding of insulin to the insulin receptor (IR) activates PI3K, which produces $PI(3,4,5)P_3$, and activates AKT pathway. Under normal conditions, activation of AKT inhibits hepatic gluconeogenesis (1), promotes glycogen synthesis (2) and de novo lipogenesis (3). (B) Activation of PKC promotes lipogenesis (3). Aberrant activation of various PKC isoforms inhibits IR by the phosphorylation of threonine residues on IR and serine residues on insulin receptor substrate (IRS). (C) Modulation of the three physiological events due to the activation of AKT and PKC pathways under normal conditions and in insulin resistance.

In the hypothalamus, insulin shares common downstream pathways with leptin signaling (Figure 1.5). The canonical leptin signaling includes activation of the Jak2/Stat3 pathway by LEPR, which induces the transcription of anorexigenic neuropeptide pro-opiomelanocortin (POMC) and reduces orexigenic neuropeptide Y/ Agouti-related protein (NPY/AgRP) expression to suppress appetite [145]. Both leptin and insulin receptors activate IR/PI3K/AKT signaling cascade [118]. IR mediated activation of AKT leads to hyperphosphorylation and subsequent degradation of FOXO1, which downregulates the expression of FOXO1 target genes NPY/AgRP and results in a reduction in food intake [146]. Deletion of IRS1 in the nestin- expressing neurons interferes with hypothalamic insulin signaling in mice and leads to obesity, hyperglycemia, and insulin resistance in a FOXO1- dependent manner [147].

Thus, aberrant activation of AKT and PKC pathways in liver, WAT, and hypothalamus leads to insulin resistance, which may progress to T2D and NAFLD [148-150].

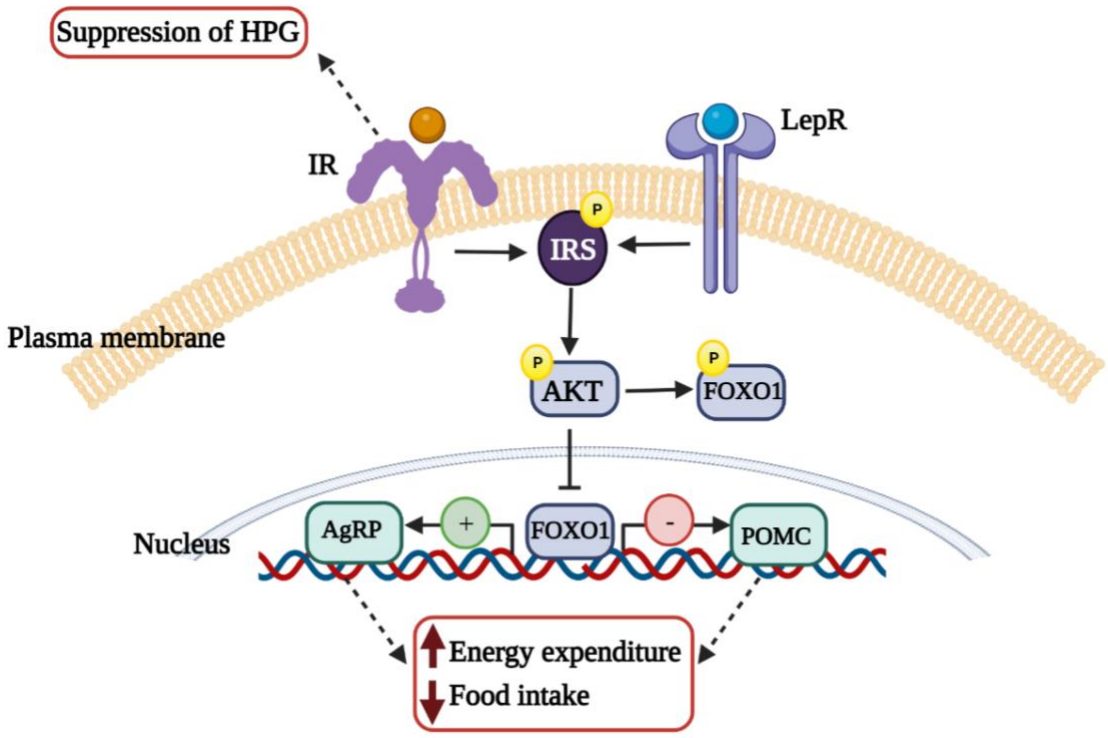


**Figure 1.5.** AKT signaling in hypothalamus
The activation of AKT pathway by insulin receptor (IR) and leptin receptor (LepR) is demonstrated. Hypothalamic insulin signaling maintains blood glucose levels by suppressing hepatic glucose production (HPG). AKT downstream FOXO1 induces anorexigenic POMC transcription and inhibits orexigenic AgRP expression, which lead to weight gain by increasing food intake and suppressing energy expenditure. AKT activation causes phosphorylation and nuclear export of FOXO1, contributing to weight control.

### 1.4.6. Role of INPP4B in Metabolic Homeostasis

Due to the role of INPP4B in the modulation of AKT and PKC pathways, our lab has investigated the function of INPP4B in metabolic health [20]. We showed that three-month-old *Inpp4b*$^{-/-}$ males fed low fat diet (LFD) developed hyperglycemia and exhibited ectopic accumulation of fat in liver. When fed high-fat diet (HFD), *Inpp4b*$^{-/-}$ males developed obesity, NAFLD, T2D, inflammation of visceral WAT, and prostate hyperplasia. The obesity in HFD *Inpp4b*$^{-/-}$ males was caused by the decreased ambulatory activity, respiratory exchange, and energy expenditure and activated lipogenesis. The differentially expressed genes from RNA-sequencing analysis of liver samples of WT and

*Inpp4b*$^{-/-}$ males on HFD showed that *Inpp4b* loss altered lipid and glucose metabolisms, drug detoxification, peroxisome biogenesis, and expression of T2D associated genes. In the liver, loss of INPP4B elevated phosphorylation of AKT, PKCζ and PKCβ, as well as the expression and proteolytic activation of SREBP1, which were exacerbated with HFD. In addition, regulation of SREBP1 signaling by feeding and fasting was abolished in *Inpp4b*$^{-/-}$ males. Furthermore, serum levels of metabolic adipokines and hormones such as leptin, insulin, C-peptide, and resistin were significantly higher in HFD *Inpp4b*$^{-/-}$ males compared to the HFD WT or LFD *Inpp4b*$^{-/-}$ mice. The analysis of patient datasets was aligned with the metabolic changes in *Inpp4b*-deficient mice. Hepatic *INPP4B* expression in patients with T2D and NAFLD was significantly reduced compared to healthy controls. Moreover, there was significant inverse correlation between steatosis score in NAFLD patients and *INPP4B* mRNA levels [20].

### 1.5. INPP4B- regulated signaling pathways in male fertility

PI3K/AKT and PLC/PKC pathways, inhibited by INPP4B, play significant roles in sperm production and testicular testosterone synthesis. At different stages of spermatogenesis, several factors activate PI3K/AKT pathway. Glial cell line-derived neurotrophic factor (GDNF) promotes proliferation and self-renewal of spermatogonial stem cells (SSCs) [151] and degradation of FOXO1 by increasing PI3K/AKT activity, which leads to the differentiation of SSCs into spermatogonia [152]. In spermatogonia, stem cell factor (SCF)/ c-kit activates PI3K/AKT/ p70S6K signaling cascade and drives cell proliferation by increasing cyclin D3 expression [153]. Conversely, inactivation of PI3K subunit p110β impairs c-kit- dependent AKT activation and halts spermatogenesis in both pre-meiotic and post-meiotic stages [154]. In Leydig cells, Kit ligand KitL promotes production of

luteinizing hormone by activating PI3K/AKT signaling to maintain steroidogenesis [155]. In the Sertoli cells, insulin and insulin growth factor (IGF-1) activate PI3K/AKT pathway to stimulate glucose and amino acid transport [156]. Concomitant knockout of insulin and IGF receptors in Sertoli cells leads to 75% reduction in testis size [157]. Follicle stimulating hormone (FSH) activates expression of the steroidogenic enzyme, aromatase, which is required for postnatal development of Sertoli cells by activating PI3K/AKT pathway [158]. PKC pathway plays important roles in spermiogenesis and fertilization. In Sertoli cells, testosterone regulates $K^{+}_{ATP}$ channels by activating GPCR-PLC-PI(4,5)$P_2$ axis to re-structure cell junctions between Sertoli and germ cells that support spermatogenesis [159]. In the sperm tail, PKC increases sperm motility by activating ERK1/2 and inhibiting p38 MAPK [160]. During capacitation, sperm specific PLCζ, hydrolyzes PI(4,5)$P_2$ to I(1,4,5)$P_3$ to activate $Ca^{2+}$ channels and facilitate fertilization [161].

Reproductive health in men is strongly affected by obesity, which leads to overactivation of AKT and PKC signaling pathways in multiple tissues. In parallel with increase of obesity in men, the average sperm count has declined more than 50% in the last 60 years, which is an alarming signal for male infertility [162]. Men suffering from obesity have impaired spermatogenesis due to decreased testosterone levels and poor semen quality. Keszthelyi et al. showed that obese men exhibit significantly lower sperm concentration and total sperm count compared to men of normal weight [163].

Thus, INPP4B-substrates and downstream signaling play essential roles in testicular homeostasis, which can be disrupted by obesity-associated signaling. However, exact mechanisms that link obesity and male sub-fertility and the role of INPP4B in these processes are not known.

## 1.6. Overview

Obesity is a major public health concern that is strongly correlated with various endocrine disorders such as metabolic diseases, subfertility, and cancer. PI products and substrates of INPP4B enzymatic activity directly regulate PI3K/AKT and PKC pathways, common signaling molecules in obesity, metabolic syndrome, infertility, and cancer [5, 8, 10, 161, 164, 165]. Thus, the focus of this dissertation was to determine the role of INPP4B in the physiological homeostasis of metabolism and reproductive organs along with rapid cancer progression. The role of INPP4B in metabolic regulation is covered in Chapter Two, in mammary gland development and carcinogenesis in Chapter Three, and in male reproductive physiology in Chapters Four and Five.

In Chapter Two, I report my findings on the regulation of metabolic homeostasis by INPP4B in female mice and the role of INPP4B in the metabolic response to HFD. In a normal diet, *Inpp4b*$^{-/-}$ females developed fatty liver without changes in body weight or blood glucose levels. Placing female *Inpp4b*$^{-/-}$ mice on HFD led to obesity, NAFLD, hyperglycemia and inflammation of visceral adipose tissue. Opposite to WT females, *Inpp4b*$^{-/-}$ females failed to show compensatory increase in lipid catabolism in response to HFD, leading to obesity. In HFD *Inpp4b*$^{-/-}$ females, obesity resulted in increased levels of circulating leptin. However, reduced hypothalamic leptin receptor expression in this group suggests leptin resistance and contributes to obesity. Concomitantly, metabolic tolerance tests revealed that HFD *Inpp4b*$^{-/-}$ mice have increased rates of gluconeogenesis and insulin resistance, resulting in increased levels of blood glucose. Impaired hypothalamic FGF1 signaling in knockout females further contributed to the elevated levels of circulating glucose. Phosphorylation of AKT and the processing of transcription factor for lipogenic

enzymes, SREBP1 were significantly higher in the livers of HFD *Inpp4b*$^{-/-}$ group compared to all other groups. Comparison of RNA-sequencing of hepatic RNAs in HFD WT and HFD *Inpp4b*$^{-/-}$ female groups showed upregulation of lipid metabolism pathways in livers of knockout females. Metabolomics analysis of serum samples was in alignment with upregulated hepatic lipid metabolism in HFD *Inpp4b*$^{-/-}$ females. Consistent with humans and other mouse models with metabolic syndrome, *Inpp4b*$^{-/-}$ females have better glucose metabolism compared to *Inpp4b*$^{-/-}$ males in either diet, and HFD *Inpp4b*$^{-/-}$ females are more obese than HFD *Inpp4b*$^{-/-}$ males. When on an HFD, hypothalamic leptin and FGF21-FGFR1 signaling play a role in the sexual dimorphism of metabolism in *Inpp4b*$^{-/-}$ males and females. Hypothalamic leptin resistance in HFD *Inpp4b*$^{-/-}$ females contributed to their increased weight gain compared to males. In addition, HFD *Inpp4b*$^{-/-}$ males showed reduction in both FGF21 and FGF1 hypothalamic signaling, while FGF21 signaling was still active in knockout females, resulting in better management of circulating glucose. Thus, *Inpp4b* deletion leads to stronger changes in the hypothalamus of male mice, resulting in higher blood glucose levels and more severe insulin resistance.

In Chapter Three, I report my findings on the role of INPP4B in normal mammary gland physiology and *ERBB2*-driven mammary gland tumorigenesis. Preliminary data from our lab demonstrated that INPP4B deletion significantly reduces PR levels *in vitro* and delays mammary gland branching *in vivo* [166]. Quantification of whole mount staining of mammary glands revealed that INPP4B loss reduces the number of mammary gland side branches. I found that pAKT and p53 protein levels were higher in mammary glands of LFD *Inpp4b*$^{-/-}$ and HFD *Inpp4b*$^{-/-}$ females compared to their corresponding WT groups. Leptin levels were significantly higher and adiponectin levels were decreased in the

mammary glands of HFD *Inpp4b*$^{-/-}$ females, along with increased inflammation. *Inpp4b* deletion accelerated *MMTV-ERBB2* driven tumor progression and increased tumorigenic effect of the HFD. I found that reduction in p53 and p21 protein levels as well as increase in inflammation contributed to increased progression of mammary tumorigenesis in HFD *Inpp4b*$^{-/-}$ females.

In Chapter Four, I discuss my analysis on the expression patterns and potential roles of INPP4B and other PI-phosphatases in human and mouse testes using publicly available datasets with various types of testicular cells, infertile patients, and mouse testes at different postnatal stages. While the mouse models for the knockout of the PI-3 phosphatases are present, we observed main expression of PI-3 phosphatases in germ cells. Similarly, PI-4 phosphatases including INPP4B also showed higher expression in the germ cells. On the other hand, the expression of PI-5 phosphatases was observed in both somatic and germ cells. In addition, some of these phosphatases are also involved in metabolic homeostasis and may impact fertility indirectly through metabolic syndrome-associated mechanisms.

In Chapter Five, I describe the role of INPP4B in testicular function. In both human and mouse testes, the expression of INPP4B was detected in the post-meiotic germ cells and partially in somatic Leydig and Sertoli cells. *Inpp4b*$^{-/-}$ mice exhibited smaller testes and fewer sperm count, which were exacerbated with HFD feeding. Consistent with smaller testes and reduced sperm count, *Inpp4b*$^{-/-}$ males had an increase in apoptosis rate. In addition, HFD *Inpp4b*$^{-/-}$ mice showed a significant reduction in meiosis and in the expression of early steroidogenic enzymes. My findings suggest that INPP4B has an important role in spermatogenesis, while diet and metabolism also contribute to INPP4B function in testis.

In conclusion, my data demonstrates that INPP4B is involved in the metabolic health of female mice under obesogenic conditions, modulates mammary gland development and ERBB2- driven tumorigenesis, and contributes to testicular homeostasis.

# 2. CHAPTER 2: INPP4B is protective against obesity and metabolic syndrome in female mice under obesogenic conditions

## 2.1. Abstract

Metabolic diseases are more prevalent in men; however, the signaling pathways which lead to this disparity between men and women are poorly characterized. Inositol polyphosphate-4- phosphatase type II B (INPP4B) is an emerging metabolic regulator. We reported that INPP4B protects male mice from diet-induced obesity, type II diabetes (T2D), and non-alcoholic fatty liver disease (NAFLD). In this study, we investigated the consequences of INPP4B loss on metabolic homeostasis in females. We find that *Inpp4b*$^{-/-}$ female mice display both common and gender-specific metabolic changes. Similar to males, *Inpp4b*$^{-/-}$ females develop diet-induced obesity, inflammation of visceral adipose tissue, and NAFLD. Unlike males, *Inpp4b*$^{-/-}$ females do not develop T2D and display only mild hyperglycemia when fed a high fat diet.

## 2.2. Introduction

The prevalence of obesity and metabolic syndrome (MetS) is increasing worldwide at an alarming rate; currently, 35% of the adult population in the US suffer from MetS [167]. It is a sexually dimorphic disorder characterized by central obesity, impaired glucose metabolism, type 2 diabetes (T2D), high triglyceride levels, chronic inflammation, and non-alcoholic fatty liver disease (NAFLD) [104, 105]. While women exhibit a higher prevalence of obesity, men are more likely to develop T2D and NAFLD [102, 110, 168]. Majority of the metabolic studies are conducted in male mice; thus the female metabolism remains under-studied.

Insulin resistance is the major reason for MetS and is observed in a substantial portion of obese individuals [169]. Immediate downstream targets of activated insulin receptor (IR) are PI3K/AKT and PKC pathways. The dysregulation of IR/PI3K/AKT pathway in the liver, central nervous system, and adipose tissue result in insulin resistance, leading to higher blood glucose levels, dysregulation of lipid metabolism, and reducing energy expenditure [122, 170-172]. Increased levels of plasma free fatty acids due to obesity activate PKC pathway which phosphorylates IR on Thr1160 and IRS on Ser1101 residues and inhibits it further reducing insulin sensitivity [139, 140, 173].

In addition to AKT and PKC pathways, adipokine leptin, leptin receptor (LEPR), metabolic fibroblast growth factors (FGF), FGF1 and FGF21, and their cognate receptor FGFR1 are hypothalamic regulators of metabolic homeostasis. Loss of function mutations of leptin or leptin receptor result in severe obesity and other endocrine abnormalities in both mice and men [115, 116, 174, 175]. Importantly, conditional knockout of *Lepr* in mouse hypothalamus causes extreme obesity [176], and hypothalamus specific transgenic overexpression of *Lepr* corrects obesity, diabetes, and insulin resistance in *db/db* mice [177]. In humans, FGF21 serum levels are positively correlated with body mass index (BMI), fasting glucose levels, and plasma triglyceride levels [178, 179]. Treatment with FGF21 analogs and FGFR1 receptor agonist lead to weight loss and reduction of plasma triglycerides [180]. In diabetic and diet-induced obese mice, while peripheral administration of FGF21 reduces body weight and improves insulin sensitivity, single intracerebroventricular injection of FGF1 leads to a sustained decrease in blood glucose levels [125, 128]. However, the downstream pathways of FGFs are still being investigated.

Inositol polyphosphate-4-phosphatase type II B (INPP4B) is a phosphatidylinositol phosphatase that was shown to inhibit AKT and PKC pathways by dephosphorylating their activating lipids $PI(3,4)P_2$, $PI(3,4,5)P_3$, and $PI(4,5)P_2$ [20, 90, 181, 182]. We have previously described that INPP4B is a metabolic regulator in male mice [20]. *Inpp4b*$^{-/-}$ males display characteristics of metabolic dysfunction even on a low fat diet (LFD): hyperglycemia, insulin resistance, and fatty liver. The symptoms in the knockout males escalate when they are fed a high fat diet (HFD): severe NAFLD, T2D, and obesity [20].

In this study, we showed that *Inpp4b*$^{-/-}$ females fed LFD develop mild fatty liver phenotype without increasing their body weight and decreasing insulin sensitivity. When fed HFD, weight gain in *Inpp4b*$^{-/-}$ females significantly exceeds that of males. Similar to HFD knockout males, HFD *Inpp4b*$^{-/-}$ females develop NAFLD and white adipose tissue (WAT) inflammation. In HFD *Inpp4b*$^{-/-}$ females, higher production and secretion of leptin from WAT and lower levels of *Lepr* in hypothalamus cause leptin resistance, resulting in obesity, with subsequent inflammation of the adipose tissue. While leptin levels are high in both genders of HFD *Inpp4b*$^{-/-}$ groups, hypothalamic *Lepr* levels are lower only in HFD *Inpp4b*$^{-/-}$ females, which contributes to higher weight gain in females. In addition, lower mRNA levels of peroxisome proliferator activated receptor alpha (*Ppara*) and its co-activators in WAT suggest reduced fat combustion contributing to obesity in HFD *Inpp4b*$^{-/-}$ females. Higher AKT phosphorylation in the livers of HFD *Inpp4b*$^{-/-}$ group indicate overactivation of insulin signaling. Activation of hepatic AKT signaling increases proteolytic processing of a transcription factor sterol regulatory binding protein 1 (SREBP1) which activates expression of lipogenic target genes including PPARG, causing ectopic accumulation of hepatic lipids in HFD *Inpp4b*$^{-/-}$ females. Surprisingly, despite the higher weight gain,

knockout females remain insulin sensitive, and their fasting blood glucose raises only to half that of the fasting HFD *Inpp4b*$^{-/-}$ males. I found that this is due in part to gender specific differences of INPP4B action of hypothalamus. While serum FGF21 levels are equally induced in both males and females, hypothalamic FGF21-FGFR1 signaling is impacted more significantly in HFD *Inpp4b*$^{-/-}$ males compared to HFD *Inpp4b*$^{-/-}$ females, resulting in higher blood glucose levels and more severe insulin resistance in male mice. Hypothalamic *Fgf21* and *Fgfr1* levels, as well as phosphorylation of FGFR1 downstream targets MAPK/ ERK1/2 are significantly downregulated in HFD *Inpp4b*$^{-/-}$ males, while remaining unchanged in *Inpp4b*$^{-/-}$ females. Thus, in females INPP4B is required for hypothalamic leptin response and FGFR1 signaling, which regulate lipid and glucose metabolism.

## 2.3. Results

### 2.3.1. Loss of INPP4B and HFD result in obesity in female mice

*Inpp4b* is widely expressed in the tissues of wild-type (WT) female mice with the highest expression in the hypothalamus (Figure 2.1. A). In WT, the expression of *Inpp4b* in WAT and hypothalamus increased in females fed HFD (Figure 2.1. B).

Our preliminary data showed that loss of INPP4B and HFD synergistically led to a significant weight gain in female mice [166]. The body composition analysis by nuclear magnetic resonance (NMR) confirmed the significant weight gain in the HFD *Inpp4b*$^{-/-}$ group (Figure 2.1. C), which was due to an increase in the body fat content and was accompanied by a reduction in the lean mass (Figure 2.1. D-E).

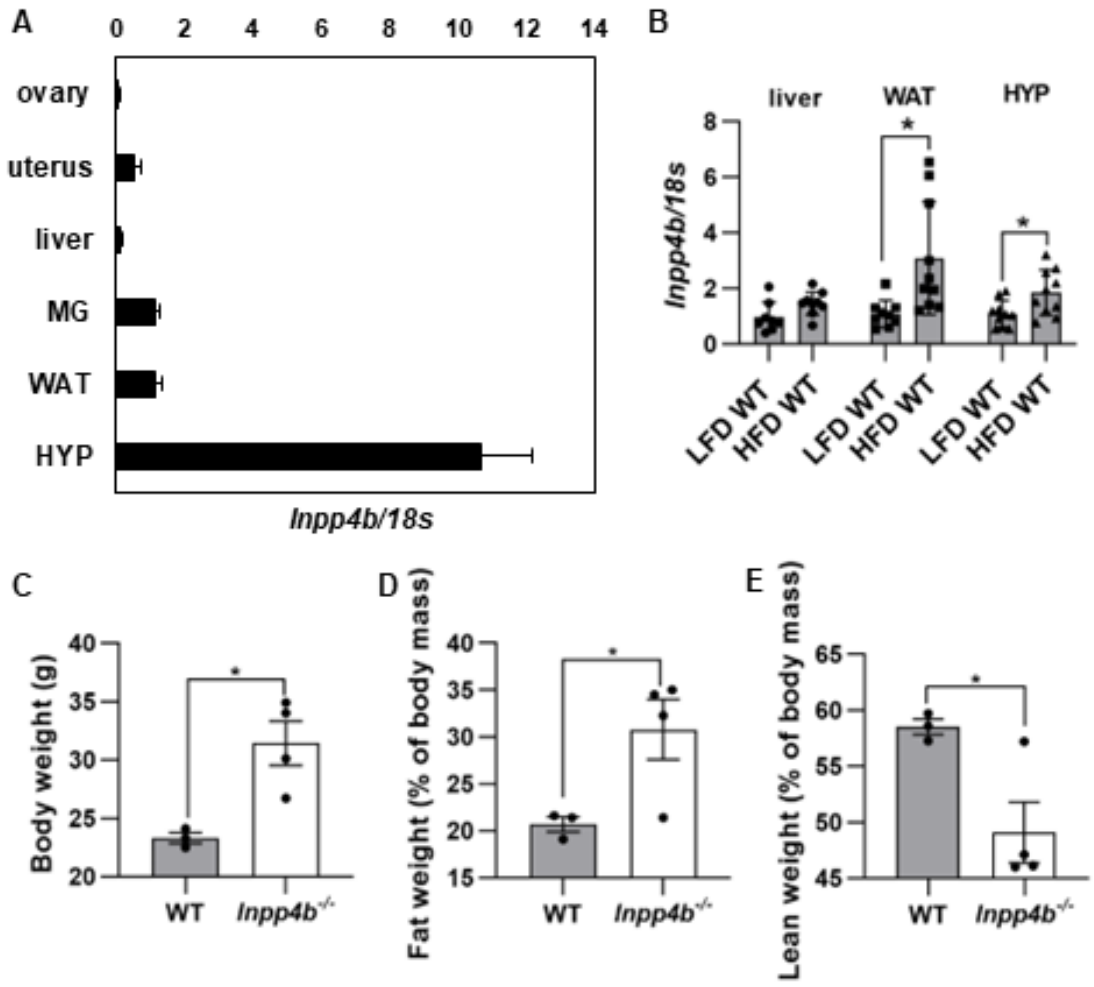


**Figure 2.1.** HFD *Inpp4b*$^{-/-}$ females are obese.
A) Expression of *Inpp4b* in ovary, uterus, liver, mammary gland (MG), white adipose tissue (WAT), and hypothalamus (HYP) of FVB female mice (N>3). B) Expression of *Inpp4b* in the liver, WAT (*p=0.0103), and HYP (*p=0.0207) of FVB female mice on LFD or HFD (N>7). C-E) Body weight and body composition analysis of 6-month-old HFD WT (N=3) and HFD *Inpp4b*$^{-/-}$ (N=4) female mice. (C) Body weights (*p=0.0158), (D) fat mass as percentage of total body mass (*p=0.0462), and (E) lean body mass as a percentage of total body mass (*p=0.0.340) were determined by NMR. Data shown as mean ± SEM. Statistical analysis was performed using two-tail student t-test.

### 2.3.2. WAT in HFD *Inpp4b*$^{-/-}$ female mice undergoes significant metabolic, secretory, and inflammatory changes

To investigate the underlying reasons for fat accumulation in HFD *Inpp4b*$^{-/-}$ females, we evaluated the expression of peroxisome proliferator-activated receptors α and γ (*Ppara and Pparg*), transcription factors that regulate glucose and lipid metabolism [183]. While PPARγ stimulates adipogenesis and promotes insulin sensitivity, PPARα modulates fatty acid oxidation pathways [184]. In WT females, gene expression analysis of WAT revealed significant HFD induced increase in the mRNA levels of *Ppara*, as well as its co-activators *Ppargc1a* and *Ppargc1b*. However, HFD failed to induce this compensatory increase in *Inpp4b*$^{-/-}$ females (Figure 2.2. A-C).

Inflammation of WAT is a common feature in obesity [185]. Consistently, the WAT in the obese HFD *Inpp4b*$^{-/-}$ females was inflamed, expressing elevated levels of pro-inflammatory markers *Tnfa* and *Il1b* (Figure 2.2. D-E), and macrophage infiltration markers CD68 and *Adgre1* (Figure 2.2. F-H).

WAT secretes adipokines that affect satiety, energy expenditure, blood glucose levels, and other metabolic functions [186]. Adipokine signaling is dysregulated in obesity and diabetes [187]. The analysis of adipokine levels in female mice showed significant increase of GLP-1, insulin, leptin, and ghrelin in sera of HFD *Inpp4b*$^{-/-}$ group (Figure 2.2. I).

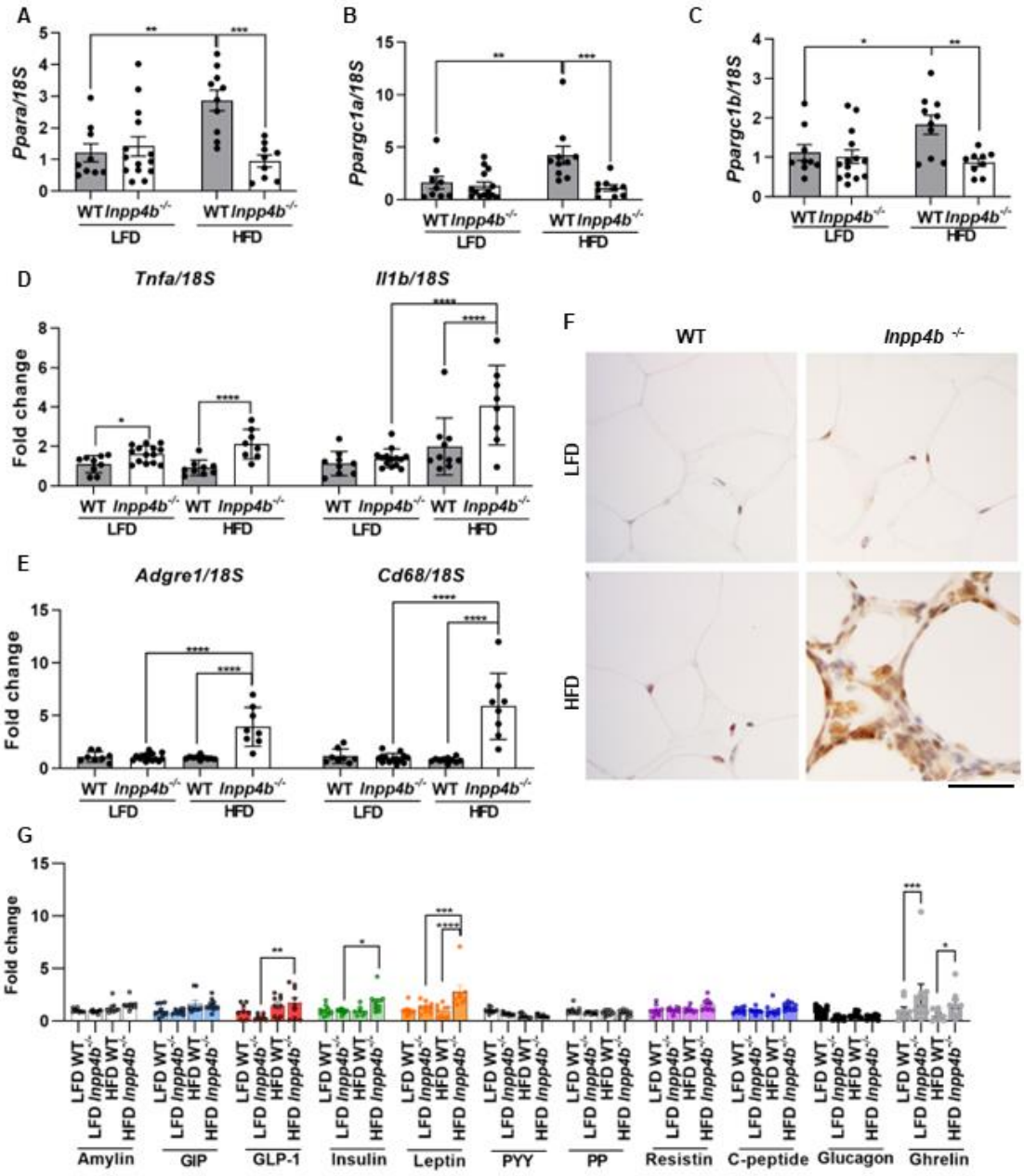


**Figure 2.2.** Adipose tissue homeostasis is disrupted in HFD *Inpp4b*$^{-/-}$ females.
A-E) RNA was extracted from WAT of LFD WT (N=9), LFD *Inpp4b*$^{-/-}$(N=14), HFD WT (N=10), and HFD *Inpp4b*$^{-/-}$ (N=9) female mice. The gene expression levels of (A) *Ppara* (**p=0.0028, ***p=0.0005), (B) *Ppargc1a* (**p=0.0056, ***p=0.0010 ), (C) *Ppargc1b* (*p=0.0132, **p=0.0076), (D) *Tnf* (*p=0.0414), and *Il1b*, (E) *Adgre1* and *Cd68* were assayed by qRT-PCR using *18S* as an internal control. F) IHC staining for CD68 was represented in the WAT of LFD WT, LFD *Inpp4b*$^{-/-}$, HFD WT, and HFD *Inpp4b*$^{-/-}$ female mice (N=3 per group). The scale represents 50 μm. G) Sera from LFD WT (N=10), LFD *Inpp4b*$^{-/-}$ (N=10), HFD WT (N=9), and HFD *Inpp4b*$^{-/-}$ (N=10) female mice were analyzed for amylin, GIP, GLP-1 (**p=0.0024), insulin (*p= 0.0369), leptin (***p=0.0002), PYY, PP, resistin, C-peptide, glucagon, and ghrelin (***p=0.0002, *p=0.0240) protein levels. ****p<0.0001. Data shown as mean ± SEM. Statistical analysis was performed using two-way ANOVA.

### 2.3.3. HFD *Inpp4b*$^{-/-}$ females develop leptin resistance

Leptin and adiponectin are adipokines that target central nervous system regulating energy expenditure and appetite [112]. Obese and MetS patients have higher leptin and lower adiponectin levels in blood [113]. In the WAT of HFD *Inpp4b*$^{-/-}$ females, leptin mRNA levels were significantly increased, while the adiponectin expression was decreased (Figure 2.3. A-C). Consistent with increased WAT leptin expression, serum leptin protein levels were also elevated in HFD *Inpp4b*$^{-/-}$ females (Figure 2.3. D).

The main target of leptin signaling is the hypothalamus [112]. We observed significant increase in hypothalamic *Lepr* levels in the HFD WT mice, but HFD *Inpp4b*$^{-/-}$ group lacked this increase despite significantly higher levels of circulating leptin (Figure 2.3. E). Lack of compensatory increase in hypothalamic *Lepr* expression in HFD *Inpp4b*$^{-/-}$ females suggests development of leptin resistance.

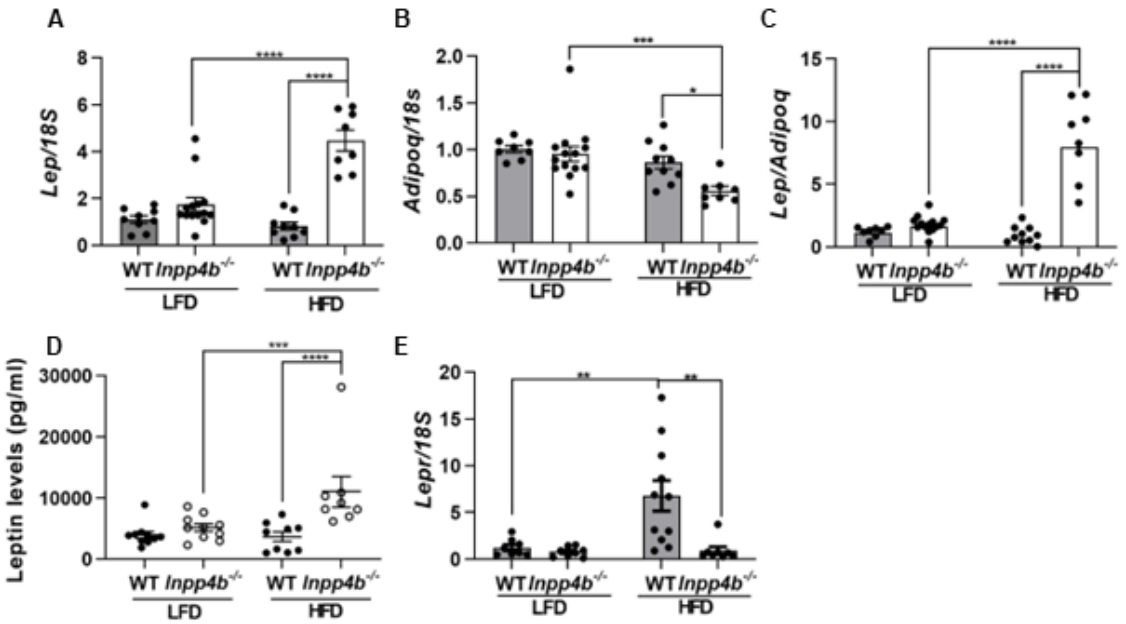


**Figure 2.3.** Leptin signaling is dysregulated in HFD *Inpp4b*$^{-/-}$ females
A-C) The gene expression for (A) *Lep*, and (B) *Adipoq* (***p=0.0007, *p=0.0148), were assayed by qRT-PCR using *18S* as an internal control. (C) *Lep/ Adipoq* ratio from panels 2.3. A-B. D) Serum leptin levels of LFD WT, LFD *Inpp4b*$^{-/-}$, HFD WT, and HFD *Inpp4b*$^{-/-}$ mice from panel 2.2. G. E) RNA was extracted from hypothalami of LFD WT (N=10), LFD *Inpp4b*$^{-/-}$ (N=10), HFD WT (N=11), and HFD *Inpp4b*$^{-/-}$ (N=9) female mice. Gene expression levels of *Lepr* (left to right: **p=0.0038, **p=0.0021) was analyzed by qRT-PCR. ****p<0.0001. Data shown as mean ± SEM. Statistical analysis was performed using two-way ANOVA.

### 2.3.4. INPP4B protects female mice from HFD-induced hyperglycemia

Obesity and inflammation are markers of MetS [188]. To confirm and further characterize metabolic changes in *Inpp4b*$^{-/-}$ females we conducted oral glucose tolerance test (OGTT), insulin tolerance test (ITT), and intraperitoneal pyruvate tolerance test (IPTT) which characterize ability to internalize glucose, respond to insulin injection, and efficiency of gluconeogenesis, respectively. As shown in Figure 2.4, WT females on either diet and LFD *Inpp4b*$^{-/-}$ females efficiently internalized ingested glucose. The HFD *Inpp4b*$^{-/-}$ females were unable to maintain normal levels of glucose and exhibited hyperglycemia (Figure 2.4.A). ITT showed that both HFD and loss of INPP4B function abolish the response to intraperitoneal insulin injections (Figure 2.4. B). IPTT showed that HFD caused a mild

increase in gluconeogenesis in WT females and a significant increase in *Inpp4b*$^{-/-}$ females (Figure 2.4. C). Consistently, HFD *Inpp4b*$^{-/-}$ females had significantly higher blood insulin levels compared to LFD *Inpp4b*$^{-/-}$ and HFD WT groups (Figure 2.4. D). Pancreatic islets for all groups were positive for insulin staining and no change in pancreatic morphology was observed (Figure 2.4. E).

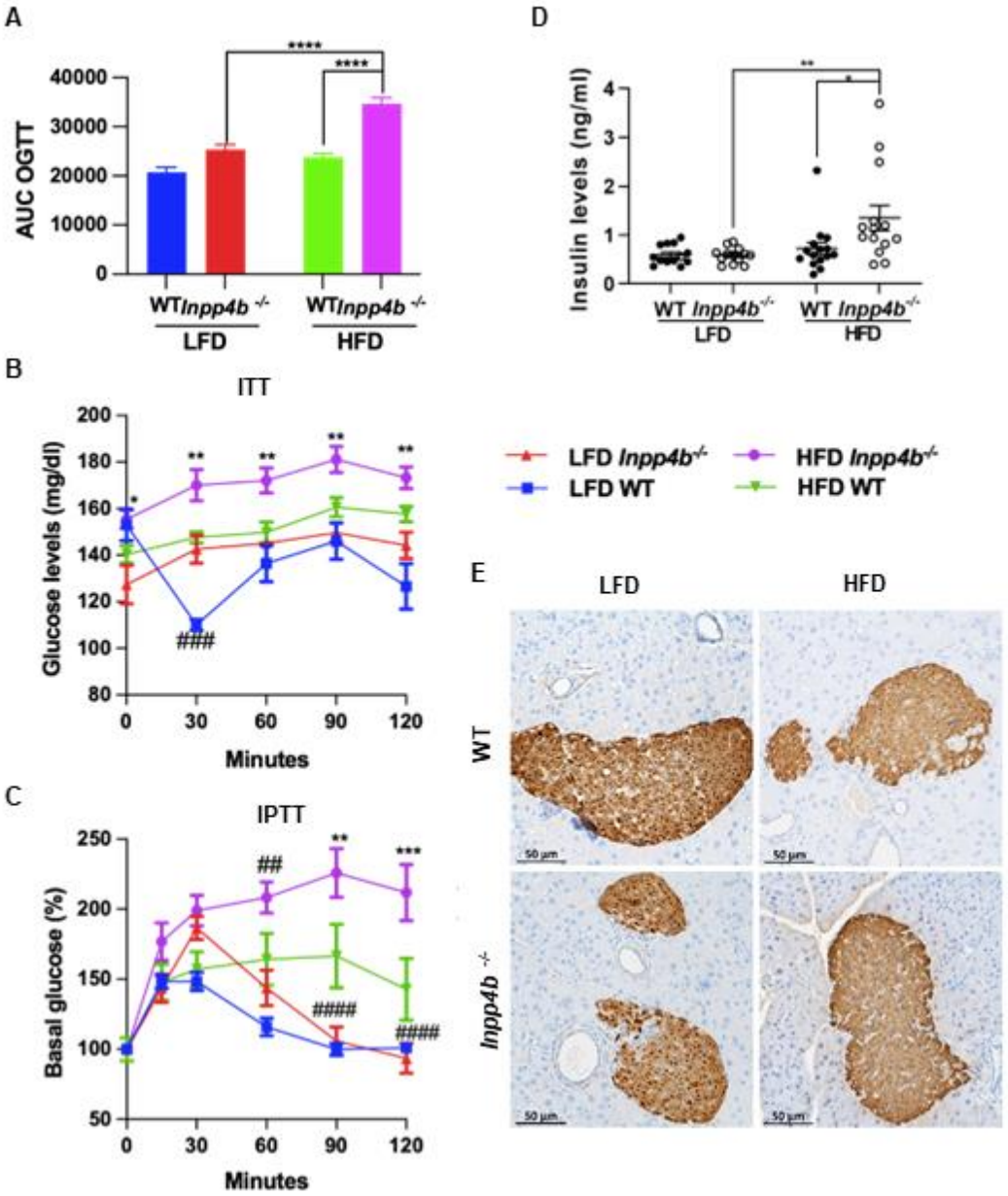


**Figure 2.4.** HFD *Inpp4b*$^{-/-}$ females are glucose intolerant and insulin resistant.
A) Area under curve (AUC) graph for OGTT in LFD WT, LFD *Inpp4b*$^{-/-}$, HFD WT, and HFD *Inpp4b*$^{-/-}$ female mice (****p<0.0001) [166]. B) ITT in LFD WT (N=5), LFD *Inpp4b*$^{-/-}$(N=5), HFD WT (N=11), and HFD *Inpp4b*$^{-/-}$ (N=9) female mice. **#** presents statistically significant differences between LFD groups, and ***** presents statistically significant differences between HFD groups (##p=0.025, *p=0.0273, left to right: **p=0.0040, **p=0.0039, **p=0.0097, **p=0.0022). C) IPTT in LFD WT (N=10), LFD *Inpp4b*$^{-/-}$(N=7), HFD WT (N=11), and HFD *Inpp4b*$^{-/-}$ (N=9) female mice. **#** represents statistically significant differences between *Inpp4b*$^{-/-}$ groups, and ***** presents statistically significant differences between HFD groups (##p=0.0076, $^{\#\#\#\#}$p<0.0001, **p=0.0056, ***p=0.0008) D) Serum insulin levels for LFD WT (N=13), LFD *Inpp4b*$^{-/-}$ (N=13), HFD WT (N=15), and HFD *Inpp4b*$^{-/-}$ (N=14) female mice were measured using ELISA kit (**p=0.0048, *p=0.0220). E) Representative pancreatic sections from LFD WT, LFD *Inpp4b*$^{-/-}$, HFD WT, and HFD *Inpp4b*$^{-/-}$ mice were stained for insulin and counterstained with hematoxylin (N=3 per group). The scale represents 50 µm. Data shown as mean ± SEM. Statistical analysis was performed using two-way ANOVA.

### 2.3.5. *Inpp4b*$^{-/-}$ females develop NAFLD

One of the strongest markers of MetS is ectopic accumulation of lipids in liver, progressing from fatty liver to NAFLD [189]. It is tightly correlated with obesity and insulin resistance [105, 108]. Since HFD *Inpp4b*$^{-/-}$ females are both obese and insulin resistant, we examined the liver morphology in *Inpp4b*- knockout female mice. The oil-red staining of livers revealed abnormally high levels of lipid droplets in livers of *Inpp4b*$^{-/-}$ females and lipid levels were increased with HFD feeding (Figure 2.5 A-B). Moreover, livers in HFD *Inpp4b*$^{-/-}$ group presented with microvesicular and macrovesicular steatosis, hepatocellular hypertrophy, pyknotic nuclei, and Mallory bodies confirming development of NAFLD (Figure 2.5. C). Hepatic mRNA levels of macrophage infiltration markers *Cd68* and *Adgre1* were elevated in the livers of HFD *Inpp4b*$^{-/-}$ mice suggesting inflammation (Figure 2.5. D-E).

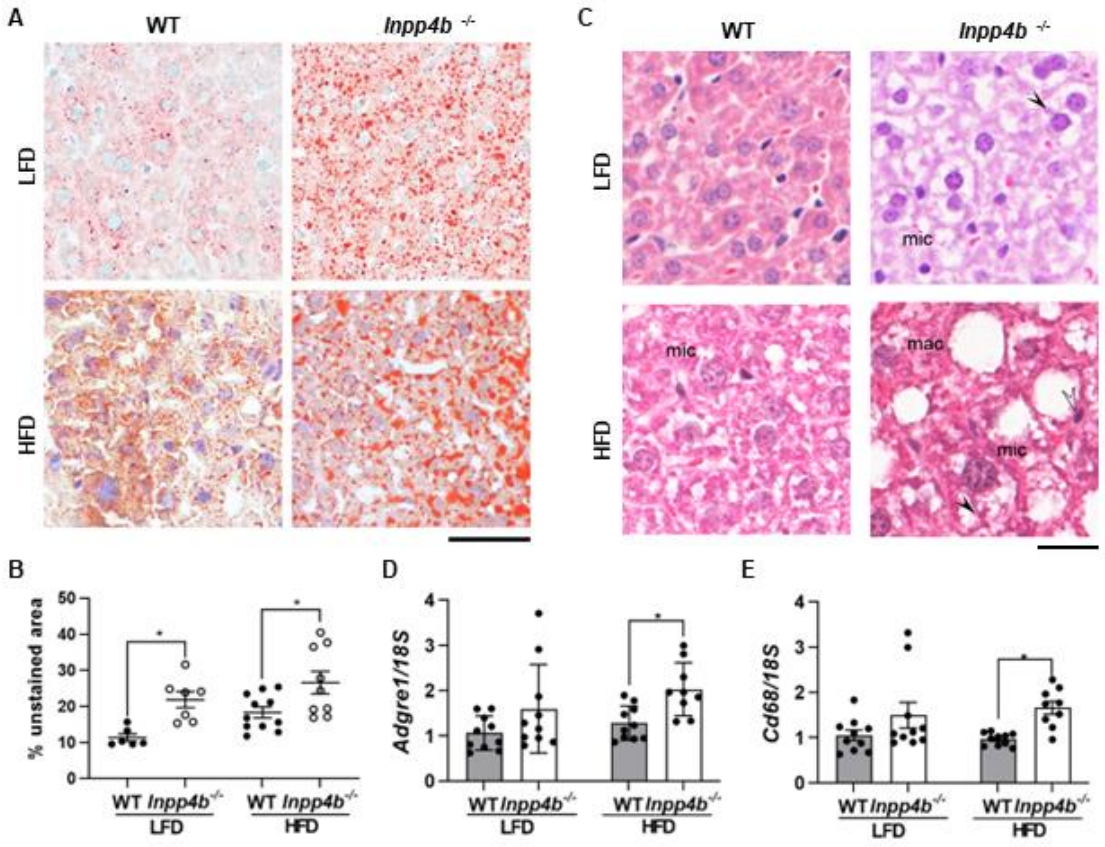


**Figure 2.5.** Loss of *Inpp4b* leads to NAFLD in female mice.
A) Representative Oil-Red staining from frozen liver sections of indicated groups and quantification of hepatic steatosis on the right panel. Scale represents 50 μm. B) Quantification of panel (A) (left to right: *p=0.0307, *p=0.0360). C) Characteristic features of hepatocellular steatosis in livers of LFD and HFD *Inpp4b*$^{-/-}$ females. Examples of microvesicular (mic) and macrovesicular (mac) steatoses, Mallory bodies (closed arrowhead), and pyknotic nuclei (open arrowhead). Scale represents 20 μm. D-E) RNA was extracted from the livers of LFD WT (N=10), LFD *Inpp4b*$^{-/-}$(N=7), HFD WT (N=11), and HFD *Inpp4b*$^{-/-}$ (N=9) female mice. Gene expression levels of macrophage infiltration markers (D) *Adgre1* (*p=0.0279) and (E) *Cd68* (*p=0.0370) were analyzed by qRT- PCR using *18S* as an internal control. Data shown as mean ± SEM. Statistical analysis was performed using two-way ANOVA.

### 2.3.6. INPP4B regulation of hepatic insulin receptor signaling cascade

Consistent with insulin resistance, some hepatic pathways at the downstream of IR were dysregulated in HFD *Inpp4b*$^{-/-}$ females. While the phosphorylation of AKT was significantly increased, phospho- PKC levels were similar in all groups (Figure 2.6. A). Since AKT and PKC pathways promote proteolytic cleavage and activation SREBP1 we

observed increased levels of processed SREBP1 in livers of HFD *Inpp4b*$^{-/-}$ females (Figure 2.6. B).

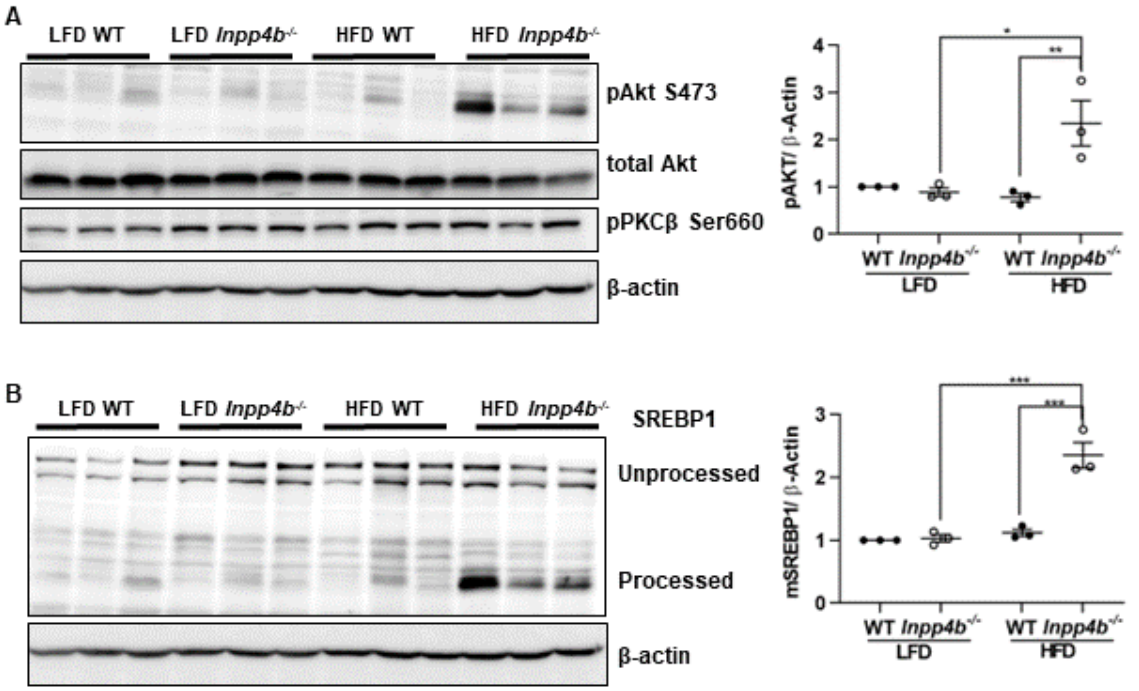


**Figure 2.6.** Insulin signaling and lipid synthesis are upregulated in the livers of HFD *Inpp4b*$^{-/-}$ mice. Protein lysates from female livers (N=3) per group were analyzed and quantified for (A) pAKT S473 (*p=0.0137, **p=0.0090), total AKT, pPKCβ S660, and (B) SREBP1 (left to right: ***p=0.0001, ***p=0.0002), and normalized by β-actin. Data shown as mean ± SEM. Statistical analysis was performed using two-way ANOVA.

To determine transcriptional changes associated with metabolic phenotype of *Inpp4b*$^{-/-}$ females we performed RNA-sequencing analysis of HFD WT and HFD *Inpp4b*$^{-/-}$ female livers (Figure 2.7 A). The pathway analysis of differentially expressed genes (DEG) by GSEA and DAVID showed an upregulation of multiple transcriptional signatures associated with the lipid metabolism in livers of HFD *Inpp4b*$^{-/-}$ females (Figure 2.7. B-C). The validation of DEGs confirmed upregulation of SREBP1 and *Pparg* target genes which are involved in fatty acid import (*Cd36*), triglyceride synthesis (*Mogat1*), and intracellular lipid storage (*Cidec* and *Plin4*) in the livers of HFD *Inpp4b*$^{-/-}$ female mice (Figure 2.7. D-I).

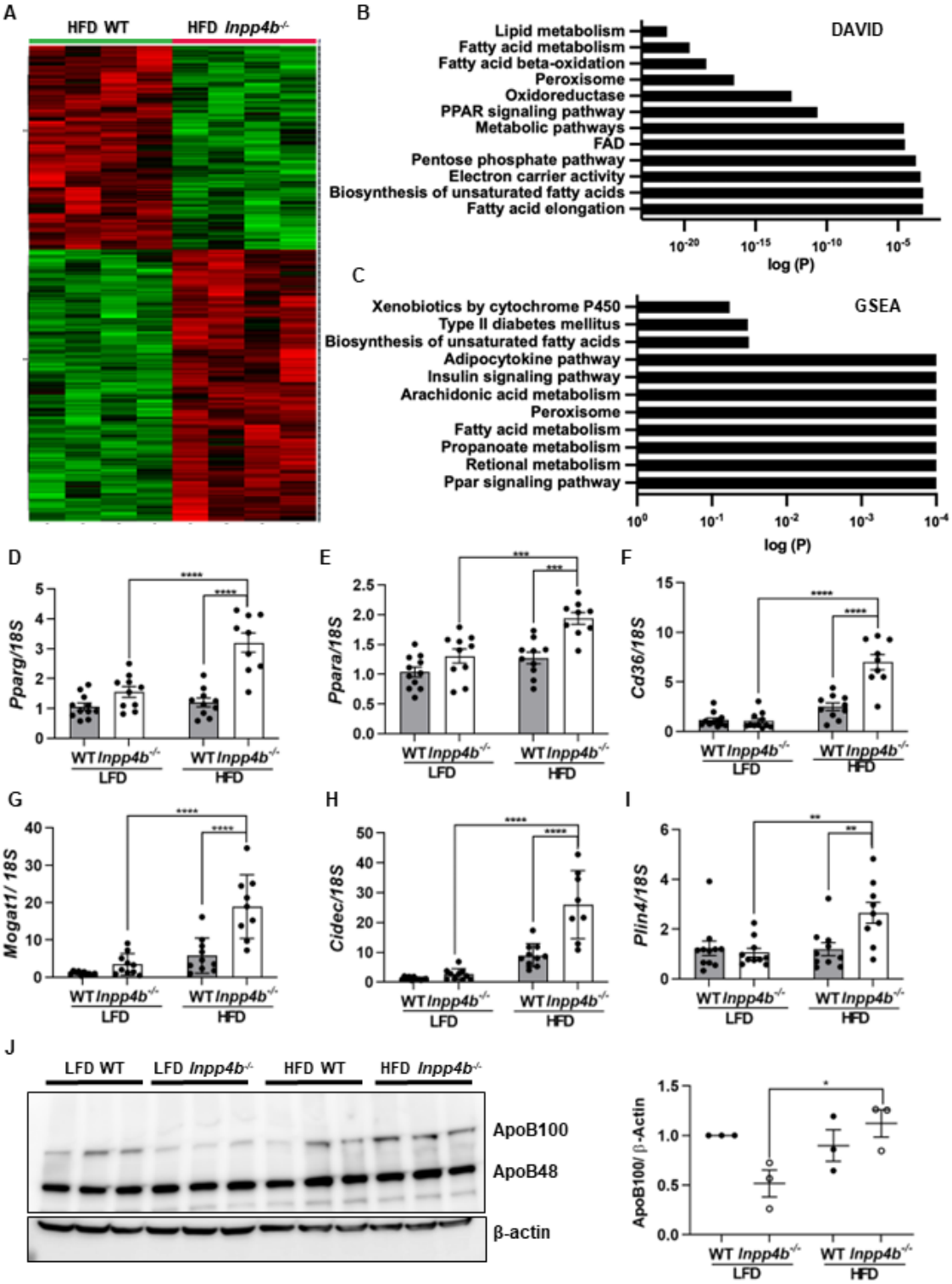


**Figure 2.7.** HFD *Inpp4b*$^{-/-}$ females have upregulated hepatic lipid signaling.
A) Heatmap for the differentially expressed genes in HFD WT and HFD *Inpp4b*$^{-/-}$ female mice. RNA samples from the livers of HFD WT (N=4) and HFD *Inpp4b*$^{-/-}$ (N=4) female mice were submitted for RNA sequencing. B-C) KEGG pathway functional enrichment analysis was done using B) DAVID functional annotation module or C) GSEA. The vertical axis represents the KEGG pathways significantly enriched in

*Inpp4b*-deficient mouse liver. The horizontal axis represents the logarithmic scale of the p values. D-I) Female liver RNA samples from panel 2.5.D were used. Gene expression levels of (D) *Pparg*, (E) *Ppara* (left to right: ***p=0.0006, ***p=0.0003), (F) *Cd36*, (G) *Mogat1*, (H) *Cidec*, and (I) *Plin4* (left to right: **p=0.0033, **p=0.0081) were analyzed by qRT- PCR using *18S* as an internal control. (J) Protein lysates from female livers (N=3) per group were analyzed and quantified ApoB48 and ApoB100 (*p=0.0377) and normalized by β-actin. ****$p < 0.0001$. Data shown as mean ± SEM. Statistical analysis was performed using two-way ANOVA.

Increased lipogenesis in livers of HFD knockout females was accompanied with a modest but significant increase in ApoB100 (Figure 2.7. J), a apolipoprotein in VLDLs that transport lipids from liver to adipose and other peripheral tissues [190].

Consistent with the upregulation of genes required for lipid metabolism in liver, metabolomics analysis of the serum samples of HFD females revealed significant increase in circulating fatty acids and triglycerides in HFD *Inpp4b*$^{-/-}$ mice (Figure 2.8. A). The metabolome pathway analysis indicated that metabolites associated with fatty acid oxidation and arachidonic acid metabolism were significantly enriched in HFD *Inpp4b*$^{-/-}$ females. In addition, the pathways that are important for glucose homeostasis such as pyruvate metabolism and gluconeogenesis were also increased between HFD WT and HFD *Inpp4b*$^{-/-}$ groups, which contributes to hyperglycemia in the latter group (Figure 2.8. B).

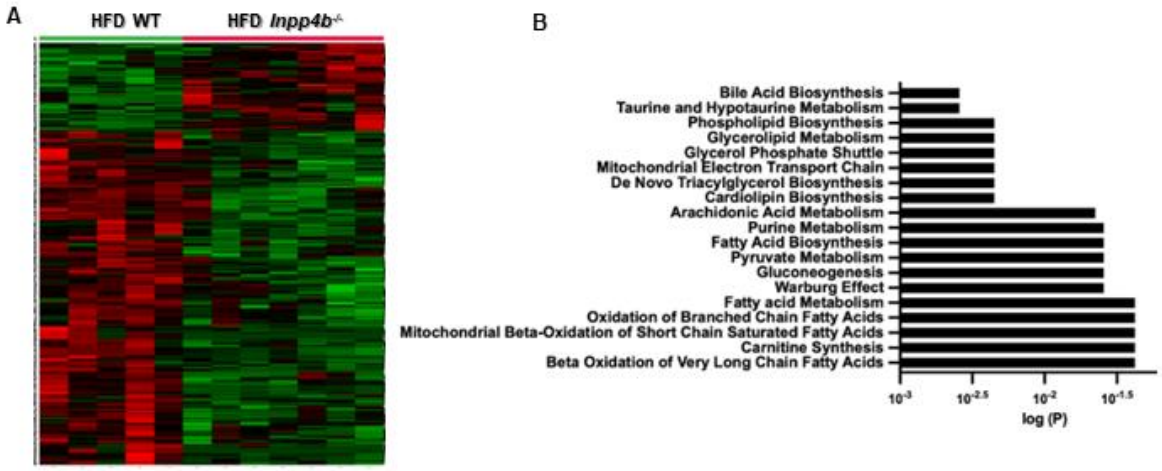


**Figure 2.8.** Serum metabolites confirm the dysregulation of glucose and lipid metabolism in HFD *Inpp4b*$^{-/-}$ females.
A) Heatmap for significantly different metabolites in HFD WT (N=5) and HFD *Inpp4b*$^{-/-}$ (N=7) female serum. B) Pathway analysis from the metabolites that are significantly changed in HFD *Inpp4b*$^{-/-}$ females using MetaboAnalyst 5.0. The horizontal axis represents the logarithmic scale of the p values.

### 2.3.7. FGF21 and FGF1 signaling pathways are dysregulated in *Inpp4b*$^{-/-}$ females

To determine whether INPP4B is required for hypothalamic regulation of circulating glucose, we examined whether endocrine FGF21 and autocrine FGF1 signaling is disrupted in hypothalami of HFD *Inpp4b*$^{-/-}$ females contributing to elevated blood glucose levels.

FGF21 is produced by the liver and adipose tissue and secreted into the bloodstream [191]. In hypothalamus, FGF21 requires a co-receptor β-klotho (*Klb*) to compensate the lack of heparan sulfate domain to bind to and activate its cognate receptor FGFR1 [191]. FGF1 is produced in multiple tissues including in hypothalamus where it acts through FGFR1 in an autocrine/paracrine klotho-independent manner [192]. Hepatic and adipose expression as well as serum protein levels of FGF21 were elevated in HFD *Inpp4b*$^{-/-}$ females (Figure 2.9. A-C). Hypothalamic *Klb* levels were significantly reduced while *Fgf21* and *Fgfr1* levels were unchanged in HFD *Inpp4b*$^{-/-}$ females (Figure 2.9. D-F). In the hypothalamus, both mRNA and protein levels of FGF1 were reduced in *Inpp4b*$^{-/-}$ mice independent of diet (Figure 2.10. A-C).

This data suggests that hypothalamic FGF21 - FGFR1/β-Klotho signaling may be reduced in HFD *Inpp4b*$^{-/-}$ females due to lower levels of *Klb* expression and FGF1/FGFR1 signaling is downregulated due to decreased levels of hypothalamic FGF1 mRNA and protein. Deficiencies in these two pathways contribute to increased circulating levels of glucose in HFD *Inpp4b*$^{-/-}$ females.

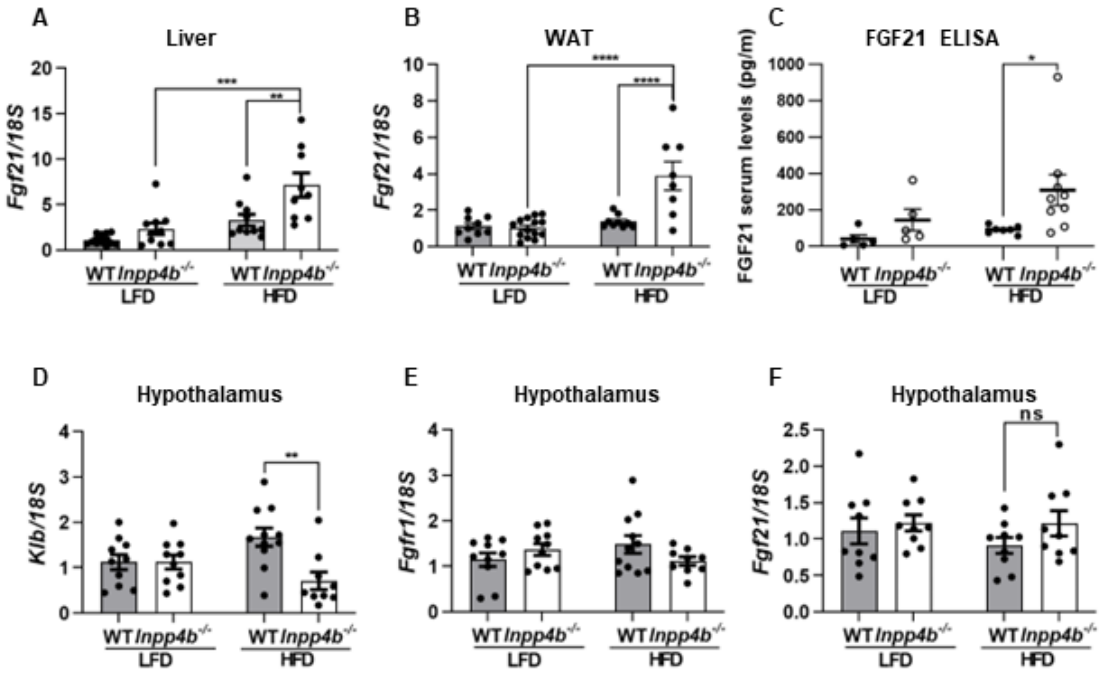


**Figure 2.9.** Hypothalamic FGF21- FGFR1 signaling is regulated via INPP4B loss and HFD in female mice.

A-B) The gene expression of *Fgf21* was analyzed by qRT- PCR using *18S* as an internal control in LFD WT, LFD *Inpp4b*$^{-/-}$, HFD WT, and HFD *Inpp4b*$^{-/-}$ female (A) liver (***p=0.0006, **p=0.0070) and (B) WAT. RNA samples from panels 2.5.B-C and 2.2. A-C were used respectively. C) FGF21 levels were assayed using ELISA in the sera of LFD WT (N=5), LFD *Inpp4b*$^{-/-}$ (N=5), HFD WT (N=7), and HFD *Inpp4b*$^{-/-}$ (N=9) female mice (*p=0.0315). D-F) Female hypothalamic RNA samples were used from panel 2.3.E. The gene expression of (D) *Klb* (**p=0.0035), (E) *Fgfr1*, and (F) *Fgf21* were analyzed by qRT- PCR using *18S* as internal control. ****p<0.0001. Data shown as mean ± SEM. Statistical analysis was performed using two-way ANOVA.

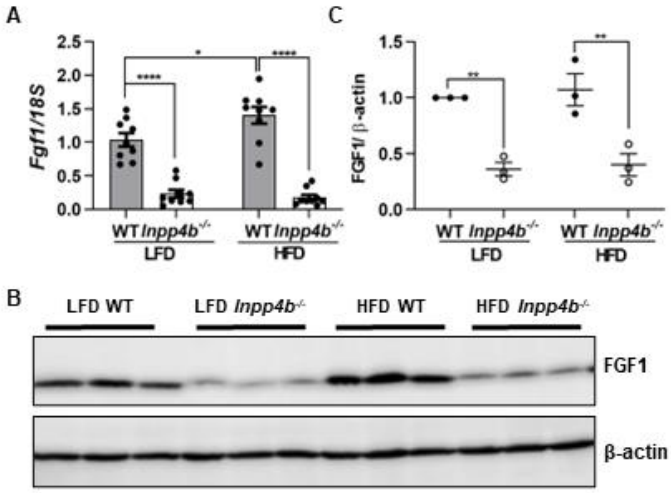


**Figure 2.10.** INPP4B loss reduces hypothalamic FGF1 expression
Female hypothalamic RNA samples were used from panel 2.3.E. The gene expression of *Fgf1* was analyzed by qRT- PCR using *18S* as an internal control in LFD WT, LFD *Inpp4b*$^{-/-}$, HFD WT, and HFD *Inpp4b*$^{-/-}$ groups (*p=0.0287). B) Protein lysates from female hypothalami (N=3 per group) were analyzed and quantified for FGF1 and normalized using β-actin. C) Quantification of panel (B) (left to right: **p=0.0052, **p=0.0038). ****p<0.0001. Data shown as mean ± SEM. Statistical analysis was performed using two-way ANOVA.

### 2.3.8. INPP4B modulates blood glucose levels in a sexually dimorphic manner

While blood glucose levels in HFD knockout females peak at 300 mg/dL in the glucose tolerance test, in HFD *Inpp4b*$^{-/-}$ males, it reaches 600 mg/dL which is associated with the T2D (Figure 2.11. A). To determine whether hypothalamic regulation of circulating glucose is differentially regulated by INPP4B, we compared changes in FGF21 and FGF1 signaling caused by INPP4B loss of function in males and females.

Similar to females, HFD *Inpp4b*$^{-/-}$ male mice had significantly higher levels of serum FGF21 (Figure 2.11. B). However, in males *Fgf21* mRNA levels in WAT were unchanged by diet and genotype, and only half that of HFD *Inpp4b*$^{-/-}$ females (Figure 2.11. C). In the hypothalamus, *Fgf1* levels were significantly lower in *Inpp4b*$^{-/-}$ males on either diet, similar to females (Figure 2.11. D). In hypothalamus, *Fgf21* expression was reduced in *Inpp4b*$^{-/-}$ males, with a further decrease caused by HFD (Figure 2.11. E). HFD *Inpp4b*$^{-/-}$ males

featured a stronger reduction in *Klb* and *Fgfr1* expression levels than HFD *Inpp4b*$^{-/-}$ males (Figure 2.11. F-G) suggesting that HFD and *Inpp4b* knockout have stronger effect on hypothalamic regulation of circulating glucose.

The activation of FGF1-FGFR1 and FGF21-FGFR1/β klotho cascades induces the phosphorylation of p44/42 MAPK to reduce blood glucose levels [128, 193]. Consistent with significantly higher blood glucose levels in HFD *Inpp4b* males, phosphorylation levels of p44/42 ERK1/2 were reduced in the hypothalami of HFD *Inpp4b*$^{-/-}$ males compared females (Figure 2.11. H).

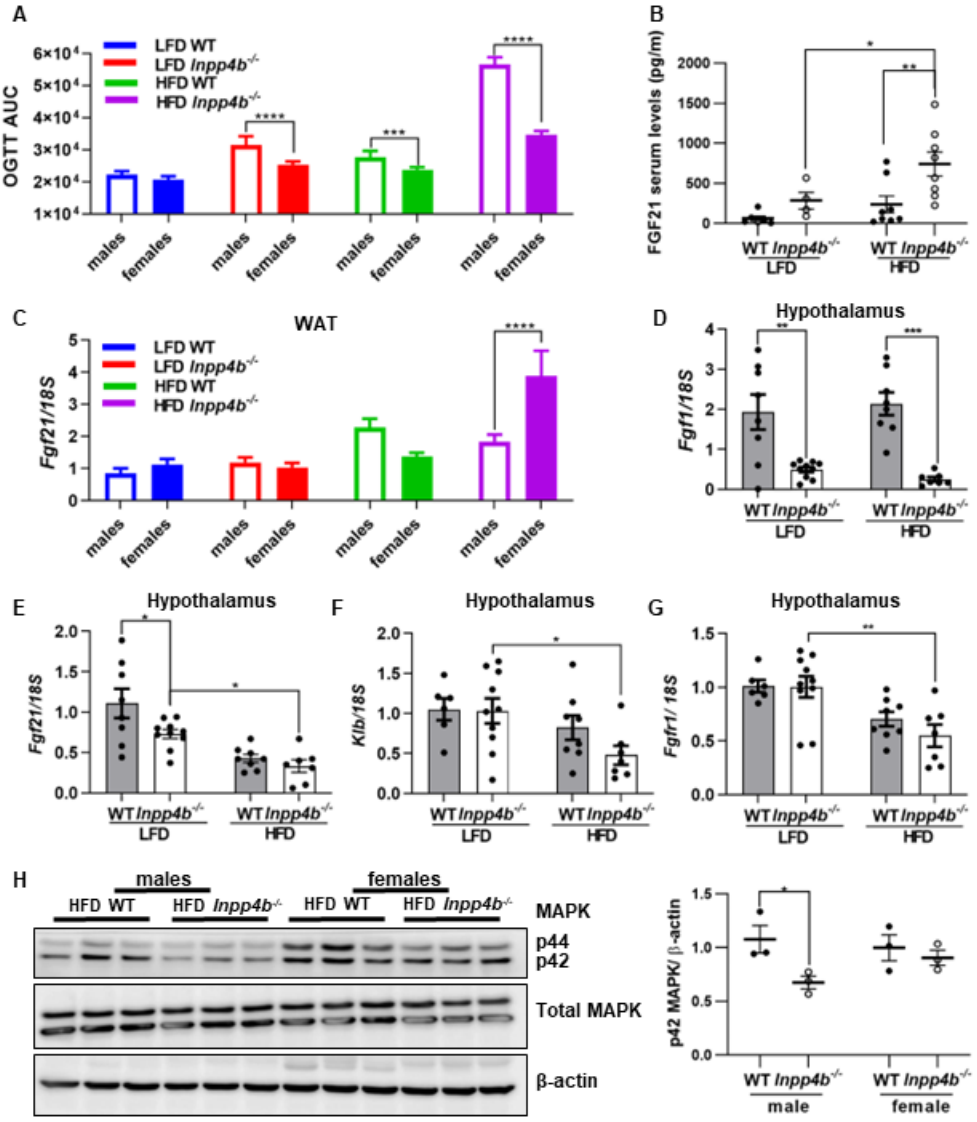


**Figure 2.11.** FGF21 and FGF1 signaling leads to sexual dimorphism of glucose handling in an INPP4B dependent manner.

A) AUC OGTT in LFD WT, LFD *Inpp4b*$^{-/-}$, HFD WT, and HFD *Inpp4b*$^{-/-}$ male and female mice, as reported previously (***p=0.0007) [166]. B) FGF21 levels were assayed using ELISA in the sera of LFD WT (N=6), LFD *Inpp4b*$^{-/-}$ (N=5), HFD WT (N=8), and HFD *Inpp4b*$^{-/-}$ (N=8) males (*p=0.0465, **p=0.0065). C) The gene expression of *Fgf21* was analyzed by qRT- PCR using *18S* as an internal control in female and male WAT. WAT RNA samples were used from panel 2.2. A for female mice, and RNA was extracted from WAT of LFD WT (N=12), LFD *Inpp4b*$^{-/-}$(N=11), HFD WT (N=8), and HFD *Inpp4b*$^{-/-}$ (N=11) male mice. D-G) RNA was extracted from hypothalami of LFD WT (N=8), LFD *Inpp4b*$^{-/-}$(N=10), HFD WT (N=8), and HFD *Inpp4b*$^{-/-}$ (N=7) male mice. The gene expression levels of (D) *Fgf1*(**p=0.0016, ***p=0.0002), (E) *Fgf21* (left to right: *p=0.0489, *p=0.0471), (F) *Klb* (*p=0.0229), and (G) *Fgfr1* (**p=0.0051) were analyzed by qRT- PCR using 18S as an internal control. H) Protein lysates from male and female hypothalami (N=3 per group) were analyzed and quantified for p-p44/42 MAPK (*p=0.0418) and total MAPK, and normalized using β-actin. ****p<0.0001. Data shown as mean ± SEM. Statistical analysis was performed using two-way ANOVA.

## 2.4. Discussion

Similar to humans, most mouse models exhibit differences between genders in metabolic homeostasis [194, 195]. We have previously reported that *Inpp4b*$^{-/-}$ male mice on HFD develop obesity, diabetes, NAFLD, and reproductive abnormalities [20]. In this study, we investigated the alterations in the female metabolism due to INPP4B loss. We observed high levels of *Inpp4b* in the female tissues, which are important for metabolic homeostasis. HFD induced *Inpp4b* levels in the WAT and hypothalamus of WT females. Unlike males, HFD WT females did not show any metabolic abnormalities, suggesting that INPP4B protects from the diet induced metabolic abnormalities in females.

Among the four experimental groups, HFD *Inpp4b*$^{-/-}$ females were the only ones with a significant weight gain, which was due to increased fat weight (Figure 2.1. C-D). Compared to the 14% increase in the weight gain between HFD WT and HFD *Inpp4b*$^{-/-}$ males [20], HFD females gained 35% of their body weight in fat. Weight gain and fat accumulation in HFD *Inpp4b*$^{-/-}$ females were due to the failure of lipid oxidation and leptin resistance (Figure 2.2 and 2.3). For both genders, mRNA *Lep* levels as well as the serum leptin protein levels were higher in the WAT of HFD *Inpp4b*$^{-/-}$ groups, with significantly higher leptin levels in females. Moreover, *Lepr* levels were elevated in the hypothalamus of both WT males and females in response to HFD; however, *Inpp4b*$^{-/-}$ mice failed to increase *Lepr* expression in response to HFD (Figure 2.3). We previously reported that HFD *Inpp4b*$^{-/-}$ males have reduced ambulatory activity, energy expenditure, and respiratory exchange ratio [20]. The downregulation of energy metabolism might be caused by lack of compensatory increase in *Lepr* expression in response to HFD in knockout males (data not shown). We anticipate that there will be a more severe reduction in the energy metabolism

in HFD *Inpp4b*$^{-/-}$ females, due to stronger downregulation of hypothalamic *Lepr* in HFD knockout females compared to that of HFD WT (Figure 2.3. E). Obesity in HFD *Inpp4b*$^{-/-}$ females was associated with inflammation of the visceral adipose tissue and accumulation of ectopic lipids in liver leading liver damage and NAFLD (Figure 2.2 and 2.5).

The evaluation of molecular pathways in liver has shown that insulin signaling was dysregulated in HFD *Inpp4b*$^{-/-}$ females due to the over-activation of AKT pathway, which led to SREBP1 processing and activating lipid anabolism (Figure 2.6). RNA-sequencing and pathway analysis of HFD livers confirmed activation of lipid metabolism in HFD *Inpp4b*$^{-/-}$ females. Using pathway analysis, we found that PPARγ signaling was among most highly activated pathways. In the livers of HFD *Inpp4b*$^{-/-}$ females, the mRNA expression of *Pparg* and PPARγ transcriptional targets were significantly increased, consistent with the development of NAFLD in this group (Figure 2.7). The results from metabolomic analysis of the serum samples were aligned with the induced hepatic lipid synthesis in HFD *Inpp4b*$^{-/-}$ females (Figure 2.8).

Metabolic fibroblast growth factors, FGF1 and FGF21, contribute significantly to maintenance of blood glucose levels via hypothalamic signaling [123, 127-129]. We observed that endocrine FGF21 signaling was dysregulated in HFD *Inpp4b*$^{-/-}$ females. FGF21 production and secretion were induced; however, the mRNA levels of co-receptor *Klb* were reduced in the hypothalami of the HFD *Inpp4b*$^{-/-}$ group. Hypothalamic expression of *Fgf1*, a paracrine peptide hormone, was significantly reduced in *Inpp4b*$^{-/-}$ mice, regardless of diet. We speculate that, unlike males, HFD *Inpp4b*$^{-/-}$ females might be protected against diabetes due to the normal levels of *Fgf21* in the hypothalamus, despite

the reduction in hypothalamic *Fgf1* levels and somewhat lower *Klb* expression (Figure 2.9-2.10).

Glucose metabolism differs in *Inpp4b*- deficient male and female mice on either diet (Figure 2.11. A). Similar to other mouse models, loss of INPP4B function is more significant in male mice [20, 166, 174, 194]. We showed that gender specific differences in INPP4B regulation of hepatic insulin and hypothalamic FGFR signaling contribute to the disparate outcomes of INPP4B loss of function in males and females. Unlike males, loss of INPP4B did not affect IR downstream signaling in females fed LFD. Hypothalamic *Fgf21* and *Fgfr1* levels were not reduced in knockout females. Lower *Fgfr1* expression in HFD *Inpp4b*$^{-/-}$ males compared to LFD *Inpp4b*$^{-/-}$ males, reduced *Fgf21* levels in LFD *Inpp4b*$^{-/-}$ males and especially HFD *Inpp4b*$^{-/-}$ males (Figures 2.9- 2.11), and reduced phosphorylation of p44/42 MAPK downstream of FGFR1 signaling worsened the phenotype in *Inpp4b*$^{-/-}$ males compared to females and led to the development of T2D in that group (Figure 2.11 H). Altogether, these factors may contribute to lower glucose levels in *Inpp4b*$^{-/-}$ females compared to *Inpp4b*$^{-/-}$ males.

In conclusion, we showed that loss of INPP4B under obesogenic conditions led to obesity, inflammation, hyperglycemia, and NAFLD in female mice due to the leptin resistance, impaired insulin signaling, alterations in lipid metabolism, and dysregulation of hypothalamic FGF1- FGFR1 and FGF21-FGFR1/β klotho signaling. In addition, the differences in serum glucose levels in HFD *Inpp4b*$^{-/-}$ male and female mice suggest that INPP4B signaling is sexually dimorphic.

## 2.5. Materials & Methods

### Animal studies

The mice were maintained at AAALAC certified facility at Florida International University and all experimental protocols were performed in accordance with the regulations of the Florida International University Institutional Animal Care and Use Committee. *Inpp4b*$^{-/-}$ mice and high-fat diet feeding strategy were described previously [18, 20, 196]. Briefly, WT and *Inpp4b*$^{-/-}$ females on FVB background were fed either LFD (LabDiet 5V75, St. Louis, MO) or HFD (TestDiet 58R3, St. Louis, MO) from gestation to dissection. To prevent any hormonal fluctuations, all LFD WT, LFD *Inpp4b*$^{-/-}$, HFD WT, and HFD *Inpp4b*$^{-/-}$ females were euthanized at the diestrus stage of the estrous cycle [197]. For the determination of estrous stage, vaginal smears were collected and stained with crystal violet for the cytological assessment as described by McLean et al. [198]. The four experimental groups were dissected at the age of 3-month and the tissues were collected for gene and protein expression, and histological analysis. Body composition of HFD WT and HFD *Inpp4b*$^{-/-}$ females was determined at the Vanderbilt Mouse Metabolic Phenotyping Center by NMR using Bruker Minispec body composition analyzer (Bruker Optics, Billerica, MA).

### Insulin tolerance test (ITT)

Three-month-old LFD WT, LFD *Inpp4b*$^{-/-}$, HFD WT, and HFD *Inpp4b*$^{-/-}$ female mice were administered 0.75 U/kg of Humulin R insulin (Eli Lilly and Company, Indianapolis, IN) by intraperitoneal injection after 3 hours of fasting. Blood glucose levels were tested from tail, before insulin administration, and 30, 60, 90, and 120 minutes after administration

using the ACCU-CHEK Nano SmartView glucometer (Roche Diagnostics, Indianapolis, IN).

**Intraperitoneal pyruvate tolerance test (IPTT)**

Three-month-old LFD WT, LFD *Inpp4b*$^{-/-}$, HFD WT, and HFD *Inpp4b*$^{-/-}$ female mice were fasted overnight, followed by intraperitoneal injection of pyruvate (1.5 g/kg, Sigma-Aldrich, St. Louis, MO). The blood glucose levels were measured before pyruvate injection and 15, 30, 60, 90, and 120 minutes after the pyruvate administration as described above.

**Measurement of metabolic adipokines, cytokines, and hormones**

The serum samples were collected from LFD WT, LFD *Inpp4b*$^{-/-}$, HFD WT, and HFD *Inpp4b*$^{-/-}$ female mice. After blood samples were incubated for 30 minutes at room temperature, centrifuged at 3000 × g for 15 min, and serum was aspirated and stored at -80$^{0}$C. The serum samples of the four experimental groups were analyzed for the following peptide hormones using the Mouse Metabolic 11-plex Arrays (Eve Technologies, Calgary, AB, Canada): Amylin (active), C-Peptide, Ghrelin, GIP (total), GLP-1(active), Glucagon, Insulin, Leptin, PP, PYY, and Resistin.

**Measurement of serum insulin and FGF21 levels by ELISA**

Blood insulin levels were determined using the Ultra Sensitive Mouse Insulin ELISA Kit (Crystal Chem, Elk Grove Village, IL) according to the manufacturer's instructions. Briefly, five µl of blood serum LFD WT, LFD *Inpp4b*$^{-/-}$, HFD WT, HFD *Inpp4b*$^{-/-}$ female mice were used for the test. Plasma FGF21 levels were determined using the Mouse and Rat FGF21 ELISA Kit (BioVendor, Catalog #RD291108200R, Brno, Czech Republic) according to the manufacturer's instructions. Hundred µl of undiluted sera from LFD WT, LFD *Inpp4b*$^{-/-}$, HFD WT, HFD *Inpp4b*$^{-/-}$ female mice were used for each experimental

measurement. The concentrations were measured using a CLARIOstar plate reader (BMG Labtech, Cary, NC).

**RNA sequencing and data analysis**

RNA was isolated from the livers of HFD WT and HFD *Inpp4b*$^{-/-}$ females and submitted to Novogene for RNA sequencing. The libraries were produced by the NEBNext® Ultra™ RNA Library Prep Kit and used for Illumina 150-bp paired-end sequencing. Quality control assessment was performed using the Illumina RNA-seq pipeline for the estimation of genomic coverage, percent alignment, and nucleotide quality. Raw reads were mapped to the reference mouse genome (the most recent build GRCm39) using HISAT2 [199] and STAR [200] software. The reads for each gene aligned using HISAT2 and were counted by HTSeq [201] software. Alignment by STAR was run with the option "—quantMode Gene Counts," which allowed the counting of reads aligned to each gene. Raw counts from HTSeq and STAR were imported into Bioconductor/R package DESeq2 [202], normalized, and tested for differential gene expression. This analysis was performed separately for the files produced by each aligner. In each analysis, the genes that meet the criteria of false discovery rate (FDR) < 0.1 and fold change (FC) > 1.3 in either direction were considered differentially expressed genes (DEGs). Genes that showed differential expression after analysis of the files from both aligners were included in further analysis.

**Pathway analysis for RNA-sequencing**

Pathways analysis for DEGs was performed using the Database for Annotation, Visualization, and Integrated Discovery (DAVID, https://david.ncifcrf.gov/home.jsp) and Gene Set Enrichment Analysis (GSEA, http://www.broad.mit.edu/gsea/index.html). The normalized enrichment score (NES) with FDR<0.25 or p<0.05 was accepted as significant.

**RNA isolation and gene expression analysis**

RNA samples from mouse tissues were prepared using Tri Reagent (Molecular Research Center, Cincinnati, OH). The RNA concentration was measured by NanoVue Plus (GE Healthcare BioSciences, Piscataway, NJ). For reverse transcription Verso cDNA synthesis Kit (Thermo Fisher Scientific) was used, and the real-time quantitative polymerase chain reaction (qRT-PCR) was performed using Roche 480 LightCycler (Roche, Basel, Switzerland). The corresponding primers and probes used in qPCR were designed by Universal Probe Library and listed in Table 3.

**Table 3.** Mouse gene primers and probes for qPCR analysis used in Chapter 2.

| Gene | Forward primer | Reverse Primer | Probe |
|---|---|---|---|
| *18S* | gcaattattccccatgaacg | Gggacttaatcaacgcaagc | 48 |
| *Adgre1* | tgtcctccttgcctggac | gagacttctgagctgacactgc | 29 |
| *Adipoq* | ccatctggaggtgggagac | ctgcatagagtccattgtggtc | 1 |
| *Cd36* | tggccttacttgggattgg | ggatttgcaagcacaatatgaa | 9 |
| *Cd68* | tccactgttggccctcac | ccccttggaccttggacta | 10 |
| *Cidec* | aagccctggcaaaagatacc | cttcttgcgctgttctgatg | 18 |
| *Il1b* | caggcaggcagtatcactca | tgtcctcatcctggaaggtc | 76 |
| *Fgf1* | cagcctgccagttcttcag | ggctgcgaaggttgtgat | 41 |
| *Fgf21* | agatggagctctctatggatcg | gggcttcagactggtacacat | 67 |
| *Fgfr1* | ccaacctctaaccgcagaac | agtgcagagagtggctgtga | 35 |
| *Klb* | caggacatcacccgcctaag | gtagttcctccggatccacg | 28 |
| *Lep* | cccaaaatgtgctgcagatag | ccagcagatggaggaggtc | 80 |
| *Lepr* | gttccaaaccccaagaattg | gacttcaaagagtgtccgttctc | 104 |
| *Lpl* | ttatcccaatggaggcactt | aatcacacggatggcttctc | 20 |
| *Mogat1* | ttcaatgggagtagccttgc | gcattatgccaaagtagtgctg | 6 |
| *Plin4* | tgcagcttacagcagcctagt | gccatacagcttgcagagg | 40 |
| *Ppargc1a* | cccatacacaaccgcagtc | gaacccttggggtcatttg | 6 |
| *Ppargc1b* | ctccagttccggctcctc | ccctctgctctcacgtctg | 17 |
| *Pparg* | ctctcagctgttcgccaag | cacgtgctctgtgacgatct | 50 |
| *Tnfa* | ttgtcttaataacgctgatttggt | gggagcagaggttcagtgat | 64 |

**Untargeted aqueous metabolomics and data analysis**

Serum samples of HFD WT and HFD *Inpp4b*$^{-/-}$ were analyzed for untargeted aqueous metabolomics in Dr. Haiwei Gu's laboratory at FIU Center for Translational Science. Untargeted metabolic profiling was performed using a Thermo Vanquish UPLC-Exploris 240 Orbitrap MS instrument. Each sample was injected twice, 10 μL for negative and 4 μL for positive ionization mode. Both chromatographic separations were performed in hydrophilic interaction chromatography (HILIC) mode on a Waters XBridge BEH Amide column. The mobile phase was composed of Solvents A (10 mM ammonium acetate, 10 mM ammonium hydroxide in 95% H2O/5% ACN) and B (10 mM ammonium acetate, 10 mM ammonium hydroxide in 95% ACN/5% H2O). After the initial 1 min isocratic elution of 90% B, the percentage of Solvent B decreased to 40% at t=11 min. The composition of Solvent B was maintained at 40% for 4 min (t=15 min), and then the percentage of B gradually increased to 90%, for the next injection. Using mass spectrometer equipped with an electrospray ionization (ESI) source, we collected untargeted data from 65 to 1000 m/z. The untargeted data was processed by Progenesis QI (version 2.1, Waters Corporation) for peak picking, alignment, and normalization. To improve rigor, the highly varied signals/peaks with CV > 20% across quality control (QC) pools, and the signals with missing values in all QC were excluded for further analysis.

**Pathway analysis for metabolomics**

The metabolite heatmap and pathway analysis were obtained using MetaboAnalyst 5.0 (https://www.metaboanalyst.ca/). In the heatmap, the significant 260 metabolites were shown. For the pathway analysis, FDR<0.05 was considered significant.

**Western blotting**

The protein extraction from mouse tissues was previously described [181]. 15-30 µg of protein samples were loaded on a 7.5% - 12.5% SDS-PAGE gel. The protein was transferred using nitrocellulose or PVDF membrane and the membrane was blocked using 5% BSA or 5% non-fat milk. The blots were incubated with primary antibodies against p-p44/42 MAPK T202/Y204 (1:1000, #4370, Cell Signaling, Danvers, MA), p44/42 MAPK (1:1000, #4695, Cell Signaling), pAKT S473 (1:1000, #4051, Cell Signaling), total AKT (1:1000, #4691, Cell Signaling), pPKCβ S660 (1:1000, #9371, Cell Signaling), SREBP1 (1:1000, NB #600-582, Novus Biologicals, Littleton, CO), ApoB48 and ApoB100 (1:1000, #20578-1, ProteinTech, Rosemont, IL), FGF1 (1:2000, #ab207321, AbCam, Cambridge, MA), and β-actin (1:10 000, A5316, Sigma, St Louis, MO ) overnight. Rabbit IgG (1:2000, W4011, Promega, Madison, WI) and mouse IgG (1:2000, W4021, Promega) were used as secondary antibodies. The signal was detected by ImageQuant LAS 500 imager and analyzed using ImageQuant TL software (GE Healthcare, Chicago, IL).

**Immunohistochemistry**

Tissue sectioning and immunohistochemistry (IHC) staining were described previously [20, 196]. Briefly, 4.5 µM sections were deparaffinized in xylene and hydrolyzed in gradient ethanol. For inhibition of endogenous hydrogen peroxidase, slides are incubated in 3% $H_2O_2$ for 20 minutes. Antigen retrieval was performed by heating slides in pH=6 10 mM sodium citrate buffer at 100$^{o}$C for 15 minutes. Sections were blocked with 5% BSA in PBS for 30 minutes, then incubated with primary antibodies insulin (1:60 000, #ab181547, AbCam) and CD68 (1:300, #ab125212, AbCam) overnight at 4°C. ABC kit (Vector Laboratories, Burlingame, CA) and Peroxidase substrate kit (Vector Laboratories)

were used to visualize the staining as suggested by manufacturer instruction, and slides were counterstained with hematoxylin.

**Oil Red O staining**

The tissue preparation and Oil Red O Staining were previously described [20]. Fresh liver samples were preserved in OCT medium. The frozen samples were cut into 12 μm sections and placed on glass slides. The slides were fixed in 4% PFA, rinsed in distilled water and in propylene glycol, then stained in oil red O, which was dissolved in hot propylene glycol, then filtered using Whatman #2 filter paper. Then the stained slides were counterstained with hematoxylin. The images were captured using an AxioCam MRc5 camera (Zeiss, Thornwood, NY).

**Statistical analysis**

Two-way ANOVA (Tukey's multiple comparison tests) for four groups and two tailed Student's t-test for two groups were performed using Prism 9.0. The p-values less than 0.05 were considered statistically significant. The data was present as mean ± SEM.

# 3. CHAPTER 3: INPP4B loss disrupts mammary gland homeostasis and promotes *ERBB2*- induced mammary gland tumorigenesis

## 3.1. Introduction

Breast cancer is the second leading cause of cancer deaths among women in the United States and overweight and obese women are at higher risk of developing and dying from breast cancer [203, 204]. Inositol polyphosphate-4-phosphatase type II B (INPP4B) is a well-documented tumor suppressor in breast cancer [78, 80, 91, 205], and we discovered that it protects from diet-induced metabolic syndrome. In this study, we tested whether INPP4B mediates high-fat diet (HFD)-induced changes in mammary gland development and protects from the obesity-associated acceleration of breast cancer initiation and progression. For that purpose, we investigated steroid hormone receptor signaling, oncogenic PI3K/AKT signaling, tumor suppressor p53 signaling, as well as intrinsic leptin signaling, which all contribute to both mammary gland development and breast cancer tumorigenesis.

Ovarian sex steroid hormones, estrogen and progesterone, are at the center of both mammary gland morphogenesis and neoplastic transformation [206]. Progesterone signals through its nuclear cognate receptor, progesterone receptor (PR), and its deletion perturbs mammary gland development [207]. Moreover, the phosphorylation of PR by various mitogenic signaling pathways including PI3K/AKT and PKC, which are inhibited by INPP4B, modulates their activity [208]. Non-genomic activities of PR induce AKT and PKC phosphorylation, leading to the promotion of cell proliferation and inhibition of apoptosis in cancer progression [209, 210]. In addition to intrinsic hormone signaling, adipokine leptin signaling contributes to mammary gland development and carcinogenesis.

The deletion of leptin (*ob/ob*) and leptin receptor (*db/db*) in mouse models results in defective mammary gland development [211], while excess leptin levels promote inflammation and mammary gland tumorigenesis [212].

One of the breast cancer subtypes with overexpression of human epidermal growth factor 2/ Erb-B2 Receptor Tyrosine Kinase 2 (HER2/ ERBB2) accounts for one- fourth of whole breast cancer cases and exhibit poor prognosis and survival rates [81]. There is accumulating clinical and research data on the correlation of HER2 and p53 in breast cancer. p53 is a well-established tumor suppressor gene that plays a role in DNA repair, cell cycle inhibition, apoptosis, and cell metabolism [213, 214]. While p53 is involved in normal mammary gland development [215], it has one of the highest mutation rates in breast cancer patients. In 70% of HER2 positive breast cancer cases, p53 mutations increase HER2 expression [216, 217].

Our findings suggest that INPP4B is involved in mammary gland branching through reduced steroid hormone receptor signaling along with other intrinsic and extrinsic signaling pathways, and it protects against *ERBB2*-driven tumorigenesis by regulating tumor suppression and metabolic factors. Using *Inpp4b* knockout mouse model, we showed that INPP4B is required for optimal ductal side branching, and pAKT, p53, and p53 target p21 levels were increased in the mammary glands of *Inpp4b*$^{-/-}$ females in a low-fat diet (LFD). In the HFD *Inpp4b*$^{-/-}$ mammary glands, fewer ductal side branches were caused by reduced PR expression and activity, while pAKT and p53 levels were increased further in this group. Moreover, leptin signaling was dysregulated and was accompanied by elevated inflammation in HFD *Inpp4b*$^{-/-}$ females. In addition to its impact in normal mammary glands, loss of *Inpp4b* resulted in faster progression of *MMTV-ERBB2/+* tumors,

which were aggravated with the combination of *Inpp4b* deletion and HFD. A reduction in p53 protein levels and activity, and upregulation of *Cd36* an *Fabp4* that are involved in lipid anabolism were observed in HFD *MMTV-ERBB2/+; Inpp4b*$^{-/-}$ tumors, contributing to the worse phenotype in this group.

## 3.2. Results

### 3.2.1. INPP4B loss and HFD impair mammary gland ductal side branching

Our preliminary data suggest that INPP4B is required for ductal branching of murine mammary glands [166]. In this study, we showed that loss of INPP4B in combination with HFD further impairs mammary gland development (Figure 3.1. A). The quantification of whole mount staining revealed that *Inpp4b*$^{-/-}$ females possess significantly fewer mammary gland branches compared to WT groups of both diets, while the number of branches showed a modest reduction in both HFD WT and HFD *Inpp4b*$^{-/-}$ groups (Figure 3.1. B). Moreover, *Inpp4b*$^{-/-}$ females exhibited smaller mammary epithelial area (MEA), which was also significantly less in HFD *Inpp4b*$^{-/-}$ females compared to the LFD *Inpp4b*$^{-/-}$ group (Figure 3.1. C).

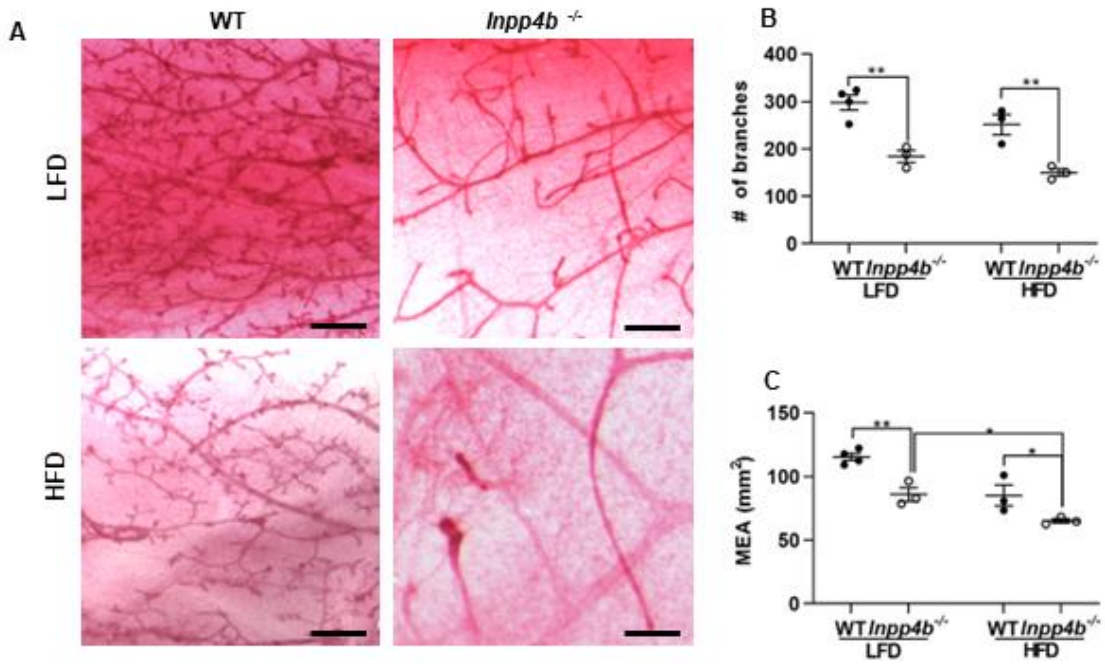


**Figure 3.1.** INPP4B and diet affect mammary gland epithelium.
(A) Representative images for the whole mount staining of the 11- month- old LFD WT (N=4), LFD *Inpp4b*$^{-/-}$ (N=3), HFD WT (N=3), and HFD *Inpp4b*$^{-/-}$ (N=3) female mammary glands. LFD groups have been reported previously [166]. (B-C) Quantification of whole mount staining for (B) number of ductal side branches (left to right: **p=0.0010, **p=0.0035) and (C) MEA (**p=0.0029, left to right: *p=0.0429, *p=0.0357). Data shown as mean ± SEM. Statistical analysis was performed using two-way ANOVA.

### 3.2.2. Loss of *Inpp4b* and HFD lead to a decrease in PR levels and activity

Estrogen and progesterone regulate mammary gland development from post-partum to pregnancy and lactation through the transcriptional activity of their cognate receptors [218]. Particularly, PR (*Pgr*) is required for the ductal side branching of mammary glands [207, 219, 220]. Thus, we investigated the impact of INPP4B loss on PR expression and activity. In invasive and metastatic breast cancer cohorts, we observed a strong correlation between *INPP4B* and *PGR* expression (r=0.5965 and r=0.3906 with p<0.0001 for both cohorts) (Figure 3.2 A-B). In the murine mammary glands, our preliminary data demonstrated that loss of *Inpp4b* causes a reduction in *Pgr* levels [166]. In this research, we investigated whether *Inpp4b* deletion and HFD alter the serum hormone levels, as well as the *Pgr* levels and the expression of PR transcriptional targets in the mammary

glands. The serum estradiol and progesterone levels remained similar in all groups (Figure 3.2. C-D). Meanwhile, the levels of *Pgr* were significantly reduced in the mammary glands of HFD *Inpp4b*$^{-/-}$ females (Figure 3.2 E). Consistent with the fewer ductal branches and lower PR levels, the gene expression levels of the PR targets that take a role in the ductal side branching — *Msx1*, *Msx2*, *Id4*, and *Wnt4* — were downregulated in the HFD *Inpp4b*$^{-/-}$ group (Figure 3.2. F-I).

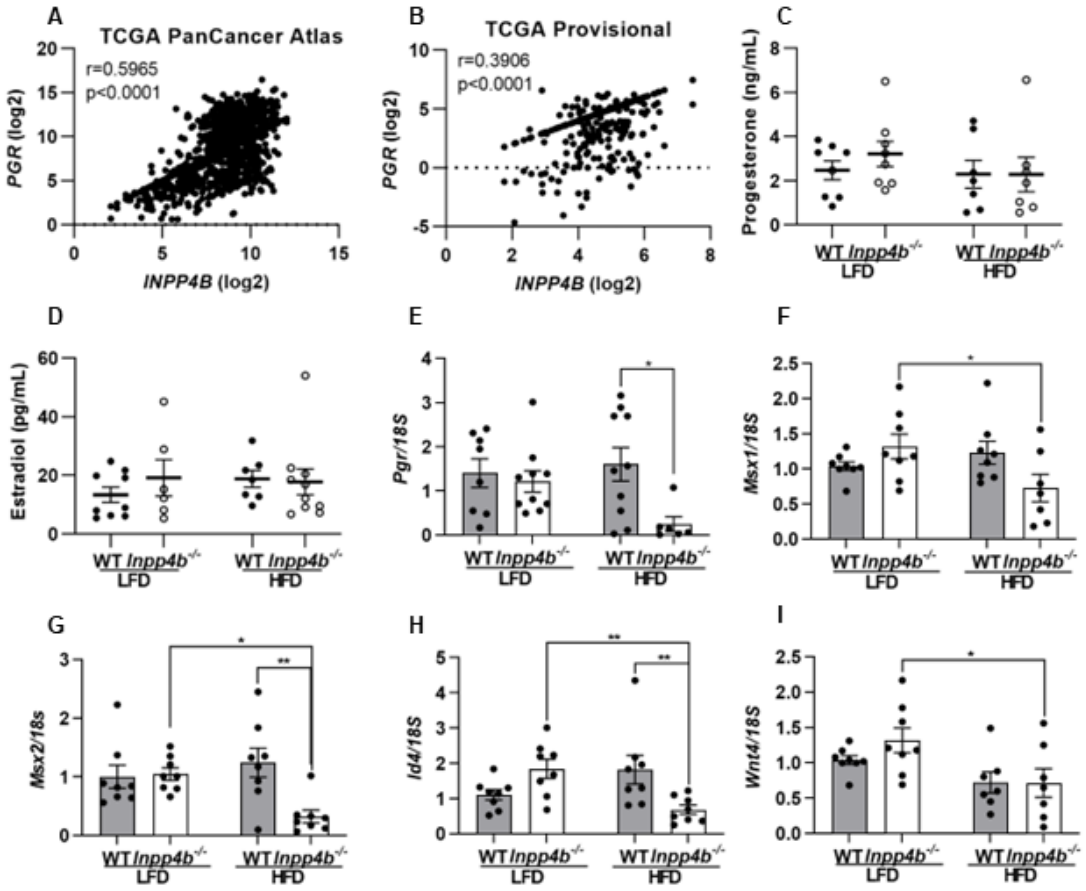


**Figure 3.2.** INPP4B is positively correlated with PR expression and activity in humans and mice. (A-B) Correlation between INPP4B and PR in (A) 992 and (B) 158 breast adenocarcinoma patient samples (TCGA). (C-D) Serum samples from LFD WT, LFD *Inpp4b*$^{-/-}$, HFD WT, and HFD *Inpp4b*$^{-/-}$ females (N=8 per group) were analyzed for (C) progesterone and (D) estradiol levels. E-I) RNA was extracted from mammary glands of LFD WT (N=8), LFD *Inpp4b*$^{-/-}$ (N=10), HFD WT (N=10), and HFD *Inpp4b*$^{-/-}$ (N=8) female mice. The gene expression levels of (E) *Pgr* (*p=0.0341), (F) *Msx1* (*p=0.0264), (G) *Msx2* (*p=0.0135, **p=0.0018), (H) *Id4* (left to right: **p=0.080, **p=0.097), and (I) *Wnt4* (*p=0.0198) were assayed by qRT-PCR using *18S* as an internal control. Data shown as mean ± SEM. Statistical analysis was performed using two-way ANOVA.

### 3.2.3. INPP4B loss regulates various oncogenic and tumor suppressor pathways

AKT and PKC pathways are both involved in mammary gland development and neoplastic transformation. While both pathways are required for ductal branching and involution in non-malignant mammary glands, the aberrant activation of AKT and PKC drives mammary gland tumorigenesis [221-223]. We previously showed higher levels of phospho- AKT *in vitro* due to INPP4B loss [166]. Similarly, we observed that phosphorylation of AKT was higher in the mammary glands of LFD *Inpp4b*$^{-/-}$ females and was significantly higher in the HFD *Inpp4b*$^{-/-}$ group (Figure 3.3. A-B).

Despite the tumor suppressor properties of INPP4B in breast cancer and increased AKT activity, *Inpp4b*$^{-/-}$ females lack mammary gland tumors. Thus, we investigated the potential signaling pathways that protect *Inpp4b*$^{-/-}$ females from mammary gland tumorigenesis. We found that INPP4B loss leads to a compensatory induction in the p53 protein expression and the p53 transcriptional target p21 levels. In the mammary glands of LFD *Inpp4b*$^{-/-}$ mice, p53 and p21 levels were drastically increased (Figure 3.3 A). Intriguingly, while p53 levels were further increased in the mammary glands of HFD *Inpp4b*$^{-/-}$ females, p21 expression remained similar in HFD *Inpp4b*$^{-/-}$ mice compared to the HFD WT group (Figure 3.3 C-D).

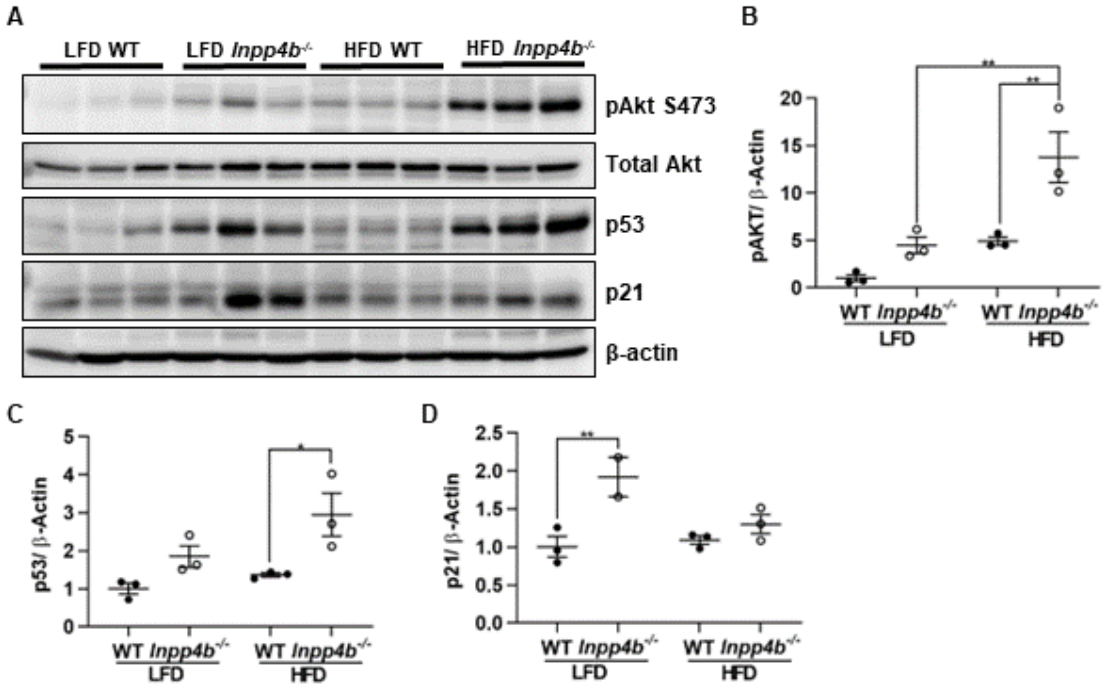


**Figure 3.3.** pAKT, p53, and p21 levels are modulated by INPP4B loss.
(A) Protein lysates from mammary glands of LFD WT, LFD *Inpp4b*$^{-/-}$, HFD WT, and HFD *Inpp4b*$^{-/-}$ females (N=3 per group) were analyzed and quantified for pAKT, total AKT, p53, and p21, and normalized using β-actin. (B-D) Quantification of panel (A) for (B) pAKT (left to right: **p=0.0036, **p=0.0047), (C) p53 (*p=0.0172) , and (D) p21 (**p=0.0059). Data shown as mean ± SEM. Statistical analysis was performed using two-way ANOVA.

.

### 3.2.4. INPP4B HFD modulate leptin signaling and inflammation

The expression and role adipokines leptin and adiponectin are implied in the mammary gland development and breast cancer progression [211, 212, 224]. Leptin has the highest expression in virgin mammary glands with the reduced expression in pregnancy and lactation and is expressed in both adipocytes and ductal epithelial cells [225]. In our knockout mice on HFD, we observed leptin mRNA and protein levels accompanied by lower adiponectin levels (Figure 3.4 A-C). Leptin promotes inflammation in breast cancer, while adiponectin shows anti-inflammatory effects [226, 227]. Consistent with the higher leptin and lower adiponectin levels in the mammary glands of HFD *Inpp4b*$^{-/-}$ females, we

observed a higher expression of macrophage infiltration markers *Cd68* and *Adgre1* in this group (Figure 3. 4 D-E).

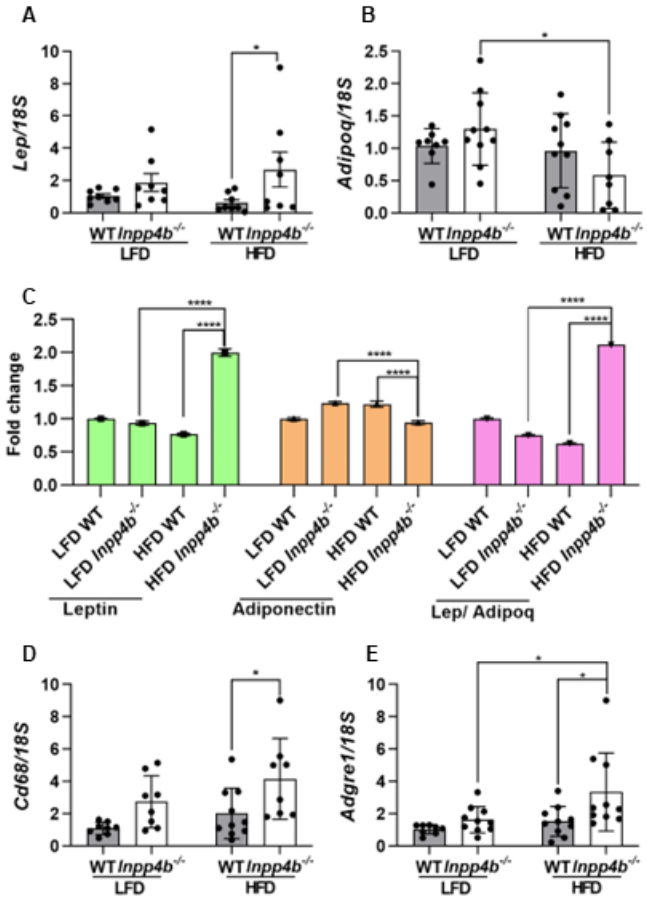


**Figure 3.4.** Leptin/Adiponectin pair and inflammation are altered in the mammary glands of HFD *Inpp4b*$^{-/-}$ females.
(A-B, D-E) The gene expression levels of (A) *Lep* (*p=0.0419), (C) *Adipoq* (*p=0.0104), (D) *Cd68* (*p=0.0228), and (E) *Adgre1* (left to right: *p=0.0200,*p=0.0131) in the mammary glands of LFD WT (N=8), LFD *Inpp4b*$^{-/-}$ (N=10), HFD WT (N=10), and HFD *Inpp4b*$^{-/-}$ (N=8) female mice were assayed by qRT-PCR using *18S* as an internal control. (B) Protein expression was determined for leptin and adiponectin in the mammary glands of the groups above (N=3 per group) using Proteome Profiler Mouse Adipokine Array Kit, ****p<0.0001. Data shown as mean ± SEM. Statistical analysis was performed using two-way ANOVA.

### 3.2.5. Loss of INPP4B leads to the fastest mammary gland tumor progression

HER2-positive breast cancer is one of the most aggressive molecular types of breast cancers, exhibiting worse clinical profile and relapse- free survival in patients with higher BMI and hyperglycemia [228, 229]. INPP4B is a well-documented tumor suppressor gene

in ER+ positive and triple negative breast cancers [78, 87, 96, 99, 230]; however, the role of INPP4B in HER2- positive breast cancer tumorigenesis was not fully explored.

Metabolic dysregulation in the HFD *Inpp4b*$^{-/-}$ group was described in Chapter 2, and we previously reported that *Inpp4b*$^{-/-}$ females on HFD exhibit hyperplasia of mammary ducts and end buds at the age of 17 weeks [166]. Despite these systemic and local abnormalities, HFD *Inpp4b*$^{-/-}$ mice do not develop mammary gland tumors. For that reason, we used transgenic mouse model with the mammary gland specific *ERBB2*- overexpression (*MMTV-ERBB2/+*) to study the role of INPP4B in breast cancer tumorigenesis. We tested whether *MMTV-ERBB2* transgenic mouse was appropriate to determine the role of INPP4B in the *ERBB2*- driven tumorigenesis by comparing the gene expression levels of *Inpp4b* in the mammary glands and tumors of normal and *ERBB2*- overexpressing females. The normal mammary glands from both WT and *MMTV-ERBB2/+*; +/+ females and mammary gland tumors of *MMTV-ERBB2/+*; +/+ mice express similar levels of *Inpp4b* (Figure 3.5. A). Thus, this model allows us to investigate the physiology of *ERBB2*- driven tumors in the presence and absence of INPP4B.

We compared tumor initiation and progression in the following 4 groups: LFD *MMTV-ERBB2/+; +/+*, LFD *MMTV-ERBB2/+; Inpp4b*$^{-/-}$, HFD *MMTV-ERBB2/+; +/+*, and HFD *MMTV-ERBB2/+; Inpp4b*$^{-/-}$. The *MMTV-ERBB2/+; Inpp4b*$^{-/-}$ groups showed worse survival rates compared to LFD *MMTV-ERBB2/+; +/+* groups in either diet (Median survival for +/+ mice: 263 days, *Inpp4b*$^{-/-}$ mice:179 days, p=0.0059 for LFD groups and Median survival for +/+ mice: 209 days, *Inpp4b*$^{-/-}$ mice:171 days, p=0.0418 for HFD groups) (Figure 3.5. B-C) without affecting tumor incidence. In addition, loss of INPP4B

accelerates tumor progression especially in HFD fed females (p=0. 0417 in LFD groups and p=0.0013 in HFD groups) (Figure 3.5 D-E).

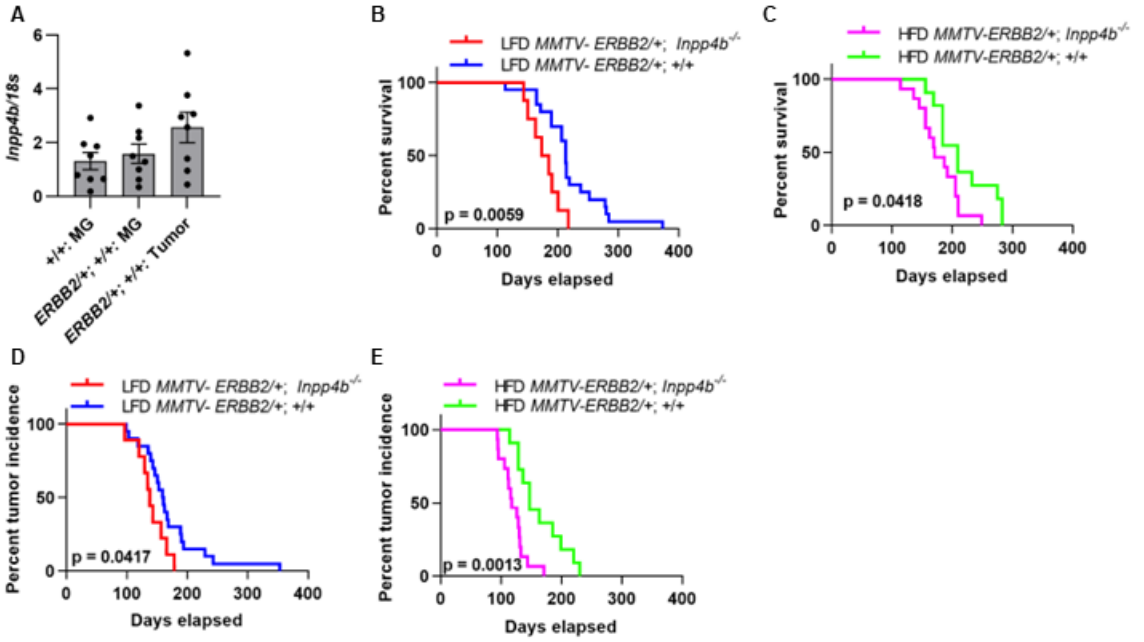


**Figure 3.5.** INPP4B and HFD take a role in tumor progression and overall survival of ERBB2- driven tumorigenesis.
(A) Gene expression of *Inpp4b* was determined in the WT mammary glands (N=8), *MMTV-ERBB2/+*; +/+ mammary glands (N=8), and *MMTV-ERBB2/+; +/+* tumors (N=8) by qRT-PCR and using *18S* as an internal control. Data shown as mean ± SEM. Statistical analysis was performed using one-way ANOVA. (B-C) Comparison of survival rates in (B) LFD *MMTV-ERBB2/+; +/+* (N=20), LFD *MMTV-ERBB2/+; Inpp4b*$^{-/-}$ (N=9), (C) HFD *MMTV-ERBB2/+; +/+* (N=11) and HFD *MMTV-ERBB2/+; Inpp4b*$^{-/-}$ (N=15) groups. (D-E) Comparison of tumor progression in the (D) LFD and (E) HFD groups described above.

### 3.2.6. Reduced p53 levels and signaling and altered lipid synthesis contribute to fastest tumor progression in HFD *MMTV-ERBB2/+; Inpp4b*$^{-/-}$ females

After assessing that INPP4B loss and HFD promote accelerated tumor progression and worse survival rates, we investigated the underlying molecular pathways which lead to this phenotype. In human breast cancer samples, we observed a positive correlation between INPP4B and p53 expression (r=0.3931, p<0.001) (Figure 3.6. A). In the tumors of HFD *MMTV-ERBB2/+; Inpp4b*$^{-/-}$ mice, we observed lower p53 protein levels as well as its

direct transcriptional target p21 (Figure 3.6. B-D). In addition, the protein levels of p53 and p21 were positively correlated in these tumors (r = 0.5691) (Figure 3.6. E). It appears that loss of INPP4B causes compensatory increase in p53 (Figure 3.3) and in order to ERBB2 driven tumors to develop, p53 has to be downregulated.

Aberrant cell metabolism is another factor that plays an important role in tumorigenesis [231, 232]. In particular, lipid metabolism is heavily dysregulated in HER2- positive breast cancers [233]. The oncogenic effects of CD36 and FABP4 in breast cancer have been shown previously [234]. In alignment with the literature, accelerated tumor progression is associated with increased expression of *Cd36* and *Fabp4* in the HFD *MMTV-ERBB2/+; Inpp4b*$^{-/-}$ group (Figure 3.6. F-G).

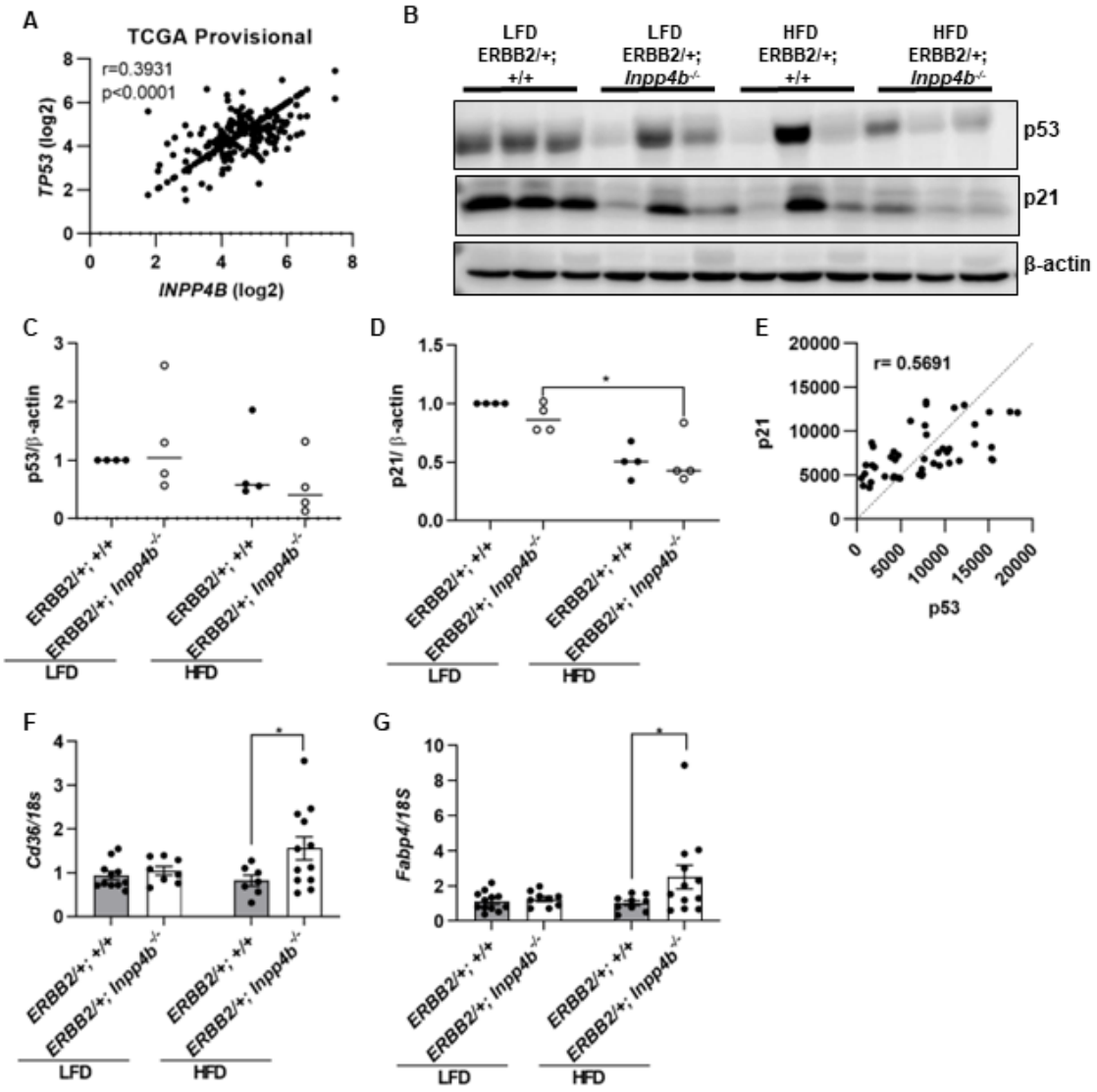


**Figure 3.6.** Driving mechanisms for faster progression in HFD *MMTV- ERBB2/+; Inpp4b*$^{-/-}$ tumors.
(A) Correlation of INPP4B and TP53 in 158 human breast cancer samples (TCGA, Provisional). (B-E) p53 and p21 expression in the tumors of LFD *MMTV-ERBB2/+;* WT, LFD *MMTV-ERBB2/+; Inpp4b*$^{-/-}$, HFD *MMTV-ERBB2/+;* WT, and HFD *MMTV-ERBB2/+; Inpp4b*$^{-/-}$ (N=9 per group). (B) Protein lysates from tumor samples of the indicated groups were analyzed for p53 and p21 and normalized using β-actin. (C-D) Quantification of panel for (C) p53 and (D) p21 (*p=0.0208). (E) Correlation of p53 and p21 in each tumor sample. (F-G) RNA was isolated from the tumors of LFD *MMTV- ERBB2/+;* WT (N=12), LFD *MMTV-ERBB2/+; Inpp4b*$^{-/-}$ (N=9), HFD *MMTV- ERBB2*; WT (N=9), and HFD *MMTV- ERBB2*; *Inpp4b*$^{-/-}$ (N=12). Gene expression levels of (F) *Cd36* (*p=0.0226), and (G) *Fabp4* (*p=0.0291) were assayed by qRT-PCR using *18S* as an internal control. *p<0.05, **p<0.01. Data shown as mean ± SEM. Statistical analysis was performed using two-way ANOVA.

## 3.3. Discussion

HER2- positive type has the second worse prognosis among the four molecular breast cancer subtypes [235]. More than 70% of breast cancers are hormone dependent; however, the most aggressive types are resistant to hormone therapies [236]. Obesity and metabolic diseases worsen postmenopausal breast cancer incidence and survival [237, 238]. Accumulating evidence suggests that obesity modulates steroid hormone receptor signaling and metabolism. Our group reported that INPP4B regulates AR transcriptional activity in normal prostate tissue and in prostate cancer [90, 181]. My data suggests that INPP4B improves insulin sensitivity and protects from diet induced obesity and inflammation of WAT in female mice. In this chapter, I showed that INPP4B protects from HFD induced changes in mammary gland development and HER2-driven tumorigenesis.

The main factor in the pubertal mammary gland branching is PR expression and transcriptional activity. The knockout of PR results in defective mammary gland morphogenesis [207, 239], while PR induces expression of various transcription factors such as Msx2 and Wnt4 in the mammary gland epithelium and leads to peripubertal lateral branching [219, 220]. We previously reported that *Inpp4b*$^{-/-}$ mice have fewer mammary gland ductal side branches, which was accompanied with reduced *Pgr* expression and its target amphiregulin levels [166]. In this research, I discovered that deletion of *Inpp4b* and HFD synergistically decreased transcriptional activity of PR, contributing to reduced ductal branching (Figure 3.1- 3.2).

Leptin and adiponectin are involved in breast cancer development through their effects on inflammation, which increases breast cancer progression [240]. Leptin shows pro-inflammatory effects and adiponectin has anti-inflammatory properties [226]. In the

mammary glands of HFD *Inpp4b*$^{-/-}$ females, I observed increased leptin and reduced adiponectin levels (Figure 3.3 A-C). Higher leptin to adiponectin ratio and induced inflammation (Figure 3.3 C-E) are aligned with the systemic leptin resistance in HFD *Inpp4b*$^{-/-}$ females and can potentially contribute to hyperplasia in this group.

INPP4B also impacts HER2/ERBB2 driven tumorigenesis. Loss of INPP4B led to worse survival in both LFD and HFD feeding. In addition, HFD accelerated tumor progression in *MMTV- ERBB2/+; Inpp4b*$^{-/-}$ females (Figure 3.5).

In both normal mammary glands and *ERBB2*- driven tumors, INPP4B loss altered p53 expression and signaling differently. In the normal mammary glands, p53 expression was higher in the *Inpp4b*$^{-/-}$ females independently of the diet; however, p21 levels were higher only in LFD *Inpp4b*$^{-/-}$ females (Figure 3.3). While this higher expression might be protective against epithelial cell proliferation and tumor development, it can contribute to the reduction of ductal side branching in the mutant females [215]. On the other hand, both p53 and p21 levels were reduced in HFD *MMTV- ERBB2/+; Inpp4b*$^{-/-}$ tumors, consistent with faster tumor development and worst survival rates (Figure 3.5- Figure 3.6), suggesting that increase in p53 has to be overcome in order for tumors to develop.

The most common metabolic dysregulation in HER2-positive breast cancers is the upregulation of lipid anabolism [241]. In our previous publication and in Chapter 2, I have reported that *Inpp4b* loss and HFD increase lipid anabolism in the livers of male and female mice, suggesting a role for INPP4B in overall lipid metabolism. Our initial findings showed that deletion of *Inpp4b* and HFD upregulate some of the lipid anabolism genes in *ERBB2*-positive tumors (Figure 3.6). However, more studies are required to reveal the role of INPP4B in the lipid metabolism of breast cancer.

In conclusion, I showed that INPP4B is involved in both normal mammary gland homeostasis and ERBB2-driven breast cancer tumorigenesis. Loss of *Inpp4b* reduced the number of ductal side branches along with the elevation of pAKT, p53, and p21 levels in normal mammary glands. Moreover, *Inpp4b* deletion and HFD led to a decrease in MEA through reduced PR expression and transcriptional activity, and also caused an increase in pAKT and p53 levels and the dysregulation of leptin signaling. In the *MMTV- ERBB2/+* tumors, *Inpp4b* loss resulted in faster tumor progression and worse survival rates. The decrease in p53 signaling and higher levels of lipid anabolism genes are contributing factors to the more severe phenotype in HFD *MMTV- ERBB2/+; Inpp4b*$^{-/-}$ females.

## 3.4. Materials & Methods

### Animal studies

*Inpp4b*-knockout mouse model and HFD strategy were described previously [18, 196] and in Chapter 2, which were used for the analysis of the normal mammary gland development and physiology. To investigate the role of INPP4B in *ERBB2*- driven mammary gland tumorigenesis, we used heterozygous FVB-Tg (MMTV-ErbB2) NK1Mul/J (referred as *MMTV- ERRB2/+* in the the text) [242]. *MMTV- ERRB2/+*; +/+ sires were bred with WT dams and *MMTV- ERRB2/+*; *Inpp4b*$^{-/-}$ sires were bred with *Inpp4b*$^{-/-}$ dams to generate offspring in desired phenotypes. The dams and litters were maintained on LFD or HFD as described in Chapter 2. For genotyping the following primers were used: Forward primer: 5'-atcaacgttttcttttccg-3', Reverse primer: 5'- atttgcctgcattaccggtc-3'. *MMTV- ERRB2/+*; +/+ and *MMTV- ERRB2/+*; *Inpp4b*$^{-/-}$ female mice on LFD or HFD were palpated twice a week after weaning to monitor tumor growth. Mice were euthanized and tumors dissected when tumors reached approximately 10% of the body weight of the mouse or when animals

exhibited signs of distress of morbidity. Tissue dissection was performed at diestrus stage of the estrous cycle, the assessment of the estrous cycle was described by Mclean et al. [198] and in Chapter 2. Tumors and organs were collected for gene, protein, and histological analysis. All experimental protocols were in accordance with the regulations of the Institutional Animal Care and Use Committees at Florida International University.

**Whole mount preparation and histological analysis of mammary glands**

The whole mount staining was described previously [166]. Briefly, inguinal murine mammary gland fat pads were flattened onto a pre-cleaned glass slide and incubated in ethanol/acetic acid (3:1) solution at room temperature for overnight. The whole mount staining solution was prepared by 0.2% Carmine red (Sigma-Aldrich, St. Louis, MO) and 0.5% aluminum potassium sulfate (Fisher, Waltham, MA) in distilled water. Fixed mammary glands were washed in 70% ethanol and distilled water. The slides were stained with Carmine Alum solution overnight. Stained mammary glands were dehydrated in graded ethanol and xylene, then were stored in toluene solution permanently (Sigma-Aldrich). The ImageJ software was used to count the number of ducts and to calculate the mammary epithelial area in LFD WT, LFD *Inpp4b*$^{-/-}$, HFD WT, and HFD *Inpp4b*$^{-/-}$ mammary glands as described by Tolg et al. and Stanko et al. respectively [243, 244].

**Adipokine array**

Protein was isolated from the mammary glands of the LFD WT, LFD *Inpp4b*$^{-/-}$, HFD WT, and HFD *Inpp4b*$^{-/-}$ females using a glass grinder and RIPA buffer with phosphatase and protease inhibitors. To measure adipokine leptin levels in the mammary glands, Proteome Profiler Mouse Adipokine Array Kit (# ARY013, R&D Systems, Minneapolis, MN) was used. The recommended protocol from the manufacturer was followed. The signal was

captured using LAS 500 imager and quantified by ImageQuant TL software (GE Healthcare, Chicago, IL).

**Determination of sex steroid hormone levels**

Serum samples from LFD WT, LFD *Inpp4b*$^{-/-}$, HFD WT, and HFD *Inpp4b*$^{-/-}$ females were sent out for the determination of sex steroid hormone levels. Collection of serum samples were described in Chapter 2. ELISA assays were performed to compare levels of estrogen (Calbiotech Inc, El Cajon, CA) and progesterone (IBL America, Minneapolis, MN) at the University of Virginia Center for Research at the Reproduction Ligand Assay and Analysis Core (University of Virginia, Charlottesville, VA).

**Gene expression analysis**

RNA was isolated from mouse tissues using Tri Reagent (Molecular Research Center, Cincinnati, OH). For the gene expression analysis in normal mammary glands, thoracic mammary glands of LFD WT, LFD *Inpp4b*$^{-/-}$, HFD WT, and HFD *Inpp4b*$^{-/-}$ were used. The RNA concentration was determined using NanoVue Plus (GE Healthcare BioSciences, Piscataway, NJ). The real-time quantitative reverse transcription (qRT-PCR) was done by Verso cDNA synthesis Kit (Thermo Fisher Scientific) and Roche 480 LightCycler (Roche, Basel, Switzerland). The corresponding primers and probes were designed from Universal Probe Library and listed in Table 4.

**Table 4.** Mouse gene primers and probes for qPCR analysis used in Chapter 3.

| Gene | Forward primer | Reverse Primer | Probe |
|---|---|---|---|
| *18S* | gcaattattccccatgaacg | gggacttaatcaacgcaagc | 48 |
| *Adgre1* | tgtcctccttgcctggac | gagacttctgagctgacactgc | 29 |
| *Adipoq* | ccatctggaggtgggagac | ctgcatagagtccattgtggtc | 1 |
| *Cd36* | tggccttacttgggattgg | ggatttgcaagcacaatatgaa | 9 |
| *Cd68* | tccactgttggccctcac | ccccttggaccttggacta | 10 |
| *Fabp4* | ggatggaaagtcgaccacaa | tggaagtcacgcctttcata | 31 |

| | | | |
|---|---|---|---|
| *Id4* | cagggtgacagcattctctg | ccggtggcttgtttctctta | 92 |
| *Lep* | cccaaaatgtgctgcagatag | ccagcagatggaggaggtc | 80 |
| *Msx1* | gacgcctttcaccacagc | tactgcttctggcggaactt | 21 |
| *Msx2* | aggagcccggcagatact | gtttcctcagggtgcaggt | 70 |
| *Pgr* | tgcacctgatctaatcctaaatga | ggtaaggcacagcgagtagaa | 17 |
| *Wnt4* | gggtggagtgcaagtgtca | cacgccagcacgtctttac | 92 |

**Western blot**

The protein was isolated from murine mammary glands or mammary gland tumors as described previously [181]. 25 µg of protein samples were loaded on 10-12.5% SDS-PAGE gels. The protein was transferred to a nitrocellulose or PVDF membrane, which was blocked using 5% BSA or 5% non-fat milk. The blot was incubated with primary antibodies against pAKT S473 (1:1000, #4051, Cell Signaling, Danvers, MA), total AKT (1:1000, #4691, Cell signaling), p53 (1:1000, #MS-187-P1, NeoMarker, Fremont, CA), p21 (1:1000, #6246, Santa Cruz, Dallas, TX), and β-actin (1:10 000, A5316, Sigma, St Louis, MO) overnight. Rabbit IgG (1:2000, W4011, Promega, Madison, WI) and mouse IgG (1:2000, W4021, Promega) were used as secondary antibodies. The signal was detected by LAS 500 imager and analyzed using ImageQuant TL software (GE Healthcare, Chicago, IL).

**Statistical analysis**

Two-way ANOVA (Sidak's multiple comparisons tests) for four groups and two tailed Student's t-test for two groups were performed using Prism 9.0. The p-values less than 0.05 were considered statistically significant. The data was present as mean ± SEM.

# 4. CHAPTER 4: Expression pattern and the roles of phosphatidylinositol phosphatases in testis

This chapter has been originally published in Biology of Reproduction, "Expression pattern and the roles of phosphatidylinositol phosphatases in testis", 2022, doi: 10.1093/biolre/ioac132

## 4.1. Abstract

Phosphoinositides (PIs) are relatively rare lipid components of the cellular membranes. Their homeostasis is tightly controlled by specific PI kinases and phosphatases. PIs play essential roles in cellular signaling, cytoskeletal organization, and secretory processes in various diseases and normal physiology. Gene targeting experiments strongly suggest that in mice with deficiency of several PI phosphatases such as *Pten*, *Mtmrs*, *Inpp4b*, and *Inpp5b*, spermatogenesis is affected, resulting in partial or complete infertility. Similarly, in men, loss of several of the PIP phosphatases is observed in infertility characterized by the lack of mature sperm. Using available gene expression databases, we compare expression of known PI phosphatases in various testicular cell types, infertility patients, and mouse age-dependent testicular gene expression, and discuss their potential roles in testis physiology and spermatogenesis.

## 4.2. Introduction

Obesity and metabolic syndrome are tightly linked with reduced fertility and these diseases are on the rise world-wide. In men, metabolic syndrome is associated with type 2 diabetes, obesity, and higher incidence of male infertility due to changes in testosterone and poor semen quality [245]. In mouse models of metabolic syndrome, *ob/ob* and *db/db*, the mutant

males have smaller testis and are infertile [246, 247]. In our recent reports, we show that *Inpp4b*$^{-/-}$ male mice develop metabolic syndrome, have smaller testis size, and reduced sperm counts, all of which are exacerbated by a high fat diet (HFD) [20, 196]. In mice, HFD alone causes reduced testis size, sperm number and motility, and impedes function of Sertoli and Leydig cells [248-253]. A major cause of metabolic syndrome is an impaired signaling by the insulin family of growth factors: insulin, IGF1, and IGF2. Sertoli cells specific knockout of insulin and IGF receptors caused 75% reduction in testis size, suggesting the importance of this pathway in testis physiology as well as metabolic syndrome [157]. Phosphoinositides are the key mediators of insulin – IGF receptors – PI3K signaling thereby activating multiple downstream pathways that are involved in metabolism, differentiation, cytoskeletal rearrangements, mitosis, and meiosis [254-256]. Single cell RNA sequencing of the human testis reveals relatively high expression in various cell types of the following PI phosphatases: PTEN, TPTE, MTMR2, MTMR5 (SBF1), INPP4A, INPP4B, TMEM55A, TMEM55B, SYNJ2, INPP5B, INPP5E, INPPL1. Genetic mutations of *Pten, Tpte, Mtmr2, Mtmr5, Inpp4b,* and *Inpp5b* resulted in various abnormal testicular phenotypes (Table 1). In this review we will focus on spatiotemporal testicular expression profiles of various PI phosphatases at different stages of mouse postnatal development, discuss their role in normal testis physiology, and review correlations between the expression of individual PI phosphatases and various types of infertility.

### 4.3. Testis morphology and function

Mammalian testis consists of two functionally and histologically distinct compartments: interstitial tissue and seminiferous tubules. Interstitial space contains Leydig cells, vascular

cells, macrophages, and some non-differentiated precursor cells [257, 258]. Leydig cells, the most abundant cell type in the interstitial compartment, are responsible for androgen synthesis, which is required for initiation of spermatogenesis [259]. Seminiferous tubules consist of peritubular myoid cells, Sertoli cells, and different stages of differentiating germ cells. Sertoli and peritubular myoid cells form the blood-testis barrier, providing support for the germ stem cells and nutrition for developing spermatogonia [260, 261] (Figure 4.1. A).

Spermatogenesis is the process of formation of mature haploid spermatozoa from the diploid spermatogonial stem cells (SSCs) through a series of mitotic and meiotic divisions and maturation of spermatids into spermatozoa in the lumen of seminiferous tubules. The first stages of spermatogenesis represent spermatocytogenesis and spermatidogenesis in which germ cell progenitors produce spermatogonia and primary and secondary spermatocytes by undergoing sequential mitosis, meiosis I, and meiosis II [262-264]. During spermiogenesis haploid spermatids no longer divide, but undergo multiple changes including cytoplasmic shedding, cytoskeleton reorganization, flagellum formation, genome condensation, and histone modifications [265, 266].

Spermatogenesis is a continuous process during adult life in both mice and men, and each stage is separated spatially in different sections of the seminiferous tubules. The time required to complete spermatogenesis from differentiation of spermatogonia to mature sperm is 64 days in men and 35 days in mice [267]. The differentiation of the first subset of spermatogonia into spermatozoa starts at birth and is called the first wave of spermatogenesis [268]. In men, mitotic divisions begin at birth and continue until prepubertal age. In mice, first mitotic division occurs between the first and eighth day

postpartum [269]. In men, meiosis is initiated between 10 and 12 years and in mice between 8-18 days postpartum, corresponding with pre-puberty for both species [263, 264, 269, 270]. Spermiogenesis starts at puberty in men and occurs between 18 and 30 days postpartum in mice [267, 269, 271].

Human and mouse testes are functionally and histologically similar [272] (Figure 4.1. A) which is supported by high degree of conservation in gene expression during testicular development and spermatogenesis in mice and men [273, 274].

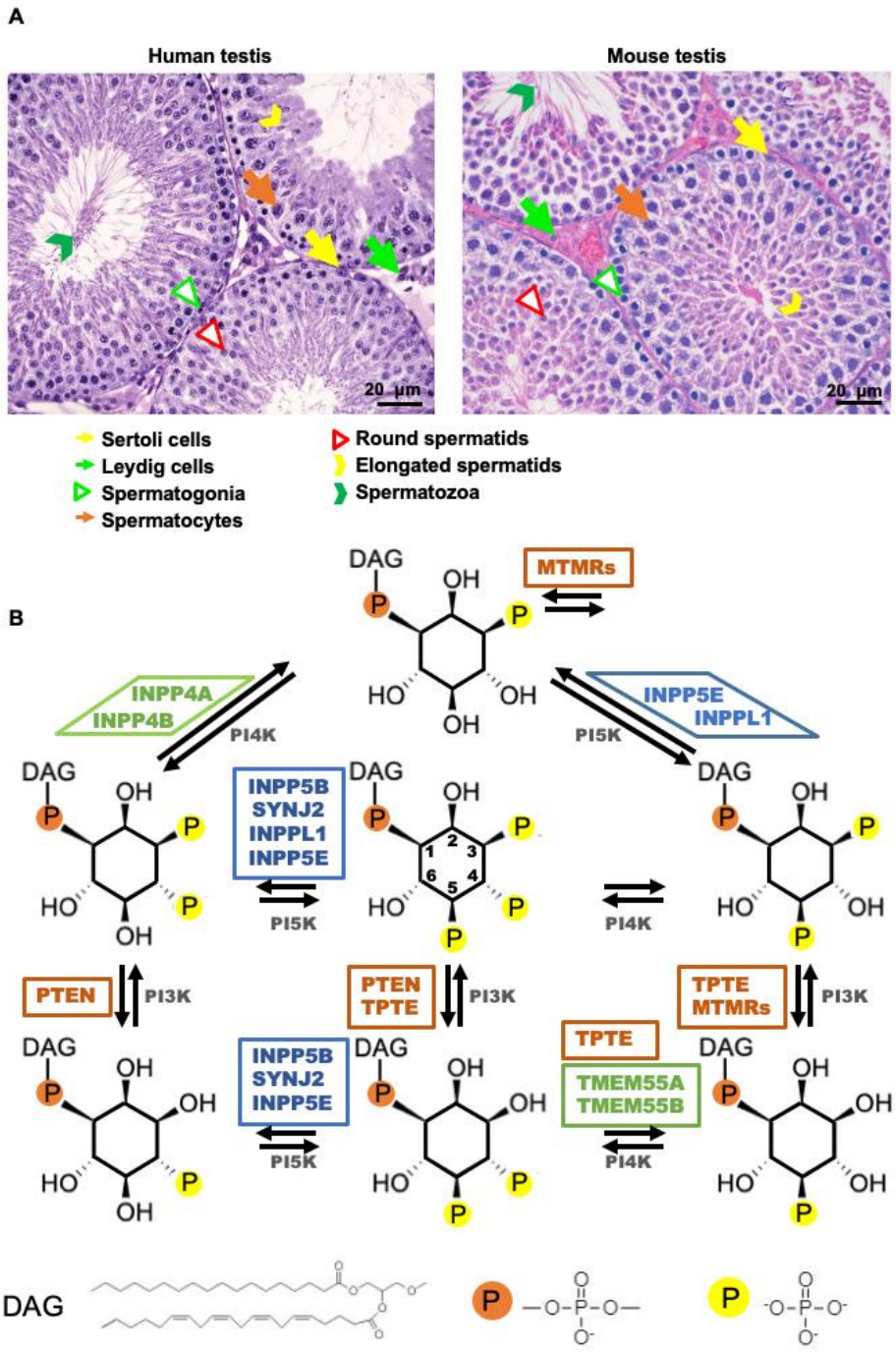


**Figure 4.1.** Testis histology and PI signaling.
A) Adult human (left) and mouse (right) testes histology. Distinct somatic and germ cells are marked with indicated arrows and arrowheads. B) Schematic diagram of PIP biogenesis and associated enzymes. Individual hydroxyl residues of the inositol group on the phosphatidylinositol molecule are phosphorylated by phosphatidylinositol 3, 4, and 5 kinases (PI3K, PI4K, and PI5K respectively) marked in gray. Site-specific phosphate groups are dephosphorylated by site-specific lipid phosphatases. Arrows indicate the direction of enzymatic reactions and kinases and phosphatases mediating these reactions are marked next to the corresponding arrow. PI-3 phosphatases are marked in red, PI-4 phosphatases in green, and PI-5 phosphatases in blue.

### 4.4. Evaluation of phosphatidylinositol signaling pathway (PIP) in testis

Phosphoinositides (PIs) are membrane phospholipids comprising two fatty acids linked via glycerol backbone to water-soluble inositol group. Phosphorylation and dephosphorylation of the hydroxyl groups on the inositol ring at D-3, D-4, or D-5 positions result in synthesis of the functionally distinct PIs: PI3P, PI4P, PI5P, PI(3,4)$P_2$, PI(4,5)$P_3$, PI(3,5)$P_2$ and PI(3,4,5)$P_3$ [21-23, 275] (Figure 4.1. B). The maintenance of phosphoinositide homeostasis is critical for the integrity of the cellular membrane, signal transduction, intracellular membrane trafficking, cytoskeleton remodeling, organelle biogenesis, and cell growth and survival [25, 26].

There is strong evidence in both *Mus musculus* and *Drosophila melanogaster* that PI signaling is obligatory for male fertility [10], suggesting an important role for PI phosphatases in testis development and physiology (Table 1). PI(3,4,5)$P_3$ is required for gonocyte proliferation [276] while dephosphorylation of PI(3,4,5)$P_3$ promotes gonocyte quiescence and differentiation [277, 278] as well as maintenance of spermatogonial stem cells [152, 279]. PI(4,5)$P_2$ itself and products of its enzymatic cleavage by PLC, diacylglycerol and inositol polyphosphate, are essential for late stages of spermatogenesis, production [280, 281] and successful capacitation of mature sperm [282], as well as the formation of adherens junctions in Sertoli cells [283].

We used reports and databases on genetically engineered mouse models, single cell RNA sequencing of human testis, and gene expression analysis in testes of healthy and infertile men to compare the roles of different phosphatases in testis physiology. Phosphatases *Pten*, *Tpte*, *Mtm1*, *Mtmr2*, *Mtmr5 (Sbf1)*, *Mtmr14*, *Inpp4b*, and *Inpp5b* have been reported to regulate testis development and spermatogenesis. Known knockout and transgenic models

of PI phosphatases are summarized in Table 5. The knockout models clearly show that PI-3, PI-4, and PI-5 phosphatases perform critical functions in spermatogenesis and are essential for optimal fertility.

**Table 5.** Testicular phenotypes in mice with genetically modified expression of the PI phosphatases.

| Group | Members | Mouse Model/ Phenotype | Reference |
|---|---|---|---|
| PI-3 phosphatases | PTEN | *$Pten^{LoxP/LoxP}$: Alpl-$Cre^{+}$* primordial germ cell specific *Pten* knockout accelerates embryonic germ cell proliferation and causes testicular teratoma.<br><br>*$Pten^{LoxP/LoxP}$: Stra8-$Cre^{+}$* and *$Pten^{LoxP/LoxP}$: Ddx4-$Cre^{+}$* postnatal germ cell *Pten* knockouts cause depletion of spermatogonial cells and infertility.<br><br>*Absence of Pten restores abnormal sperm count and testis size in $Pten^{LoxP/LoxP}$; $Insr^{LoxP/LoxP}$; $Igf1r^{Loxp/LoxP}$; Amh-$Cre^{+}$ mouse model.*<br><br>*Pten $^{LoxP/LoxP}$; $Ctnnb1^{Lox(ex3)/+}$; Amhr2-$Cre^{+}$* mice experience seminiferous tubule degeneration and testicular tumorigenesis. | [152, 276, 279, 284, 285] |
| | TPTE | *$Tpte^{-/-}$* mice have reduced sperm motility during capacitation. | [282] |
| | MTM/MTMRs | Hemizygous *Mtm1* p.R69C mutant males have severely reduced reproductive capacity resulting in infertility.<br><br>*$Mtmr2^{-/-}$* mice have azoospermia.<br><br>*$Sbf1^{-/-}$* (*$Mtmr5^{-/-}$*) mice have smaller testis size and are infertile due to azoospermia.<br><br>*$Mtmr14^{-/-}$* mice have smaller testis and reduced fertility due to decreased acrosomal reaction. | [286-289] |

| | | | |
|---|---|---|---|
| PI-4 phosphatase | INPP4B | *Inpp4b*$^{-/-}$ knockout mice display smaller testis size and reduced sperm count. | [196] |
| PI-5 phosphatase | INPP5B | *Inpp5b*$^{-/-}$ knockout mice display reduced sperm motility, reduced fertilization and accumulation of abnormal vacuoles in Sertoli cells. | [283, 290] |

Recent reports of single cell RNA sequencing of human testis allowed for comparison of expression levels and cell type specificity of phosphatases expression (Fig. 2-4). To compare expression of various PI phosphatases in distinct testicular cell pools, we investigated the Human Testis Atlas created by Guo *et al.* [291] (https://humantestisatlas.shinyapps.io/humantestisatlas1/), (GSE120508), which contains scRNA-seq data from the testes of three healthy adults at the ages of 17, 24, and 25. The cells were sorted into eight different stages of spermatogenesis spanning SSC to mature sperm and five types of stromal cell pools: macrophages, endothelial cells, myoid cells, Sertoli, and Leydig cells. To investigate changes in expression of PI phosphatases in various types of human male infertility, we used a dataset (E-TABM-1214) from the study performed by Chalmel *et al.* [292]. Testes from pre-pubertal cryptorchid men with low levels of spermatogonial cells (N=10), infertile patients with empty seminiferous tubules or tubules with Sertoli only (N=8), spermatogonia only (N=3), spermatogonia and spermatocytes (n=8), and different stages of spermatids (N=11) as well as healthy control men (n=8) were used to create this dataset. To compare the expression of PI phosphatases in mice, we used GSE12769 dataset which reported testicular gene expression in postnatal 0-, 3-, 6-, 8-, 10-, 14-, 18-, 20-, 30- and 35-day old mice. The expression data were averaged in three age groups: mitotic (day 0-8, N=8), meiotic (day 10-18, N=6), and complete

spermiogenesis (day 20-35, N=6). For male infertility and mouse postnatal testis expression values, the data were presented as mean ±SEM. One-way ANOVA (Dunnett's multiple comparison test) and two tailed t-test were performed using Prism 9.3, and a p-value <0.05 was considered statistically significant. Only genes that were detected in all three datasets were used for comparison. The graphical abstract was created in part with BioRender.com.

### 4.5. PI-3 phosphatases

**PTEN**

Phosphatase and tensin homolog (PTEN) is a dual specificity phosphatase that dephosphorylates $PI(3,4,5)P_3$ and $PI(3,4)P_2$ on the D-3 position of the inositol ring as well as phospho-tyrosine residues [293-295]. Previous studies demonstrated that PTEN acts as a tumor suppressor and metabolic regulator by inhibiting PI3K/AKT pathways [296-298]. The role of PTEN in metabolism was investigated by the conditional knockout of *Pten* in mouse models in several organs such as liver, skeletal muscle, or fat tissue. The liver specific knockout of *Pten*, $Pten^{LoxP/LoxP}$*: Alb-*$Cre^{+}$, caused insulin hypersensitivity, hepatosteatosis, dysregulation of lipid metabolism, and hepatocellular carcinoma [299]. Increasing the dose of *Pten* by transgenesis of BAC carrying *Pten* gene and its regulatory regions in mouse ($Pten^{tg}$) increased mouse lifespan, energy expenditure, and protected from metabolic dysfunction [300]. Significantly, metabolic disorders negatively affect testicular function and fertility in both mice and men [301-305]. Mutations in *PTEN* lead to hereditary disorders such as Cowden's syndrome, which are associated with the development of various neoplasms, including testicular tumors [306]. In human and mouse testes, PTEN is expressed in both germ and stromal cells (Figure 4.2. A) [307]. *Pten*

knockout in primordial germ cells, *Pten$^{LoxP/LoxP}$: Alpl-Cre$^{+}$*, resulted in higher pluripotency of the primordial germ cells, increased proliferation, and apoptosis in embryonic testis, and development of testicular teratomas after birth [276]. Conditional inactivation of *Pten* in postnatal male germ cells, *Pten$^{LoxP/LoxP}$: Ddx4-Cre$^{+}$*, caused smaller testis and led to infertility due to a depletion of the SSC population and absence of round spermatids by 21 days postpartum (dpp), making most of the seminiferous tubules appear empty by 28 dpp [152]. In *Pten$^{LoxP/LoxP}$: Stra8-Cre$^{+}$* mouse model, *Pten* deletion in postnatal germ cells reduced SSC self-renewal capacity. This particular *Pten* deficiency caused early spermatogonial differentiation and abnormal growth of testis at 50 days of age. After 60 dpp, spermatogenesis was impaired, and the males became infertile [279]. As a suppressor of AKT signaling, PTEN affected the function of Sertoli cells by regulating the IGF/insulin/PI3K/AKT signaling cascade. The knockout of *Insr* and *Igf1* caused a reduction in testis size, sperm production, and Sertoli cell proliferation. The conditional knockout of *Pten* in Sertoli cells and the absence of *Igf1* and *Insr*, *Pten$^{LoxP/LoxP}$;Insr$^{LoxP/LoxP}$;Igf1r$^{Loxp/LoxP}$; Amh-Cre$^{+}$*, restored the testis size and sperm count, while *Pten* ablation alone affected neither testis size nor sperm production [284]. The *Pten* knockout with a concomitant expression of stabilized form of β-catenin [308] in Sertoli cells, *Pten$^{LoxP/LoxP}$; Ctnnb1$^{Lox(ex3)/+}$; Amhr2-Cre$^{+}$*, males caused degeneration in the seminiferous tubules due to loss of germ cells and formation of large vacuoles in Sertoli cells at 21 dpp [285]. Microtumors formed in 100% *of the* mice by 5 weeks of age, with bilateral tumors at 6 months. Metastasis to the lungs begun to appear at 4 months. However, conditional ablation of *Pten* alone using *Amhr2-Cre* did not cause any testicular degeneration, abnormal cell proliferation, or neoplastic transformation [285]. These

findings suggested that conditional knockout of *Pten* in germ cells results in infertility, however, *Pten* ablation in Sertoli cells is insufficient to induce testicular degeneration. Thus, in germ cells PTEN is required for spermatogenesis and SSC maintenance. In Sertoli cells, PTEN suppresses PI3K/AKT and Wnt/ β-catenin signaling, maintaining Sertoli cell proliferation and ability to support maturation of germ cells.

Comparison of the *PTEN* total testicular expression between healthy men and men with various types of infertilities showed no significant differences due to relatively high expression of PTEN in all testicular cells (Figure 4.2. B). In mice, *Pten* expression did not change with the onset of the spermatogenesis in testis between days 0 to 8 (mitotic stage), days 10 to 18 (meiotic stage), and days 20 to 35 (spermiogenesis) consistent with the ubiquitous pattern of its expression (Figure 4.2. C). Our analysis shows that PTEN is abundant in all fractions of testis in both humans and mice and that loss of specific cell populations associated with infertility is not associated with changes in *PTEN* expression.

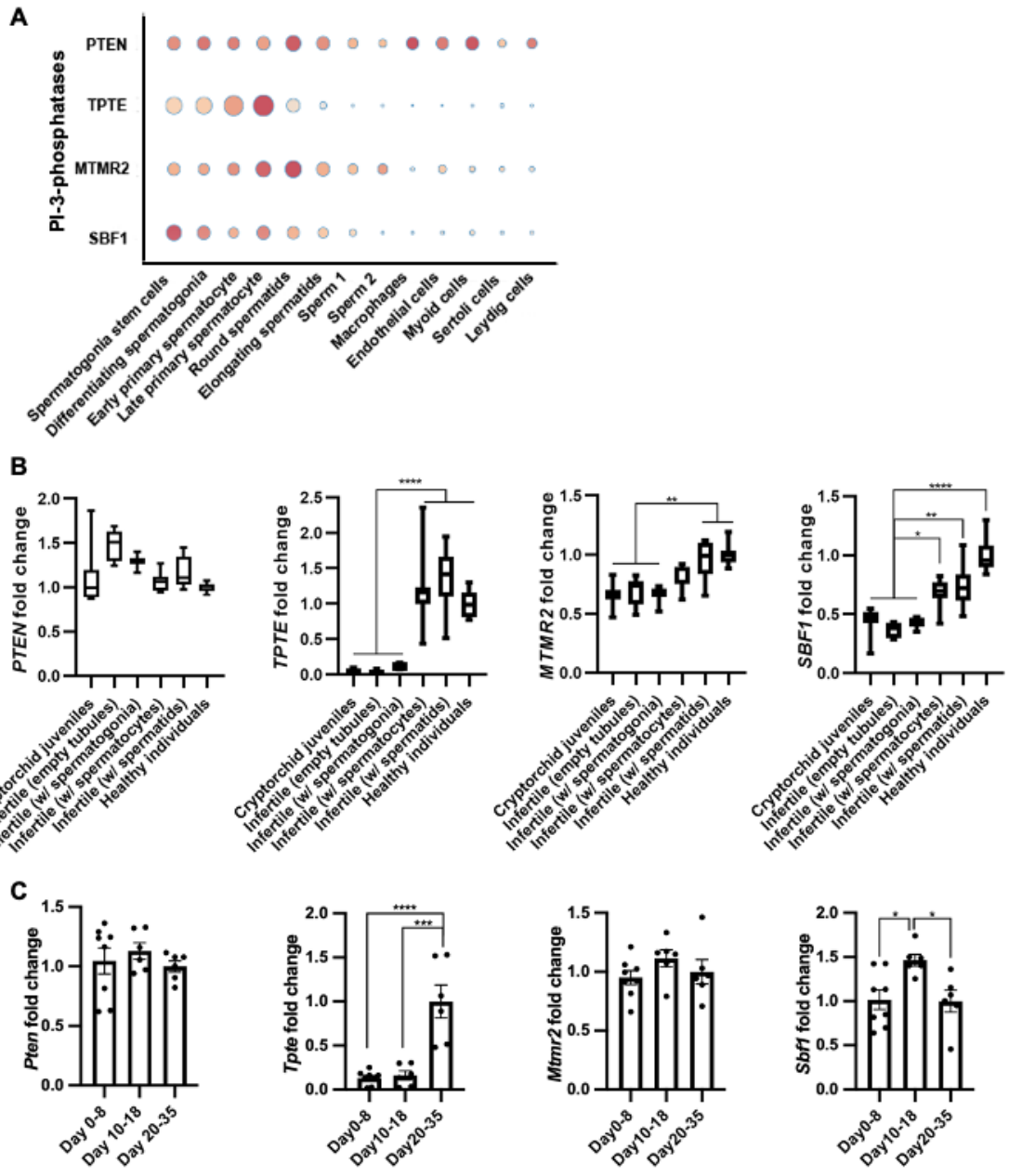


**Figure 4.2.** Expression profiles of 3-phosphatases

The changes in expression levels of 3-phoshatases *PTEN*, *TPTE*, *MTMR2* and *MTMR5* in different human testicular cell populations (A), in patients with different types of infertility (E-TABM-1214) (B), and mouse postnatal testis development study (GSE12769) (C). For panels B and C, one-way ANOVA was used. *p<0.05, **p<0.01, ***p<0.001, ****p<0.0001.

**TPTE (PTEN2)**

Transmembrane Phosphatase with Tensin homology (TPTE) is a member of the voltage-sensitive phosphatase (VSP) family and a highly conserved homolog of PTEN [309, 310], which dephosphorylates $PI(3,4,5)P_3$ and $PI(3,5)P_2$ on the D-3 position, as well as $PI(4,5)P_2$ on D-4 position of the inositol ring [282, 311]. There are two paralogs, *TPTE* and *TPTE2* (TPIP), in primates and a single ortholog, *Tpte,* in rodents [311, 312]. TPTE is defined as a Cancer/Testis (CT) antigen, and antibodies against CT are found in lung and head and neck cancers [313, 314]. In both human and mouse testes, *TPTE* (*Tpte* in mice) is expressed in several types of germ cells (Figure 4.2. A and 4.2. C), most highly in spermatocytes and early spermatids [315]. *Tpte*$^{-/-}$ knockout mice exhibited abnormal motility during capacitation and lower fertilization rate, caused by the high levels of $PI(4,5)P_2$, and $Ca^{2+}$ influx in sperm tail [282].

According to data from the human infertility study, the expression of *TPTE* in the healthy control men and infertile men with spermatocytes and spermatids is five times higher than in cryptorchid individuals and other severely infertile groups that lack spermatids and mature sperm (Figure 4.2. B). In mice, the expression of *Tpte* increases significantly after the first wave of meiosis, when spermatids are first differentiated (Figure 4.2. C). Our findings and accumulated data suggest that TPTE may play a role in the later stages of spermatogenesis in both species and is important for male fertility [315].

**MTM/MTMRs:**

The myotubularin (MTM) / myotubularin- related (MTMR) proteins are members of a PI-3 phosphatase family that dephosphorylate PI(3)P and $PI(3,5)P_2$ [316-320]. The mutations of *MTM1* and *MTMR2/5/13* result in myo- and neuropathies, X-linked myotubular

myopathy (XLMTM), and Charcot-Marie-Tooth disease, respectively [321-323]. Some members of MTM/MTMR family, such as *Mtm1, Mtmr2, Sbf1 (Mtmr5)* and *Mtmr14*, regulate both metabolic health and male infertility. While *Mtm1*$^{-/-}$ pups die at birth, hemizygote p.R69C mutant males are viable but have reduced fertility. In addition to reduced fertility, *Mtm1* p.R69C mice display muscular weakness mimicking XLMTM. They do not, however, lack mature sperm or have testicular defects. Thus, the reduced fertility in *Mtm1* p.R69C mice may be secondary to muscle weakness, rather than abnormalities in spermatogenesis [288]. While SFB1 is catalytically inactive, it forms a heterodimer with the catalytically active MTMR2, thus enhancing its enzymatic activity [324]. In seminiferous tubules, MTMR2-SFB1 complexes are found at Sertoli and germ cell membrane junctions contributing to maintenance of the blood-testis barrier [325, 326]. By 4 months, *Mtmr2*$^{-/-}$ males exhibited disrupted spermatogenesis due to depletion of elongated spermatids [286]. *Sbf1*$^{-/-}$ mice displayed smaller testis size and were infertile due to lack of epididymal sperm. By 17 dpp, the deficiency of SBF1 led to abnormalities in Sertoli cells, vacuoles in seminiferous tubules, and interruptions in the meiotic division of spermatogonia [287]. Consistent with the phenotype of *Sbf1*$^{-/-}$ males, infertile patients with testicular failure and nonobstructive azoospermia revealed high rate of heterozygous SNP in *SBF1* gene locus [327]. *Mtmr14*$^{-/-}$ mice displayed both metabolic and reproductive phenotypes. The knockout males fed HFD exhibited weight gain, hyperglycemia, obesity, and inflammation [328]. In addition, *Mtmr14*$^{-/-}$ males showed smaller testis size, decreased muscle force of the vas deferens, reduced total sperm count and increase in immobile sperm caused by high apoptosis rate, and decreased acrosomal reaction caused by $Ca^{2+}$ imbalance

[289]. It is likely that some of the reproductive defects of *Mtmr14*$^{-/-}$ males were secondary to their metabolic dysfunction.

Consistent with their heterodimeric mode of action, *MTMR2* and *SBF1* expression in men showed significant spatial overlap with the highest mRNA levels in germ cells (Figure 4.2. A). Expression of *MTMR2* and *SBF1* is lower in cryptorchid patients and in severely infertile individuals with Sertoli cells or spermatogonia-only tubules compared to the infertile individuals with spermatids and the healthy control men (Figure 4.2. B), supporting their role in early stages of spermatogenesis. The mouse data showed little change in *Mtmr2* expression in testis with the onset of spermatogenesis and a small burst of expression of *Sbf1* with the first wave of spermatogenesis suggesting functional differences between human and murine orthologs in testis development (Figure 4.2. C).

### 4.6. PI-4 phosphatases

**INPP4A & INPP4B:**

Inositol polyphosphate 4- phosphatase type-II A and type-II-B (INPP4A and INPP4B) are PI-4 phosphatases that dephosphorylate D-4 position of PI(3,4)$P_2$ [329, 330]. INPP4A is expressed in the brain, and its loss causes neurodegeneration and inflammation [331, 332]. INPP4B is expressed more broadly and functions as a tissue-specific tumor suppressor and a metabolic regulator [20, 88, 91, 182].

The role of INPP4A in testis has not been investigated. In human testis, *INPP4A* is expressed in the early stages of spermatogenesis, mostly in SSCs and spermatogonia (Figure 4.3. A). Expression of *INPP4A* is significantly higher in cryptorchid individuals due to arrest of spermatogenesis at the spermatogonia stage and relative increase in abundance of SSC and spermatogonia compared to testes of healthy men and men with

other types of infertility (Figure 4.3. B). *Inpp4a* expression in mouse testis is similar at the different stages of mouse testis development suggesting a divergent expression pattern for these orthologs (Figure 4.3. C).

Recently, we have shown that INPP4B is highly expressed in post-meiotic germ cells in both humans and mice [196]. *Inpp4b*-deficient male mice exhibited significantly smaller testes size and decreased sperm production. A higher rate of apoptosis, decrease in the expression of meiotic marker γH2A.X, and lower testicular gene expression of critical steroidogenic enzymes were observed in testes of *Inpp4b*$^{-/-}$ males. HFD exacerbated both metabolic and reproductive changes in knockout males [196]. In men, *INPP4B* testicular expression was highest in the post-meiotic germ cell populations, round and elongating spermatids, and in sperm (Figure 4.3. A). Comparison of *INPP4B* expression in infertile patients showed high expression only when spermatids were present with further increase in healthy men (Figure 4.3. B). Similarly, *Inpp4b* expression in mice is low before the appearance of spermatids at 20 dpp (Figure 4.3. C). The expression pattern of *INPP4B* in post-meiotic germ cells in both species suggests that it plays a role in the later stages of spermatogenesis. In addition, some of the fertility defects in the *Inpp4b*$^{-/-}$ males, especially when they are fed HFD, could be secondary to their metabolic syndrome [20].

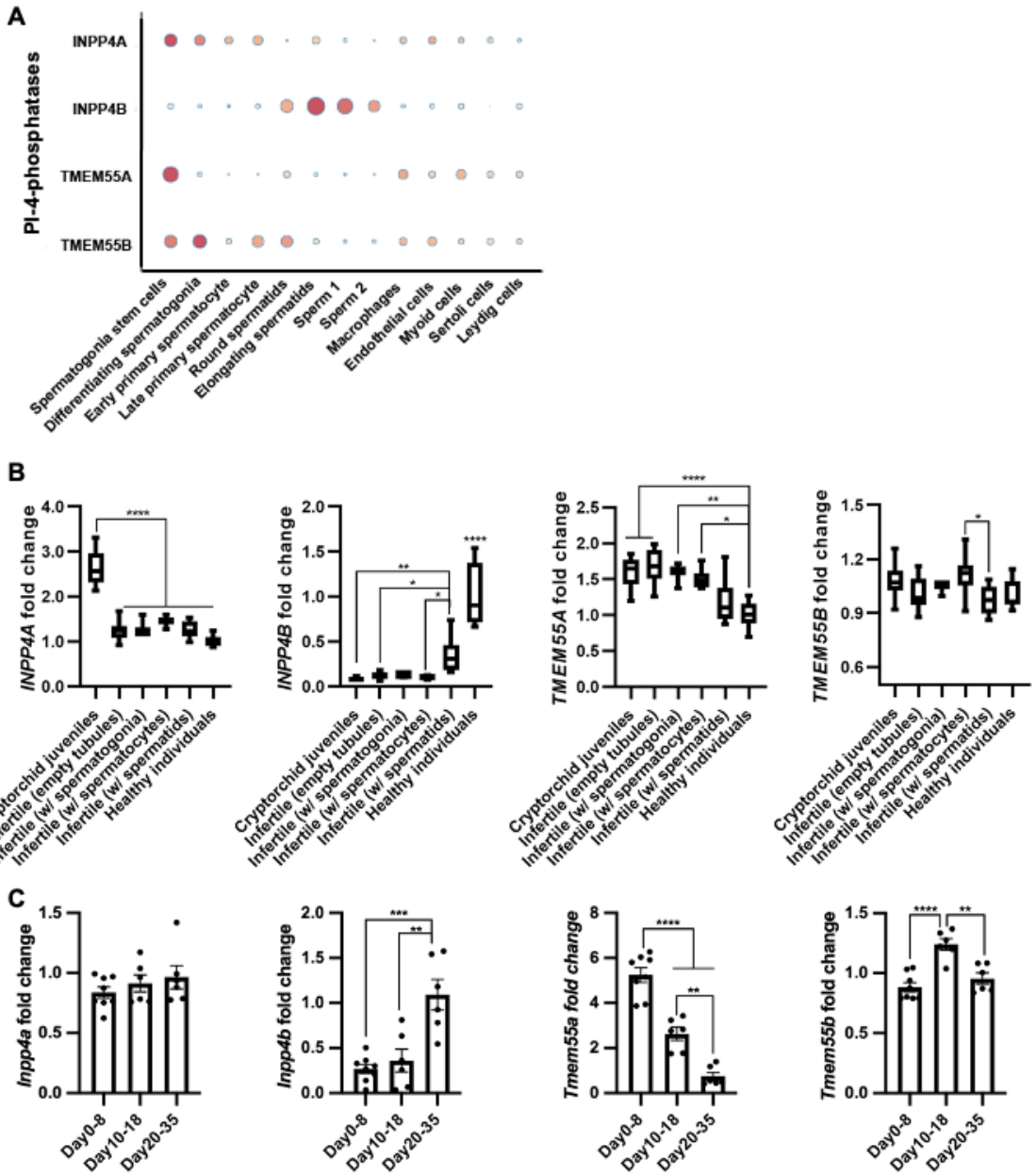


**Figure 4.3.** Expression profiles for 4-phosphatases.
The changes in expression levels of 4-phoshatases *INPP4A*, *INPP4B*, *TMEM55A* and *TMEM55B* in different human testicular cell populations (A), testes of patients with different types of infertility (E-TABM-1214) (B), and mouse postnatal testis development study (GSE12769) (C). For panels B and C, one-way ANOVA was used. *p<0.05, **p<0.01, ***p<0.001, ****p<0.0001

### TMEM55A & TMEM55B:

Transmembrane proteins 55A and 55B (TMEM55A and TMEM55B) belong to PI-4 phosphatases family, and dephosphorylate $PI(4,5)P_2$ [333]. TMEM55A activity is

inversely correlated with phagocytosis in macrophages [334], and TMEM55B is important for lysosomal homeostasis [335, 336]. TMEM55B also has an important role in cholesterol metabolism; HFD-fed *Tmem55b* knockdown mice show an increase in blood cholesterol levels and impaired lysosomal LDLR degradation in hepatocytes [337, 338].

The role of TMEM55 phosphatases in testis has not been reported. In men, expression of *TMEM55A* is restricted mainly to the SSC population and *TMEM55B* expression is relatively high in mitotic to early post-meiotic cells (Figure 4.3. A). No biologically significant difference in expression of *TMEM55A* and *TMEM55B* is apparent in various types of infertility (Figure 4.3. B). Surprisingly in mice, *Tmem55a* expression plunges with onset of spermiogenesis (day 20-35) with little change in *Tmem55b* levels (Figure 4.3. C). Expression of TMEM55A and TMEM55B in SSC warrants further investigation of their function in spermatogenesis.

### 4.7. PI-5 phosphatases

**INPP5B**

Inositol polyphosphate 5- phosphatase B (INPP5B) is a member of type II PI-5 phosphatases, which dephosphorylates PI(3,4,5)$P_3$ and PI(4,5)$P_2$ at D-5 position of the inositol ring. *Inpp5b*$^{-/-}$ male mice had impaired epididymal maturation resulting in reduced sperm count, motility, and velocity and inability to fertilize zona pellucida (ZP)-intact eggs [290]. Since haploid sperm-specific knockout *Inpp5b*$^{LoxP/LoxP}$: *Prm-Cre*$^{+}$ was fully fertile, abnormalities in sperm maturation and function in *Inpp5b*$^{-/-}$ males are not intrinsic to sperm themselves, but rather are the consequence of abnormal Sertoli development. Sertoli cells of the knockout males accumulated abnormal early endosomes due to disrupted endocytosis and recycling of plasma membranes containing adherens junction complexes.

Elevated levels of $PI(4,5)P_2$, the INPP5B substrate, affected the polymerization of actin cytoskeleton and internalization of the membrane junction protein complexes [283].

In men, *INPP5B* expression is abundant in Sertoli cells and all pre-meiotic cells with the highest expression level in the SSC (Figure 4.4. A). The expression of *INPP5B* is slightly higher in the infertile individuals with SSC and spermatogonia than in healthy control men (Figure 4.4. B), which can be explained by relatively high ratio of early germ cells in this infertile group that lack sperm. In mouse testis, the expression of *Inpp5b* is approximately two times higher in the meiotic stage than premeiotic stage and in late spermiogenesis (Figure 4.4. C). Thus, INPP5B may have a role in the early stages of spermatogenesis in addition to its role in membrane recycling demonstrated in the mouse knockout studies.

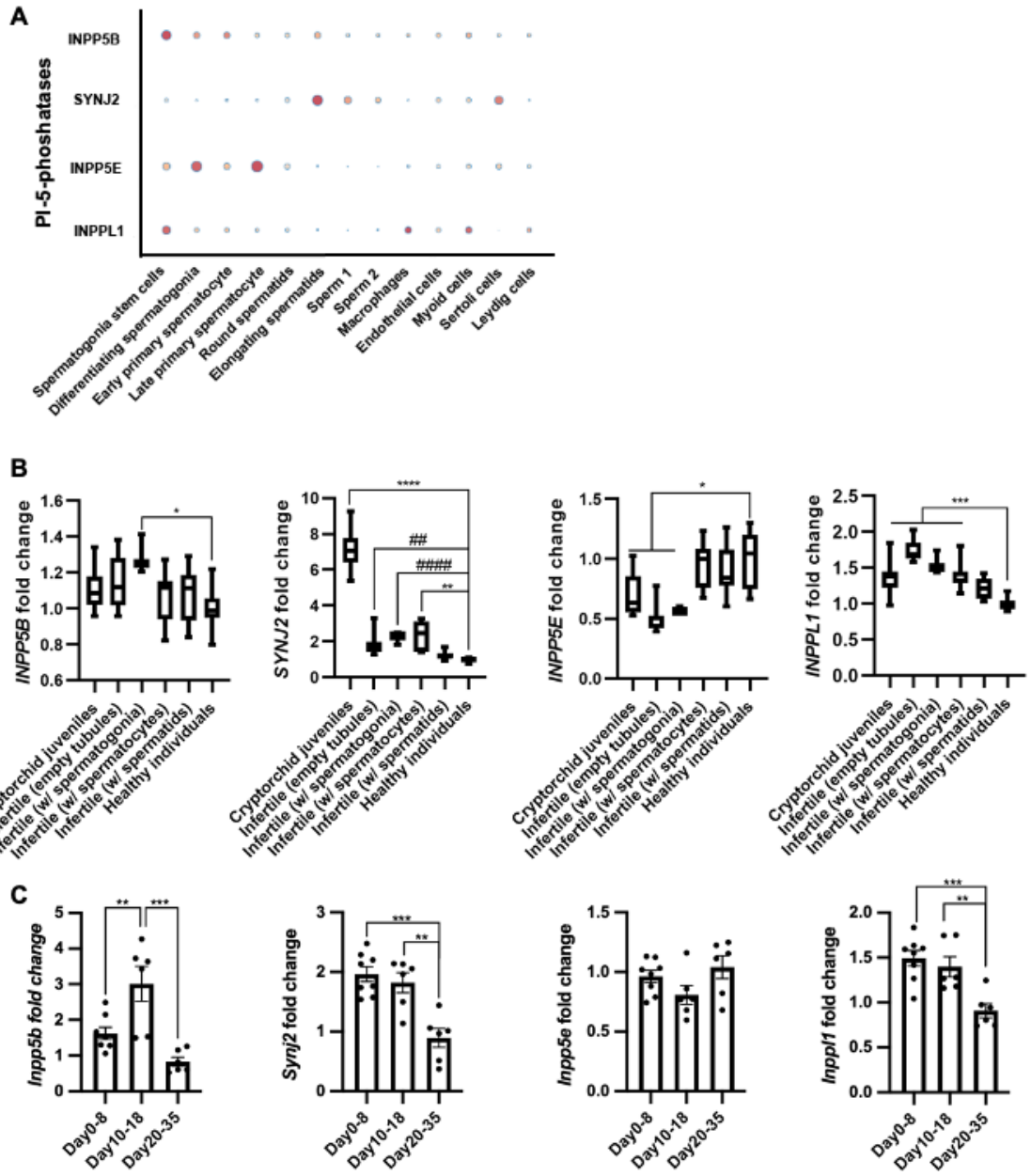


**Figure 4.4.** Expression profiles for 5-phosphatases.
The changes in expression levels of 5-phoshatases *INPP5B*, *SYNJ2*, *INPP5E* and *INPPL1* in different human testicular cell populations (A), testes of patients with different types of infertility (E-TABM-1214) (B), and mouse postnatal testis development study (GSE12769) (C). For panels B and C, one-way ANOVA was used. *p<0.05, **p<0.01, ***p<0.001, ****p<0.0001. For panel B, two tailed t-test was used to evaluate changes in *SYNJ2* expression in testes of healthy men and infertile men with empty tubules and tubules with spermatogonia only. ##p=0.0033, ####p<0.00001.

**Synaptojanins:**

Synaptojanins 1 and 2 are paralogs (SYNJ1 and SYNJ2) and type II PI-5 phosphatases. They have two phosphatase domains: inositol-5-phosphatase domain and suppressor of actin1 (Sac-1)-like phosphatase domain with broader phosphoinositide phosphatase activity [339-341]. SYNJ1 was absent in the Human infertility dataset (E-TABM-1214). SYNJ2 is associated with perinuclear manchette, bundles of microtubules surrounding the nucleus of elongated spermatids, that are required for nuclear shaping during spermiogenesis [342]. Consequently, *SYNJ2* expression in men was detected in later stages of spermatogenesis, elongated spermatids, and mature sperm, and in Sertoli cells (Figure 4.4. A). *SYNJ2* testicular expression was significantly higher in cryptorchid individuals than in other infertile groups and healthy men (Figure 4B), which may be explained by the higher relative ratio of Sertoli cells compared to the other cell types in cryptorchid men. In mouse testis, *Synj2* expression decreases with sexual maturity, potentially suggesting higher expression of *Synj2* in somatic cell populations (Figure 4.4. C).

**INPP5E**

Inositol polyphosphate 5- phosphatase E (INPP5E) is the only member of type IV PI-5 phosphatases. It dephosphorylates $PI(3,4,5)P_3$, $PI(3,5)P_2$, and $PI(4,5)P_2$ at D-5 position of the inositol ring [343-345]. INPP5E is highly expressed in both the testis and the brain. In the hypothalamus INPP5E inhibits IRS/PI3K signaling, suppressing appetite, and preventing obesity [346]. Though expression of INPP5E has been detected in mouse spermatocytes at both gene and protein levels, its role in testis remains elusive [347]. Expression of *INPP5E* in men is observed in spermatogonia, spermatocytes, and Sertoli cells (Figure 4A). No significant correlation of *INPP5E* expression was detected with

various types of infertility and various developmental stages of mouse testis (Figure 4. 4. B and 4.4. C). It is possible that, similar to PTEN, INPP5E suppresses testicular insulin and IGF signaling.

**INPPL1 (SHIP2) and INPP5D (SHIP1):**

Inositol polyphosphate phosphatase like 1 (INPPL1) and Inositol polyphosphate 5-phosphatase D (INPP5D) are type III PI-5 phosphatases which dephosphorylate $PI(3,4,5)P_3$, $PI(3,5)P_2$, and $PI(4,5)P_2$ [348, 349]. INPP5D, a homolog of INPPL1, inhibits the PI3K/ AKT signaling pathway and reduces cell proliferation and survival in various cancers [350-352]. INPPL1 is able to activate the PI3K/ AKT pathway and stimulates metastatic spread in tumor cells that lack INPP4B due to accumulation of $PI(3,4)P_2$, a potent activator of AKT and Focal Adhesion Kinase [353]. Transgenic ubiquitous overexpression of *Inppl1* in mice led to the development of the type 2 diabetes when they were fed with HFD [354]. Conversely, *Inppl1*$^{-/-}$ mice are resistant to diet induced obesity [355]. We have not included INPP5D in our analysis because it was absent in Human infertility dataset (E-TABM-1214). The INPPL1 protein was detected in the membranes of spermatids but not in spermatogonia, spermatocytes, or Sertoli cells. [356].

In human testis, testicular expression of *INPPL1* is observed in macrophages and myoid cells and in the SSC population (Figure 4.4. A). In men, the expression of *INPPL1* is elevated in the cryptorchid and infertile groups lacking spermatids and mature sperm (Figure 4.4. B), which is consistent with the higher proportion of somatic cells in the testes of these patients. Similarly in mice, *Inppl1* expression is lower in the fully mature testis than before and during early stages of the first wave of spermatogenesis (Figure 4.4. C).

The expression pattern of INPPL1 in testis may reflect its function in stromal cells during spermatogenesis or may be secondary to its role in systemic metabolism.

### 4.8. Discussion:

Male infertility is the cause of approximately 50% of couples with fertility problems. Remarkably, recent reports indicated that the average sperm count in men, a prominent marker of male fertility, declined by more than 50% in the last 60 years [357, 358]. Male subfertility may result from congenital, acquired, or idiopathic factors, with the latter constituting 30-50% of the cases [359, 360]. Obesity and metabolic syndrome are some of the idiopathic factors which become more critical in male fertility with their increasing prevalence [245]. In both metabolic disorders and male infertility, the phosphatidylinositol pathway plays a crucial role since PIPs modulate various cellular activities including cell division, cytoskeletal rearrangements, motility, endocytosis, autophagy, and other processes [361-363]. Recently, the importance of PIPs in testicular function and spermatogenesis has been demonstrated in multiple species [10, 196, 280, 281, 283].

For PI-3 phosphatases, we analyzed the expression of PTEN, TPTE, MTMR2, and SBF1 (Figure 4.2). Except for PTEN, all PI-3 phosphatases are expressed primarily in germ cells. PTEN is expressed ubiquitously across all germ and stromal cells in both men and mice [307]. SBF1 is predominantly expressed in pre-meiotic germ cells, and TPTE and MTMR2 in meiotic and post-meiotic germ cells. Consistent with their expression patterns, infertility associated with the loss of spermatids or spermatocytes does not change relative expression of PTEN, but leads to the decline in TPTE, MTMR2, and SBF1 expression.

Among PI-4 phosphatases, testicular phenotype was evaluated only in *Inpp4b*$^{-/-}$ mouse model. *Inpp4b* is highly expressed in post-meiotic germ cells and its loss caused reduced testis size, lowered the rate of meiosis reducing sperm count, and affected expression of some steroidogenic enzymes [196]. *Inpp4b* levels in mouse testis increased concomitantly with the appearance of mature sperm after day 18 (Figure 4.3. C). Infertile men that lacked spermatids showed very low levels of testicular INPP4B expression (Figure 3B). The role of PI-4 phosphatases, INPP4A, TMEM55A, and TMEM55B, in testis is much less clear. *INPP4A*, *TMEM55A*, and *TMEM55B* were expressed primarily in pre-meiotic and meiotic cells and at lower levels in stromal cells. Since INPP4B and TMEM55B protect mice from metabolic disorders, their loss may also affect fertility indirectly through metabolic syndrome-associated pathways [20, 337].

Among PI-5 phosphatases, only the role of INPP5B in testicular function was investigated in a mouse model showing its importance in Sertoli cell function and sperm quality [283, 290]. There was a spike in *SYNJ2* expression in cryptorchid prepubescent testes and higher levels of its ortholog in testes of mice prior to sexual maturity suggesting a higher expression and functional significance in spermatogonial cells (Figure 4.4. B-C). INPP5E has the broadest substrate specificity and was the only phosphatase decreased in infertile patients with defects in early spermatogenesis (Figure 4.4 B). INPPL1 showed some expression in SSC, macrophages, and myoid cells, and the groups with a higher relative fraction of somatic cells have somewhat elevated levels of INPPL1 expression in both species (Figure 4.4. B-C).

The analysis described in this manuscript possesses some inherent limitations. Firstly, the data sets used for analysis were obtained using different methodology: Human Testis Atlas

is derived from single cell RNA-seq data, and the gene expression in healthy and infertile men and postnatal murine testis were evaluated using tissue RNA microarrays. A whole tissue specimen was used for RNA microarrays for the human infertility study and to determine stage specific gene expression in mouse testis. Increase in gene expression in the whole tissue may reflect proportional increase in cell representation rather than actual increase in expression in a specific cell pool. In addition, an intriguing hypothesis by Xia *et al.*, proposes the transcriptional scanning model, which suggests that many genes highly expressed during spermatogenesis engage in transcription-coupled repair rather than perform an important function in maturing germ cells. [364]. Thus, high expression of some phosphatases may be an evolutionary mechanism to prevent mutations in the germ lineage rather than a functional requirement for spermatogenesis. This is particularly plausible for phosphatases required for embryonic development, such as PTEN, MTM1, TMEM55B, since these gene knockouts are embryonically lethal [288, 335, 365].

### 4.9. Conclusions:

The expression of PI phosphatases in testis has an indispensable role in testicular function and spermatogenesis. The knockouts of certain PI phosphatases cause infertility in male mice due to structural and/or functional defects in specific testicular cells (Table 5). Indirectly, germ line mutations in some phosphatases lead to metabolic disorders which can also negatively affect male fertility [366, 367]. PTEN, MTMR14, INPP4B, TMEM55B, INPP5E, and INPPL1 are important regulators of metabolic health [20, 299, 300, 328, 337, 346, 354, 355], and the targeted or germ line knockouts of *Pten*, *Mtmr14*, and *Inpp4b* cause various characteristics of metabolic syndrome as well as smaller testes, suggesting additional modes of regulation of testicular function [152, 196, 279, 289]. The

importance of PI-phosphatases expression in testicular cells underscores the role of PI signaling in spermatogonial stem cell maintenance, spermatogenesis, spermiogenesis, and capacitation, as well as in function of the supporting stromal cells.

# 5. CHAPTER 5: Deletion of Inositol Polyphosphate 4-Phosphatase Type-II B Affects Spermatogenesis in Mice

This chapter has been originally published in PLoS One, "Deletion of Inositol Polyphosphate 4-Phosphatase Type-II B Affects Spermatogenesis in Mice", 2020, doi: 10.1371/journal.pone.0233163

## 5.1. Abstract

Inositol polyphosphate-4-phosphatase type II (INPP4B) is a dual-specificity phosphatase that acts as a tumor suppressor in multiple cancers. INPP4B dephosphorylates phospholipids at the 4th position of the inositol ring and inhibits AKT and PKC signaling by hydrolyzing of PI(3,4)P2 and PI(4,5)P2, respectively. INPP4B protein phosphatase targets include phospho-tyrosines on AKT and phospho-serine and phospho-threonine on PTEN. INPP4B is highly expressed in testes, suggesting its role in testes development and physiology. The objective of this study was to determine whether *Inpp4b* deletion impacts testicular function in mice. In testis, *Inpp4b* expression was the highest in postmeiotic germ cells in both mice and men. The testes of *Inpp4b* knockout male mice were significantly smaller compared to the testes of wild-type (WT) males. *Inpp4b*$^{-/-}$ males produced fewer mature sperm cells compared to WT, and this difference increased with age and high fat diet (HFD). Reduction in early steroidogenic enzymes and luteinizing hormone (LH) receptor gene expression was detected, although androgen receptor (AR) protein level was similar in WT and *Inpp4b*$^{-/-}$ testes. Germ cell apoptosis was significantly increased in the knockout mice, while expression of meiotic marker γH2A.X was decreased. Our data demonstrate that INPP4B plays a role in maintenance of male germ cell differentiation and protects testis functions against deleterious effects of aging and high fat diet.

## 5.2. Introduction

Male infertility accounts for approximately half of failed conceptions after 12 or more months of regular, unprotected sexual intercourse [368]. A substantial portion of men have suboptimal sperm parameters such as low sperm count, poor mobility or abnormal morphology, which can all contribute to infertility. Testicular abnormalities, aberrant hormone production, and failed spermatogenesis are the most common causes of congenital male infertility [369, 370]. In addition to genetic factors, environmental factors also play an important role in male infertility. One of the most studied environmental factors affecting fertility is obesity [371, 372]. Obesity is correlated with a reduction in sperm quality and low rates of pregnancy [373, 374]. However, some obese patients do not develop these defects, suggesting the existence of molecular mechanisms protecting testicular function against environmental insults.

The phosphatidylinositol signaling pathway is critical to the regulation of a variety of cellular activities including cell metabolism, morphogenesis, cell cycle, cytoskeletal organization, cell polarity, and membrane trafficking. The main mechanism of regulation in this pathway relies on the controlled phosphorylation and de-phosphorylation of specific membrane bound lipids, phosphatidylinositol polyphosphates (PIPs), at the 3-, 4-, and 5-positions of the inositol ring [375]. Two best described phosphatases, phosphatase and tensin homolog (PTEN) and inositol polyphosphate 4-phosphatase II (INPP4B), dephosphorylate PIPs at the 3- and 4-inositol positions respectively, inhibiting the AKT signaling pathway. Both PTEN and INPP4B are widely expressed and function as tumor suppressors in multiple cancers. Recent data in fruit flies, frogs, mice and other species indicate the importance of kinases and phosphatases in the PIP pathway in the development

of male germ cells [10]. INPP4B is a cytosolic membrane dual specificity phosphatase that dephosphorylates both phospholipids and phosphoproteins. It possesses an N-terminal, C2 lipid-binding domain, an internal NHR2 (Nervy Homology 2) domain, and the conserved dual phosphatase motif, CX5R, within the C-terminal phosphatase domain [15, 16]. Our lab and others have shown that INPP4B participates in a variety of signaling pathways including PI3K/AKT and PKC. Notably, the loss of INPP4B correlates with poor prognosis in human cancer, including cancers of the male reproductive system [78, 90, 91]. However, the INPP4B role in healthy organs remains largely unknown.

Recent studies confirmed that INPP4B and PTEN are highly expressed in the adult human [376, 377] and mouse [378, 379] testis. Here we report the cell specific expression pattern of INPP4B in human and mouse testis and describe morphological and functional changes in mouse testis lacking functional INPP4B. We show that INPP4B is highly expressed in postmeiotic germ cells. Analysis of circulating hormones revealed reduced testosterone and LH concentrations in the serum of *Inpp4b*-deficient males. This reduction was associated with decreased expression of critical steroidogenic enzymes, reduced testes size, and decreased sperm production that worsens with age. There was a higher rate of apoptosis and a decrease in the expression of meiosis marker γH2A.X in *Inpp4b*$^{-/-}$ testis. A high fat diet exacerbated the effects of INPP4B loss in testicular function. The results suggest an important role for INPP4B in testicular physiology.

## 5.3. Results

### 5.3.1. INPP4B expression is highest in post-meiotic germ cells

To understand the function of *INPP4B* in the testes, we analyzed the expression pattern of *INPP4B* in various testicular cell populations. Using a previously generated transcriptional

cell atlas [291] derived from human testicular single-cell RNA sequencing, we detected the highest level of *INPP4B* expression in the round and elongating spermatids and in differentiating sperm (Figure 5.1. A). A lower level of expression was also present in Leydig and Sertoli cells. Interestingly, *PTEN* was expressed ubiquitously in stromal and germ cells of the testis (Figure 5.1. A). Clustering gene analysis and gene ontology analysis showed that the top 222 genes upregulated with correlation coefficient cut-off value 0.4 in *INPP4B*-positive cells are involved in fertilization, reproductive development, cellular signaling pathways and various stages of spermatogenesis (Figure 5.1. B). Thus, *INPP4B*-positive cells represent germ rather than somatic cell populations in testis.

We next used the microarray data from Chalmel et al. [292], and analyzed *INPP4B* expression in the testes of men with cryptorchidism or infertility and compared it to *INPP4B* expression in healthy adult individuals. We divided the infertile population into two groups, those who had spermatids present in the seminiferous tubules and those who did not. Among all groups, *INPP4B* expression was highest in healthy controls, and it was significantly decreased in cryptorchid testes. Within the infertile population, *INPP4B* expression was significantly lower in the group lacking spermatids (Figure 5.2. A).

The first cycle of spermatogenesis in mice is synchronized over seminiferous tubules. This timely process allows the comparison of the gene expression within distinct stages of germ cell differentiation. We compared *Inpp4b* and *Pten* expression in the testes at three important time-points during germ cell development: day 8, when the testes contain pre-meiotic diploid differentiating germ cells up to the type B spermatogonia stage; day 20, when the germ cells are differentiated into round spermatids; and after day 35, when testes contain all stages of germ cells [380]. We also analyzed adult testes from 2-month-old

*Rxfp2*$^{-/-}$ males with high intraabdominal cryptorchidism, which lack all stages of spermatogenesis past the spermatogonial cells, with only a few early spermatocytes present [381]. When compared to adult WT mice, *Inpp4b* expression in these mutants was significantly lower in the testes of 8- and 20-day old mice, and cryptorchid adult mice (Figure 5.2. B). Cryptorchid testes show a somewhat lower level of expression compared to 20-day old WT testis (Figure 5.2. B), although this difference does not reach statistical significance ($p=0.868$). Thus, as in human, in mouse germ cells *Inpp4b* expression was highest during the late stages of spermatogenesis. The variation of PTEN expression was significantly less pronounced in the same groups (Figure 5.2. C). IHC staining indicated robust expression of INPP4B was present in elongated spermatids and lower expression was observed in round spermatids, Leydig and Sertoli cells in WT mouse testes (Figure 5.2. D).

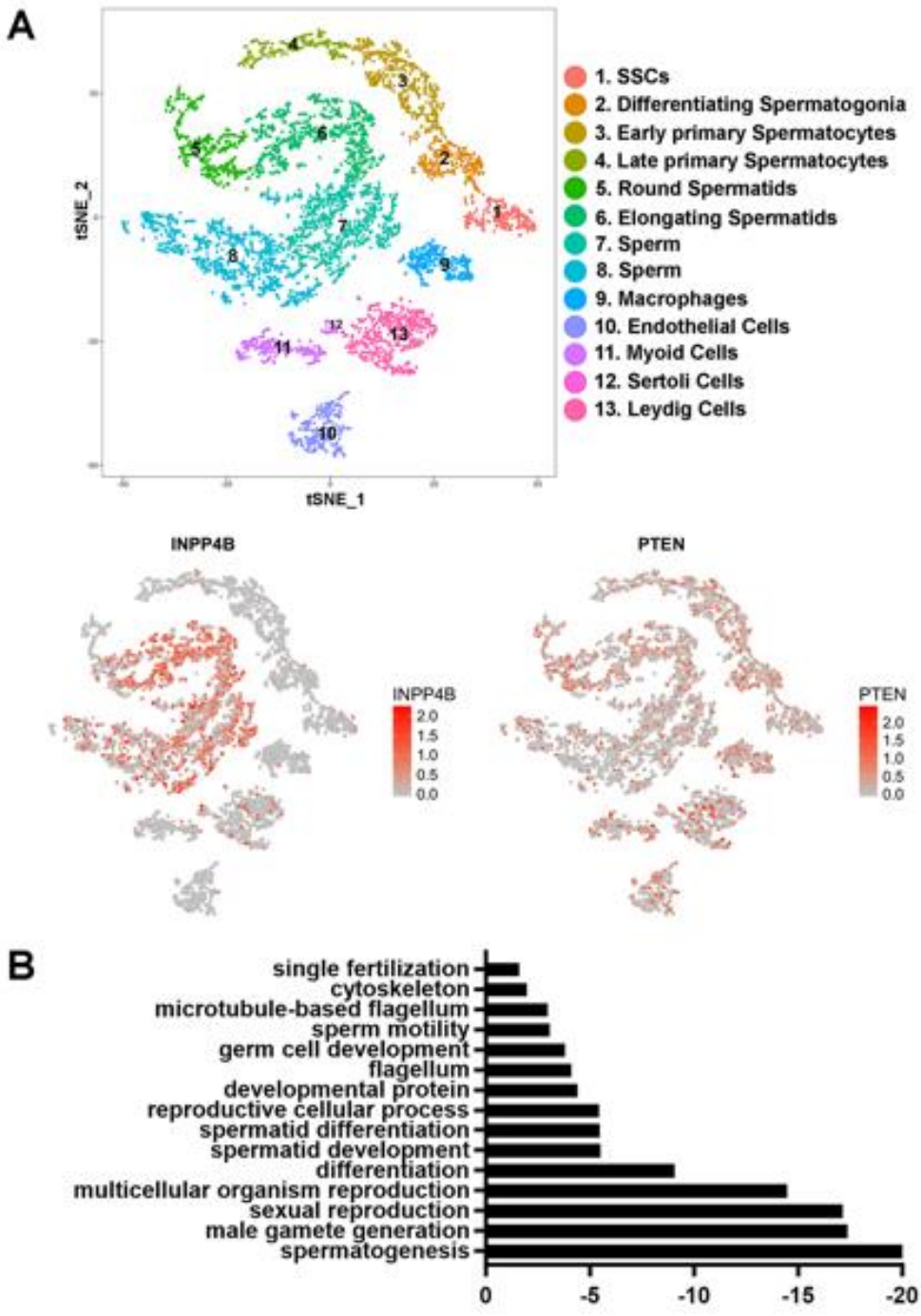


**Figure 5.1.** *INPP4B* is preferentially expressed in the post-meiotic germ cells in human testis.
A) *INPP4B* and *PTEN* expression map in different compartments of testis, obtained by the analysis of single cell RNA-Seq data. The map for the different cell fractions was adapted from [291]. B) Gene ontology pathways regulated by top 222 genes upregulated in *INPP4B*-positive germ cells. The vertical axis shows the top 15 pathways that correlate with high INPP4B levels and the horizontal axis represents the logarithmic scale of p values. The data was obtained by analyzing single cell RNA-Seq data sets [291].

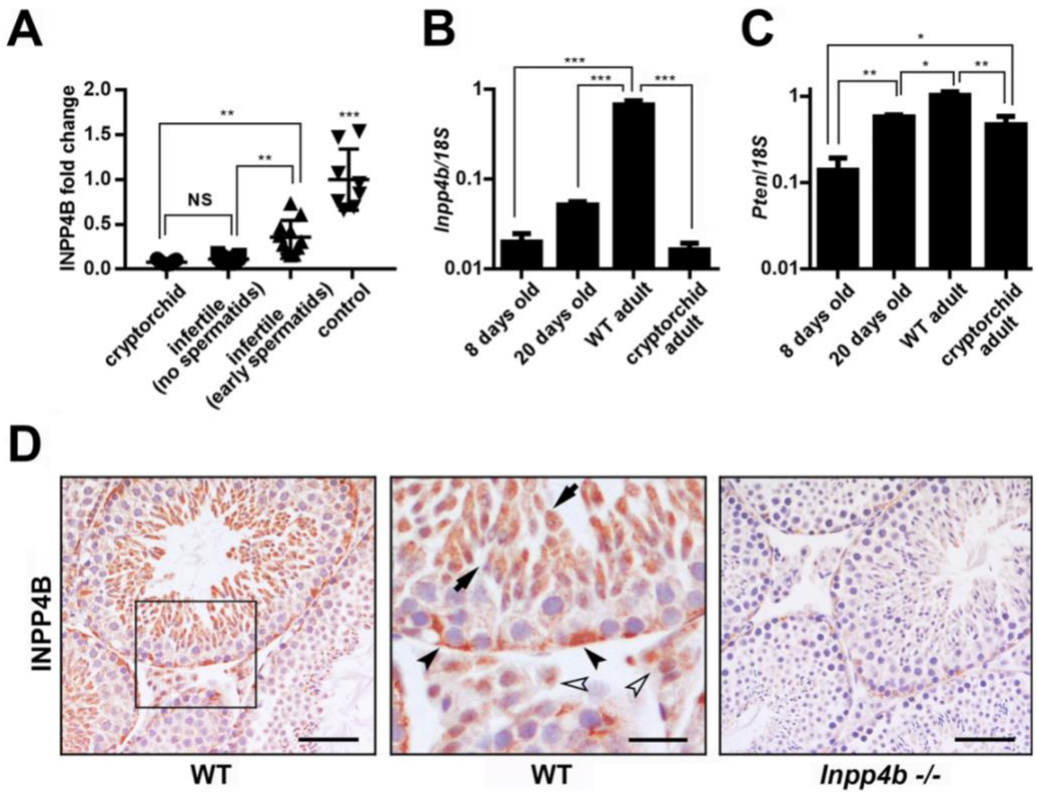


**Figure 5.2.** INPP4B and PTEN gene expression during spermatogenesis.
A) Expression analysis of *INPP4B* in cryptorchid, infertile patients without spermatids, infertile patients with spermatids and control groups using microarray data from Chalmel et al [292]. The control group has higher *INPP4B* expression compared to all other groups. **p<0.01, ***p<0.001. B) *Inpp4b* and C) *Pten* expression in postnatal mouse testes analyzed by qRT-PCR. RNA was extracted from 8-day old (N=10), 20-day old (N=6), WT adult (N=6), and cryptorchid adult (N=8) whole testis. Gene expression was normalized to *18S*. Data shown as mean ± SEM. Statistical analysis was performed using 1-way ANOVA. *p<0.05, **p<0.01, ***p<0.001. D) INPP4B IHC of 2-month-old mouse testes. Testis sections from age-matched WT (left panel) and *Inpp4b*$^{-/-}$ males (right panel) were stained for INPP4B and counterstained with hematoxylin. The middle panel represents a magnified section of WT testis. Elongated spermatids showed by arrows, Leydig and Sertoli cells showed by white and black arrowheads respectively. No staining was detected in *Inpp4b*-deficient testis sections. Scale bars represent 100 µm for right and left images and 20 µm for the middle image.

### 5.3.2. Testis weight and sperm counts are decreased in *Inpp4b*$^{-/-}$ males

To characterize the effect of INPP4B loss, we measured body, testes, and seminal vesicle weight and the epididymal sperm count of 2-, 3-, 4- and 6-month-old WT and *Inpp4b*$^{-/-}$ mice. Body weight remained comparable among age groups until 6-months of age, when *Inpp4b*$^{-/-}$ mice weighed slightly less (Figure 5.3. A). In *Inpp4b*$^{-/-}$ males, testes weight was

consistently smaller when compared to WT controls, and this difference increased with age (Figure 5.3. B). There were no statistically significant differences in seminal vesicle weight between WT and *Inpp4b*$^{-/-}$ mice at any age (Figure 5.3. C) or visible changes in mutant epididymides. Epididymal sperm counts were higher in the WT groups. The difference was not statistically significant between 2-month-old and 3-month-old males, but it became significant in 4- and 6-month-old groups. (Figure 5.3. D). Additionally, there were no differences in the diameter of the seminiferous tubules between WT and *Inpp4b*$^{-/-}$ testes at any age group (data not shown).

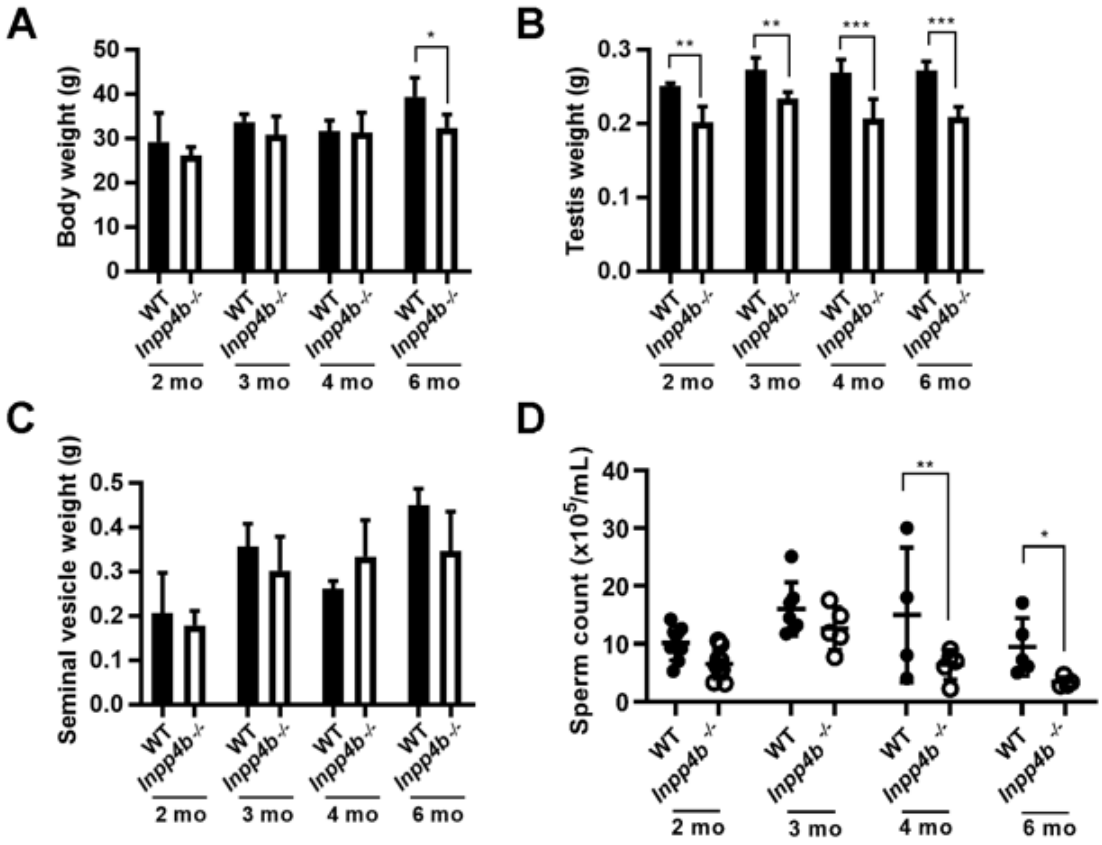


**Figure 5.3.** Testicular weight and epididymal sperm count in *Inpp4b*$^{-/-}$ mice.
A) Body weights for 2-, 3-, 4-, and 6-month-old mice. B) Testes weights of 2-, 3-, 4- and 6-month-old mice. C) Seminal vesicle weights for 2-, 3-, 4- and 6-month-old mice. D) Epididymal sperm count for 2-, 3-, 4- and 6-month-old mice. *p<0.05, **p<0.01, ***p<0.001; N>4/group. Data shown as mean ± SEM. Statistical analysis was performed using 2-way ANOVA.

### 5.3.3. INPP4B deficiency causes a shift from haploid to diploid cell population in testis

Since *Inpp4b*$^{-/-}$ males had significantly decreased sperm counts in aged groups, we used flow cytometry to evaluate changes in the ploidy of germ cells in 6-month-old WT and mutant testes [382, 383]. We compared the percentages of testicular haploid, diploid, and tetraploid populations. In the haploid populations, we examined round (1C) and hypostained (HC) elongated spermatids separately to determine whether the reduction in sperm counts was due to a reduction in meiosis (round spermatids) or spermiogenesis (elongated spermatids) stages (Figure 5.4. A-B) [384]. The percentage of elongated spermatids was significantly decreased in *Inpp4b*$^{-/-}$ males (WT – 21.8 %, *Inpp4b*$^{-/-}$ – 8.7 %, p=0.0032), whereas the percentage of diploid cells in knockout males was increased (WT – 16.6 %, *Inpp4b*$^{-/-}$ – 25.8 %, p=0.0434). The percentages of round spermatids and tetraploid cells were not statistically different between WT and *Inpp4b*$^{-/-}$ groups (Figure 5.4. C).

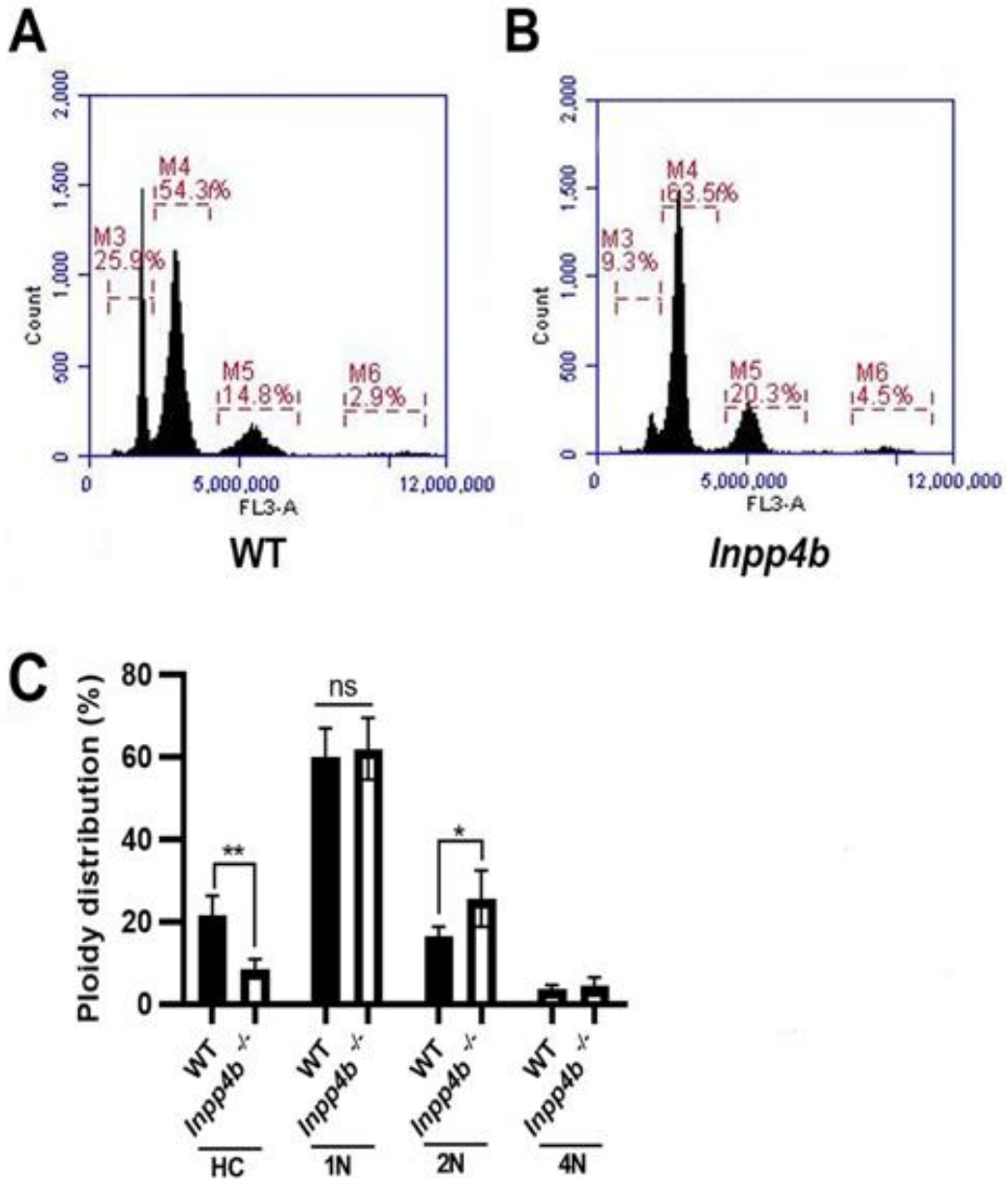


**Figure 5.4.** Flow cytometry analysis of testes from WT and *Inpp4b*$^{-/-}$ mice.
Flow cytometry histograms of A) wild type B) *Inpp4b*$^{-/-}$ testes. Testicular cells have four cell populations distinguished by DNA intensity on the Y axis: M3 (1N, haploid, elongated spermatids), M4 (1N, haploid, round spermatids), M5 (2N, diploid), and M6 (4N, quadriploid). A representative histogram from a 6-month-old male in each group is shown. C) Quantitative analysis of cell populations, N= 4/group (*$p<0.05$, **$p<0.01$). Data shown as mean ± SEM. Statistical analysis was performed using 2-way ANOVA.

### 5.3.4. High fat diet exacerbates the effects of INPP4B deficiency on testis functions

Since INPP4B is a key regulator of PIP substrates that participate in metabolic signaling pathways, we examined if a high fat diet (HFD) can exacerbate the effects of INPP4B loss on spermatogenesis. Body weight and seminal vesicle weights showed no difference when comparing 3-month-old *Inpp4b*$^{-/-}$ and WT mice fed either diet (Figure 5.5. A-B). The testes of *Inpp4b*$^{-/-}$ mice weighed significantly less than testes of the WT controls (Figure 5.5. C) and the consumption of a HFD significantly decreased sperm count in *Inpp4b*$^{-/-}$ mice when compared to WT (Figure 5.5. D). The LFD group is the same as the 3-month-old group used in Figure 5.3.

Since the hypothalamic-pituitary-gonadal (HPG) hormonal axis has an important role in the regulation of spermatogenesis [385, 386], we compared the levels of testosterone and luteinizing hormone (LH) in the serum of mutant and WT males on a LFD or a HFD. While there was a trend suggesting that *Inpp4b*$^{-/-}$ mice produce less testosterone than WT controls, this difference was not statistically significant (Figure 5.5. E). In testis, LH stimulates the production of testosterone in Leydig cells. Notably, in the HFD group, the LH levels were significantly lower in the *Inpp4b*$^{-/-}$ group than in WT mice (Figure 5.5. F).

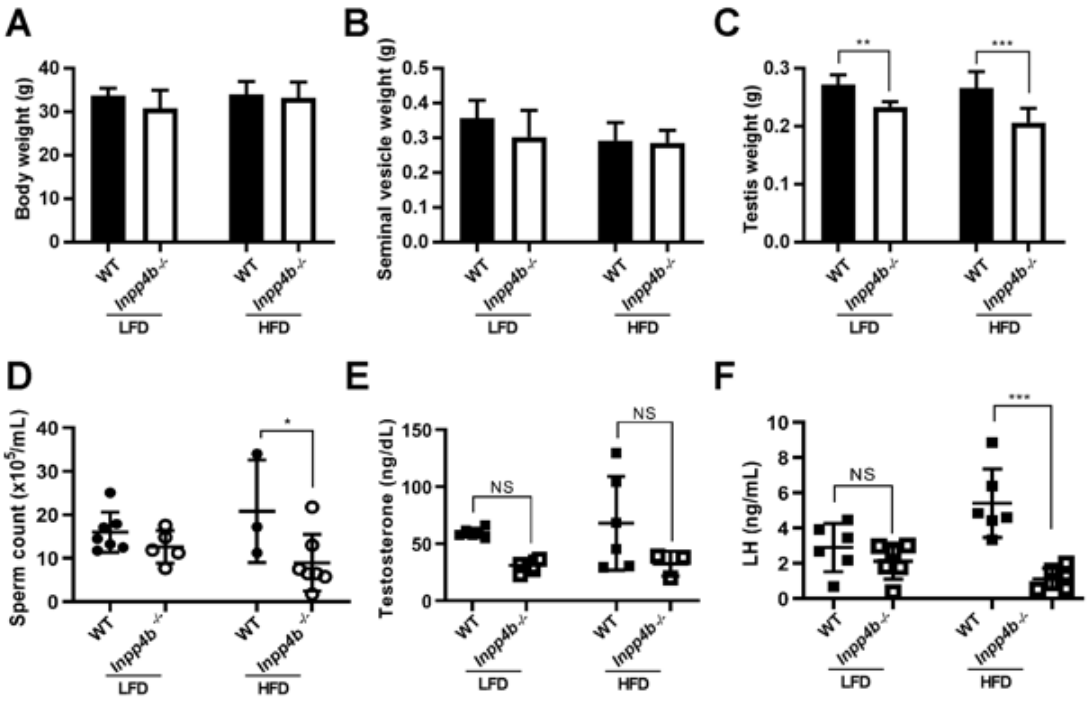


**Figure 5.5.** Effect of HFD on testicular phenotype of *Inpp4b*$^{-/-}$ males.
A) Body weights, B) Seminal vesicle weights, C) Testes weights, D) Epididymal sperm counts, E) Testosterone and F) Luteinizing hormone levels for 3-month-old mice on LFD and HFD. *p<0.05, **p<0.01, ***p<0.001; N>4/group. Data shown as mean ± SEM. Statistical analysis was performed using 2-way ANOVA.

Steroidogenic hormone synthesis in testis is controlled by a series of enzymatic steps (Figure 5.6. A). We compared the gene expression of the key steroidogenic enzymes *Cyp11a1, Cyp17a1, Hsd3b6, Hsd17b3, Cyp19* and *Srd5a1*, steroidogenic factor-1 *Nr5a1*, the cholesterol transporting protein *Star,* and the LH receptor, *Lhcgr*, in WT and mutant testes in LFD and HFD groups. *Cyp11a1* expression was significantly lower in the *Inpp4b*$^{-/-}$ LFD group when compared to WT mice, but this decrease was not significant in HFD groups (Figure 5.6. B). *Cyp17a1* and *Lhcgr* expression was significantly lower in the LFD mutant group and in mice on HFD when compared with the WT LFD group (Figure 5.6. B). *Srd5a1* expression was not changed between LFD groups, but it was significantly decreased in *Inpp4b*$^{-/-}$ HFD mice when compared with the WT HFD group. The expression

of *Nr5a1*, *Star*, *Hsd3b6*, *Hsd17b3*, and *Cyp19* were not affected by the loss of INPP4B or the diet (Figure 5.6. B).

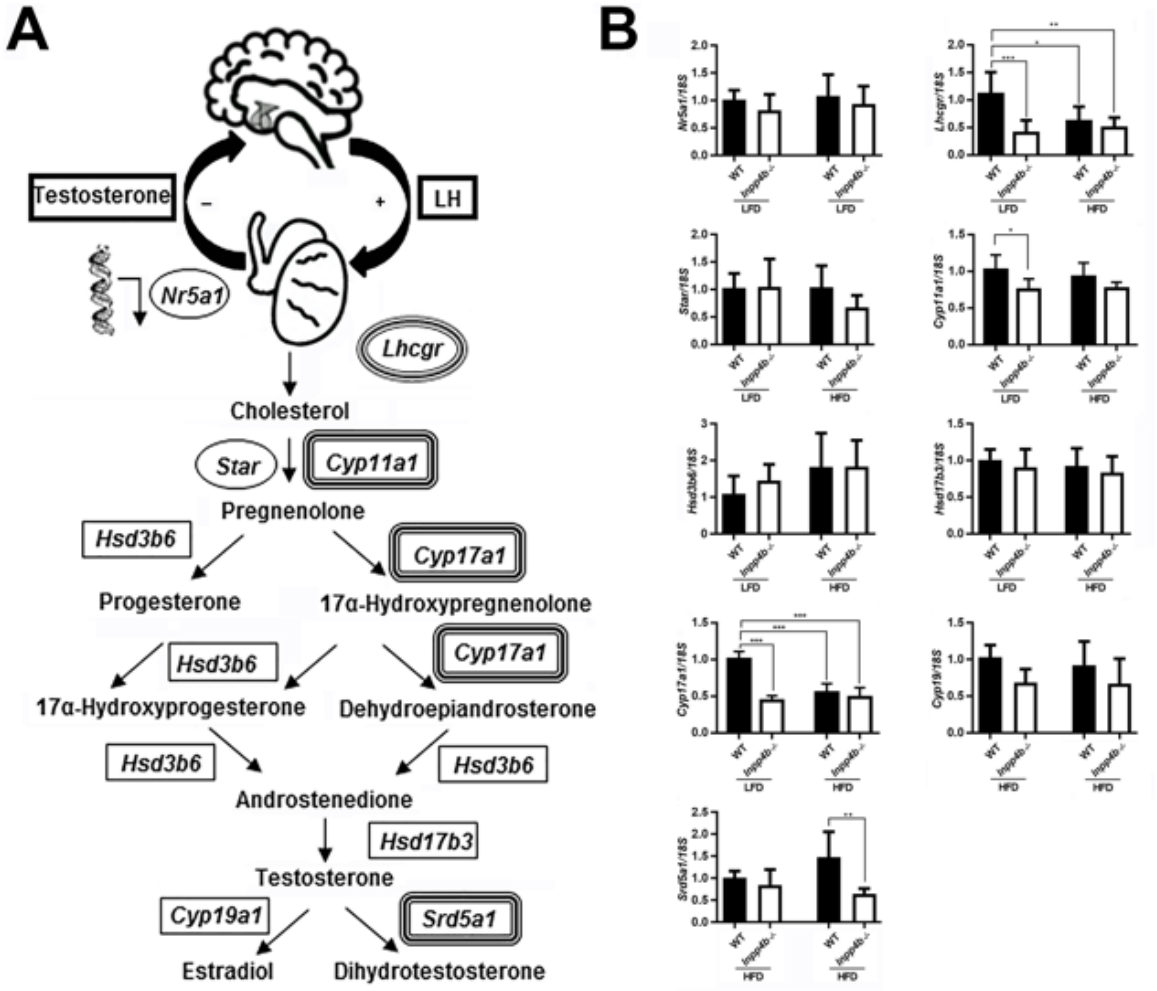


**Figure 5.6.** INPP4B deficiency and HFD effect on steroid hormone metabolism
A) Schematic diagram for hypothalamic–pituitary–gonadal hormonal axis and testosterone synthesis in testis. Key enzymes of the steroidogenic pathway are shown; corresponding genes showing different level of expression in mutant animals or on HFD are double-circled. B) Expression of genes in the steroidogenic pathway analyzed by qRT-PCR. The expression level for all genes was normalized to *18S*. *p<0.05, ***p<0.001; N=7/group. Data shown as mean ± SEM. Statistical analysis was performed using 2-way ANOVA.

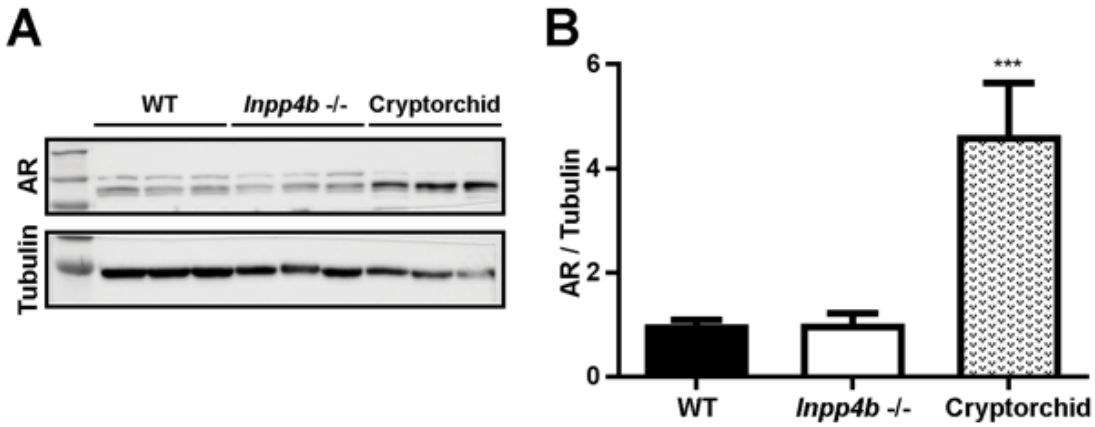


**Figure 5.7.** Androgen receptor expression in *Inpp4b*$^{-/-}$ testis.
A) AR expression in testes of WT, *Inpp4b*-/- and cryptorchid mice was analyzed by Western blot hybridization. B) Densitometric analysis of the Western blots. ***p<0.001; N=3/group. Data shown as mean ± SEM. Statistical analysis was performed using 2-way ANOVA.

Additionally, there was no difference in testicular androgen receptor (AR) protein levels between WT and *Inpp4b* $^{-/-}$ groups (Figure 5.7). There was a significantly higher level of AR expression in the cryptorchid testes, likely due to the lack of a germ cell population beyond the spermatogonia stage. As the germ cells do not express AR, cryptorchid testes have a higher proportion of AR-positive stromal cells compared to WT [387].

### 5.3.5. Loss of INPP4B increases apoptosis rate in early spermatogenesis

A decrease in the haploid testicular cell population and an increase in diploid cells indicated an abnormality in meiosis or spermiogenesis. We analyzed the rate of apoptosis in testes from 3-month-old WT and *Inpp4b*$^{-/-}$ testes in LFD and in age-matched HFD groups (Figure 5.8). The apoptosis rate was significantly higher in the mutant group compared to WT testes, independent of the diet (Figure 5.8. B). Apoptosis in testis was mainly observed in spermatogonia cells and in primary spermatocytes (Figure 5.8. C).

We next analyzed the expression of a meiosis marker, phosphorylated form of histone 2A.X (γH2A.X), which marks the double strand breaks in preleptotene through zygotene

spermatocytes and sex bodies in pachytene spermatocytes. It is highly expressed in B type spermatogonia, primary spermatocytes from preleptotene to pachytene stages and elongated spermatids [388-391] (Figure 5.9. A). Based on their position within the seminiferous tubules and cellular morphology at stage VIII-XI, the γH2A.X-positive cells were primary spermatocytes from preleptotene to pachytene spermatocytes, a population of actively dividing cells that determines efficiency of sperm production, and elongated spermatids (Figure 5.9. C). The number of γH2A.X-positive cells were significantly lower in the LFD *Inpp4b*$^{-/-}$ group compared to LFD WT controls ($p = 0.0178$). Consistent with reduced sperm count in HFD *Inpp4b*$^{-/-}$ males, there was a significantly lower number of γH2A.X-positive cells in the HFD *Inpp4b*$^{-/-}$ group when compared to HFD WT ($p = 0.0348$) or LFD mutant testes ($p = 0.0258$) (Figure 5.9. B). Among the prophase I primary spermatocytes, the γH2A.X positive pachytene spermatocyte count was significantly higher in LFD WT males (37.63 cells per tubule) than in the LFD *Inpp4b*$^{-/-}$ (31.82 cells/per tubule, $p = 0.0135$) and HFD *Inpp4b*$^{-/-}$ (26.30 cells per tubule, $p = 0.0002$) groups.

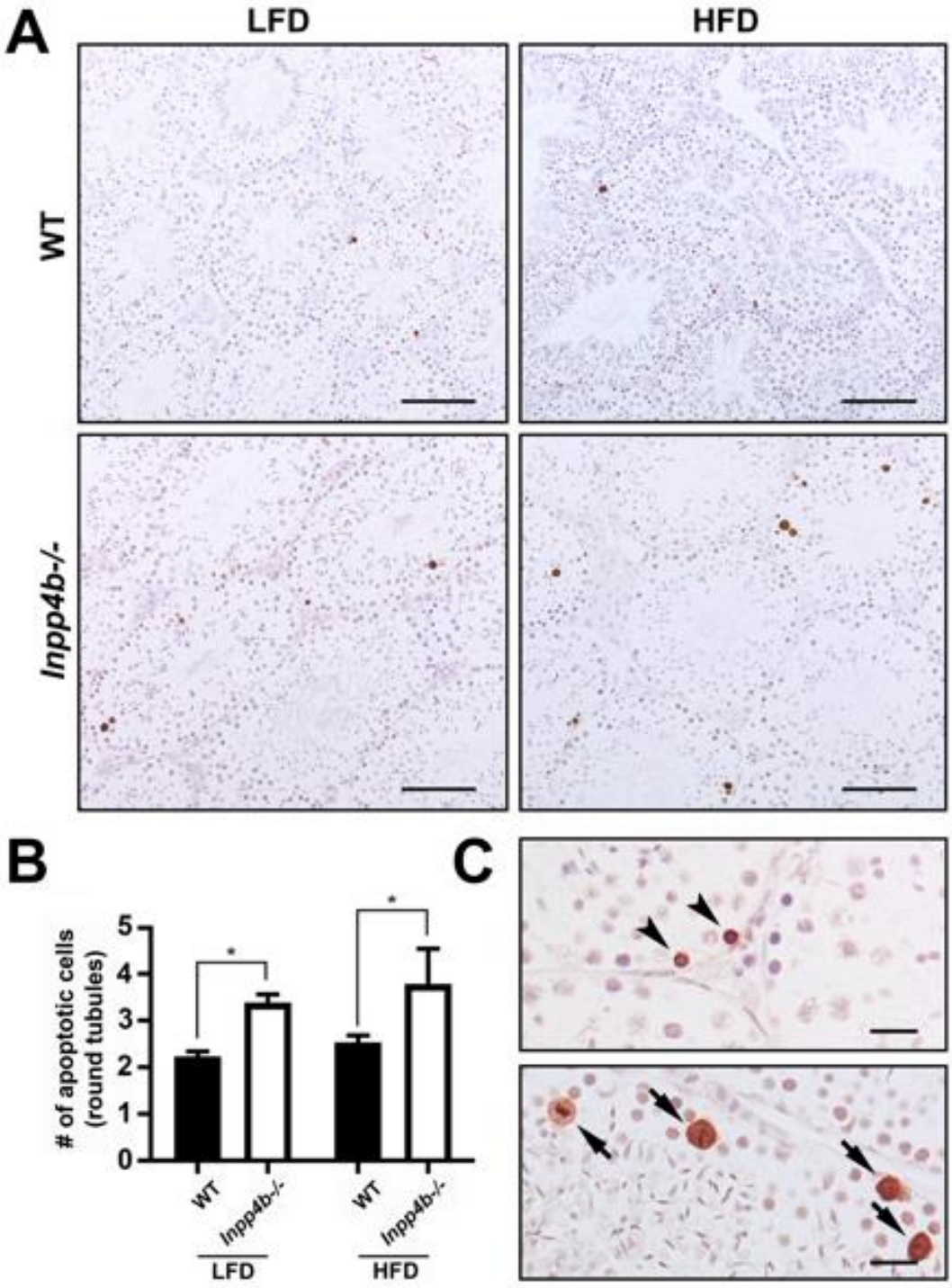


**Figure 5.8.** Apoptosis in *Inpp4b*$^{-/-}$ testis.
A) Increased apoptosis in *Inpp4b*$^{-/-}$ testes of 3-month-old males on LFD and HFD mice. Cell apoptosis was analyzed by TUNEL assay. A representative image from each group is shown. Scale bar represents 200 µm. B) Apoptotic cells (brown) were counted per field under 20X objective in at least 5 fields in each of 2 sections per animal. *$p<0.05$; N=3/group. Data shown as mean ± SEM. Statistical analysis was performed using 2-way ANOVA. C) Magnified sections from *Inpp4b*$^{-/-}$ males on HFD. Spermatogonia and cells in meiotic metaphase showed by arrowheads and arrows respectively. Scale bar is 20 µm.

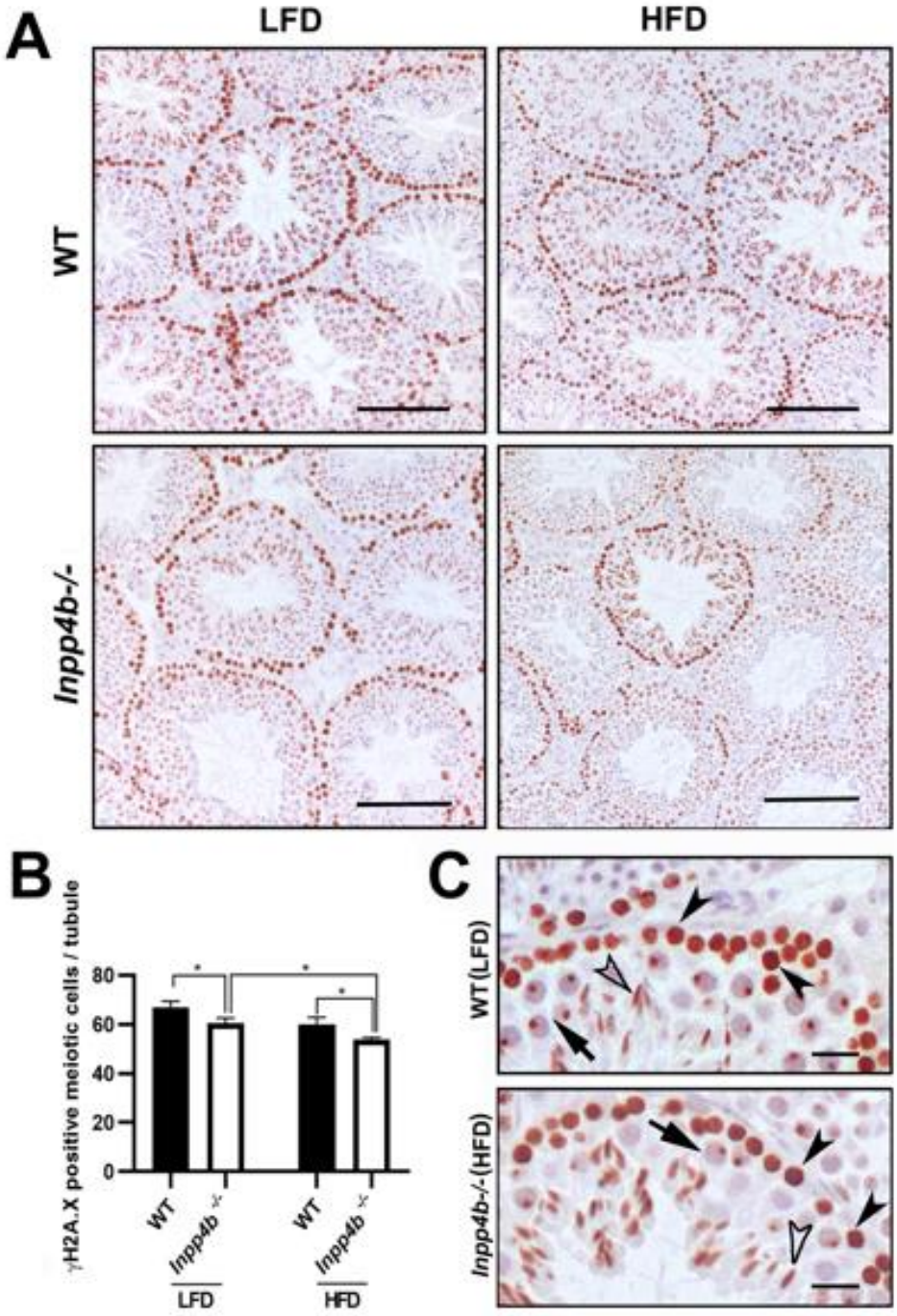


**Figure 5.9.** Expression of meiotic marker ϒH2A.X in *Inpp4b*$^{-/-}$ testis.
A) ϒH2A.X positive cells from the 3-month-old WT and *Inpp4b*$^{-/-}$ males on LFD or HFD. A representative image from each group is shown. Scale bar represents 200 µm. B) The ϒH2A.X-positive cells (brown staining) at prophase I in stage VIII-XI tubules were counted under 40X objective in at least 10 tubules that appear circular on the slide per animal. *$p<0.05$; N=3/group. Data shown as mean ± SEM. Statistical analysis was performed using 2-way ANOVA. C) Magnified sections from WT males on LFD and *Inpp4b*$^{-/-}$ males on HFD, pre-leptone to zygotene spermatocytes, pachytene spermatocytes and elongated spermatids showed by black arrowheads, arrows and white arrowheads respectively. Scale bar is 20 µm.

### 5.3.6. Expression of cytokines is altered in INPP4B deficient testis

Cytokines like interleukins (ILs) and tumor necrosis factors (TNFs) have been shown to play an important role in testicular homeostasis and spermatogenesis [392]. In testis, IL1β, IL6 and TNFα are produced by Sertoli, Leydig, and germ cells in a cyclical manner, stimulating Sertoli cell function, spermatogenesis, and steroidogenesis in Leydig cells [393]. We compared the expression of *Il1b*, *Il6* and *Tnfa* in 4-month-old WT and *Inpp4b*$^{-/-}$ testis on LFD (Figure 5.10. A) and in 3-month-old WT and *Inpp4b*$^{-/-}$ testes in mice on LFD and HFD (Figure 5.10. B). At three months no significant difference was observed in *Il1b* and *Il6* expression, however, *Il1b* and *Il6* expression was significantly higher in the WT than in *Inpp4b*$^{-/-}$ testes in 4-month-old males. The expression of *Tnfa* showed no significant difference between any groups (Figure 5.10).

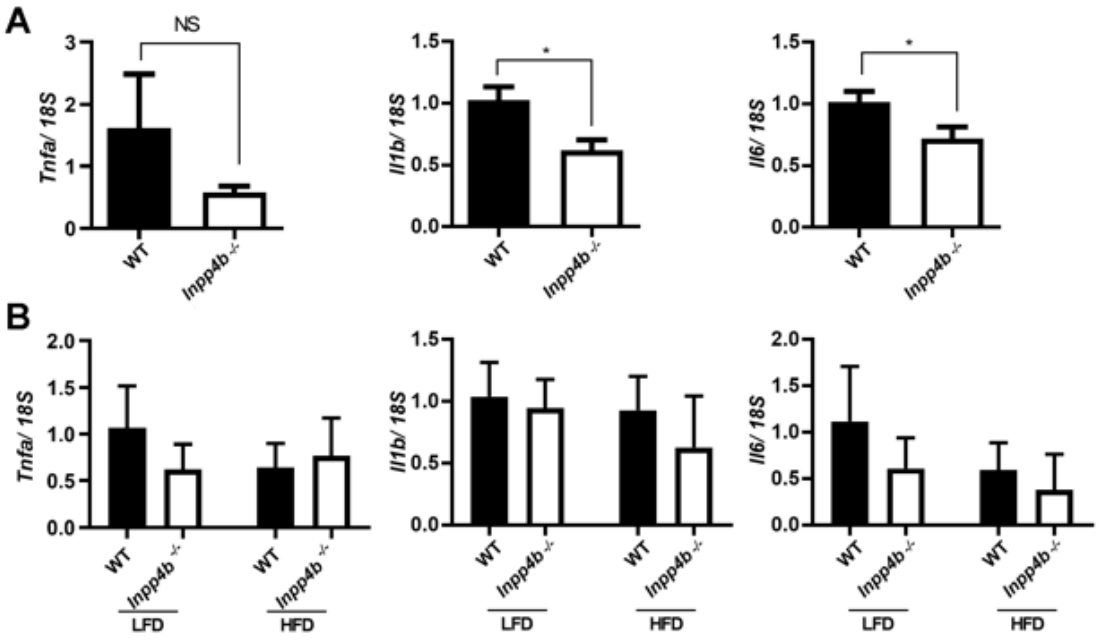


**Figure 5.10.** Expression of pro-inflammatory markers in *Inpp4b*$^{-/-}$ testis**.**
A) Reduced expression of *Il1b* and *Il6* in *Inpp4b*$^{-/-}$ testes from 4-month-old males on LFD. qRT-PCR data were normalized to the expression of 18S. *p<0.05; n=8/group. Statistical analysis was performed using Student's t-test. B) Expression of pro-inflammatory markers in testes from 3-month-old WT and *Inpp4b*$^{-/-}$ on LFD and HFD. N=7/group. Analyzed by 2-way ANOVA. Data shown as mean ± SEM.

## 5.4. Discussion

Recent data demonstrated that PIP signaling plays an important role in spermatogenesis and germ cell maintenance [10]. The involvement of members of this pathway in testicular functions was revealed through analysis of loss-of-function mutants. It was shown the PTEN/ PI3K/AKT pathway is important in controlling the proliferation and division of spermatogonial stem cells in mouse testis. Disruption of this signaling through knockout of the key genes in this pathway leads to the loss of spermatogonial cells and infertility in males [10, 152, 279]. Studies performed on Drosophila indicate that PI(4,5)P2 and PI(4)P are central regulators in germ cell meiosis and spermiogenesis, however the role of this pathway in mammals is less clear.

In this study we analyzed the expression and function of INPP4B in testes. INPP4B antagonizes the PI3K-AKT/PKB signaling pathway by dephosphorylating phosphoinositides and thereby modulating cell cycle progression and cell survival. We have shown that during spermatogenesis, in mice and men, INPP4B expression significantly increases at the round spermatid stage and continues into the mature sperm stage. Infertile men with no spermatids and cryptorchid male mice with spermatogenesis arrest at the spermatogonial-spermatocyte stage both had significantly lower levels of testicular INPP4B expression. Analysis of testicular phenotype in *Inpp4b*$^{-/-}$ males showed reduced testis weight, lower sperm count, increased apoptosis rate, and lower LH concentrations. The expression of certain enzymes mediating early stages of androgen synthesis was also reduced in mutant testes. Importantly, some of these abnormalities were exacerbated in animals maintained on a high fat diet, suggesting that INPP4B plays a role in male germ cell differentiation.

In both mice and men, high fat diet correlates with impaired intratesticular signaling and spermatogenesis [394, 395]. PKC pathway dysregulation caused by diet with high fat content leads to disruption in several pathways such as lipid metabolism and reactive oxygen species (ROS) formation, which are important for normal testis functions [396, 397].The synergistic stimulatory effect of *Inpp4b* loss and HFD on the PKC pathway might have a negative impact on testosterone metabolism and spermatogenesis. Expression of steroidogenic enzyme *Cyp17a1* and luteinizing hormone receptor *Lhcgr* were decreased in the HFD groups which, in combination with the decrease of *Srd5a1*, led to a reduction in sperm count in *Inpp4b*$^{-/-}$ mice when compared to the LFD group. Increased germ cell apoptosis and the reduction of expression of meiotic marker γH2A.X in the HFD mutant group support this conclusion. It should be pointed out that the relatively modest effects of the HFD in younger males might be due to the resistance of the FVB mouse strain to HFD induced obesity [398].

Analysis of previously reported gene expression datasets revealed a high level of expression of INPP4B in human and mouse testes [376, 378]. In cryptorchid mice, in which the testes are devoid of germ cells beyond the early spermatocyte stage, there was a low level of *Inpp4b* gene expression. The same was true when we analyzed previously published data on gene expression in infertile men with no detectable spermatids [381]. The advance of single cell RNA sequencing allowed us to map the highest *INPP4B* expression to postmeiotic germ cells beginning from the round spermatids; the conclusion was also supported by IHC analysis in mouse testis. Consistently, the genes positively correlated with expression of *INPP4B* were associated with pathways activated during spermatogenesis, such as spermatid differentiation, flagellum formation, and fertilization.

The question arises as to whether INPP4B plays any functional role in these processes or whether it is just a marker for specific stages of spermatogenesis. Our data suggest that the former might be true. INPP4B mainly catalyzes the hydrolysis of the phosphate located in the $4^{th}$ position of inositol ring of PI(3,4)P2, PI(4,5)P2, and inositol 1, 3, 4-trisphosphate. Experiments in Drosophila clearly show that PI4P cell signaling in germ cells has the same pattern: it is most prominent in spermatocyte through spermatid stages of differentiation, showing modest effects on the premeiotic population. Germline stem cells are affected by the PI3K pathway, mediated by insulin receptor and FOXO transcription factors. All these pathways are nutritionally regulated [10]. Activation of the PI3K pathway (especially isoform PI3KDN) in somatic cyst cells improves the transition from germline stem cells to spermatocytes [399]. PI4P and PI(4,5)P2 are regulators of meiotic cytokinesis in Drosophila spermatocytes [10]. Deletion of *four wheel drive* (*fwd)* encoding Drosophila PI 4-kinase IIIβ (PI4KIIIβ) [400], Class I PI transfer protein (PITP) [401, 402], trafficking factors such as GOLPH3, a Golgi PI4P-binding protein [402], and other members of PIP pathway all lead to abnormal cytokinesis. Involvement of the homologous genes in spermatogenesis in mice is less clear. Here we showed that INPP4B is highly expressed in postmeiotic germ cells during spermatogenesis in mice and men, and the deletion of this gene in mice leads to a decrease in mature sperm. However, the mild effect of *Inpp4b* deficiency is likely due to compensation by other members of the pathway, by modifier genes, or the relatively young age of the analyzed mice.

The deletion of another member of the INPP family, INPP5B, causes male infertility in mice due to a reduced sperm count, motility, and fertilization defects [403]. Interestingly, that backcrossing of the mutant allele on FVB/N inbred background, the same genetic

background as in our mice, partially rescued mutant male infertility, suggesting the existence of genetic modifier gene(s) in this mouse line. Conditional deletion of *Inpp5b* in germ cells resulted in normal male fertility [403], indicating that the abnormalities in mutant sperm function and maturation were not due to a deletion of the gene in germ cells. Further analysis of *Inpp5b*$^{-/-}$ mutant Sertoli cells revealed the appearance of abnormal vacuoles affecting germ cell adhesion [283]. A similar effect of *Inpp4b* deletion in somatic testicular cells may account for the observed increase of apoptosis in spermatogonial and spermatocyte cells detected in *Inpp4b*$^{-/-}$ mutants. One possible explanation of this phenomenon is that it might be related to a decrease in testosterone production in mutants along with the reduced expression of several steroidogenesis genes in mutant testis. The role of INPP4B targets, such as PI3K/AKT, in the survival of Leydig cells and steroidogenesis has been previously demonstrated [404]. Additionally, decreased expression of cytokines such as *Il1b* and *Il6* in mutant Sertoli cells might have caused reduced testosterone production, resulting in impaired spermatogenesis [371]. Ablation of AR signaling in Leydig, Sertoli, or peritubular myoid cells all leads to deficient spermatogenesis [405]. This is also consistent with our findings of prostate hyperplasia in one year old *Inpp4b* mutant males [181]. Thus, it is possible that in addition to a direct effect of *Inpp4b* deletion in germ cells, indirect effects of reduced testosterone and LH signaling in testicular somatic cells may be responsible for the observed phenotype. Further analysis of conditional *Inpp4b* deletion in various testicular cells might define the role of this gene in spermatogenesis.

## 5.5. Materials and Methods

### Analysis of single cell RNA-sequencing, clustering and gene ontology (GO) pathway analysis

RNA sequencing and gene clustering was performed using Seurat and previously reported data [291]. The Gene Ontology pathway analysis of genes positively correlated with INPP4B expression in testis was performed using DAVID bioinformatics functional annotation tool using data for all testicular cells for comparison [406, 407]. Since single cell RNA data results in a high dropout rate (~50%), R=0.4 was used for cutoff. The adjusted p values less than 0.05 were accepted as significant. To detect the expression of a gene in various human testicular cells, the Human Testis Atlas Browser (https://humantestisatlas.shinyapps.io/humantestisatlas1/) was used [291].

### Animal studies

Mice were maintained at the AAALAC accredited animal facility at Florida International University and all experimental protocols were performed in accordance with the regulations of the Institutional Animal Care and Use Committees at FIU and the National Academy of Science Guide for Care and Use of Laboratory Animals. The Institutional Animal Care and Use Committees at Florida International University approved this research, protocol AN18-055.

Generation of conventional knockout *Inpp4b*$^{-/-}$ [18, 181] and cryptorchid *Rxfp2*$^{-/-}$ [408] mouse models were described previously. Mice with the *Inpp4b* knockout allele were backcrossed to FVB/N inbred strain for 4 generations and then intercrossed to obtain *Inpp4b*$^{-/-}$ homozygotes in order to decrease genomic background variability. Mice were fed with low fat diet (LFD) with 12.9% fat, 63.8% carbohydrate, and 23.2% protein (total 13.6

kJ/g) (LabDiet 5V75, St. Louis, MO) or high fat diet (HFD) with 59.4% fat, 25.7% carbohydrate, and 14.9% protein (total 22.8 kJ/g) content (TestDiet 58R3, St. Louis, MO) [409]. For the HFD group, the females were on HFD for a month prior, during the pregnancy, and after delivery until weaning and the pups were on HFD from weaning until the euthanasia [409]. It was shown that under this protocol, male pups displayed more drastic changes in the urogenital system. Age-matched WT and *Inpp4b* $^{-/-}$ male mice were used in our studies at 2, 3, 4 and 6 months of age. Mice were euthanized by isoflurane (Patterson Veterinary, Greeley, CO) overexposure and testes and seminal vesicles were dissected and weighed.

Sperm count was performed as described by Huang *et al* [408], with minor modification. Briefly, sperm was released from the cauda epididymis into PBS, then diluted at a 1:5 ratio with distilled water, loaded into a hemocytometer and counted manually under the microscope by two investigators.

**Hormone measurement**

Testosterone (T) and LH levels were determined in male blood serum. The mice were euthanized, and blood collected from 3-month-old mice, with 6 males per group. The serum was collected after centrifugation at 3000 × *g* for 15 min and frozen until hormonal analysis. Testosterone and LH levels were determined in the University of Virginia Center for Research at the Reproduction Ligand Assay and Analysis Core (University of Virginia, Charlottesville, VA) using mouse/rat testosterone ELISA (IBL America, Minneapolis, MN) and RIA (in house protocol) assays respectively.

**Gene expression analysis**

mRNA samples were isolated from mouse testes using Tri-Reagent (Molecular Research Center, Cincinnati, OH) and reverse transcribed using the Verso cDNA synthesis Kit (Thermo Fisher Scientific, Waltham, MA). For quantitative PCR, primers were designed using online software (Roche, Basel, Switzerland) and probes were purchased from Universal ProbeLibrary (Roche). Roche 480 LightCycler (Roche) was used for probe-based real-time PCR. GoTaq qPCR master mix (Promega, Madison, WI) was used for experiments using BRYT dye on the Mastercycler RealPlex$^2$ system (Eppendorf, Westbury, NY). The relative fold change in gene mRNA level was calculated by the comparative cycle threshold ($2^{-\Delta\Delta Ct}$) method using 18S rRNA for normalization of the expression data. Primer sequences are shown in Table 6. The number of animals used in each group is shown in figure legends.

**Table 6.** Mouse gene primers and probes used for qRT-PCR used in Chapter 5.

| Gene | Forward primer | Reverse primer | Probe |
|---|---|---|---|
| *18S* | gcaattattccccatgaacg | gggacttaatcaacgcaagc | 48 |
| *Inpp4b* | tgaccctgaggacattcagtt | attccaactgtggctcgttc | 89 |
| *Pten* | aggcacaagaggccctagat | ctgactgggaattgtgactcc | 60 |
| *Tnfα* | ttgtcttaataacgctgatttggt | gggagcagaggttcagtgat | 64 |
| *Il1b* | caggcaggcagtatcactca | tgtcctcatcctggaaggtc | 76 |
| *Il6* | gctaccaaactggatataatcagga | ccaggtagctatggtactccagaa | 6 |
| *Hsd17b3* | tggtcccctataacagagcttca | gaaaagtcctgcccatttgt | 5 |
| *Hsd3b6* | accatccttccacagttctagc | acagtgaccctggagatggt | 95 |
| *Cyp11a1* | cctgagaaccccatcctctt | agtgttgtcttttctggtcacg | 11 |
| *Cyp17a1* | catcccacacaaggctaaca | cagtgcccagagattgatga | BRYT |
| *Cyp19* | cgaagcagcaatcctgaaggag | ccaagtccacaacaggctggta | BRYT |
| *Star* | ggaagtccctccaagactaaac | tggttgatgattgtcttcgg | BRYT |
| *Lhcgr* | caggaatttgccgaagaaag | tggagtgtcttgggtgaaca | BRYT |
| *Srd5a1* | gatggtgggctcttcctacg | aaaaccagcgtcctttgcac | BRYT |
| *Nr5a1* | gtgcatggtctttaaggagctgg | ggatgctgtcttccttgccgta | BRYT |

**Western blotting**

Testes from WT, *Inpp4b* $^{-/-}$ and cryptorchid *Rxfp2* $^{-/-}$ mice were homogenized with a glass tissue grinder in ice-cold RIPA buffer supplemented with protease and phosphatase inhibitors [181]. The lysates were diluted tenfold and 20-30 μg of protein were resolved on SDS-PAGE and transferred to PVDF membrane. For immunoblotting, rabbit polyclonal primary antibody against AR (1:1000 dilution, catalog number 06-680, Millipore, Carlsbad, CA) and mouse monoclonal β-tubulin (1:5000, #05-661, Millipore) were used. Signal was visualized using ImageQuant LAS 500 imaging system (GE Healthcare Life Sciences, Marlborough, MA) and quantitative analysis was performed with ImageQuant TL software.

**Propidium iodide staining and flow cytometry:**

Testis digestion and flow cytometry experiments were performed as previously described [381]. Six-month-old WT and *Inpp4b*$^{-/-}$ mice were used (n=4 for each group). Seminiferous tubules were washed with 1X HBSS, digested with collagenase and trypsin, and filtered. Next, cells were washed with 0.1% BSA in PBS, centrifuged at 400 g for 2 minutes, counted, and resuspended at $2x10^6$ cells/ml. Cells were fixed in 70% ethanol and stained for 30 minutes with 25 μg/ml of propidium iodide dissolved in 0.1% BSA in PBS. Analysis was performed using Accuri C6 flow cytometer (Becton-Dickinson, Franklin Lakes, NJ).

**Histology and immunohistochemistry (IHC)**

Testis samples were fixed in 4% PFA overnight and embedded in paraffin. The embedded tissue was sectioned at 4.5 μm. H&E staining and IHC were performed as previously described [410]. Rabbit polyclonal antibodies to INPP4B (1:150 dilution, #8450, Cell Signaling, Danvers, MA) and γH2A.X (1:700, #2577, Cell Signaling, Danvers, MA) were

used as primary antibodies and sections were counterstained with hematoxylin (Millipore). For TUNEL assay, ApopTag Plus Peroxidase *In Situ* Apoptosis Detection Kit (Millipore) was used following manufacturer protocol. Three mice were analyzed for each group and minimum ten circular tubules were counted per mouse. The images were captured using a Carl Zeiss Axio A1 microscope with an AxioCam MRc5 CCD camera (Carl Zeiss, New York, NY).

**Statistical analysis**

Two tailed Student's t-test for two groups, one-way ANOVA and two-way ANOVA (Tukey's multiple comparisons test) for more than two groups were used to assess the significance of differences using Prism 7.0 software (GraphPad Software, La Jolla, CA). All data are presented as mean ± SEM. p values less than 0.05 ($p<0.05$) were accepted as significant. The number of samples analyzed is shown in figure legends.

# 6. CHAPTER 6: Conclusions and future directions

Despite the high expression levels of INPP4B during the development of multiple tissues, its role has been investigated mainly as a tumor suppressor and an oncogene in various cancers. In this dissertation, I explored the role of INPP4B in normal physiology.

I showed that INPP4B protects against NAFLD and diet-induced obesity, hyperglycemia, and adipose tissue inflammation in female mice. I found that this protection is due to the regulatory effect of INPP4B on hepatic lipid metabolism, insulin sensitivity, and hypothalamic control of blood glucose levels, as well as INPP4B-modulated suppression of adipose inflammation. While both *Inpp4b*$^{-/-}$ males and females had the symptoms of the HFD-induced metabolic syndrome, females exhibited a significantly milder phenotype compared to males. The disparities between HFD *Inpp4b*$^{-/-}$ males and females are due in part to hypothalamic leptin and FGF21-FGFR1 pathways, revealing a novel and sexually dimorphic role of INPP4B in the central nervous system, which is responsible for metabolic homeostasis. We will continue to explore the molecular mechanisms that are regulated by INPP4B, which lead to the differences in the metabolic phenotype of males and females. Of note, we observed this phenotype due to the global knockout of *Inpp4b.* In the future, we will investigate which tissue-specific knockouts of *Inpp4b* would recapitulate individual aspects of *Inpp4b*$^{-/-}$ metabolic phenotype. For that reason, we will expand our metabolic research in the liver and hypothalamus-specific *Inpp4b*- knockout mouse models.

Furthermore, I demonstrated that INPP4B is involved in mammary gland ductal branching and *ERBB2*-driven tumorigenesis. It promotes mammary gland side branching through supporting PR expression and activity. We previously reported that HFD *Inpp4b*$^{-/-}$ females

develop mammary gland hyperplasia but not mammary gland tumors [166]. While higher pAKT levels, more leptin expression, and induced inflammation contribute to hyperplasia in this group, the compensatory increase in p53 levels might be preventing mammary gland tumor development in *Inpp4b*$^{-/-}$ females in either diet. Thus, my findings imply a protective role for INPP4B in mammary gland tumorigenesis.

Mammary glands consist of epithelial, myoepithelial, and adipose components, playing distinct roles in mammary gland development through different signaling pathways [411]. PR signaling is one of the main drivers of ductal branching in the mammary gland [207, 219, 220]. However, we observed lower PR signaling only in the combination of INPP4B loss and HFD feeding. In the future, we will investigate the signaling pathways that lead to the reduction in ductal branching in *Inpp4b*$^{-/-}$ mice. Since all experiments are conducted in whole mammary glands, we will continue our analyses by examining the different mammary gland cell types separately, including investigating the altered pathways in LFD *Inpp4b*$^{-/-}$ mice such as AKT and p53 signaling.

Besides affecting normal mammary glands, I reported that INPP4B inhibits *ERBB2*-driven tumorigenesis by modulating p53 signaling. In *MMTV-ERBB2/+*; *Inpp4b*$^{-/-}$ mice on HFD, I observed a reduction of p53 protein levels and activity, as well as increased lipid metabolism. The reduction of p53 levels in the tumors of *ERBB2*/+; *Inpp4b*$^{-/-}$ females leads to accelerated tumor progression. Thus, my findings reveal a new mechanism for the tumor suppressor properties of INPP4B at advanced stage and under obesogenic conditions. Other than mammary glands and tumors, we have additional data that show alterations in the expression of p53 in various tissues and there is accumulating data which suggest a direct link between INPP4B and p53 expression [86, 91]. In the future, we will investigate

whether INPP4B regulates p53 expression and signaling in the context of both metabolic health and cancer biology.

In addition, the upregulation of lipid synthesis in the tumors due to *Inpp4b* loss and HFD, suggests a direct effect of INPP4B in the control of lipid metabolism in both normal and neoplastic physiology. Furthermore, I did not observe changes in PI3K/AKT pathway, apoptosis, and proliferation, which are frequently altered in cancer progression. I believe this indifference is caused by the collection of the tumors at an advanced stage. In the future, we will dissect and analyze tumors at earlier stages.

Lastly, I investigated the expression and role of INPP4B in testicular function. I showed that INPP4B is mainly expressed in post-meiotic germ cells, along with somatic Leydig and Sertoli cells in both men and mice, while the expression of INPP4B is significantly lower in infertile men, suggesting that INPP4B is a potential marker for male infertility. Moreover, *Inpp4b*$^{-/-}$ male mice have smaller testis and fewer sperm count due to induced apoptosis. While both factors are aggravated with HFD feeding, HFD *Inpp4b*$^{-/-}$ mice also show reduced steroidogenic activity and meiosis. My findings are the first to show a distinct role for INPP4B in testis; however, the molecular pathways that result in the subfertile phenotype of *Inpp4b*$^{-/-}$ males are yet unknown. In the future, we will investigate these pathways that are affected by INPP4B using testicular cell specific knockouts of *Inpp4b*.

Moreover, I observed some differences in the sex steroid hormone receptor signaling between *Inpp4b*$^{-/-}$ males and females, in addition to metabolic homeostasis. In either gender, the levels of respective sex steroid hormones—testosterone, estradiol, and progesterone—do not change by INPP4B loss. In males, the gene and protein expression

of AR remains similar, but AR transcriptional activity is reprogrammed in *Inpp4b*$^{-/-}$ prostates in either diet [20]. In females, I detected a decrease in both gene expression and transcriptional activity for PR in mammary glands when there is a combination of *Inpp4b* loss and HFD. My findings suggest that INPP4B promotes steroid receptor stability and transcriptional activity at different degrees in males and females depending on the diet. In addition, INPP4B inhibits the AKT pathway in both male and female reproductive tissues. Since PI3K/AKT pathway has distinct roles in different organs [222, 412], the suppression of this pathway by INPP4B will have corresponding consequences in these organs.

In conclusion, I illustrated that INPP4B is indispensable in the normal physiology of reproductive organs and is protective against metabolic diseases and cancer in female mice under obesogenic conditions. In the future, it is crucial to understand further mechanisms that regulated by INPP4B in order to define potential targets for the treatment of obesity and associated diseases.

REFERENCES

1. WHO. Obesity and Overweight 2021. Available from: https://www.who.int/news-room/fact-sheets/detail/obesity-and-overweight.

2. CDC. Overweight & Obesity: Adult Obesity Facts.

3. (WHO) WHO. Noncommunicable diseases 2021. Available from: https://www.who.int/news-room/fact-sheets/detail/noncommunicable-diseases.

4. Mokdad AH, Ford ES, Bowman BA, Dietz WH, Vinicor F, Bales VS, et al. Prevalence of obesity, diabetes, and obesity-related health risk factors, 2001. JAMA. 2003;289(1):76-9. Epub 2002/12/31. doi: 10.1001/jama.289.1.76. PubMed PMID: 12503980.

5. Huang X, Liu G, Guo J, Su Z. The PI3K/AKT pathway in obesity and type 2 diabetes. Int J Biol Sci. 2018;14(11):1483-96. Epub 2018/09/29. doi: 10.7150/ijbs.27173. PubMed PMID: 30263000; PubMed Central PMCID: PMCPMC6158718.

6. Yang J, Nie J, Ma X, Wei Y, Peng Y, Wei X. Targeting PI3K in cancer: mechanisms and advances in clinical trials. Mol Cancer. 2019;18(1):26. Epub 2019/02/21. doi: 10.1186/s12943-019-0954-x. PubMed PMID: 30782187; PubMed Central PMCID: PMCPMC6379961.

7. Garg R, Benedetti LG, Abera MB, Wang H, Abba M, Kazanietz MG. Protein kinase C and cancer: what we know and what we do not. Oncogene. 2014;33(45):5225-37. Epub 2013/12/18. doi: 10.1038/onc.2013.524. PubMed PMID: 24336328; PubMed Central PMCID: PMCPMC4435965.

8. Luo J, Manning BD, Cantley LC. Targeting the PI3K-Akt pathway in human cancer. Cancer Cell. 2003;4(4):257-62. doi: 10.1016/s1535-6108(03)00248-4.

9. Chen KQ, Wei BH, Hao SL, Yang WX. The PI3K/AKT signaling pathway: How does it regulate development of Sertoli cells and spermatogenic cells? Histol Histopathol. 2022:18457. Epub 2022/04/08. doi: 10.14670/HH-18-457. PubMed PMID: 35388905.

10. Brill JA, Yildirim S, Fabian L. Phosphoinositide signaling in sperm development. Seminars in cell & developmental biology. 2016;59:2-9. doi: 10.1016/j.semcdb.2016.06.010. PubMed PMID: 27321976.

11. Billcliff PG, Lowe M. Inositol lipid phosphatases in membrane trafficking and human disease. Biochem J. 2014;461(2):159-75. Epub 2014/06/27. doi: 10.1042/BJ20140361. PubMed PMID: 24966051.

12. Norris FA, Auethavekiat V, Majerus PW. The isolation and characterization of cDNA encoding human and rat brain inositol polyphosphate 4-phosphatase. J Biol Chem. 1995;270(27):16128-33. Epub 1995/07/07. doi: 10.1074/jbc.270.27.16128. PubMed PMID: 7608176.

13. Norris FA, Atkins RC, Majerus PW. The cDNA cloning and characterization of inositol polyphosphate 4-phosphatase type II. Evidence for conserved alternative splicing in the 4-phosphatase family. J Biol Chem. 1997;272(38):23859-64. Epub 1997/09/20. doi: 10.1074/jbc.272.38.23859. PubMed PMID: 9295334.

14. Ferron M, Vacher J. Characterization of the murine Inpp4b gene and identification of a novel isoform. Gene. 2006;376(1):152-61. Epub 2006/04/25. doi: 10.1016/j.gene.2006.02.022. PubMed PMID: 16631325.

15. Agoulnik IU, Hodgson MC, Bowden WA, Ittmann MM. INPP4B: the new kid on the PI3K block. Oncotarget. 2011;2(4):321-8. Epub 2011/04/14. doi: 10.18632/oncotarget.260. PubMed PMID: 21487159; PubMed Central PMCID: PMCPMC3248162.

16. Lopez SM, Hodgson MC, Packianathan C, Bingol-Ozakpinar O, Uras F, Rosen BP, et al. Determinants of the tumor suppressor INPP4B protein and lipid phosphatase activities. Biochem Biophys Res Commun. 2013;440(2):277-82. Epub 2013/09/28. doi: 10.1016/j.bbrc.2013.09.077. PubMed PMID: 24070612; PubMed Central PMCID: PMCPMC4578723.

17. Kofuji S, Kimura H, Nakanishi H, Nanjo H, Takasuga S, Liu H, et al. INPP4B Is a PtdIns(3,4,5)P3 Phosphatase That Can Act as a Tumor Suppressor. Cancer Discov. 2015;5(7):730-9. Epub 2015/04/18. doi: 10.1158/2159-8290.CD-14-1329. PubMed PMID: 25883023.

18. Ferron M, Boudiffa M, Arsenault M, Rached M, Pata M, Giroux S, et al. Inositol polyphosphate 4-phosphatase B as a regulator of bone mass in mice and humans. Cell Metab. 2011;14(4):466-77. Epub 2011/10/11. doi: 10.1016/j.cmet.2011.08.013. PubMed PMID: 21982707; PubMed Central PMCID: PMCPMC3204353.

19. Guo ST, Chi MN, Yang RH, Guo XY, Zan LK, Wang CY, et al. INPP4B is an oncogenic regulator in human colon cancer. Oncogene. 2016;35(23):3049-61. Epub 2015/09/29. doi: 10.1038/onc.2015.361. PubMed PMID: 26411369; PubMed Central PMCID: PMCPMC4908438.

20. Zhang M, Ceyhan Y, Kaftanovskaya EM, Vasquez JL, Vacher J, Knop FK, et al. INPP4B protects from metabolic syndrome and associated disorders. Commun Biol. 2021;4(1):416. Epub 2021/03/28. doi: 10.1038/s42003-021-01940-6. PubMed PMID: 33772116.

21. De Craene JO, Bertazzi DL, Bar S, Friant S. Phosphoinositides, Major Actors in Membrane Trafficking and Lipid Signaling Pathways. Int J Mol Sci. 2017;18(3). doi: 10.3390/ijms18030634. PubMed PMID: 28294977; PubMed Central PMCID: PMCPMC5372647.

22. Epand RM. Introduction to membrane lipids. Methods Mol Biol. 2015;1232:1-6. doi: 10.1007/978-1-4939-1752-5_1. PubMed PMID: 25331123.

23. Kim YJ, Jahan N, Bahk YY. Biochemistry and structure of phosphoinositide phosphatases. BMB Rep. 2013;46(1):1-8. doi: 10.5483/bmbrep.2013.46.1.261. PubMed PMID: 23351377; PubMed Central PMCID: PMCPMC4133831.

24. Dyson JM, Fedele CG, Davies EM, Becanovic J, Mitchell CA. Phosphoinositide phosphatases: just as important as the kinases. Subcell Biochem. 2012;58:215-79. Epub 2012/03/10. doi: 10.1007/978-94-007-3012-0_7. PubMed PMID: 22403078.

25. McCrea HJ, De Camilli P. Mutations in phosphoinositide metabolizing enzymes and human disease. Physiology (Bethesda). 2009;24:8-16. Epub 2009/02/07. doi: 10.1152/physiol.00035.2008. PubMed PMID: 19196647; PubMed Central PMCID: PMCPMC3499097.

26. Liu Y, Bankaitis VA. Phosphoinositide phosphatases in cell biology and disease. Prog Lipid Res. 2010;49(3):201-17. doi: 10.1016/j.plipres.2009.12.001. PubMed PMID: 20043944; PubMed Central PMCID: PMCPMC2873057.

27. Manning BD, Toker A. AKT/PKB Signaling: Navigating the Network. Cell. 2017;169(3):381-405. Epub 2017/04/22. doi: 10.1016/j.cell.2017.04.001. PubMed PMID: 28431241; PubMed Central PMCID: PMCPMC5546324.

28. Sabatini DM. Twenty-five years of mTOR: Uncovering the link from nutrients to growth. Proc Natl Acad Sci U S A. 2017;114(45):11818-25. Epub 2017/10/29. doi: 10.1073/pnas.1716173114. PubMed PMID: 29078414; PubMed Central PMCID: PMCPMC5692607.

29. Liu P, Gan W, Chin YR, Ogura K, Guo J, Zhang J, et al. PtdIns(3,4,5)P3-Dependent Activation of the mTORC2 Kinase Complex. Cancer Discov. 2015;5(11):1194-209. Epub 2015/08/22. doi: 10.1158/2159-8290.CD-15-0460. PubMed PMID: 26293922; PubMed Central PMCID: PMCPMC4631654.

30. Marat AL, Wallroth A, Lo WT, Muller R, Norata GD, Falasca M, et al. mTORC1 activity repression by late endosomal phosphatidylinositol 3,4-bisphosphate. Science. 2017;356(6341):968-72. Epub 2017/06/03. doi: 10.1126/science.aaf8310. PubMed PMID: 28572395.

31. Aoki M, Jiang H, Vogt PK. Proteasomal degradation of the FoxO1 transcriptional regulator in cells transformed by the P3k and Akt oncoproteins. Proc Natl Acad Sci U S A. 2004;101(37):13613-7. Epub 2004/09/03. doi: 10.1073/pnas.0405454101. PubMed PMID: 15342912; PubMed Central PMCID: PMCPMC518802.

32. Furukawa-Hibi Y, Kobayashi Y, Chen C, Motoyama N. FOXO transcription factors in cell-cycle regulation and the response to oxidative stress. Antioxid Redox Signal. 2005;7(5-6):752-60. Epub 2005/05/14. doi: 10.1089/ars.2005.7.752. PubMed PMID: 15890021.

33. Duvel K, Yecies JL, Menon S, Raman P, Lipovsky AI, Souza AL, et al. Activation of a metabolic gene regulatory network downstream of mTOR complex 1. Mol Cell. 2010;39(2):171-83. Epub 2010/07/31. doi: 10.1016/j.molcel.2010.06.022. PubMed PMID: 20670887; PubMed Central PMCID: PMCPMC2946786.

34. Liu Z, Xu E, Zhao HT, Cole T, West AB. LRRK2 and Rab10 coordinate macropinocytosis to mediate immunological responses in phagocytes. EMBO J. 2020;39(20):e104862. Epub 2020/08/28. doi: 10.15252/embj.2020104862. PubMed PMID: 32853409; PubMed Central PMCID: PMCPMC7560233.

35. Klarlund JK, Rameh LE, Cantley LC, Buxton JM, Holik JJ, Sakelis C, et al. Regulation of GRP1-catalyzed ADP ribosylation factor guanine nucleotide exchange by phosphatidylinositol 3,4,5-trisphosphate. J Biol Chem. 1998;273(4):1859-62. Epub 1998/01/27. doi: 10.1074/jbc.273.4.1859. PubMed PMID: 9442017.

36. Mazloumi Gavgani F, Slinning MS, Morovicz AP, Arnesen VS, Turcu DC, Ninzima S, et al. Nuclear Phosphatidylinositol 3,4,5-Trisphosphate Interactome Uncovers an Enrichment in Nucleolar Proteins. Mol Cell Proteomics. 2021;20:100102. Epub 2021/05/29. doi: 10.1016/j.mcpro.2021.100102. PubMed PMID: 34048982; PubMed Central PMCID: PMCPMC8255942.

37. Chen M, Choi S, Wen T, Chen C, Thapa N, Lee JH, et al. A p53-phosphoinositide signalosome regulates nuclear AKT activation. Nat Cell Biol. 2022;24(7):1099-113. Epub 2022/07/08. doi: 10.1038/s41556-022-00949-1. PubMed PMID: 35798843.

38. Gozzelino L, De Santis MC, Gulluni F, Hirsch E, Martini M. PI(3,4)P2 Signaling in Cancer and Metabolism. Front Oncol. 2020;10:360. Epub 2020/04/17. doi: 10.3389/fonc.2020.00360. PubMed PMID: 32296634; PubMed Central PMCID: PMCPMC7136497.

39. Castro-Castro A, Marchesin V, Monteiro P, Lodillinsky C, Rosse C, Chavrier P. Cellular and Molecular Mechanisms of MT1-MMP-Dependent Cancer Cell Invasion. Annu Rev Cell Dev Biol. 2016;32:555-76. Epub 2016/08/09. doi: 10.1146/annurev-cellbio-111315-125227. PubMed PMID: 27501444.

40. Lagarrigue F, Vikas Anekal P, Lee HS, Bachir AI, Ablack JN, Horwitz AF, et al. A RIAM/lamellipodin-talin-integrin complex forms the tip of sticky fingers that guide cell migration. Nat Commun. 2015;6:8492. Epub 2015/10/01. doi: 10.1038/ncomms9492. PubMed PMID: 26419705; PubMed Central PMCID: PMCPMC4589889.

41. Posor Y, Eichhorn-Gruenig M, Puchkov D, Schoneberg J, Ullrich A, Lampe A, et al. Spatiotemporal control of endocytosis by phosphatidylinositol-3,4-bisphosphate. Nature. 2013;499(7457):233-7. Epub 2013/07/05. doi: 10.1038/nature12360. PubMed PMID: 23823722.

42. Hogan A, Yakubchyk Y, Chabot J, Obagi C, Daher E, Maekawa K, et al. The phosphoinositol 3,4-bisphosphate-binding protein TAPP1 interacts with syntrophins and regulates actin cytoskeletal organization. J Biol Chem. 2004;279(51):53717-24. Epub 2004/10/16. doi: 10.1074/jbc.M410654200. PubMed PMID: 15485858.

43. Sun HQ, Yamamoto M, Mejillano M, Yin HL. Gelsolin, a multifunctional actin regulatory protein. J Biol Chem. 1999;274(47):33179-82. Epub 1999/11/24. doi: 10.1074/jbc.274.47.33179. PubMed PMID: 10559185.

44. Tan X, Thapa N, Choi S, Anderson RA. Emerging roles of PtdIns(4,5)P2--beyond the plasma membrane. J Cell Sci. 2015;128(22):4047-56. Epub 2015/11/18. doi: 10.1242/jcs.175208. PubMed PMID: 26574506; PubMed Central PMCID: PMCPMC4712784.

45. Newton AC. Diacylglycerol's affair with protein kinase C turns 25. Trends Pharmacol Sci. 2004;25(4):175-7. Epub 2004/05/01. doi: 10.1016/j.tips.2004.02.010. PubMed PMID: 15116719.

46. Hansen SB, Tao X, MacKinnon R. Structural basis of PIP2 activation of the classical inward rectifier K+ channel Kir2.2. Nature. 2011;477(7365):495-8. Epub 2011/08/30. doi: 10.1038/nature10370. PubMed PMID: 21874019; PubMed Central PMCID: PMCPMC3324908.

47. Yen HY, Hoi KK, Liko I, Hedger G, Horrell MR, Song W, et al. PtdIns(4,5)P2 stabilizes active states of GPCRs and enhances selectivity of G-protein coupling. Nature. 2018;559(7714):423-7. Epub 2018/07/12. doi: 10.1038/s41586-018-0325-6. PubMed PMID: 29995853; PubMed Central PMCID: PMCPMC6059376.

48. Stack JH, DeWald DB, Takegawa K, Emr SD. Vesicle-mediated protein transport: regulatory interactions between the Vps15 protein kinase and the Vps34 PtdIns 3-kinase essential for protein sorting to the vacuole in yeast. J Cell Biol. 1995;129(2):321-34. Epub 1995/04/01. doi: 10.1083/jcb.129.2.321. PubMed PMID: 7721937; PubMed Central PMCID: PMCPMC2199917.

49. Nezis IP, Sagona AP, Schink KO, Stenmark H. Divide and ProsPer: the emerging role of PtdIns3P in cytokinesis. Trends Cell Biol. 2010;20(11):642-9. Epub 2010/10/01. doi: 10.1016/j.tcb.2010.08.010. PubMed PMID: 20880709.

50. Nascimbeni AC, Codogno P, Morel E. Phosphatidylinositol-3-phosphate in the regulation of autophagy membrane dynamics. FEBS J. 2017;284(9):1267-78. Epub 2016/12/16. doi: 10.1111/febs.13987. PubMed PMID: 27973739.

51. Saffi GT, Wang CA, Mangialardi EM, Vacher J, Botelho RJ, Salmena L. Inhibition of lipid kinase PIKfyve reveals a role for phosphatase Inpp4b in the regulation

of PI(3)P-mediated lysosome dynamics through VPS34 activity. J Biol Chem. 2022;298(8):102187. Epub 2022/06/28. doi: 10.1016/j.jbc.2022.102187. PubMed PMID: 35760104; PubMed Central PMCID: PMCPMC9304791.

52. Gaullier JM, Simonsen A, D'Arrigo A, Bremnes B, Stenmark H, Aasland R. FYVE fingers bind PtdIns(3)P. Nature. 1998;394(6692):432-3. Epub 1998/08/11. doi: 10.1038/28767. PubMed PMID: 9697764.

53. Marat AL, Haucke V. Phosphatidylinositol 3-phosphates-at the interface between cell signalling and membrane traffic. EMBO J. 2016;35(6):561-79. Epub 2016/02/19. doi: 10.15252/embj.201593564. PubMed PMID: 26888746; PubMed Central PMCID: PMCPMC4801949.

54. Ajazi A, Bruhn C, Shubassi G, Lucca C, Ferrari E, Cattaneo A, et al. Endosomal trafficking and DNA damage checkpoint kinases dictate survival to replication stress by regulating amino acid uptake and protein synthesis. Dev Cell. 2021;56(18):2607-22 e6. Epub 2021/09/18. doi: 10.1016/j.devcel.2021.08.019. PubMed PMID: 34534458.

55. Jin N, Mao K, Jin Y, Tevzadze G, Kauffman EJ, Park S, et al. Roles for PI(3,5)P2 in nutrient sensing through TORC1. Mol Biol Cell. 2014;25(7):1171-85. Epub 2014/01/31. doi: 10.1091/mbc.E14-01-0021. PubMed PMID: 24478451; PubMed Central PMCID: PMCPMC3967979.

56. Bridges D, Ma JT, Park S, Inoki K, Weisman LS, Saltiel AR. Phosphatidylinositol 3,5-bisphosphate plays a role in the activation and subcellular localization of mechanistic target of rapamycin 1. Mol Biol Cell. 2012;23(15):2955-62. Epub 2012/06/15. doi: 10.1091/mbc.E11-12-1034. PubMed PMID: 22696681; PubMed Central PMCID: PMCPMC3408421.

57. Rodgers SJ, Jones EI, Arumugam S, Hamila SA, Danne J, Gurung R, et al. Endosome maturation links PI3Kalpha signaling to lysosome repopulation during basal autophagy. EMBO J. 2022:e110398. Epub 2022/08/16. doi: 10.15252/embj.2021110398. PubMed PMID: 35968799.

58. Rodgers SJ, Jones EI, Mitchell CA, McGrath MJ. Sequential conversion of PtdIns3P to PtdIns(3,5)P2 via endosome maturation couples nutrient signaling to lysosome reformation and basal autophagy. Autophagy. 2022. Epub 2022/09/15. doi: 10.1080/15548627.2022.2124499. PubMed PMID: 36103410.

59. Grainger DL, Tavelis C, Ryan AJ, Hinchliffe KA. The emerging role of PtdIns5P: another signalling phosphoinositide takes its place. Biochem Soc Trans. 2012;40(1):257-61. Epub 2012/01/21. doi: 10.1042/BST20110617. PubMed PMID: 22260701.

60. Karabiyik C, Vicinanza M, Son SM, Rubinsztein DC. Glucose starvation induces autophagy via ULK1-mediated activation of PIKfyve in an AMPK-dependent manner. Dev Cell. 2021;56(13):1961-75 e5. Epub 2021/06/10. doi: 10.1016/j.devcel.2021.05.010. PubMed PMID: 34107300.

61. Vicinanza M, Korolchuk VI, Ashkenazi A, Puri C, Menzies FM, Clarke JH, et al. PI(5)P regulates autophagosome biogenesis. Mol Cell. 2015;57(2):219-34. Epub 2015/01/13. doi: 10.1016/j.molcel.2014.12.007. PubMed PMID: 25578879; PubMed Central PMCID: PMCPMC4306530.

62. Sbrissa D, Ikonomov OC, Strakova J, Shisheva A. Role for a novel signaling intermediate, phosphatidylinositol 5-phosphate, in insulin-regulated F-actin stress fiber breakdown and GLUT4 translocation. Endocrinology. 2004;145(11):4853-65. Epub 2004/07/31. doi: 10.1210/en.2004-0489. PubMed PMID: 15284192.

63. Grainger DL, Tavelis C, Ryan AJ, Hinchliffe KA. Involvement of phosphatidylinositol 5-phosphate in insulin-stimulated glucose uptake in the L6 myotube model of skeletal muscle. Pflugers Arch. 2011;462(5):723-32. Epub 2011/08/19. doi: 10.1007/s00424-011-1008-4. PubMed PMID: 21847559.

64. Viaud J, Lagarrigue F, Ramel D, Allart S, Chicanne G, Ceccato L, et al. Phosphatidylinositol 5-phosphate regulates invasion through binding and activation of Tiam1. Nat Commun. 2014;5:4080. Epub 2014/06/07. doi: 10.1038/ncomms5080. PubMed PMID: 24905281.

65. Oppelt A, Haugsten EM, Zech T, Danielsen HE, Sveen A, Lobert VH, et al. PIKfyve, MTMR3 and their product PtdIns5P regulate cancer cell migration and invasion through activation of Rac1. Biochem J. 2014;461(3):383-90. Epub 2014/05/21. doi: 10.1042/BJ20140132. PubMed PMID: 24840251.

66. Zou J, Marjanovic J, Kisseleva MV, Wilson M, Majerus PW. Type I phosphatidylinositol-4,5-bisphosphate 4-phosphatase regulates stress-induced apoptosis. Proc Natl Acad Sci U S A. 2007;104(43):16834-9. Epub 2007/10/18. doi: 10.1073/pnas.0708189104. PubMed PMID: 17940011; PubMed Central PMCID: PMCPMC2040409.

67. Jones DR, Bultsma Y, Keune WJ, Halstead JR, Elouarrat D, Mohammed S, et al. Nuclear PtdIns5P as a transducer of stress signaling: an in vivo role for PIP4Kbeta. Mol Cell. 2006;23(5):685-95. Epub 2006/09/05. doi: 10.1016/j.molcel.2006.07.014. PubMed PMID: 16949365.

68. Wong KK, Engelman JA, Cantley LC. Targeting the PI3K signaling pathway in cancer. Curr Opin Genet Dev. 2010;20(1):87-90. Epub 2009/12/17. doi: 10.1016/j.gde.2009.11.002. PubMed PMID: 20006486; PubMed Central PMCID: PMCPMC2822054.

69. Urtreger AJ, Kazanietz MG, Bal de Kier Joffe ED. Contribution of individual PKC isoforms to breast cancer progression. IUBMB Life. 2012;64(1):18-26. Epub 2011/11/19. doi: 10.1002/iub.574. PubMed PMID: 22095874.

70. Samuel VT, Shulman GI. Nonalcoholic Fatty Liver Disease as a Nexus of Metabolic and Hepatic Diseases. Cell Metab. 2018;27(1):22-41. Epub 2017/09/05. doi: 10.1016/j.cmet.2017.08.002. PubMed PMID: 28867301; PubMed Central PMCID: PMCPMC5762395.

71. Hopkins BD, Goncalves MD, Cantley LC. Insulin-PI3K signalling: an evolutionarily insulated metabolic driver of cancer. Nat Rev Endocrinol. 2020;16(5):276-83. Epub 2020/03/05. doi: 10.1038/s41574-020-0329-9. PubMed PMID: 32127696; PubMed Central PMCID: PMCPMC7286536.

72. Lemcke S, Muller S, Moller S, Schillert A, Ziegler A, Cepok-Kauffeld S, et al. Nerve conduction velocity is regulated by the inositol polyphosphate-4-phosphatase II gene. Am J Pathol. 2014;184(9):2420-9. Epub 2014/08/19. doi: 10.1016/j.ajpath.2014.05.021. PubMed PMID: 25129256.

73. Ji L, Kim NH, Huh SO, Rhee HJ. Depletion of Inositol Polyphosphate 4-Phosphatase II Suppresses Callosal Axon Formation in the Developing Mice. Mol Cells. 2016;39(6):501-7. Epub 2016/04/26. doi: 10.14348/molcells.2016.0058. PubMed PMID: 27109423; PubMed Central PMCID: PMCPMC4916402.

74. Hamila SA, Ooms LM, Rodgers SJ, Mitchell CA. The INPP4B paradox: Like PTEN, but different. Adv Biol Regul. 2021;82:100817. Epub 2021/07/04. doi: 10.1016/j.jbior.2021.100817. PubMed PMID: 34216856.

75. Fragomeni SM, Sciallis A, Jeruss JS. Molecular Subtypes and Local-Regional Control of Breast Cancer. Surg Oncol Clin N Am. 2018;27(1):95-120. Epub 2017/11/15. doi: 10.1016/j.soc.2017.08.005. PubMed PMID: 29132568; PubMed Central PMCID: PMCPMC5715810.

76. National Cancer Institute (NIH): Survaillance E, and End Results Program (SEER). . Cancer Stat Facts: Female Breast Cancer Subtypes 2021. Available from: https://seer.cancer.gov/statfacts/html/breast-subtypes.html.

77. Boonyaratanakornkit V, Hamilton N, Marquez-Garban DC, Pateetin P, McGowan EM, Pietras RJ. Extranuclear signaling by sex steroid receptors and clinical implications in breast cancer. Mol Cell Endocrinol. 2018;466:51-72. Epub 2017/11/18. doi: 10.1016/j.mce.2017.11.010. PubMed PMID: 29146555; PubMed Central PMCID: PMCPMC5878997.

78. Fedele CG, Ooms LM, Ho M, Vieusseux J, O'Toole SA, Millar EK, et al. Inositol polyphosphate 4-phosphatase II regulates PI3K/Akt signaling and is lost in human basal-like breast cancers. Proc Natl Acad Sci U S A. 2010;107(51):22231-6. Epub 2010/12/04. doi: 10.1073/pnas.1015245107. PubMed PMID: 21127264; PubMed Central PMCID: PMCPMC3009830.

79. Rimawi MF, Schiff R, Osborne CK. Targeting HER2 for the treatment of breast cancer. Annu Rev Med. 2015;66:111-28. Epub 2015/01/15. doi: 10.1146/annurev-med-042513-015127. PubMed PMID: 25587647.

80. Won JR, Gao D, Chow C, Cheng J, Lau SY, Ellis MJ, et al. A survey of immunohistochemical biomarkers for basal-like breast cancer against a gene expression profile gold standard. Mod Pathol. 2013;26(11):1438-50. Epub 2013/05/25. doi: 10.1038/modpathol.2013.97. PubMed PMID: 23702728.

81. Lv Q, Meng Z, Yu Y, Jiang F, Guan D, Liang C, et al. Molecular Mechanisms and Translational Therapies for Human Epidermal Receptor 2 Positive Breast Cancer. Int J Mol Sci. 2016;17(12). Epub 2016/12/17. doi: 10.3390/ijms17122095. PubMed PMID: 27983617; PubMed Central PMCID: PMCPMC5187895.

82. Yarden Y, Sliwkowski MX. Untangling the ErbB signalling network. Nat Rev Mol Cell Biol. 2001;2(2):127-37. Epub 2001/03/17. doi: 10.1038/35052073. PubMed PMID: 11252954.

83. Hellyer NJ, Kim MS, Koland JG. Heregulin-dependent activation of phosphoinositide 3-kinase and Akt via the ErbB2/ErbB3 co-receptor. J Biol Chem. 2001;276(45):42153-61. Epub 2001/09/08. doi: 10.1074/jbc.M102079200. PubMed PMID: 11546794.

84. Pereira B, Chin SF, Rueda OM, Vollan HK, Provenzano E, Bardwell HA, et al. The somatic mutation profiles of 2,433 breast cancers refines their genomic and transcriptomic landscapes. Nat Commun. 2016;7:11479. Epub 2016/05/11. doi: 10.1038/ncomms11479. PubMed PMID: 27161491; PubMed Central PMCID: PMCPMC4866047.

85. Zhang B, Wang W, Li C, Liu R. Inositol polyphosphate-4-phosphatase type II plays critical roles in the modulation of cadherin-mediated adhesion dynamics of pancreatic ductal adenocarcinomas. Cell Adh Migr. 2018;12(6):548-63. Epub 2018/06/29. doi: 10.1080/19336918.2018.1491496. PubMed PMID: 29952716; PubMed Central PMCID: PMCPMC6363046.

86. Tang W, Yang L, Yang T, Liu M, Zhou Y, Lin J, et al. INPP4B inhibits cell proliferation, invasion and chemoresistance in human hepatocellular carcinoma. Onco Targets Ther. 2019;12:3491-507. Epub 2019/05/28. doi: 10.2147/OTT.S196832. PubMed PMID: 31123408; PubMed Central PMCID: PMCPMC6511246.

87. Liu H, Paddock MN, Wang H, Murphy CJ, Geck RC, Navarro AJ, et al. The INPP4B Tumor Suppressor Modulates EGFR Trafficking and Promotes Triple-Negative Breast Cancer. Cancer Discov. 2020;10(8):1226-39. Epub 2020/06/10. doi: 10.1158/2159-8290.CD-19-1262. PubMed PMID: 32513774; PubMed Central PMCID: PMCPMC7415683.

88. Li Chew C, Lunardi A, Gulluni F, Ruan DT, Chen M, Salmena L, et al. In Vivo Role of INPP4B in Tumor and Metastasis Suppression through Regulation of PI3K-AKT Signaling at Endosomes. Cancer Discov. 2015;5(7):740-51. Epub 2015/04/18. doi: 10.1158/2159-8290.CD-14-1347. PubMed PMID: 25883022; PubMed Central PMCID: PMCPMC4497843.

89. Hsu I, Yeh CR, Slavin S, Miyamoto H, Netto GJ, Tsai YC, et al. Estrogen receptor alpha prevents bladder cancer via INPP4B inhibited akt pathway in vitro and in vivo. Oncotarget. 2014;5(17):7917-35. Epub 2014/10/04. doi: 10.18632/oncotarget.1421. PubMed PMID: 25277204; PubMed Central PMCID: PMCPMC4202170.

90. Hodgson MC, Shao LJ, Frolov A, Li R, Peterson LE, Ayala G, et al. Decreased expression and androgen regulation of the tumor suppressor gene INPP4B in prostate cancer. Cancer Res. 2011;71(2):572-82. Epub 2011/01/13. doi: 10.1158/0008-5472.CAN-10-2314. PubMed PMID: 21224358; PubMed Central PMCID: PMCPMC3077543.

91. Gewinner C, Wang ZC, Richardson A, Teruya-Feldstein J, Etemadmoghadam D, Bowtell D, et al. Evidence that inositol polyphosphate 4-phosphatase type II is a tumor suppressor that inhibits PI3K signaling. Cancer Cell. 2009;16(2):115-25. doi: 10.1016/j.ccr.2009.06.006. PubMed PMID: 19647222; PubMed Central PMCID: PMCPMC2957372.

92. Strotbek M, Schmid S, Sanchez-Gonzalez I, Boerries M, Busch H, Olayioye MA. miR-181 elevates Akt signaling by co-targeting PHLPP2 and INPP4B phosphatases in luminal breast cancer. Int J Cancer. 2017;140(10):2310-20. Epub 2017/02/23. doi: 10.1002/ijc.30661. PubMed PMID: 28224609.

93. Sun Y, Ding H, Liu X, Li X, Li L. INPP4B overexpression enhances the antitumor efficacy of PARP inhibitor AG014699 in MDA-MB-231 triple-negative breast cancer cells. Tumour Biol. 2014;35(5):4469-77. Epub 2014/01/15. doi: 10.1007/s13277-013-1589-y. PubMed PMID: 24420152.

94. Dai X, Fagerholm R, Khan S, Blomqvist C, Nevanlinna H. INPP4B and RAD50 have an interactive effect on survival after breast cancer. Breast Cancer Res Treat. 2015;149(2):363-71. Epub 2014/12/22. doi: 10.1007/s10549-014-3241-y. PubMed PMID: 25528023.

95. Chen X, Theobard R, Zhang J, Dai X. Genetic interactions between INPP4B and RAD50 is prognostic of breast cancer survival. Biosci Rep. 2020;40(1). Epub 2019/12/25. doi: 10.1042/BSR20192546. PubMed PMID: 31872854; PubMed Central PMCID: PMCPMC6954369.

96. Gasser JA, Inuzuka H, Lau AW, Wei W, Beroukhim R, Toker A. SGK3 mediates INPP4B-dependent PI3K signaling in breast cancer. Mol Cell. 2014;56(4):595-607. Epub 2014/12/03. doi: 10.1016/j.molcel.2014.09.023. PubMed PMID: 25458846; PubMed Central PMCID: PMCPMC4255362.

97. Chi MN, Guo ST, Wilmott JS, Guo XY, Yan XG, Wang CY, et al. INPP4B is upregulated and functions as an oncogenic driver through SGK3 in a subset of melanomas. Oncotarget. 2015;6(37):39891-907. Epub 2015/11/18. doi:

10.18632/oncotarget.5359. PubMed PMID: 26573229; PubMed Central PMCID: PMCPMC4741868.

98. Jin H, Yang L, Wang L, Yang Z, Zhan Q, Tao Y, et al. INPP4B promotes cell survival via SGK3 activation in NPM1-mutated leukemia. J Exp Clin Cancer Res. 2018;37(1):8. Epub 2018/01/19. doi: 10.1186/s13046-018-0675-9. PubMed PMID: 29343273; PubMed Central PMCID: PMCPMC5773044.

99. Rodgers SJ, Ooms LM, Oorschot VMJ, Schittenhelm RB, Nguyen EV, Hamila SA, et al. INPP4B promotes PI3Kalpha-dependent late endosome formation and Wnt/beta-catenin signaling in breast cancer. Nat Commun. 2021;12(1):3140. Epub 2021/05/27. doi: 10.1038/s41467-021-23241-6. PubMed PMID: 34035258; PubMed Central PMCID: PMCPMC8149851.

100. Hill JO, Wyatt HR, Peters JC. The Importance of Energy Balance. Eur Endocrinol. 2013;9(2):111-5. Epub 2013/08/01. doi: 10.17925/EE.2013.09.02.111. PubMed PMID: 29922364; PubMed Central PMCID: PMCPMC6003580.

101. Wu BN, O'Sullivan AJ. Sex differences in energy metabolism need to be considered with lifestyle modifications in humans. J Nutr Metab. 2011;2011:391809. Epub 2011/07/21. doi: 10.1155/2011/391809. PubMed PMID: 21773020; PubMed Central PMCID: PMCPMC3136178.

102. Diseases NIoDaDaK. Overweight & Obesity Statistics 2017-2018 [updated September 2021]. Available from: https://www.niddk.nih.gov/health-information/health-statistics/overweight-obesity.

103. Flegal KM, Carroll MD, Kit BK, Ogden CL. Prevalence of obesity and trends in the distribution of body mass index among US adults, 1999-2010. JAMA. 2012;307(5):491-7. Epub 2012/01/19. doi: 10.1001/jama.2012.39. PubMed PMID: 22253363.

104. Wildman RP, Muntner P, Reynolds K, McGinn AP, Rajpathak S, Wylie-Rosett J, et al. The obese without cardiometabolic risk factor clustering and the normal weight with cardiometabolic risk factor clustering: prevalence and correlates of 2 phenotypes among the US population (NHANES 1999-2004). Arch Intern Med. 2008;168(15):1617-24. Epub 2008/08/13. doi: 10.1001/archinte.168.15.1617. PubMed PMID: 18695075.

105. Saklayen MG. The Global Epidemic of the Metabolic Syndrome. Curr Hypertens Rep. 2018;20(2):12. Epub 2018/02/27. doi: 10.1007/s11906-018-0812-z. PubMed PMID: 29480368; PubMed Central PMCID: PMCPMC5866840.

106. American Diabetes A. Economic costs of diabetes in the U.S. in 2012. Diabetes Care. 2013;36(4):1033-46. Epub 2013/03/08. doi: 10.2337/dc12-2625. PubMed PMID: 23468086; PubMed Central PMCID: PMCPMC3609540.

107. Fabbrini E, Sullivan S, Klein S. Obesity and nonalcoholic fatty liver disease: biochemical, metabolic, and clinical implications. Hepatology. 2010;51(2):679-89. Epub 2009/12/31. doi: 10.1002/hep.23280. PubMed PMID: 20041406; PubMed Central PMCID: PMCPMC3575093.

108. Godoy-Matos AF, Silva Junior WS, Valerio CM. NAFLD as a continuum: from obesity to metabolic syndrome and diabetes. Diabetol Metab Syndr. 2020;12:60. Epub 2020/07/21. doi: 10.1186/s13098-020-00570-y. PubMed PMID: 32684985; PubMed Central PMCID: PMCPMC7359287.

109. Saeedi P, Petersohn I, Salpea P, Malanda B, Karuranga S, Unwin N, et al. Global and regional diabetes prevalence estimates for 2019 and projections for 2030 and 2045: Results from the International Diabetes Federation Diabetes Atlas, 9(th) edition. Diabetes Res Clin Pract. 2019;157:107843. Epub 2019/09/14. doi: 10.1016/j.diabres.2019.107843. PubMed PMID: 31518657.

110. Jeong EH, Jun DW, Cho YK, Choe YG, Ryu S, Lee SM, et al. Regional prevalence of non-alcoholic fatty liver disease in Seoul and Gyeonggi-do, Korea. Clin Mol Hepatol. 2013;19(3):266-72. Epub 2013/10/18. doi: 10.3350/cmh.2013.19.3.266. PubMed PMID: 24133664; PubMed Central PMCID: PMCPMC3796676.

111. Fain JN, Madan AK, Hiler ML, Cheema P, Bahouth SW. Comparison of the release of adipokines by adipose tissue, adipose tissue matrix, and adipocytes from visceral and subcutaneous abdominal adipose tissues of obese humans. Endocrinology. 2004;145(5):2273-82. Epub 2004/01/17. doi: 10.1210/en.2003-1336. PubMed PMID: 14726444.

112. Munzberg H, Morrison CD. Structure, production and signaling of leptin. Metabolism. 2015;64(1):13-23. Epub 2014/10/12. doi: 10.1016/j.metabol.2014.09.010. PubMed PMID: 25305050; PubMed Central PMCID: PMCPMC4267896.

113. Farr OM, Gavrieli A, Mantzoros CS. Leptin applications in 2015: what have we learned about leptin and obesity? Curr Opin Endocrinol Diabetes Obes. 2015;22(5):353-9. Epub 2015/08/28. doi: 10.1097/MED.0000000000000184. PubMed PMID: 26313897; PubMed Central PMCID: PMCPMC4610373.

114. Ingalls AM, Dickie MM, Snell GD. Obese, a new mutation in the house mouse. J Hered. 1950;41(12):317-8. Epub 1950/12/01. doi: 10.1093/oxfordjournals.jhered.a106073. PubMed PMID: 14824537.

115. Suriano F, Vieira-Silva S, Falony G, Roumain M, Paquot A, Pelicaen R, et al. Novel insights into the genetically obese (ob/ob) and diabetic (db/db) mice: two sides of the same coin. Microbiome. 2021;9(1):147. Epub 2021/06/30. doi: 10.1186/s40168-021-01097-8. PubMed PMID: 34183063; PubMed Central PMCID: PMCPMC8240277.

116. Clement K, Vaisse C, Lahlou N, Cabrol S, Pelloux V, Cassuto D, et al. A mutation in the human leptin receptor gene causes obesity and pituitary dysfunction. Nature. 1998;392(6674):398-401. Epub 1998/04/16. doi: 10.1038/32911. PubMed PMID: 9537324.

117. Cohen P, Zhao C, Cai X, Montez JM, Rohani SC, Feinstein P, et al. Selective deletion of leptin receptor in neurons leads to obesity. J Clin Invest. 2001;108(8):1113-21. Epub 2001/10/17. doi: 10.1172/JCI13914. PubMed PMID: 11602618; PubMed Central PMCID: PMCPMC209535.

118. Thon M, Hosoi T, Ozawa K. Possible Integrative Actions of Leptin and Insulin Signaling in the Hypothalamus Targeting Energy Homeostasis. Front Endocrinol (Lausanne). 2016;7:138. Epub 2016/11/05. doi: 10.3389/fendo.2016.00138. PubMed PMID: 27812350; PubMed Central PMCID: PMCPMC5071376.

119. Brüning JC, Gautam D, Burks DJ, Gillette J, Schubert M, Orban PC, et al. Role of brain insulin receptor in control of body weight and reproduction. Science. 2000;289(5487):2122-5. Epub 2000/09/23. doi: 10.1126/science.289.5487.2122. PubMed PMID: 11000114.

120. Nazarians-Armavil A, Menchella JA, Belsham DD. Cellular insulin resistance disrupts leptin-mediated control of neuronal signaling and transcription. Mol Endocrinol. 2013;27(6):990-1003. Epub 2013/04/13. doi: 10.1210/me.2012-1338. PubMed PMID: 23579487; PubMed Central PMCID: PMCPMC5415275.

121. Zhang J, Liu F. Tissue-specific insulin signaling in the regulation of metabolism and aging. IUBMB Life. 2014;66(7):485-95. Epub 2014/08/05. doi: 10.1002/iub.1293. PubMed PMID: 25087968; PubMed Central PMCID: PMCPMC4140976.

122. Konner AC, Janoschek R, Plum L, Jordan SD, Rother E, Ma X, et al. Insulin action in AgRP-expressing neurons is required for suppression of hepatic glucose production. Cell Metab. 2007;5(6):438-49. Epub 2007/06/07. doi: 10.1016/j.cmet.2007.05.004. PubMed PMID: 17550779.

123. Jonker JW, Suh JM, Atkins AR, Ahmadian M, Li P, Whyte J, et al. A PPARgamma-FGF1 axis is required for adaptive adipose remodelling and metabolic homeostasis. Nature. 2012;485(7398):391-4. Epub 2012/04/24. doi: 10.1038/nature10998. PubMed PMID: 22522926; PubMed Central PMCID: PMCPMC3358516.

124. Badman MK, Koester A, Flier JS, Kharitonenkov A, Maratos-Flier E. Fibroblast growth factor 21-deficient mice demonstrate impaired adaptation to ketosis. Endocrinology. 2009;150(11):4931-40. Epub 2009/10/13. doi: 10.1210/en.2009-0532. PubMed PMID: 19819944; PubMed Central PMCID: PMCPMC2775979.

125. Scarlett JM, Rojas JM, Matsen ME, Kaiyala KJ, Stefanovski D, Bergman RN, et al. Central injection of fibroblast growth factor 1 induces sustained remission of diabetic hyperglycemia in rodents. Nat Med. 2016;22(7):800-6. Epub 2016/05/24. doi: 10.1038/nm.4101. PubMed PMID: 27213816; PubMed Central PMCID: PMCPMC4938755.

126. Morton GJ, Matsen ME, Bracy DP, Meek TH, Nguyen HT, Stefanovski D, et al. FGF19 action in the brain induces insulin-independent glucose lowering. J Clin Invest. 2013;123(11):4799-808. Epub 2013/10/03. doi: 10.1172/JCI70710. PubMed PMID: 24084738; PubMed Central PMCID: PMCPMC3809800.

127. Owen BM, Ding X, Morgan DA, Coate KC, Bookout AL, Rahmouni K, et al. FGF21 acts centrally to induce sympathetic nerve activity, energy expenditure, and weight loss. Cell Metab. 2014;20(4):670-7. Epub 2014/08/19. doi: 10.1016/j.cmet.2014.07.012. PubMed PMID: 25130400; PubMed Central PMCID: PMCPMC4192037.

128. BonDurant LD, Ameka M, Naber MC, Markan KR, Idiga SO, Acevedo MR, et al. FGF21 Regulates Metabolism Through Adipose-Dependent and -Independent Mechanisms. Cell Metab. 2017;25(4):935-44 e4. Epub 2017/04/06. doi:

10.1016/j.cmet.2017.03.005. PubMed PMID: 28380381; PubMed Central PMCID: PMCPMC5494834.

129. Sancar G, Liu S, Gasser E, Alvarez JG, Moutos C, Kim K, et al. FGF1 and insulin control lipolysis by convergent pathways. Cell Metab. 2022;34(1):171-83 e6. Epub 2022/01/06. doi: 10.1016/j.cmet.2021.12.004. PubMed PMID: 34986332; PubMed Central PMCID: PMCPMC8863067.

130. De Meyts P. The Insulin Receptor and Its Signal Transduction Network. In: Dungan K, editor. Diabetes Mellitus and Carbohydrate Metabolism---DiabetesManager: Endotext (Online); 2016.

131. Taniguchi CM, Emanuelli B, Kahn CR. Critical nodes in signalling pathways: insights into insulin action. Nat Rev Mol Cell Biol. 2006;7(2):85-96. Epub 2006/02/24. doi: 10.1038/nrm1837. PubMed PMID: 16493415.

132. Shepherd PR, Withers DJ, Siddle K. Phosphoinositide 3-kinase: the key switch mechanism in insulin signalling. Biochem J. 1998;333 ( Pt 3):471-90. Epub 1998/07/25. doi: 10.1042/bj3330471. PubMed PMID: 9677303; PubMed Central PMCID: PMCPMC1219607.

133. Haeusler RA, Kaestner KH, Accili D. FoxOs function synergistically to promote glucose production. J Biol Chem. 2010;285(46):35245-8. Epub 2010/10/01. doi: 10.1074/jbc.C110.175851. PubMed PMID: 20880840; PubMed Central PMCID: PMCPMC2975147.

134. MacAulay K, Blair AS, Hajduch E, Terashima T, Baba O, Sutherland C, et al. Constitutive activation of GSK3 down-regulates glycogen synthase abundance and glycogen deposition in rat skeletal muscle cells. J Biol Chem. 2005;280(10):9509-18. Epub 2005/01/06. doi: 10.1074/jbc.M411648200. PubMed PMID: 15632169.

135. Taniguchi CM, Kondo T, Sajan M, Luo J, Bronson R, Asano T, et al. Divergent regulation of hepatic glucose and lipid metabolism by phosphoinositide 3-kinase via Akt and PKClambda/zeta. Cell Metab. 2006;3(5):343-53. Epub 2006/05/09. doi: 10.1016/j.cmet.2006.04.005. PubMed PMID: 16679292.

136. Matsumoto M, Ogawa W, Akimoto K, Inoue H, Miyake K, Furukawa K, et al. PKClambda in liver mediates insulin-induced SREBP-1c expression and determines both hepatic lipid content and overall insulin sensitivity. J Clin Invest. 2003;112(6):935-44.

Epub 2003/09/17. doi: 10.1172/JCI18816. PubMed PMID: 12975478; PubMed Central PMCID: PMCPMC193669.

137. Porstmann T, Santos CR, Griffiths B, Cully M, Wu M, Leevers S, et al. SREBP activity is regulated by mTORC1 and contributes to Akt-dependent cell growth. Cell Metab. 2008;8(3):224-36. Epub 2008/09/03. doi: 10.1016/j.cmet.2008.07.007. PubMed PMID: 18762023; PubMed Central PMCID: PMCPMC2593919.

138. Turban S, Hajduch E. Protein kinase C isoforms: mediators of reactive lipid metabolites in the development of insulin resistance. FEBS Lett. 2011;585(2):269-74. Epub 2010/12/24. doi: 10.1016/j.febslet.2010.12.022. PubMed PMID: 21176778.

139. Samuel VT, Liu ZX, Wang A, Beddow SA, Geisler JG, Kahn M, et al. Inhibition of protein kinase Cepsilon prevents hepatic insulin resistance in nonalcoholic fatty liver disease. J Clin Invest. 2007;117(3):739-45. Epub 2007/02/24. doi: 10.1172/JCI30400. PubMed PMID: 17318260; PubMed Central PMCID: PMCPMC1797607.

140. Li Y, Soos TJ, Li X, Wu J, Degennaro M, Sun X, et al. Protein kinase C Theta inhibits insulin signaling by phosphorylating IRS1 at Ser(1101). J Biol Chem. 2004;279(44):45304-7. Epub 2004/09/15. doi: 10.1074/jbc.C400186200. PubMed PMID: 15364919.

141. Imamura T, Huang J, Usui I, Satoh H, Bever J, Olefsky JM. Insulin-induced GLUT4 translocation involves protein kinase C-lambda-mediated functional coupling between Rab4 and the motor protein kinesin. Mol Cell Biol. 2003;23(14):4892-900. Epub 2003/07/02. doi: 10.1128/MCB.23.14.4892-4900.2003. PubMed PMID: 12832475; PubMed Central PMCID: PMCPMC162221.

142. Liu XJ, Yang C, Gupta N, Zuo J, Chang YS, Fang FD. Protein kinase C-zeta regulation of GLUT4 translocation through actin remodeling in CHO cells. J Mol Med (Berl). 2007;85(8):851-61. Epub 2007/07/11. doi: 10.1007/s00109-007-0232-z. PubMed PMID: 17619838.

143. Sano H, Kane S, Sano E, Mîinea CP, Asara JM, Lane WS, et al. Insulin-stimulated phosphorylation of a Rab GTPase-activating protein regulates GLUT4 translocation. J Biol Chem. 2003;278(17):14599-602. Epub 2003/03/15. doi: 10.1074/jbc.C300063200. PubMed PMID: 12637568.

144. Brandon AE, Liao BM, Diakanastasis B, Parker BL, Raddatz K, McManus SA, et al. Protein Kinase C Epsilon Deletion in Adipose Tissue, but Not in Liver, Improves Glucose Tolerance. Cell Metab. 2019;29(1):183-91 e7. Epub 2018/10/16. doi: 10.1016/j.cmet.2018.09.013. PubMed PMID: 30318338.

145. Bates SH, Stearns WH, Dundon TA, Schubert M, Tso AWK, Wang Y, et al. STAT3 signalling is required for leptin regulation of energy balance but not reproduction. Nature. 2003;421(6925):856-9. doi: 10.1038/nature01388.

146. Kim M-S, Pak YK, Jang P-G, Namkoong C, Choi Y-S, Won J-C, et al. Role of hypothalamic Foxo1 in the regulation of food intake and energy homeostasis. Nature Neuroscience. 2006;9(7):901-6. doi: 10.1038/nn1731.

147. Taguchi A, Wartschow LM, White MF. Brain IRS2 signaling coordinates life span and nutrient homeostasis. Science. 2007;317(5836):369-72. Epub 2007/07/21. doi: 10.1126/science.1142179. PubMed PMID: 17641201.

148. Samuel VT, Shulman GI. Mechanisms for insulin resistance: common threads and missing links. Cell. 2012;148(5):852-71. Epub 2012/03/06. doi: 10.1016/j.cell.2012.02.017. PubMed PMID: 22385956; PubMed Central PMCID: PMCPMC3294420.

149. Sajan MP, Standaert ML, Nimal S, Varanasi U, Pastoor T, Mastorides S, et al. The critical role of atypical protein kinase C in activating hepatic SREBP-1c and NFkappaB in obesity. J Lipid Res. 2009;50(6):1133-45. Epub 2009/02/10. doi: 10.1194/jlr.M800520-JLR200. PubMed PMID: 19202134; PubMed Central PMCID: PMCPMC2681395.

150. Perry RJ, Samuel VT, Petersen KF, Shulman GI. The role of hepatic lipids in hepatic insulin resistance and type 2 diabetes. Nature. 2014;510(7503):84-91. Epub 2014/06/06. doi: 10.1038/nature13478. PubMed PMID: 24899308; PubMed Central PMCID: PMCPMC4489847.

151. Lee J, Kanatsu-Shinohara M, Inoue K, Ogonuki N, Miki H, Toyokuni S, et al. Akt mediates self-renewal division of mouse spermatogonial stem cells. Development. 2007;134(10):1853-9. Epub 2007/04/13. doi: 10.1242/dev.003004. PubMed PMID: 17428826.

152. Goertz MJ, Wu Z, Gallardo TD, Hamra FK, Castrillon DH. Foxo1 is required in mouse spermatogonial stem cells for their maintenance and the initiation of spermatogenesis. J Clin Invest. 2011;121(9):3456-66. doi: 10.1172/JCI57984. PubMed PMID: 21865646; PubMed Central PMCID: PMCPMC3163967.

153. Feng LX, Ravindranath N, Dym M. Stem cell factor/c-kit up-regulates cyclin D3 and promotes cell cycle progression via the phosphoinositide 3-kinase/p70 S6 kinase pathway in spermatogonia. J Biol Chem. 2000;275(33):25572-6. Epub 2000/06/13. doi: 10.1074/jbc.M002218200. PubMed PMID: 10849422.

154. Ciraolo E, Morello F, Hobbs RM, Wolf F, Marone R, Iezzi M, et al. Essential role of the p110beta subunit of phosphoinositide 3-OH kinase in male fertility. Mol Biol Cell. 2010;21(5):704-11. Epub 2010/01/08. doi: 10.1091/mbc.E09-08-0744. PubMed PMID: 20053680; PubMed Central PMCID: PMCPMC2828958.

155. Rothschild G, Sottas CM, Kissel H, Agosti V, Manova K, Hardy MP, et al. A role for kit receptor signaling in Leydig cell steroidogenesis. Biol Reprod. 2003;69(3):925-32. Epub 2003/05/30. doi: 10.1095/biolreprod.102.014548. PubMed PMID: 12773427.

156. Escott GM, Jacobus AP, Loss ES. PI3K-dependent actions of insulin and IGF-I on seminiferous tubules from immature rats. Pflugers Arch. 2013;465(10):1497-505. Epub 2013/05/03. doi: 10.1007/s00424-013-1287-z. PubMed PMID: 23636775.

157. Pitetti JL, Calvel P, Zimmermann C, Conne B, Papaioannou MD, Aubry F, et al. An essential role for insulin and IGF1 receptors in regulating sertoli cell proliferation, testis size, and FSH action in mice. Mol Endocrinol. 2013;27(5):814-27. Epub 2013/03/23. doi: 10.1210/me.2012-1258. PubMed PMID: 23518924; PubMed Central PMCID: PMCPMC5416760.

158. McDonald CA, Millena AC, Reddy S, Finlay S, Vizcarra J, Khan SA, et al. Follicle-stimulating hormone-induced aromatase in immature rat Sertoli cells requires an active phosphatidylinositol 3-kinase pathway and is inhibited via the mitogen-activated protein kinase signaling pathway. Mol Endocrinol. 2006;20(3):608-18. Epub 2005/11/05. doi: 10.1210/me.2005-0245. PubMed PMID: 16269516.

159. Loss ES, Jacobsen M, Costa ZS, Jacobus AP, Borelli F, Wassermann GF. Testosterone modulates K(+)ATP channels in Sertoli cell membrane via the PLC-PIP2 pathway. Horm Metab Res. 2004;36(8):519-25. Epub 2004/08/25. doi: 10.1055/s-2004-825753. PubMed PMID: 15326560.

160. Almog T, Lazar S, Reiss N, Etkovitz N, Milch E, Rahamim N, et al. Identification of extracellular signal-regulated kinase 1/2 and p38 MAPK as regulators of human sperm motility and acrosome reaction and as predictors of poor spermatozoan quality. J Biol Chem. 2008;283(21):14479-89. Epub 2008/03/29. doi: 10.1074/jbc.M710492200. PubMed PMID: 18372245.

161. Yu Y, Nomikos M, Theodoridou M, Nounesis G, Lai FA, Swann K. PLCzeta causes Ca(2+) oscillations in mouse eggs by targeting intracellular and not plasma membrane PI(4,5)P(2). Mol Biol Cell. 2012;23(2):371-80. Epub 2011/11/25. doi: 10.1091/mbc.E11-08-0687. PubMed PMID: 22114355; PubMed Central PMCID: PMCPMC3258180.

162. Levine H, Jorgensen N, Martino-Andrade A, Mendiola J, Weksler-Derri D, Mindlis I, et al. Temporal trends in sperm count: a systematic review and meta-regression analysis. Hum Reprod Update. 2017;23(6):646-59. Epub 2017/10/06. doi: 10.1093/humupd/dmx022. PubMed PMID: 28981654; PubMed Central PMCID: PMCPMC6455044.

163. Keszthelyi M, Gyarmathy VA, Kaposi A, Kopa Z. The potential role of central obesity in male infertility: body mass index versus waist to hip ratio as they relate to selected semen parameters. Bmc Public Health. 2020;20(1). doi: ARTN 307 10.1186/s12889-020-8413-6. PubMed PMID: WOS:000521103400002.

164. He S, Li Q, Huang Q, Cheng J. Targeting Protein Kinase C for Cancer Therapy. Cancers (Basel). 2022;14(5). Epub 2022/03/11. doi: 10.3390/cancers14051104. PubMed PMID: 35267413; PubMed Central PMCID: PMCPMC8909172.

165. Itani SI, Zhou Q, Pories WJ, MacDonald KG, Dohm GL. Involvement of protein kinase C in human skeletal muscle insulin resistance and obesity. Diabetes. 2000;49(8):1353-8. Epub 2000/08/03. doi: 10.2337/diabetes.49.8.1353. PubMed PMID: 10923637.

166. Zhang M. The Role of inositol Polyphosphate-4-Phosphatase Type II b (INPP4B) in Obese Models and Endocrine Cancers [Dissertation]: Florida International University; 2019.

167. Hirode G, Wong RJ. Trends in the Prevalence of Metabolic Syndrome in the United States, 2011-2016. JAMA. 2020;323(24):2526-8. Epub 2020/06/24. doi: 10.1001/jama.2020.4501. PubMed PMID: 32573660; PubMed Central PMCID: PMCPMC7312413.

168. Menke A, Casagrande S, Geiss L, Cowie CC. Prevalence of and Trends in Diabetes Among Adults in the United States, 1988-2012. JAMA. 2015;314(10):1021-9. Epub 2015/09/09. doi: 10.1001/jama.2015.10029. PubMed PMID: 26348752.

169. Bluher M. The distinction of metabolically 'healthy' from 'unhealthy' obese individuals. Curr Opin Lipidol. 2010;21(1):38-43. Epub 2009/11/17. doi: 10.1097/MOL.0b013e3283346ccc. PubMed PMID: 19915462.

170. Vazirani RP, Verma A, Sadacca LA, Buckman MS, Picatoste B, Beg M, et al. Disruption of Adipose Rab10-Dependent Insulin Signaling Causes Hepatic Insulin Resistance. Diabetes. 2016;65(6):1577-89. Epub 2016/05/22. doi: 10.2337/db15-1128. PubMed PMID: 27207531; PubMed Central PMCID: PMCPMC4878419.

171. Titchenell PM, Lazar MA, Birnbaum MJ. Unraveling the Regulation of Hepatic Metabolism by Insulin. Trends Endocrinol Metab. 2017;28(7):497-505. Epub 2017/04/19. doi: 10.1016/j.tem.2017.03.003. PubMed PMID: 28416361; PubMed Central PMCID: PMCPMC5477655.

172. Osorio-Fuentealba C, Contreras-Ferrat AE, Altamirano F, Espinosa A, Li Q, Niu W, et al. Electrical stimuli release ATP to increase GLUT4 translocation and glucose uptake via PI3Kgamma-Akt-AS160 in skeletal muscle cells. Diabetes. 2013;62(5):1519-26. Epub 2013/01/01. doi: 10.2337/db12-1066. PubMed PMID: 23274898; PubMed Central PMCID: PMCPMC3636621.

173. Lyu K, Zhang Y, Zhang D, Kahn M, Ter Horst KW, Rodrigues MRS, et al. A Membrane-Bound Diacylglycerol Species Induces PKC-Mediated Hepatic Insulin Resistance. Cell Metab. 2020;32(4):654-64 e5. Epub 2020/09/04. doi: 10.1016/j.cmet.2020.08.001. PubMed PMID: 32882164; PubMed Central PMCID: PMCPMC7544641.

174. Hummel KP, Dickie MM, Coleman DL. Diabetes, a new mutation in the mouse. Science. 1966;153(3740):1127-8. Epub 1966/09/02. doi: 10.1126/science.153.3740.1127. PubMed PMID: 5918576.

175. Chaves C, Kay T, Anselmo J. Early onset obesity due to a mutation in the human leptin receptor gene. Endocrinol Diabetes Metab Case Rep. 2022;2022. Epub 2022/08/25. doi: 10.1530/EDM-21-0124. PubMed PMID: 36001025; PubMed Central PMCID: PMCPMC9422261.

176. Ren Z, Liu Y, Hong W, Pan X, Gong P, Liu Q, et al. Conditional knockout of leptin receptor in neural stem cells leads to obesity in mice and affects neuronal differentiation in the hypothalamus early after birth. Mol Brain. 2020;13(1):109. Epub 2020/08/05. doi: 10.1186/s13041-020-00647-9. PubMed PMID: 32746867; PubMed Central PMCID: PMCPMC7398062.

177. de Luca C, Kowalski TJ, Zhang Y, Elmquist JK, Lee C, Kilimann MW, et al. Complete rescue of obesity, diabetes, and infertility in db/db mice by neuron-specific LEPR-B transgenes. J Clin Invest. 2005;115(12):3484-93. Epub 2005/11/15. doi: 10.1172/JCI24059. PubMed PMID: 16284652; PubMed Central PMCID: PMCPMC1280964.

178. Lee Y, Lim S, Hong ES, Kim JH, Moon MK, Chun EJ, et al. Serum FGF21 concentration is associated with hypertriglyceridaemia, hyperinsulinaemia and pericardial fat accumulation, independently of obesity, but not with current coronary artery status. Clin Endocrinol (Oxf). 2014;80(1):57-64. Epub 2013/01/03. doi: 10.1111/cen.12134. PubMed PMID: 23278761.

179. An SY, Lee MS, Yi SA, Ha ES, Han SJ, Kim HJ, et al. Serum fibroblast growth factor 21 was elevated in subjects with type 2 diabetes mellitus and was associated with the presence of carotid artery plaques. Diabetes Res Clin Pract. 2012;96(2):196-203. Epub 2012/02/02. doi: 10.1016/j.diabres.2012.01.004. PubMed PMID: 22293928.

180. Keuper M, Haring HU, Staiger H. Circulating FGF21 Levels in Human Health and Metabolic Disease. Exp Clin Endocrinol Diabetes. 2020;128(11):752-70. Epub 2019/05/21. doi: 10.1055/a-0879-2968. PubMed PMID: 31108554.

181. Zhang M, Suarez E, Vasquez JL, Nathanson L, Peterson LE, Rajapakshe K, et al. Inositol polyphosphate 4-phosphatase type II regulation of androgen receptor activity. Oncogene. 2019;38(7):1121-35. Epub 2018/09/20. doi: 10.1038/s41388-018-0498-3. PubMed PMID: 30228349; PubMed Central PMCID: PMCPMC6377303.

182. Hodgson MC, Deryugina EI, Suarez E, Lopez SM, Lin D, Xue H, et al. INPP4B suppresses prostate cancer cell invasion. Cell Commun Signal. 2014;12:61. Epub 2014/09/25. doi: 10.1186/s12964-014-0061-y. PubMed PMID: 25248616; PubMed Central PMCID: PMCPMC4181726.

183. Ahmadian M, Suh JM, Hah N, Liddle C, Atkins AR, Downes M, et al. PPARgamma signaling and metabolism: the good, the bad and the future. Nat Med.

2013;19(5):557-66. Epub 2013/05/09. doi: 10.1038/nm.3159. PubMed PMID: 23652116; PubMed Central PMCID: PMCPMC3870016.

184. Evans RM, Barish GD, Wang Y-X. PPARs and the complex journey to obesity. Nature Medicine. 2004;10(4):355-61. doi: 10.1038/nm1025.

185. Ellulu MS, Patimah I, Khaza'ai H, Rahmat A, Abed Y. Obesity and inflammation: the linking mechanism and the complications. Arch Med Sci. 2017;13(4):851-63. Epub 2017/07/20. doi: 10.5114/aoms.2016.58928. PubMed PMID: 28721154; PubMed Central PMCID: PMCPMC5507106.

186. Derosa G, Catena G, Gaudio G, D'Angelo A, Maffioli P. Adipose tissue dysfunction and metabolic disorders: Is it possible to predict who will develop type 2 diabetes mellitus? Role of markErs in the progreSsion of dIabeteS in obese paTIeNts (The RESISTIN trial). Cytokine. 2020;127:154947. Epub 2019/12/08. doi: 10.1016/j.cyto.2019.154947. PubMed PMID: 31811995.

187. Würfel M, Breitfeld J, Gebhard C, Scholz M, Baber R, Riedel-Heller SG, et al. Interplay between adipose tissue secreted proteins, eating behavior and obesity. European Journal of Nutrition. 2022;61(2):885-99. doi: 10.1007/s00394-021-02687-w.

188. Qatanani M, Lazar MA. Mechanisms of obesity-associated insulin resistance: many choices on the menu. Genes Dev. 2007;21(12):1443-55. Epub 2007/06/19. doi: 10.1101/gad.1550907. PubMed PMID: 17575046.

189. Takahashi Y, Fukusato T. Histopathology of nonalcoholic fatty liver disease/nonalcoholic steatohepatitis. World J Gastroenterol. 2014;20(42):15539-48. Epub 2014/11/18. doi: 10.3748/wjg.v20.i42.15539. PubMed PMID: 25400438; PubMed Central PMCID: PMCPMC4229519.

190. Ipsen DH, Lykkesfeldt J, Tveden-Nyborg P. Molecular mechanisms of hepatic lipid accumulation in non-alcoholic fatty liver disease. Cell Mol Life Sci. 2018;75(18):3313-27. Epub 2018/06/25. doi: 10.1007/s00018-018-2860-6. PubMed PMID: 29936596; PubMed Central PMCID: PMCPMC6105174.

191. Suzuki M, Uehara Y, Motomura-Matsuzaka K, Oki J, Koyama Y, Kimura M, et al. betaKlotho is required for fibroblast growth factor (FGF) 21 signaling through FGF receptor (FGFR) 1c and FGFR3c. Mol Endocrinol. 2008;22(4):1006-14. Epub

2008/01/12. doi: 10.1210/me.2007-0313. PubMed PMID: 18187602; PubMed Central PMCID: PMCPMC5419549.

192. Gasser E, Sancar G, Downes M, Evans RM. Metabolic Messengers: fibroblast growth factor 1. Nat Metab. 2022;4(6):663-71. Epub 2022/06/11. doi: 10.1038/s42255-022-00580-2. PubMed PMID: 35681108.

193. Brown JM, Bentsen MA, Rausch DM, Phan BA, Wieck D, Wasanwala H, et al. Role of hypothalamic MAPK/ERK signaling and central action of FGF1 in diabetes remission. iScience. 2021;24(9):102944. Epub 2021/08/26. doi: 10.1016/j.isci.2021.102944. PubMed PMID: 34430821; PubMed Central PMCID: PMCPMC8368994.

194. Lukowicz C, Ellero-Simatos S, Regnier M, Oliviero F, Lasserre F, Polizzi A, et al. Dimorphic metabolic and endocrine disorders in mice lacking the constitutive androstane receptor. Sci Rep. 2019;9(1):20169. Epub 2019/12/29. doi: 10.1038/s41598-019-56570-0. PubMed PMID: 31882815; PubMed Central PMCID: PMCPMC6934754.

195. Chella Krishnan K, Floyd RR, Sabir S, Jayasekera DW, Leon-Mimila PV, Jones AE, et al. Liver Pyruvate Kinase Promotes NAFLD/NASH in Both Mice and Humans in a Sex-Specific Manner. Cell Mol Gastroenterol Hepatol. 2021;11(2):389-406. Epub 2020/09/18. doi: 10.1016/j.jcmgh.2020.09.004. PubMed PMID: 32942044; PubMed Central PMCID: PMCPMC7788245.

196. Ceyhan Y, Zhang M, Guo J, Sandoval CG, Vacher J, Kaftanovskaya EM, et al. Deletion of inositol polyphosphate 4-phosphatase type-II B affects spermatogenesis in mice. PLoS One. 2020;15(5):e0233163. Epub 2020/05/16. doi: 10.1371/journal.pone.0233163. PubMed PMID: 32413098; PubMed Central PMCID: PMCPMC7228085.

197. Fernandez MO, Hsueh K, Park HT, Sauceda C, Hwang V, Kumar D, et al. Astrocyte-Specific Deletion of Peroxisome-Proliferator Activated Receptor-gamma Impairs Glucose Metabolism and Estrous Cycling in Female Mice. J Endocr Soc. 2017;1(11):1332-50. Epub 2017/12/22. doi: 10.1210/js.2017-00242. PubMed PMID: 29264458; PubMed Central PMCID: PMCPMC5686676.

198. McLean AC, Valenzuela N, Fai S, Bennett SA. Performing vaginal lavage, crystal violet staining, and vaginal cytological evaluation for mouse estrous cycle staging identification. J Vis Exp. 2012;(67):e4389. Epub 2012/09/26. doi: 10.3791/4389. PubMed PMID: 23007862; PubMed Central PMCID: PMCPMC3490233.

199. Kim D, Langmead B, Salzberg SL. HISAT: a fast spliced aligner with low memory requirements. Nat Methods. 2015;12(4):357-60. Epub 2015/03/10. doi: 10.1038/nmeth.3317. PubMed PMID: 25751142; PubMed Central PMCID: PMCPMC4655817.

200. Dobin A, Gingeras TR. Mapping RNA-seq Reads with STAR. Curr Protoc Bioinformatics. 2015;51:11 4 1- 4 9. Epub 2015/09/04. doi: 10.1002/0471250953.bi1114s51. PubMed PMID: 26334920; PubMed Central PMCID: PMCPMC4631051.

201. Anders S, Pyl PT, Huber W. HTSeq--a Python framework to work with high-throughput sequencing data. Bioinformatics. 2015;31(2):166-9. Epub 2014/09/28. doi: 10.1093/bioinformatics/btu638. PubMed PMID: 25260700; PubMed Central PMCID: PMCPMC4287950.

202. Love MI, Huber W, Anders S. Moderated estimation of fold change and dispersion for RNA-seq data with DESeq2. Genome Biol. 2014;15(12):550. Epub 2014/12/18. doi: 10.1186/s13059-014-0550-8. PubMed PMID: 25516281; PubMed Central PMCID: PMCPMC4302049.

203. Arnold M, Pandeya N, Byrnes G, Renehan AG, Stevens GA, Ezzati M, et al. Global burden of cancer attributable to high body-mass index in 2012: a population-based study. The Lancet Oncology. 2015;16(1):36-46. doi: 10.1016/s1470-2045(14)71123-4.

204. Whiteman DC, Wilson LF. The fractions of cancer attributable to modifiable factors: A global review. Cancer Epidemiol. 2016;44:203-21. Epub 2016/07/28. doi: 10.1016/j.canep.2016.06.013. PubMed PMID: 27460784.

205. Asleh K, Lyck Carstensen S, Tykjaer Jorgensen CL, Burugu S, Gao D, Won JR, et al. Basal biomarkers nestin and INPP4B predict gemcitabine benefit in metastatic breast cancer: Samples from the phase III SBG0102 clinical trial. Int J Cancer. 2019;144(10):2578-86. Epub 2018/11/10. doi: 10.1002/ijc.31969. PubMed PMID: 30411790.

206. Stingl J. Estrogen and progesterone in normal mammary gland development and in cancer. Horm Cancer. 2011;2(2):85-90. Epub 2011/07/16. doi: 10.1007/s12672-010-0055-1. PubMed PMID: 21761331.

207. Mulac-Jericevic B, Lydon JP, DeMayo FJ, Conneely OM. Defective mammary gland morphogenesis in mice lacking the progesterone receptor B isoform. Proc Natl Acad Sci U S A. 2003;100(17):9744-9. Epub 2003/08/05. doi: 10.1073/pnas.1732707100. PubMed PMID: 12897242; PubMed Central PMCID: PMCPMC187836.

208. Grimm SL, Ward RD, Obr AE, Franco HL, Fernandez-Valdivia R, Kim JS, et al. A role for site-specific phosphorylation of mouse progesterone receptor at serine 191 in vivo. Mol Endocrinol. 2014;28(12):2025-37. Epub 2014/10/22. doi: 10.1210/me.2014-1206. PubMed PMID: 25333515; PubMed Central PMCID: PMCPMC4250360.

209. Schwartz N, Verma A, Bivens CB, Schwartz Z, Boyan BD. Rapid steroid hormone actions via membrane receptors. Biochim Biophys Acta. 2016;1863(9):2289-98. Epub 2016/06/12. doi: 10.1016/j.bbamcr.2016.06.004. PubMed PMID: 27288742.

210. Diep CH, Ahrendt H, Lange CA. Progesterone induces progesterone receptor gene (PGR) expression via rapid activation of protein kinase pathways required for cooperative estrogen receptor alpha (ER) and progesterone receptor (PR) genomic action at ER/PR target genes. Steroids. 2016;114:48-58. Epub 2016/09/20. doi: 10.1016/j.steroids.2016.09.004. PubMed PMID: 27641443; PubMed Central PMCID: PMCPMC5068826.

211. Hu X, Juneja SC, Maihle NJ, Cleary MP. Leptin--a growth factor in normal and malignant breast cells and for normal mammary gland development. J Natl Cancer Inst. 2002;94(22):1704-11. Epub 2002/11/21. doi: 10.1093/jnci/94.22.1704. PubMed PMID: 12441326.

212. Tenvooren I, Jenks MZ, Rashid H, Cook KL, Muhlemann JK, Sistrunk C, et al. Elevated leptin disrupts epithelial polarity and promotes premalignant alterations in the mammary gland. Oncogene. 2019;38(20):3855-70. Epub 2019/01/24. doi: 10.1038/s41388-019-0687-8. PubMed PMID: 30670780; PubMed Central PMCID: PMCPMC6525037.

213. Gasco M, Shami S, Crook T. The p53 pathway in breast cancer. Breast Cancer Res. 2002;4(2):70-6. Epub 2002/03/07. doi: 10.1186/bcr426. PubMed PMID: 11879567; PubMed Central PMCID: PMCPMC138723.

214. Freed-Pastor WA, Mizuno H, Zhao X, Langerod A, Moon SH, Rodriguez-Barrueco R, et al. Mutant p53 disrupts mammary tissue architecture via the mevalonate

pathway. Cell. 2012;148(1-2):244-58. Epub 2012/01/24. doi: 10.1016/j.cell.2011.12.017. PubMed PMID: 22265415; PubMed Central PMCID: PMCPMC3511889.

215. Gatza CE, Dumble M, Kittrell F, Edwards DG, Dearth RK, Lee AV, et al. Altered mammary gland development in the p53+/m mouse, a model of accelerated aging. Dev Biol. 2008;313(1):130-41. Epub 2007/11/13. doi: 10.1016/j.ydbio.2007.10.004. PubMed PMID: 17996864; PubMed Central PMCID: PMCPMC2234269.

216. Silwal-Pandit L, Vollan HK, Chin SF, Rueda OM, McKinney S, Osako T, et al. TP53 mutation spectrum in breast cancer is subtype specific and has distinct prognostic relevance. Clin Cancer Res. 2014;20(13):3569-80. Epub 2014/05/08. doi: 10.1158/1078-0432.CCR-13-2943. PubMed PMID: 24803582.

217. Fedorova O, Daks A, Shuvalov O, Kizenko A, Petukhov A, Gnennaya Y, et al. Attenuation of p53 mutant as an approach for treatment Her2-positive cancer. Cell Death Discov. 2020;6:100. Epub 2020/10/22. doi: 10.1038/s41420-020-00337-4. PubMed PMID: 33083021; PubMed Central PMCID: PMCPMC7548004.

218. Arendt LM, Kuperwasser C. Form and function: how estrogen and progesterone regulate the mammary epithelial hierarchy. J Mammary Gland Biol Neoplasia. 2015;20(1-2):9-25. Epub 2015/07/21. doi: 10.1007/s10911-015-9337-0. PubMed PMID: 26188694; PubMed Central PMCID: PMCPMC4596764.

219. Satoh K, Hovey RC, Malewski T, Warri A, Goldhar AS, Ginsburg E, et al. Progesterone enhances branching morphogenesis in the mouse mammary gland by increased expression of Msx2. Oncogene. 2007;26(54):7526-34. Epub 2007/06/05. doi: 10.1038/sj.onc.1210555. PubMed PMID: 17546050.

220. Brisken C, Heineman A, Chavarria T, Elenbaas B, Tan J, Dey SK, et al. Essential function of Wnt-4 in mammary gland development downstream of progesterone signaling. Genes Dev. 2000;14(6):650-4. Epub 2000/03/25. PubMed PMID: 10733525; PubMed Central PMCID: PMCPMC316462.

221. Morrison MM, Young CD, Wang S, Sobolik T, Sanchez VM, Hicks DJ, et al. mTOR Directs Breast Morphogenesis through the PKC-alpha-Rac1 Signaling Axis. PLoS Genet. 2015;11(7):e1005291. Epub 2015/07/02. doi: 10.1371/journal.pgen.1005291. PubMed PMID: 26132202; PubMed Central PMCID: PMCPMC4488502.

222. Schwertfeger KL, Richert MM, Anderson SM. Mammary gland involution is delayed by activated Akt in transgenic mice. Mol Endocrinol. 2001;15(6):867-81. Epub 2001/05/29. doi: 10.1210/mend.15.6.0663. PubMed PMID: 11376107.

223. Allen-Petersen BL, Miller MR, Neville MC, Anderson SM, Nakayama KI, Reyland ME. Loss of protein kinase C delta alters mammary gland development and apoptosis. Cell Death Dis. 2010;1:e17. Epub 2010/01/01. doi: 10.1038/cddis.2009.20. PubMed PMID: 21364618; PubMed Central PMCID: PMCPMC3032509.

224. Wang Y, Lam JB, Lam KS, Liu J, Lam MC, Hoo RL, et al. Adiponectin modulates the glycogen synthase kinase-3beta/beta-catenin signaling pathway and attenuates mammary tumorigenesis of MDA-MB-231 cells in nude mice. Cancer Res. 2006;66(23):11462-70. Epub 2006/12/06. doi: 10.1158/0008-5472.CAN-06-1969. PubMed PMID: 17145894.

225. Lin Y, Li Q. Expression and function of leptin and its receptor in mouse mammary gland. Sci China C Life Sci. 2007;50(5):669-75. Epub 2007/09/20. doi: 10.1007/s11427-007-0077-2. PubMed PMID: 17879067.

226. Jarde T, Caldefie-Chezet F, Goncalves-Mendes N, Mishellany F, Buechler C, Penault-Llorca F, et al. Involvement of adiponectin and leptin in breast cancer: clinical and in vitro studies. Endocr Relat Cancer. 2009;16(4):1197-210. Epub 2009/08/08. doi: 10.1677/ERC-09-0043. PubMed PMID: 19661131.

227. Garcia-Estevez L, Gonzalez-Martinez S, Moreno-Bueno G. The Leptin Axis and Its Association With the Adaptive Immune System in Breast Cancer. Front Immunol. 2021;12:784823. Epub 2021/12/07. doi: 10.3389/fimmu.2021.784823. PubMed PMID: 34868066; PubMed Central PMCID: PMCPMC8634160.

228. Ligorio F, Zambelli L, Bottiglieri A, Castagnoli L, Zattarin E, Lobefaro R, et al. Hormone receptor status influences the impact of body mass index and hyperglycemia on the risk of tumor relapse in early-stage HER2-positive breast cancer patients. Ther Adv Med Oncol. 2021;13:17588359211006960. Epub 2021/05/06. doi: 10.1177/17588359211006960. PubMed PMID: 33948122; PubMed Central PMCID: PMCPMC8053837.

229. Slamon DJ, Clark GM, Wong SG, Levin WJ, Ullrich A, McGuire WL. Human breast cancer: correlation of relapse and survival with amplification of the HER-2/neu oncogene. Science. 1987;235(4785):177-82. Epub 1987/01/09. doi: 10.1126/science.3798106. PubMed PMID: 3798106.

230. Reed DE, Shokat KM. INPP4B and PTEN Loss Leads to PI-3,4-P2 Accumulation and Inhibition of PI3K in TNBC. Mol Cancer Res. 2017;15(6):765-75. Epub 2017/02/16. doi: 10.1158/1541-7786.MCR-16-0183. PubMed PMID: 28196852; PubMed Central PMCID: PMCPMC5502826.

231. Liu W, Chakraborty B, Safi R, Kazmin D, Chang CY, McDonnell DP. Dysregulated cholesterol homeostasis results in resistance to ferroptosis increasing tumorigenicity and metastasis in cancer. Nat Commun. 2021;12(1):5103. Epub 2021/08/26. doi: 10.1038/s41467-021-25354-4. PubMed PMID: 34429409; PubMed Central PMCID: PMCPMC8385107.

232. Garrido P, Moran J, Alonso A, Gonzalez S, Gonzalez C. 17beta-estradiol activates glucose uptake via GLUT4 translocation and PI3K/Akt signaling pathway in MCF-7 cells. Endocrinology. 2013;154(6):1979-89. Epub 2013/04/03. doi: 10.1210/en.2012-1558. PubMed PMID: 23546602.

233. Kim S, Lee Y, Koo JS. Differential expression of lipid metabolism-related proteins in different breast cancer subtypes. PLoS One. 2015;10(3):e0119473. Epub 2015/03/10. doi: 10.1371/journal.pone.0119473. PubMed PMID: 25751270; PubMed Central PMCID: PMCPMC4353724.

234. Gyamfi J, Yeo JH, Kwon D, Min BS, Cha YJ, Koo JS, et al. Interaction between CD36 and FABP4 modulates adipocyte-induced fatty acid import and metabolism in breast cancer. NPJ Breast Cancer. 2021;7(1):129. Epub 2021/09/26. doi: 10.1038/s41523-021-00324-7. PubMed PMID: 34561446; PubMed Central PMCID: PMCPMC8463699.

235. Howlader N, Cronin KA, Kurian AW, Andridge R. Differences in Breast Cancer Survival by Molecular Subtypes in the United States. Cancer Epidemiol Biomarkers Prev. 2018;27(6):619-26. Epub 2018/03/30. doi: 10.1158/1055-9965.EPI-17-0627. PubMed PMID: 29593010.

236. Clarke R, Tyson JJ, Dixon JM. Endocrine resistance in breast cancer--An overview and update. Mol Cell Endocrinol. 2015;418 Pt 3:220-34. Epub 2015/10/13. doi: 10.1016/j.mce.2015.09.035. PubMed PMID: 26455641; PubMed Central PMCID: PMCPMC4684757.

237. Senie RT, Rosen PP, Rhodes P, Lesser ML, Kinne DW. Obesity at diagnosis of breast carcinoma influences duration of disease-free survival. Ann Intern Med. 1992;116(1):26-32. Epub 1992/01/01. doi: 10.7326/0003-4819-116-1-26. PubMed PMID: 1727092.

238. Kaplan MA, Pekkolay Z, Kucukoner M, Inal A, Urakci Z, Ertugrul H, et al. Type 2 diabetes mellitus and prognosis in early stage breast cancer women. Med Oncol. 2012;29(3):1576-80. Epub 2011/11/16. doi: 10.1007/s12032-011-0109-4. PubMed PMID: 22083554.

239. Conneely OM, Jericevic BM, Lydon JP. Progesterone receptors in mammary gland development and tumorigenesis. J Mammary Gland Biol Neoplasia. 2003;8(2):205-14. Epub 2003/11/26. doi: 10.1023/a:1025952924864. PubMed PMID: 14635795.

240. Iyengar NM, Hudis CA, Dannenberg AJ. Obesity and inflammation: new insights into breast cancer development and progression. Am Soc Clin Oncol Educ Book. 2013:46-51. Epub 2013/05/30. doi: 10.1200/EdBook_AM.2013.33.46 10.14694/EdBook_AM.2013.33.46. PubMed PMID: 23714453; PubMed Central PMCID: PMCPMC3897299.

241. Wang L, Zhang S, Wang X. The Metabolic Mechanisms of Breast Cancer Metastasis. Front Oncol. 2020;10:602416. Epub 2021/01/26. doi: 10.3389/fonc.2020.602416. PubMed PMID: 33489906; PubMed Central PMCID: PMCPMC7817624.

242. Muller WJ, Sinn E, Pattengale PK, Wallace R, Leder P. Single-step induction of mammary adenocarcinoma in transgenic mice bearing the activated c-neu oncogene. Cell. 1988;54(1):105-15. doi: 10.1016/0092-8674(88)90184-5.

243. Tolg C, Cowman M, Turley EA. Mouse Mammary Gland Whole Mount Preparation and Analysis. Bio Protoc. 2018;8(13):e2915. Epub 2018/07/05. doi: 10.21769/BioProtoc.2915. PubMed PMID: 34395744; PubMed Central PMCID: PMCPMC8328583.

244. Stanko JP, Fenton SE. Quantifying Branching Density in Rat Mammary Gland Whole-mounts Using the Sholl Analysis Method. J Vis Exp. 2017;(125). Epub 2017/07/27. doi: 10.3791/55789. PubMed PMID: 28745626; PubMed Central PMCID: PMCPMC5612270.

245. Martins AD, Majzoub A, Agawal A. Metabolic Syndrome and Male Fertility. World J Mens Health. 2019;37(2):113-27. Epub 2018/10/24. doi: 10.5534/wjmh.180055. PubMed PMID: 30350486; PubMed Central PMCID: PMCPMC6479081.

246. Kuhn-Velten N, Codjambopoulo P, Herberg L, Kley HK, Staib W. In-vitro studies of the development of pituitary and testicular functions in diabetes (C57Bl/KsJ-db/db) mutant mice. Horm Metab Res. 1985;17(11):576-9. Epub 1985/11/01. doi: 10.1055/s-2007-1013610. PubMed PMID: 3000907.

247. Swerdloff RS, Batt RA, Bray GA. Reproductive hormonal function in the genetically obese (ob/ob) mouse. Endocrinology. 1976;98(6):1359-64. Epub 1976/06/01. doi: 10.1210/endo-98-6-1359. PubMed PMID: 1278106.

248. Jarvis S, Gethings LA, Samanta L, Pedroni SMA, Withers DJ, Gray N, et al. High fat diet causes distinct aberrations in the testicular proteome. International Journal of Obesity. 2020;44(9):1958-69. doi: 10.1038/s41366-020-0595-6.

249. Wang F, Chen H, Chen Y, Cheng Y, Li J, Zheng L, et al. Diet-induced obesity is associated with altered expression of sperm motility-related genes and testicular post-translational modifications in a mouse model. Theriogenology. 2020;158:233-8. Epub 2020/09/28. doi: 10.1016/j.theriogenology.2020.09.023. PubMed PMID: 32980686.

250. Fan Y, Liu Y, Xue K, Gu G, Fan W, Xu Y, et al. Diet-induced obesity in male C57BL/6 mice decreases fertility as a consequence of disrupted blood-testis barrier. PLoS One. 2015;10(4):e0120775. Epub 2015/04/18. doi: 10.1371/journal.pone.0120775. PubMed PMID: 25886196; PubMed Central PMCID: PMCPMC4401673.

251. Ghanayem BI, Bai R, Kissling GE, Travlos G, Hoffler U. Diet-induced obesity in male mice is associated with reduced fertility and potentiation of acrylamide-induced reproductive toxicity. Biol Reprod. 2010;82(1):96-104. Epub 2009/08/22. doi: 10.1095/biolreprod.109.078915. PubMed PMID: 19696015; PubMed Central PMCID: PMCPMC2802115.

252. Peng Y, Zhao W, Qu F, Jing J, Hu Y, Liu Y, et al. Proteomic alterations underlie an association with teratozoospermia in obese mice sperm. Reprod Biol Endocrinol. 2019;17(1):82. Epub 2019/10/28. doi: 10.1186/s12958-019-0530-7. PubMed PMID: 31651332; PubMed Central PMCID: PMCPMC6813985.

253. Jiang Q, Maresch CC, Petry SF, Paradowska-Dogan A, Bhushan S, Chang Y, et al. Elevated CCL2 causes Leydig cell malfunction in metabolic syndrome. JCI Insight. 2020;5(21). Epub 2020/11/06. doi: 10.1172/jci.insight.134882. PubMed PMID: 33148888; PubMed Central PMCID: PMCPMC7710294.

254. Gagnon A, Dods P, Roustan-Delatour N, Chen CS, Sorisky A. Phosphatidylinositol-3,4,5-trisphosphate is required for insulin-like growth factor 1-mediated survival of 3T3-L1 preadipocytes. Endocrinology. 2001;142(1):205-12. Epub 2001/01/06. doi: 10.1210/endo.142.1.7902. PubMed PMID: 11145583.

255. Zheng P, Baibakov B, Wang XH, Dean J. PtdIns(3,4,5)P3 is constitutively synthesized and required for spindle translocation during meiosis in mouse oocytes. J Cell Sci. 2013;126(Pt 3):715-21. Epub 2012/12/25. doi: 10.1242/jcs.118042. PubMed PMID: 23264738; PubMed Central PMCID: PMCPMC3619807.

256. Kwik J, Boyle S, Fooksman D, Margolis L, Sheetz MP, Edidin M. Membrane cholesterol, lateral mobility, and the phosphatidylinositol 4,5-bisphosphate-dependent organization of cell actin. Proc Natl Acad Sci U S A. 2003;100(24):13964-9. Epub 2003/11/13. doi: 10.1073/pnas.2336102100. PubMed PMID: 14612561; PubMed Central PMCID: PMCPMC283529.

257. Svingen T, Koopman P. Building the mammalian testis: origins, differentiation, and assembly of the component cell populations. Genes Dev. 2013;27(22):2409-26. Epub 2013/11/19. doi: 10.1101/gad.228080.113. PubMed PMID: 24240231; PubMed Central PMCID: PMCPMC3841730.

258. Potter SJ, DeFalco T. Role of the testis interstitial compartment in spermatogonial stem cell function. Reproduction. 2017;153(4):R151-R62. Epub 2017/01/25. doi: 10.1530/REP-16-0588. PubMed PMID: 28115580; PubMed Central PMCID: PMCPMC5326597.

259. Smith LB, Walker WH. The regulation of spermatogenesis by androgens. Semin Cell Dev Biol. 2014;30:2-13. Epub 2014/03/07. doi: 10.1016/j.semcdb.2014.02.012. PubMed PMID: 24598768; PubMed Central PMCID: PMCPMC4043871.

260. Combes AN, Wilhelm D, Davidson T, Dejana E, Harley V, Sinclair A, et al. Endothelial cell migration directs testis cord formation. Dev Biol. 2009;326(1):112-20. Epub 2008/12/02. doi: 10.1016/j.ydbio.2008.10.040. PubMed PMID: 19041858.

261. Costanzo LS. Reproductive Physiology. 6 ed: Elsevier; 2018 8th May 2017. 258 p.

262. Muciaccia B, Boitani C, Berloco BP, Nudo F, Spadetta G, Stefanini M, et al. Novel stage classification of human spermatogenesis based on acrosome development.

Biol Reprod. 2013;89(3):60. Epub 2013/08/16. doi: 10.1095/biolreprod.113.111682. PubMed PMID: 23946533.

263. Zindy F, den Besten W, Chen B, Rehg JE, Latres E, Barbacid M, et al. Control of spermatogenesis in mice by the cyclin D-dependent kinase inhibitors p18(Ink4c) and p19(Ink4d). Mol Cell Biol. 2001;21(9):3244-55. Epub 2001/04/05. doi: 10.1128/MCB.21.9.3244-3255.2001. PubMed PMID: 11287627; PubMed Central PMCID: PMCPMC86968.

264. Cheng CY, editor. Molecular Mechanisms in Spermatogenesis. USA: Springer Nature International Publishing AG; 2008.

265. White-Cooper H, Davidson I. Unique aspects of transcription regulation in male germ cells. Cold Spring Harb Perspect Biol. 2011;3(7). Epub 2011/05/11. doi: 10.1101/cshperspect.a002626. PubMed PMID: 21555408; PubMed Central PMCID: PMCPMC3119912.

266. Pacheco SE, Houseman EA, Christensen BC, Marsit CJ, Kelsey KT, Sigman M, et al. Integrative DNA methylation and gene expression analyses identify DNA packaging and epigenetic regulatory genes associated with low motility sperm. PLoS One. 2011;6(6):e20280. Epub 2011/06/16. doi: 10.1371/journal.pone.0020280. PubMed PMID: 21674046; PubMed Central PMCID: PMCPMC3107223.

267. Adler I-D. Comparison of the duration of spermatogenesis between male rodents and humans. Mutation Research/Fundamental and Molecular Mechanisms of Mutagenesis. 1996;352(1-2):169-72. doi: 10.1016/0027-5107(95)00223-5.

268. Geyer CB. Setting the stage: the first round of spermatogenesis. In: Oatley JM GM, editor. The Biology of Mammalian Spermatogonia. NY: Springer Nature; 2017. p. 39-63.

269. Janca FC, Jost LK, Evenson DP. Mouse testicular and sperm cell development characterized from birth to adulthood by dual parameter flow cytometry. Biol Reprod. 1986;34(4):613-23. Epub 1986/05/01. doi: 10.1095/biolreprod34.4.613. PubMed PMID: 3708046.

270. Paniagua R, Nistal M. Morphological and histometric study of human spermatogonia from birth to the onset of puberty. J Anat. 1984;139 ( Pt 3):535-52. Epub 1984/10/01. PubMed PMID: 6490534; PubMed Central PMCID: PMCPMC1165067.

271. Leblond CP, Clermont Y. Spermiogenesis of rat, mouse, hamster and guinea pig as revealed by the periodic acid-fuchsin sulfurous acid technique. Am J Anat. 1952;90(2):167-215. Epub 1952/03/01. doi: 10.1002/aja.1000900202. PubMed PMID: 14923625.

272. Working PK. Male reproductive toxicology: comparison of the human to animal models. Environ Health Perspect. 1988;77:37-44. doi: 10.1289/ehp.887737. PubMed PMID: 3289906; PubMed Central PMCID: PMCPMC1474524.

273. Chalmel F, Rolland AD, Niederhauser-Wiederkehr C, Chung SS, Demougin P, Gattiker A, et al. The conserved transcriptome in human and rodent male gametogenesis. Proc Natl Acad Sci U S A. 2007;104(20):8346-51. Epub 2007/05/08. doi: 10.1073/pnas.0701883104. PubMed PMID: 17483452; PubMed Central PMCID: PMCPMC1864911.

274. Sha J, Zhou Z, Li J, Yin L, Yang H, Hu G, et al. Identification of testis development and spermatogenesis-related genes in human and mouse testes using cDNA arrays. Mol Hum Reprod. 2002;8(6):511-7. doi: 10.1093/molehr/8.6.511. PubMed PMID: 12029067.

275. Dyson JM, Fedele, C.G., Davies, E.M., Becanovic, J., Mitchell, C.A. Phosphoinositide Phosphatases: Just as Important as the Kinases. 2012. In: Phosphoinositides I: Enzymes of Synthesis and Degradation [Internet]. SpringerSubcellular Biochemistry; [215-75].

276. Kimura T, Suzuki A, Fujita Y, Yomogida K, Lomeli H, Asada N, et al. Conditional loss of PTEN leads to testicular teratoma and enhances embryonic germ cell production. Development. 2003;130(8):1691-700. Epub 2003/03/07. doi: 10.1242/dev.00392. PubMed PMID: 12620992.

277. Bowles J, Koopman P. Retinoic acid, meiosis and germ cell fate in mammals. Development. 2007;134(19):3401-11. Epub 2007/08/24. doi: 10.1242/dev.001107. PubMed PMID: 17715177.

278. Koubova J, Menke DB, Zhou Q, Capel B, Griswold MD, Page DC. Retinoic acid regulates sex-specific timing of meiotic initiation in mice. Proc Natl Acad Sci U S A. 2006;103(8):2474-9. Epub 2006/02/08. doi: 10.1073/pnas.0510813103. PubMed PMID: 16461896; PubMed Central PMCID: PMCPMC1413806.

279. Zhou W, Shao H, Zhang D, Dong J, Cheng W, Wang L, et al. PTEN signaling is required for the maintenance of spermatogonial stem cells in mouse, by regulating the expressions of PLZF and UTF1. Cell Biosci. 2015;5:42. Epub 2015/07/30. doi: 10.1186/s13578-015-0034-x. PubMed PMID: 26221533; PubMed Central PMCID: PMCPMC4517568.

280. Bhandari R, Juluri KR, Resnick AC, Snyder SH. Gene deletion of inositol hexakisphosphate kinase 1 reveals inositol pyrophosphate regulation of insulin secretion, growth, and spermiogenesis. Proc Natl Acad Sci U S A. 2008;105(7):2349-53. Epub 2008/02/13. doi: 10.1073/pnas.0712227105. PubMed PMID: 18268345; PubMed Central PMCID: PMCPMC2268139.

281. Hasegawa H, Noguchi J, Yamashita M, Okada R, Sugimoto R, Furuya M, et al. Phosphatidylinositol 4-phosphate 5-kinase is indispensable for mouse spermatogenesis. Biol Reprod. 2012;86(5):136, 1-12. Epub 2012/02/11. doi: 10.1095/biolreprod.110.089896. PubMed PMID: 22321832.

282. Kawai T, Miyata H, Nakanishi H, Sakata S, Morioka S, Sasaki J, et al. Polarized PtdIns(4,5)P2 distribution mediated by a voltage-sensing phosphatase (VSP) regulates sperm motility. Proc Natl Acad Sci U S A. 2019;116(51):26020-8. Epub 2019/11/30. doi: 10.1073/pnas.1916867116. PubMed PMID: 31776261; PubMed Central PMCID: PMCPMC6925991.

283. Hellsten E, Bernard DJ, Owens JW, Eckhaus M, Suchy SF, Nussbaum RL. Sertoli cell vacuolization and abnormal germ cell adhesion in mice deficient in an inositol polyphosphate 5-phosphatase. Biol Reprod. 2002;66(5):1522-30. doi: 10.1095/biolreprod66.5.1522. PubMed PMID: 11967219.

284. Neirijnck Y, Kuhne F, Mayere C, Pavlova E, Sararols P, Foti M, et al. Tumor Suppressor PTEN Regulates Negatively Sertoli Cell Proliferation, Testis Size, and Sperm Production In Vivo. Endocrinology. 2019;160(2):387-98. doi: 10.1210/en.2018-00892. PubMed PMID: 30576429.

285. Boyer A, Paquet M, Lague MN, Hermo L, Boerboom D. Dysregulation of WNT/CTNNB1 and PI3K/AKT signaling in testicular stromal cells causes granulosa cell tumor of the testis. Carcinogenesis. 2009;30(5):869-78. Epub 2009/02/25. doi: 10.1093/carcin/bgp051. PubMed PMID: 19237610; PubMed Central PMCID: PMCPMC2675650.

286. Bolino A, Bolis A, Previtali SC, Dina G, Bussini S, Dati G, et al. Disruption of Mtmr2 produces CMT4B1-like neuropathy with myelin outfolding and impaired spermatogenesis. J Cell Biol. 2004;167(4):711-21. Epub 2004/11/24. doi: 10.1083/jcb.200407010. PubMed PMID: 15557122; PubMed Central PMCID: PMCPMC2172586.

287. Firestein R, Nagy PL, Daly M, Huie P, Conti M, Cleary ML. Male infertility, impaired spermatogenesis, and azoospermia in mice deficient for the pseudophosphatase Sbf1. J Clin Invest. 2002;109(9):1165-72. Epub 2002/05/08. doi: 10.1172/JCI12589. PubMed PMID: 11994405; PubMed Central PMCID: PMCPMC150957.

288. Pierson CR, Dulin-Smith AN, Durban AN, Marshall ML, Marshall JT, Snyder AD, et al. Modeling the human MTM1 p.R69C mutation in murine Mtm1 results in exon 4 skipping and a less severe myotubular myopathy phenotype. Hum Mol Genet. 2012;21(4):811-25. Epub 2011/11/10. doi: 10.1093/hmg/ddr512. PubMed PMID: 22068590; PubMed Central PMCID: PMCPMC3263994.

289. Wen N, Yu MF, Liu J, Cai C, Liu QH, Shen J. Deficiency of MTMR14 impairs male fertility in Mus musculus. PLoS One. 2018;13(11):e0206224. Epub 2018/11/10. doi: 10.1371/journal.pone.0206224. PubMed PMID: 30412589; PubMed Central PMCID: PMCPMC6226155 commercial affiliation/institutions do not alter our adherence to PLOS ONE policies on sharing data and materials.

290. Hellsten E, Evans JP, Bernard DJ, Janne PA, Nussbaum RL. Disrupted sperm function and fertilin beta processing in mice deficient in the inositol polyphosphate 5-phosphatase Inpp5b. Dev Biol. 2001;240(2):641-53. doi: 10.1006/dbio.2001.0476. PubMed PMID: 11784089.

291. Guo J, Grow EJ, Mlcochova H, Maher GJ, Lindskog C, Nie X, et al. The adult human testis transcriptional cell atlas. Cell Res. 2018;28(12):1141-57. Epub 2018/10/14. doi: 10.1038/s41422-018-0099-2. PubMed PMID: 30315278; PubMed Central PMCID: PMCPMC6274646.

292. Chalmel F, Lardenois A, Evrard B, Mathieu R, Feig C, Demougin P, et al. Global human tissue profiling and protein network analysis reveals distinct levels of transcriptional germline-specificity and identifies target genes for male infertility. Hum Reprod. 2012;27(11):3233-48. Epub 2012/08/29. doi: 10.1093/humrep/des301. PubMed PMID: 22926843.

293. Malek M, Kielkowska A, Chessa T, Anderson KE, Barneda D, Pir P, et al. PTEN Regulates PI(3,4)P2 Signaling Downstream of Class I PI3K. Mol Cell. 2017;68(3):566-80 e10. Epub 2017/10/24. doi: 10.1016/j.molcel.2017.09.024. PubMed PMID: 29056325; PubMed Central PMCID: PMCPMC5678281.

294. Maehama T, Dixon JE. The tumor suppressor, PTEN/MMAC1, dephosphorylates the lipid second messenger, phosphatidylinositol 3,4,5-trisphosphate. J Biol Chem. 1998;273(22):13375-8. Epub 1998/06/05. doi: 10.1074/jbc.273.22.13375. PubMed PMID: 9593664.

295. Myers MP, Stolarov JP, Eng C, Li J, Wang SI, Wigler MH, et al. P-TEN, the tumor suppressor from human chromosome 10q23, is a dual-specificity phosphatase. Proc Natl Acad Sci U S A. 1997;94(17):9052-7. Epub 1997/08/19. doi: 10.1073/pnas.94.17.9052. PubMed PMID: 9256433; PubMed Central PMCID: PMCPMC23024.

296. Li J, Yen C, Liaw D, Podsypanina K, Bose S, Wang SI, et al. PTEN, a putative protein tyrosine phosphatase gene mutated in human brain, breast, and prostate cancer. Science. 1997;275(5308):1943-7. Epub 1997/03/28. doi: 10.1126/science.275.5308.1943. PubMed PMID: 9072974.

297. Myers MP, Pass I, Batty IH, Van der Kaay J, Stolarov JP, Hemmings BA, et al. The lipid phosphatase activity of PTEN is critical for its tumor supressor function. Proc Natl Acad Sci U S A. 1998;95(23):13513-8. Epub 1998/11/13. doi: 10.1073/pnas.95.23.13513. PubMed PMID: 9811831; PubMed Central PMCID: PMCPMC24850.

298. Butler M, McKay RA, Popoff IJ, Gaarde WA, Witchell D, Murray SF, et al. Specific inhibition of PTEN expression reverses hyperglycemia in diabetic mice. Diabetes. 2002;51(4):1028-34. Epub 2002/03/28. doi: 10.2337/diabetes.51.4.1028. PubMed PMID: 11916922.

299. Horie Y, Suzuki A, Kataoka E, Sasaki T, Hamada K, Sasaki J, et al. Hepatocyte-specific Pten deficiency results in steatohepatitis and hepatocellular carcinomas. J Clin Invest. 2004;113(12):1774-83. Epub 2004/06/17. doi: 10.1172/JCI20513. PubMed PMID: 15199412; PubMed Central PMCID: PMCPMC420505.

300. Ortega-Molina A, Efeyan A, Lopez-Guadamillas E, Munoz-Martin M, Gomez-Lopez G, Canamero M, et al. Pten positively regulates brown adipose function, energy

expenditure, and longevity. Cell Metab. 2012;15(3):382-94. Epub 2012/03/13. doi: 10.1016/j.cmet.2012.02.001. PubMed PMID: 22405073.

301. Lotti F, Corona G, Degli Innocenti S, Filimberti E, Scognamiglio V, Vignozzi L, et al. Seminal, ultrasound and psychobiological parameters correlate with metabolic syndrome in male members of infertile couples. Andrology. 2013;1(2):229-39. Epub 2013/01/15. doi: 10.1111/j.2047-2927.2012.00031.x. PubMed PMID: 23315971.

302. Mounzih K, Lu R, Chehab FF. Leptin treatment rescues the sterility of genetically obese ob/ob males. Endocrinology. 1997;138(3):1190-3. Epub 1997/03/01. doi: 10.1210/endo.138.3.5024. PubMed PMID: 9048626.

303. Leisegang K, Udodong A, Bouic PJ, Henkel RR. Effect of the metabolic syndrome on male reproductive function: a case-controlled pilot study. Andrologia. 2014;46(2):167-76. Epub 2013/01/03. doi: 10.1111/and.12060. PubMed PMID: 23278477.

304. Rama Raju GA, Jaya Prakash G, Murali Krishna K, Madan K, Siva Narayana T, Ravi Krishna CH. Noninsulin-dependent diabetes mellitus: effects on sperm morphological and functional characteristics, nuclear DNA integrity and outcome of assisted reproductive technique. Andrologia. 2012;44 Suppl 1:490-8. Epub 2011/08/03. doi: 10.1111/j.1439-0272.2011.01213.x. PubMed PMID: 21806668.

305. Bhat GK, Sea TL, Olatinwo MO, Simorangkir D, Ford GD, Ford BD, et al. Influence of a leptin deficiency on testicular morphology, germ cell apoptosis, and expression levels of apoptosis-related genes in the mouse. J Androl. 2006;27(2):302-10. Epub 2005/11/24. doi: 10.2164/jandrol.05133. PubMed PMID: 16304204.

306. Woodhouse J, Ferguson MM. Multiple hyperechoic testicular lesions are a common finding on ultrasound in Cowden disease and represent lipomatosis of the testis. Br J Radiol. 2006;79(946):801-3. Epub 2006/09/19. doi: 10.1259/bjr/50628431. PubMed PMID: 16980675.

307. Di Vizio D, Cito L, Boccia A, Chieffi P, Insabato L, Pettinato G, et al. Loss of the tumor suppressor gene PTEN marks the transition from intratubular germ cell neoplasias (ITGCN) to invasive germ cell tumors. Oncogene. 2005;24(11):1882-94. Epub 2005/01/28. doi: 10.1038/sj.onc.1208368. PubMed PMID: 15674339.

308. Harada N, Tamai Y, Ishikawa T, Sauer B, Takaku K, Oshima M, et al. Intestinal polyposis in mice with a dominant stable mutation of the beta-catenin gene. EMBO J. 1999;18(21):5931-42. Epub 1999/11/02. doi: 10.1093/emboj/18.21.5931. PubMed PMID: 10545105; PubMed Central PMCID: PMCPMC1171659.

309. Chen H, Rossier C, Morris MA, Scott HS, Gos A, Bairoch A, et al. A testis-specific gene, TPTE, encodes a putative transmembrane tyrosine phosphatase and maps to the pericentromeric region of human chromosomes 21 and 13, and to chromosomes 15, 22, and Y. Hum Genet. 1999;105(5):399-409. doi: 10.1007/s004390051122. PubMed PMID: 10598804.

310. Sutton KA, Jungnickel MK, Jovine L, Florman HM. Evolution of the Voltage Sensor Domain of the Voltage-Sensitive Phosphoinositide Phosphatase VSP/TPTE Suggests a Role as a Proton Channel in Eutherian Mammals. Mol Biol Evol. 2012;29(9):2147-55. doi: 10.1093/molbev/mss083. PubMed PMID: WOS:000308851600008.

311. Wu Y, Dowbenko D, Pisabarro MT, Dillard-Telm L, Koeppen H, Lasky LA. PTEN 2, a Golgi-associated testis-specific homologue of the PTEN tumor suppressor lipid phosphatase. J Biol Chem. 2001;276(24):21745-53. doi: 10.1074/jbc.M101480200. PubMed PMID: 11279206.

312. Walker SM, Downes CP, Leslie NR. TPIP: a novel phosphoinositide 3-phosphatase. Biochem J. 2001;360(Pt 2):277-83. doi: 10.1042/0264-6021:3600277. PubMed PMID: 11716755; PubMed Central PMCID: PMCPMC1222227.

313. Atanackovic D, Blum I, Cao Y, Wenzel S, Bartels K, Faltz C, et al. Expression of cancer-testis antigens as possible targets for antigen-specific immunotherapy in head and neck squamous cell carcinoma. Cancer Biol Ther. 2006;5(9):1218-25. doi: 10.4161/cbt.5.9.3174. PubMed PMID: 16929165.

314. Kuemmel A, Simon P, Breitkreuz A, Rohlig J, Luxemburger U, Elsasser A, et al. Humoral immune responses of lung cancer patients against the Transmembrane Phosphatase with TEnsin homology (TPTE). Lung Cancer. 2015;90(2):334-41. doi: 10.1016/j.lungcan.2015.07.012. PubMed PMID: 26350112.

315. Tapparel C, Reymond A, Girardet C, Guillou L, Lyle R, Lamon C, et al. The TPTE gene family: cellular expression, subcellular localization and alternative splicing. Gene. 2003;323:189-99. doi: 10.1016/j.gene.2003.09.038. PubMed PMID: 14659893.

316. Taylor GS, Maehama T, Dixon JE. Myotubularin, a protein tyrosine phosphatase mutated in myotubular myopathy, dephosphorylates the lipid second messenger, phosphatidylinositol 3-phosphate. Proc Natl Acad Sci U S A. 2000;97(16):8910-5. Epub 2000/07/20. doi: 10.1073/pnas.160255697. PubMed PMID: 10900271; PubMed Central PMCID: PMCPMC16795.

317. Begley MJ, Taylor GS, Brock MA, Ghosh P, Woods VL, Dixon JE. Molecular basis for substrate recognition by MTMR2, a myotubularin family phosphoinositide phosphatase. Proc Natl Acad Sci U S A. 2006;103(4):927-32. Epub 2006/01/18. doi: 10.1073/pnas.0510006103. PubMed PMID: 16410353; PubMed Central PMCID: PMCPMC1347996.

318. Schaletzky J, Dove SK, Short B, Lorenzo O, Clague MJ, Barr FA. Phosphatidylinositol-5-Phosphate Activation and Conserved Substrate Specificity of the Myotubularin Phosphatidylinositol 3-Phosphatases. Current Biology. 2003;13(6):504-9. doi: 10.1016/s0960-9822(03)00132-5.

319. Blondeau F, Laporte J, Bodin S, Superti-Furga G, Payrastre B, Mandel JL. Myotubularin, a phosphatase deficient in myotubular myopathy, acts on phosphatidylinositol 3-kinase and phosphatidylinositol 3-phosphate pathway. Hum Mol Genet. 2000;9(15):2223-9. Epub 2000/09/26. doi: 10.1093/oxfordjournals.hmg.a018913. PubMed PMID: 11001925.

320. Tosch V, Rohde HM, Tronchere H, Zanoteli E, Monroy N, Kretz C, et al. A novel PtdIns3P and PtdIns(3,5)P2 phosphatase with an inactivating variant in centronuclear myopathy. Hum Mol Genet. 2006;15(21):3098-106. Epub 2006/09/30. doi: 10.1093/hmg/ddl250. PubMed PMID: 17008356.

321. Laporte J, Guiraud-Chaumeil C, Vincent MC, Mandel JL, Tanner SM, Liechti-Gallati S, et al. Mutations in the MTM1 gene implicated in X-linked myotubular myopathy. ENMC International Consortium on Myotubular Myopathy. European Neuro-Muscular Center. Hum Mol Genet. 1997;6(9):1505-11. Epub 1997/09/26. doi: 10.1093/hmg/6.9.1505. PubMed PMID: 9305655.

322. Bolino A, Muglia M, Conforti FL, LeGuern E, Salih MA, Georgiou DM, et al. Charcot-Marie-Tooth type 4B is caused by mutations in the gene encoding myotubularin-related protein-2. Nat Genet. 2000;25(1):17-9. Epub 2000/05/10. doi: 10.1038/75542. PubMed PMID: 10802647.

323. Azzedine H, Bolino A, Taieb T, Birouk N, Di Duca M, Bouhouche A, et al. Mutations in MTMR13, a new pseudophosphatase homologue of MTMR2 and Sbf1, in two families with an autosomal recessive demyelinating form of Charcot-Marie-Tooth disease associated with early-onset glaucoma. Am J Hum Genet. 2003;72(5):1141-53. Epub 2003/04/11. doi: 10.1086/375034. PubMed PMID: 12687498; PubMed Central PMCID: PMCPMC1180267.

324. Kim SA, Vacratsis PO, Firestein R, Cleary ML, Dixon JE. Regulation of myotubularin-related (MTMR)2 phosphatidylinositol phosphatase by MTMR5, a catalytically inactive phosphatase. Proc Natl Acad Sci U S A. 2003;100(8):4492-7. Epub 2003/04/02. doi: 10.1073/pnas.0431052100. PubMed PMID: 12668758; PubMed Central PMCID: PMCPMC153583.

325. Li JC, Lee TW, Mruk TD, Cheng CY. Regulation of Sertoli cell myotubularin (rMTM) expression by germ cells in vitro. J Androl. 2001;22(2):266-77. Epub 2001/03/07. PubMed PMID: 11229801.

326. Zhang J, Wong CH, Xia W, Mruk DD, Lee NP, Lee WM, et al. Regulation of Sertoli-germ cell adherens junction dynamics via changes in protein-protein interactions of the N-cadherin-beta-catenin protein complex which are possibly mediated by c-Src and myotubularin-related protein 2: an in vivo study using an androgen suppression model. Endocrinology. 2005;146(3):1268-84. Epub 2004/12/14. doi: 10.1210/en.2004-1194. PubMed PMID: 15591133.

327. Kuzmin A, Jarvi K, Lo K, Spencer L, Chow GY, Macleod G, et al. Identification of potentially damaging amino acid substitutions leading to human male infertility. Biol Reprod. 2009;81(2):319-26. Epub 2009/04/17. doi: 10.1095/biolreprod.109.076000. PubMed PMID: 19369647; PubMed Central PMCID: PMCPMC2849822.

328. Yin L, Yong-Bo P, Meng-Fei Y, Weiwei C, Ping Z, Lu X, et al. Mice lacking myotubularin-related protein 14 show accelerated high-fat diet-induced lipid accumulation and inflammation. J Physiol Biochem. 2017;73(1):17-28. Epub 2016/11/04. doi: 10.1007/s13105-016-0520-6. PubMed PMID: 27807764.

329. Norris FA, Majerus PW. Hydrolysis of phosphatidylinositol 3,4-bisphosphate by inositol polyphosphate 4-phosphatase isolated by affinity elution chromatography. Journal of Biological Chemistry. 1994;269(12):8716-20. doi: 10.1016/s0021-9258(17)37027-8.

330. Maekawa M, Terasaka S, Mochizuki Y, Kawai K, Ikeda Y, Araki N, et al. Sequential breakdown of 3-phosphorylated phosphoinositides is essential for the completion of macropinocytosis. Proc Natl Acad Sci U S A. 2014;111(11):E978-87. Epub 2014/03/05. doi: 10.1073/pnas.1311029111. PubMed PMID: 24591580; PubMed Central PMCID: PMCPMC3964036.

331. Sasaki J, Kofuji S, Itoh R, Momiyama T, Takayama K, Murakami H, et al. The PtdIns(3,4)P(2) phosphatase INPP4A is a suppressor of excitotoxic neuronal death. Nature. 2010;465(7297):497-501. Epub 2010/05/14. doi: 10.1038/nature09023. PubMed PMID: 20463662.

332. Aich J, Mabalirajan U, Ahmad T, Agrawal A, Ghosh B. Loss-of-function of inositol polyphosphate-4-phosphatase reversibly increases the severity of allergic airway inflammation. Nat Commun. 2012;3:877. Epub 2012/06/08. doi: 10.1038/ncomms1880. PubMed PMID: 22673904.

333. Ungewickell A, Hugge C, Kisseleva M, Chang SC, Zou J, Feng Y, et al. The identification and characterization of two phosphatidylinositol-4,5-bisphosphate 4-phosphatases. Proc Natl Acad Sci U S A. 2005;102(52):18854-9. Epub 2005/12/21. doi: 10.1073/pnas.0509740102. PubMed PMID: 16365287; PubMed Central PMCID: PMCPMC1323219.

334. Morioka S, Nigorikawa K, Okada E, Tanaka Y, Kasuu Y, Yamada M, et al. TMEM55a localizes to macrophage phagosomes to downregulate phagocytosis. J Cell Sci. 2018;131(5). Epub 2018/01/31. doi: 10.1242/jcs.213272. PubMed PMID: 29378918.

335. Hashimoto Y, Shirane M, Nakayama KI. TMEM55B contributes to lysosomal homeostasis and amino acid-induced mTORC1 activation. Genes Cells. 2018;23(6):418-34. Epub 2018/04/13. doi: 10.1111/gtc.12583. PubMed PMID: 29644770.

336. Takemasu S, Nigorikawa K, Yamada M, Tsurumi G, Kofuji S, Takasuga S, et al. Phosphorylation of TMEM55B by Erk/MAPK regulates lysosomal positioning. J Biochem. 2019;166(2):175-85. Epub 2019/07/23. doi: 10.1093/jb/mvz026. PubMed PMID: 31329883.

337. Qin Y, Ting F, Kim MJ, Strelnikov J, Harmon J, Gao F, et al. Phosphatidylinositol-(4,5)-Bisphosphate Regulates Plasma Cholesterol Through LDL (Low-Density Lipoprotein) Receptor Lysosomal Degradation. Arterioscler Thromb Vasc Biol. 2020;40(5):1311-24. Epub 2020/03/20. doi: 10.1161/ATVBAHA.120.314033. PubMed PMID: 32188273; PubMed Central PMCID: PMCPMC7197750.

338. Medina MW, Bauzon F, Naidoo D, Theusch E, Stevens K, Schilde J, et al. Transmembrane protein 55B is a novel regulator of cellular cholesterol metabolism. Arterioscler Thromb Vasc Biol. 2014;34(9):1917-23. Epub 2014/07/19. doi: 10.1161/ATVBAHA.113.302806. PubMed PMID: 25035345; PubMed Central PMCID: PMCPMC4141484.

339. Woscholski R, Finan PM, Radley E, Totty NF, Sterling AE, Hsuan JJ, et al. Synaptojanin is the major constitutively active phosphatidylinositol-3,4,5-trisphosphate 5-phosphatase in rodent brain. J Biol Chem. 1997;272(15):9625-8. Epub 1997/04/11. doi: 10.1074/jbc.272.15.9625. PubMed PMID: 9092489.

340. McPherson PS, Garcia EP, Slepnev VI, David C, Zhang X, Grabs D, et al. A presynaptic inositol-5-phosphatase. Nature. 1996;379(6563):353-7. Epub 1996/01/25. doi: 10.1038/379353a0. PubMed PMID: 8552192.

341. Mitchell CA, Gurung R, Kong AM, Dyson JM, Tan A, Ooms LM. Inositol polyphosphate 5-phosphatases: lipid phosphatases with flair. IUBMB Life. 2002;53(1):25-36. Epub 2002/05/23. doi: 10.1080/15216540210815. PubMed PMID: 12018404.

342. Nemoto Y, Wenk MR, Watanabe M, Daniell L, Murakami T, Ringstad N, et al. Identification and characterization of a synaptojanin 2 splice isoform predominantly expressed in nerve terminals. J Biol Chem. 2001;276(44):41133-42. doi: 10.1074/jbc.M106404200. PubMed PMID: 11498538.

343. Hakim S, Bertucci MC, Conduit SE, Vuong DL, Mitchell CA. Inositol polyphosphate phosphatases in human disease. Curr Top Microbiol Immunol. 2012;362:247-314. doi: 10.1007/978-94-007-5025-8_12. PubMed PMID: 23086422.

344. Kisseleva MV, Wilson MP, Majerus PW. The isolation and characterization of a cDNA encoding phospholipid-specific inositol polyphosphate 5-phosphatase. J Biol Chem. 2000;275(26):20110-6. Epub 2000/04/15. doi: 10.1074/jbc.M910119199. PubMed PMID: 10764818.

345. Hasegawa J, Iwamoto R, Otomo T, Nezu A, Hamasaki M, Yoshimori T. Autophagosome-lysosome fusion in neurons requires INPP5E, a protein associated with Joubert syndrome. EMBO J. 2016;35(17):1853-67. Epub 2016/06/25. doi: 10.15252/embj.201593148. PubMed PMID: 27340123; PubMed Central PMCID: PMCPMC5007553.

346. Bertelli DF, Araujo EP, Cesquini M, Stoppa GR, Gasparotto-Contessotto M, Toyama MH, et al. Phosphoinositide-specific inositol polyphosphate 5-phosphatase IV inhibits inositide trisphosphate accumulation in hypothalamus and regulates food intake and body weight. Endocrinology. 2006;147(11):5385-99. Epub 2006/08/19. doi: 10.1210/en.2006-0280. PubMed PMID: 16916951.

347. Kong AM, Speed CJ, O'Malley CJ, Layton MJ, Meehan T, Loveland KL, et al. Cloning and characterization of a 72-kDa inositol-polyphosphate 5-phosphatase localized to the Golgi network. J Biol Chem. 2000;275(31):24052-64. doi: 10.1074/jbc.M000874200. PubMed PMID: 10806194.

348. Nakatsu F, Perera RM, Lucast L, Zoncu R, Domin J, Gertler FB, et al. The inositol 5-phosphatase SHIP2 regulates endocytic clathrin-coated pit dynamics. J Cell Biol. 2010;190(3):307-15. Epub 2010/08/04. doi: 10.1083/jcb.201005018. PubMed PMID: 20679431; PubMed Central PMCID: PMCPMC2922640.

349. Chi Y, Zhou B, Wang WQ, Chung SK, Kwon YU, Ahn YH, et al. Comparative mechanistic and substrate specificity study of inositol polyphosphate 5-phosphatase Schizosaccharomyces pombe Synaptojanin and SHIP2. J Biol Chem. 2004;279(43):44987-95. Epub 2004/08/19. doi: 10.1074/jbc.M406416200. PubMed PMID: 15316017.

350. Hibbs ML, Raftery AL, Tsantikos E. Regulation of hematopoietic cell signaling by SHIP-1 inositol phosphatase: growth factors and beyond. Growth Factors. 2018;36(5-6):213-31. Epub 2019/02/16. doi: 10.1080/08977194.2019.1569649. PubMed PMID: 30764683.

351. Hamilton MJ, Ho VW, Kuroda E, Ruschmann J, Antignano F, Lam V, et al. Role of SHIP in cancer. Exp Hematol. 2011;39(1):2-13. Epub 2010/11/09. doi: 10.1016/j.exphem.2010.11.002. PubMed PMID: 21056081.

352. Hamilton MJ, Halvorsen EC, LePard NE, Bosiljcic M, Ho VW, Lam V, et al. SHIP represses lung inflammation and inhibits mammary tumor metastasis in BALB/c mice. Oncotarget. 2016;7(4):3677-91. doi: DOI 10.18632/oncotarget.6611. PubMed PMID: WOS:000369952400003.

353. Ghosh S, Scozzaro S, Ramos AR, Delcambre S, Chevalier C, Krejci P, et al. Inhibition of SHIP2 activity inhibits cell migration and could prevent metastasis in breast cancer cells. J Cell Sci. 2018;131(16). Epub 2018/07/18. doi: 10.1242/jcs.216408. PubMed PMID: 30012834.

354. Kagawa S, Soeda Y, Ishihara H, Oya T, Sasahara M, Yaguchi S, et al. Impact of transgenic overexpression of SH2-containing inositol 5'-phosphatase 2 on glucose metabolism and insulin signaling in mice. Endocrinology. 2008;149(2):642-50. Epub 2007/11/28. doi: 10.1210/en.2007-0820. PubMed PMID: 18039790.

355. Sleeman MW, Wortley KE, Lai KM, Gowen LC, Kintner J, Kline WO, et al. Absence of the lipid phosphatase SHIP2 confers resistance to dietary obesity. Nat Med. 2005;11(2):199-205. Epub 2005/01/18. doi: 10.1038/nm1178. PubMed PMID: 15654325.

356. Liu QR, Shalaby F, Jones J, Bouchard D, Dumont DJ. The SH2-Containing inositol polyphosphate 5-phosphatase, Ship, is expressed during hematopoiesis and spermatogenesis. Blood. 1998;91(8):2753-9. PubMed PMID: WOS:000073012000017.

357. Carlsen E, Giwercman A, Keiding N, Skakkebaek NE. Evidence for decreasing quality of semen during past 50 years. BMJ. 1992;305(6854):609-13. Epub 1992/09/12. doi: 10.1136/bmj.305.6854.609. PubMed PMID: 1393072; PubMed Central PMCID: PMCPMC1883354.

358. Swan SH, Elkin EP, Fenster L. The question of declining sperm density revisited: an analysis of 101 studies published 1934-1996. Environ Health Perspect. 2000;108(10):961-6. Epub 2000/10/26. doi: 10.1289/ehp.00108961. PubMed PMID: 11049816; PubMed Central PMCID: PMCPMC1240129.

359. de Kretser DM. Male infertility. The Lancet. 1997;349(9054):787-90. doi: 10.1016/s0140-6736(96)08341-9.

360. Agarwal A, Baskaran S, Parekh N, Cho C-L, Henkel R, Vij S, et al. Male infertility. The Lancet. 2021;397(10271):319-33. doi: 10.1016/s0140-6736(20)32667-2.

361. Sagona AP, Nezis IP, Pedersen NM, Liestol K, Poulton J, Rusten TE, et al. PtdIns(3)P controls cytokinesis through KIF13A-mediated recruitment of FYVE-CENT to the midbody. Nat Cell Biol. 2010;12(4):362-71. Epub 2010/03/09. doi: 10.1038/ncb2036. PubMed PMID: 20208530.

362. Rohatgi R, Ho HY, Kirschner MW. Mechanism of N-WASP activation by CDC42 and phosphatidylinositol 4, 5-bisphosphate. J Cell Biol. 2000;150(6):1299-310. Epub 2000/09/20. doi: 10.1083/jcb.150.6.1299. PubMed PMID: 10995436; PubMed Central PMCID: PMCPMC2150699.

363. Chew CL, Chen M, Pandolfi PP. Endosome and INPP4B. Oncotarget. 2016;7(1):5-6. doi: 10.18632/oncotarget.6663. PubMed PMID: 26700619; PubMed Central PMCID: PMCPMC4807978.

364. Xia B, Yan Y, Baron M, Wagner F, Barkley D, Chiodin M, et al. Widespread Transcriptional Scanning in the Testis Modulates Gene Evolution Rates. Cell. 2020;180(2):248-62 e21. Epub 2020/01/25. doi: 10.1016/j.cell.2019.12.015. PubMed PMID: 31978344.

365. Di Cristofano A, Pesce B, Cordon-Cardo C, Pandolfi PP. Pten is essential for embryonic development and tumour suppression. Nat Genet. 1998;19(4):348-55. doi: 10.1038/1235. PubMed PMID: 9697695.

366. Boeri L, Capogrosso P, Ventimiglia E, Pederzoli F, Frego N, Cazzaniga W, et al. Undiagnosed prediabetes is highly prevalent in primary infertile men - results from a cross-sectional study. BJU Int. 2019;123(6):1070-7. Epub 2018/10/18. doi: 10.1111/bju.14558. PubMed PMID: 30328251.

367. Ferlin A, Garolla A, Ghezzi M, Selice R, Palego P, Caretta N, et al. Sperm Count and Hypogonadism as Markers of General Male Health. Eur Urol Focus. 2021;7(1):205-13. Epub 2019/08/21. doi: 10.1016/j.euf.2019.08.001. PubMed PMID: 31427194.

368. Katz D, Teloken P, Shoshany O. Male infertility – The other side of the equation. Australian Family Physician. 2017;46(9):641-6.

369. Barratt CLR, Bjorndahl L, De Jonge CJ, Lamb DJ, Osorio Martini F, McLachlan R, et al. The diagnosis of male infertility: an analysis of the evidence to support the development of global WHO guidance-challenges and future research opportunities. Hum Reprod Update. 2017;23(6):660-80. Epub 2017/10/06. doi: 10.1093/humupd/dmx021. PubMed PMID: 28981651; PubMed Central PMCID: PMCPMC5850791.

370. Song SH, Chiba K, Ramasamy R, Lamb DJ. Recent advances in the genetics of testicular failure. Asian J Androl. 2016;18(3):350-5. Epub 2016/04/07. doi: 10.4103/1008-682X.178857. PubMed PMID: 27048782; PubMed Central PMCID: PMCPMC4854078.

371. Zhang J, Li K, Yuan M, Zhang J, Huang G, Ao J, et al. A high-fat diet impairs reproduction by decreasing the IL1beta level in mice treated at immature stage. Sci Rep.

2017;7(1):567. Epub 2017/04/05. doi: 10.1038/s41598-017-00505-0. PubMed PMID: 28373640; PubMed Central PMCID: PMCPMC5428732.

372. Crean AJ, Senior AM. High-fat diets reduce male reproductive success in animal models: A systematic review and meta-analysis. Obes Rev. 2019;20(6):921-33. doi: 10.1111/obr.12827. PubMed PMID: 30756459.

373. Palmer NO, Bakos HW, Fullston T, Lane M. Impact of obesity on male fertility, sperm function and molecular composition. Spermatogenesis. 2012;2(4):253-63. Epub 2012/12/19. doi: 10.4161/spmg.21362. PubMed PMID: 23248766; PubMed Central PMCID: PMCPMC3521747.

374. Hammoud AO, Wilde N, Gibson M, Parks A, Carrell DT, Meikle AW. Male obesity and alteration in sperm parameters. Fertil Steril. 2008;90(6):2222-5. Epub 2008/01/08. doi: 10.1016/j.fertnstert.2007.10.011. PubMed PMID: 18178190.

375. Bunney TD, Katan M. Phosphoinositide signalling in cancer: beyond PI3K and PTEN. Nat Rev Cancer. 2010;10(5):342-52. Epub 2010/04/24. doi: 10.1038/nrc2842. PubMed PMID: 20414202.

376. Sato T, Kaneda A, Tsuji S, Isagawa T, Yamamoto S, Fujita T, et al. PRC2 overexpression and PRC2-target gene repression relating to poorer prognosis in small cell lung cancer. Sci Rep. 2013;3:1911. Epub 2013/05/30. doi: 10.1038/srep01911. PubMed PMID: 23714854; PubMed Central PMCID: PMCPMC3665955.

377. Mengual L, Burset M, Ars E, Lozano JJ, Villavicencio H, Ribal MJ, et al. DNA microarray expression profiling of bladder cancer allows identification of noninvasive diagnostic markers. J Urol. 2009;182(2):741-8. Epub 2009/06/23. doi: 10.1016/j.juro.2009.03.084. PubMed PMID: 19539325.

378. Lattin JE, Schroder K, Su AI, Walker JR, Zhang J, Wiltshire T, et al. Expression analysis of G Protein-Coupled Receptors in mouse macrophages. Immunome Res. 2008;4:5. Epub 2008/04/30. doi: 10.1186/1745-7580-4-5. PubMed PMID: 18442421; PubMed Central PMCID: PMCPMC2394514.

379. Thorrez L, Van Deun K, Tranchevent LC, Van Lommel L, Engelen K, Marchal K, et al. Using ribosomal protein genes as reference: a tale of caution. PLoS One. 2008;3(3):e1854. Epub 2008/03/28. doi: 10.1371/journal.pone.0001854. PubMed PMID: 18365009; PubMed Central PMCID: PMCPMC2267211.

380. Bellve AR, Cavicchia JC, Millette CF, O'Brien DA, Bhatnagar YM, Dym M. Spermatogenic cells of the prepuberal mouse. Isolation and morphological characterization. J Cell Biol. 1977;74(1):68-85. doi: 10.1083/jcb.74.1.68. PubMed PMID: 874003; PubMed Central PMCID: PMCPMC2109873.

381. Ferguson L, How JJ, Agoulnik AI. The fate of spermatogonial stem cells in the cryptorchid testes of RXFP2 deficient mice. PLoS One. 2013;8(10):e77351. Epub 2013/10/08. doi: 10.1371/journal.pone.0077351. PubMed PMID: 24098584; PubMed Central PMCID: PMCPMC3789668.

382. Baksi A, Vasan SS, Dighe RR. DNA Flow cytometric analysis of the human testicular tissues to investigate the status of spermatogenesis in azoospermic patients. Sci Rep. 2018;8(1):11117. Epub 2018/07/26. doi: 10.1038/s41598-018-29369-8. PubMed PMID: 30042518; PubMed Central PMCID: PMCPMC6057995.

383. Suresh R, Aravindan GR, Moudgal NR. Quantitation of spermatogenesis by DNA flow cytometry: Comparative study among six species of mammals. Journal of Biosciences. 1992;17(4):413-9. doi: 10.1007/bf02720096.

384. Krishnamurthy H, Danilovich N, Morales CR, Sairam MR. Qualitative and quantitative decline in spermatogenesis of the follicle-stimulating hormone receptor knockout (FORKO) mouse. Biol Reprod. 2000;62(5):1146-59. doi: 10.1095/biolreprod62.5.1146. PubMed PMID: 10775161.

385. Clavijo RI, Hsiao W. Update on male reproductive endocrinology. Transl Androl Urol. 2018;7(Suppl 3):S367-S72. Epub 2018/08/31. doi: 10.21037/tau.2018.03.25. PubMed PMID: 30159243; PubMed Central PMCID: PMCPMC6087844.

386. O'Shaughnessy PJ. Hormonal control of germ cell development and spermatogenesis. Seminars in cell & developmental biology. 2014;29:55-65. doi: 10.1016/j.semcdb.2014.02.010. PubMed PMID: 24598767.

387. Tsai MY, Yeh SD, Wang RS, Yeh S, Zhang C, Lin HY, et al. Differential effects of spermatogenesis and fertility in mice lacking androgen receptor in individual testis cells. Proc Natl Acad Sci U S A. 2006;103(50):18975-80. doi: 10.1073/pnas.0608565103. PubMed PMID: 17142319; PubMed Central PMCID: PMCPMC1748162.

388. Hamer G, Roepers-Gajadien HL, van Duyn-Goedhart A, Gademan IS, Kal HB, van Buul PP, et al. DNA double-strand breaks and gamma-H2AX signaling in the testis.

Biol Reprod. 2003;68(2):628-34. doi: 10.1095/biolreprod.102.008672. PubMed PMID: 12533428.

389. Bellani MA, Romanienko PJ, Cairatti DA, Camerini-Otero RD. SPO11 is required for sex-body formation, and Spo11 heterozygosity rescues the prophase arrest of Atm-/- spermatocytes. J Cell Sci. 2005;118(Pt 15):3233-45. doi: 10.1242/jcs.02466. PubMed PMID: 15998665.

390. Endo T, Freinkman E, de Rooij DG, Page DC. Periodic production of retinoic acid by meiotic and somatic cells coordinates four transitions in mouse spermatogenesis. Proc Natl Acad Sci U S A. 2017;114(47):E10132-E41. doi: 10.1073/pnas.1710837114. PubMed PMID: 29109271; PubMed Central PMCID: PMCPMC5703301.

391. Leduc F, Maquennehan V, Nkoma GB, Boissonneault G. DNA damage response during chromatin remodeling in elongating spermatids of mice. Biol Reprod. 2008;78(2):324-32. Epub 2007/11/23. doi: 10.1095/biolreprod.107.064162. PubMed PMID: 18032420.

392. Hedger MP, Meinhardt A. Cytokines and the immune-testicular axis. Journal of Reproductive Immunology. 2003;58(1):1-26. doi: 10.1016/s0165-0378(02)00060-8.

393. Loveland KL, Klein B, Pueschl D, Indumathy S, Bergmann M, Loveland BE, et al. Cytokines in Male Fertility and Reproductive Pathologies: Immunoregulation and Beyond. Front Endocrinol (Lausanne). 2017;8:307. Epub 2017/12/19. doi: 10.3389/fendo.2017.00307. PubMed PMID: 29250030; PubMed Central PMCID: PMCPMC5715375.

394. Duale N, Steffensen IL, Andersen J, Brevik A, Brunborg G, Lindeman B. Impaired sperm chromatin integrity in obese mice. Andrology. 2014;2(2):234-43. Epub 2014/01/25. doi: 10.1111/j.2047-2927.2013.00178.x. PubMed PMID: 24459046.

395. Mu Y, Yan WJ, Yin TL, Zhang Y, Li J, Yang J. Diet-induced obesity impairs spermatogenesis: a potential role for autophagy. Sci Rep. 2017;7:43475. Epub 2017/03/10. doi: 10.1038/srep43475. PubMed PMID: 28276438; PubMed Central PMCID: PMCPMC5343591.

396. Sharma RP, Schuhmacher M, Kumar V. Review on crosstalk and common mechanisms of endocrine disruptors: Scaffolding to improve PBPK/PD model of EDC

mixture. Environ Int. 2017;99:1-14. Epub 2016/10/05. doi: 10.1016/j.envint.2016.09.016. PubMed PMID: 27697394.

397. Darbandi M, Darbandi S, Agarwal A, Sengupta P, Durairajanayagam D, Henkel R, et al. Reactive oxygen species and male reproductive hormones. Reprod Biol Endocrinol. 2018;16(1):87. Epub 2018/09/13. doi: 10.1186/s12958-018-0406-2. PubMed PMID: 30205828; PubMed Central PMCID: PMCPMC6134507.

398. Kim DH, Gutierrez-Aguilar R, Kim HJ, Woods SC, Seeley RJ. Increased adipose tissue hypoxia and capacity for angiogenesis and inflammation in young diet-sensitive C57 mice compared with diet-resistant FVB mice. Int J Obes (Lond). 2013;37(6):853-60. doi: 10.1038/ijo.2012.141. PubMed PMID: 22964790; PubMed Central PMCID: PMCPMC3525796.

399. Gupta S, Ray K. Somatic PI3K activity regulates transition to the spermatocyte stages in Drosophila testis. Journal of Biosciences. 2017;42(2):285-97. doi: 10.1007/s12038-017-9678-5.

400. Brill JA, Hime GR, Scharer-Schuksz M, Fuller MT. A phospholipid kinase regulates actin organization and intercellular bridge formation during germline cytokinesis. Development (Cambridge, England). 2000;127(17):3855-64. PubMed PMID: Medline:10934029.

401. Gatt MK, Glover DM. The Drosophila phosphatidylinositol transfer protein encoded by vibrator is essential to maintain cleavage-furrow ingression in cytokinesis. Journal of cell science. 2006;119(Pt 11):2225-35. PubMed PMID: Medline:16684816.

402. Giansanti MG, Bonaccorsi S, Kurek R, Farkas RM, Dimitri P, Fuller MT, et al. The class I PITP giotto is required for Drosophila cytokinesis. Current biology : CB. 2006;16(2):195-201. PubMed PMID: Medline:16431372.

403. Hellsten E, Evans JP, Bernard DJ, Janne PA, Nussbaum RL. Disrupted sperm function and fertilin beta processing in mice deficient in the inositol polyphosphate 5-phosphatase Inpp5b. Developmental biology. 2001;240(2):641-53. PubMed PMID: Medline:11784089.

404. Lai MS, Cheng YS, Chen PR, Tsai SJ, Huang BM. Fibroblast growth factor 9 activates akt and MAPK pathways to stimulate steroidogenesis in mouse leydig cells.

PLoS One. 2014;9(3):e90243. doi: 10.1371/journal.pone.0090243. PubMed PMID: 24603862; PubMed Central PMCID: PMCPMC3946167.

405. De Gendt K, Verhoeven G. Tissue- and cell-specific functions of the androgen receptor revealed through conditional knockout models in mice. Mol Cell Endocrinol. 2012;352(1-2):13-25. Epub 2011/08/30. doi: 10.1016/j.mce.2011.08.008. PubMed PMID: 21871526.

406. Huang da W, Sherman BT, Lempicki RA. Systematic and integrative analysis of large gene lists using DAVID bioinformatics resources. Nat Protoc. 2009;4(1):44-57. doi: 10.1038/nprot.2008.211. PubMed PMID: 19131956.

407. Huang da W, Sherman BT, Lempicki RA. Bioinformatics enrichment tools: paths toward the comprehensive functional analysis of large gene lists. Nucleic Acids Res. 2009;37(1):1-13. doi: 10.1093/nar/gkn923. PubMed PMID: 19033363; PubMed Central PMCID: PMCPMC2615629.

408. Huang Z, Rivas B, Agoulnik AI. Insulin-like 3 signaling is important for testicular descent but dispensable for spermatogenesis and germ cell survival in adult mice. Biol Reprod. 2012;87(6):143. Epub 2012/10/27. doi: 10.1095/biolreprod.112.103382. PubMed PMID: 23100620; PubMed Central PMCID: PMCPMC4435430.

409. Benesh EC, Humphrey PA, Wang Q, Moley KH. Maternal high-fat diet induces hyperproliferation and alters Pten/Akt signaling in prostates of offspring. Sci Rep. 2013;3:3466. Epub 2013/12/11. doi: 10.1038/srep03466. PubMed PMID: 24322661; PubMed Central PMCID: PMCPMC3857567.

410. Hodgson MC, VanOstran G, Alghamdi S, Poppiti RJ, Agoulnik AI, Agoulnik IU. Reduced Androgen Receptor Expression Accelerates the Onset of ERBB2 Induced Breast Tumors in Female Mice. PLoS One. 2013;8(4).

411. Macias H, Hinck L. Mammary gland development. Wiley Interdiscip Rev Dev Biol. 2012;1(4):533-57. Epub 2012/07/31. doi: 10.1002/wdev.35. PubMed PMID: 22844349; PubMed Central PMCID: PMCPMC3404495.

412. Deng CY, Lv M, Luo BH, Zhao SZ, Mo ZC, Xie YJ. The Role of the PI3K/AKT/mTOR Signalling Pathway in Male Reproduction. Curr Mol Med. 2021;21(7):539-48. Epub 2020/12/05. doi: 10.2174/1566524020666201203164910. PubMed PMID: 33272176.

# VITA

## YASEMIN CEYHAN

Miami, Florida

| | |
|---|---|
| 2012-2016 | B.S., Molecular Biology and Genetics<br>Middle East Technical University<br>Ankara, TURKEY |
| 2014-2017 | B.S., Chemistry<br>Middle East Technical University<br>Ankara, TURKEY |
| 2017-2022 | Ph.D., Biomedical Sciences<br>Florida International University<br>Miami, Florida |
| 2018-2021 | Teaching Assistant<br>Florida International University<br>Miami, Florida |
| 2021-2022 | Research Assistant<br>Florida International University<br>Miami, Florida |
| 2022 | Dissertation Year Fellowship<br>Florida International University<br>Miami, Florida |

## PUBLICATIONS AND PRESENTATIONS

Ceyhan, Y., Zhang, M., Guo, J., Sandoval, C. G., Vacher, J., Kaftanovskaya, E. M., Agoulnik, A. I., Agoulnik, I. U. (2020). Deletion of inositol polyphosphate 4-phosphatase type-II B affects spermatogenesis in mice. PLoS One, 15(5), e0233163. doi:10.1371/journal.pone.0233163

Ceyhan, Y., Zhang, M., Sandoval, C. G., Agoulnik, A. I., Agoulnik, I. U. (2022). Expression pattern and the roles of phosphatidylinositol phosphatases in testis. Biol Rep. ioac132, doi: 10.1093/biolre/ioac132

Zhang, M., Ceyhan, Y., Kaftanovskaya, E. M., Vasquez, J.L., Vacher, J., Knop, F.K., Nathanson, L., Agoulnik, A. I., Ittman, M. M., Agoulnik, I. U. (2021). INPP4B protects

from metabolic syndrome and associated disorders. Commun Biol 4, 416. doi: 10.1038/s42003-021-01940-6

Ceyhan, Y., Zhang, M., Agoulnik, I.U. INPP4B prevents PIN via EZH2 and p53 signaling. Poster presented at: 2022 Herbert Wertheim College of Medicine 8th Annual Research Symposium; 2022 April 22, Miami, FL.

Ceyhan, Y., Zhang, M., Agoulnik, I.U. Regulation of p53 by INPP4B and high fat diet in mouse prostate. Poster presented at: Annual AACR Meeting 2022; 2022 April 8-13, New Orleans, LA.

Ceyhan, Y., Zhang, M., Kaftanovskaya E.M., Vasquez, J.L., Nathanson L., Agoulnik, A.I., Agoulnik, I.U. INPP4B improves insulin resistance by suppressing SREBP1 lipogenic activity in liver. Poster presented at: Florida International University Biomolecular Sciences Institute Research Symposium; 2021 April 30, Virtual Meeting.

Ceyhan, Y., Zhang, M., Agoulnik, I.U. INPP4B protects mice against BPH. Poster presented at: Annual AACR Meeting 2021; 2021 April 10-15, Virtual Meeting.

Ceyhan, Y., Zhang, M., Kaftanovskaya E.M., Vasquez, J.L., Nathanson L., Agoulnik, A.I., Agoulnik, I.U. INPP4B protects against NAFLD. Poster presented at: Keystone Symposium; 2021 March 22-24, Virtual Meeting.

Ceyhan, Y., Zhang, M., Lai, Y., Vasquez, J.L., Liu, Y., Agoulnik, I.U., Tse-Dinh, Y.C. (2020). Natamycin reduces prostate cancer proliferation by inhibiting base-excision repair mechanism. Poster presented at: 27th Annual PCF Scientific Retreat; 2020 October 20-23, Virtual Meeting.

Ceyhan, Y., Kaftanovskaya, E.M., Zhang, M., Myhr, C., Agoulnik, A.I., Agoulnik, I.U. Inositol Polyphosphate 4-Phosphatase Type-II B Is Required for Optimal Spermatogenesis in Mice. Poster presented at: Florida International University Biomolecular Sciences Institute Research Symposium; 2020 July 30-31, Virtual Meeting.